Einfluss des Chemokinrezeptors 4 (CXCR4) und seiner Liganden auf die systemische Inflammation

Dissertation

zur Erlangung des akademischen Grades

doctor rerum naturalium (Dr. rer. nat.)

vorgelegt dem Rat der Medizinischen Fakultät der

Friedrich-Schiller-Universität Jena

von Apotheker Semjon Seemann,

geboren am 24.04.1991 in Riga, Lettland

Gutachter

1. **apl. Prof. Dr. med. Amelie Lupp**
   Institut für Pharmakologie und Toxikologie, Universitätsklinikum Jena,
   Friedrich-Schiller-Universität Jena

2. **Prof. Dr. rer. nat. K.E. Gerhard Scriba**
   Institut für Pharmazeutische Chemie,
   Friedrich-Schiller-Universität Jena

3. **Prof. Dr. med. dent. habil. Tomasz Gedrange**
   Universitätsklinikum der Technischen Universität Dresden,
   UniversitätsZahnMedizin, Poliklinik für Kieferorthopädie

Tag der öffentlichen Verteidigung: 06.02.2018

Inhaltsverzeichnis

Abkürzungsverzeichnis

ALAT	Alanin-Aminotransferase
ASAT	Aspartat-Aminotransferase
Bcl-2	B-Zell-Lymphom 2 (B-cell lymphoma 2)
cAMP	Cyclisches Adenosinmonophosphat
CASP	Colon-ascendens-Stent-Peritonitis
CD3	Unterscheidungsgruppe 3 (Cluster of differentiation 3)
CLP	Blinddarm-Ligatur und Punktion (Cecal ligation and puncture)
COX-2	Cyclooxygenase-2
CREB	cAMP-Antwort-Element-bindendes Protein (response element-binding protein)
CRP	C-reaktives Protein
CXCL12	CXC-Motiv-Chemokin 12
CXCR4	CXC-Motiv-Chemokinrezeptor 4
CXCR7	CXC-Motiv-Chemokinrezeptor 7
CYP	Cytochrom P450
DAG	Diacylglycerin
ELAM-1	Endothel-Leukozyten-Adhäsionsmolekül 1 (Endothelial-leukocyte adhesion molecule 1)
GSH	Glutathion
HEK	Humane embryonale Niere (Human embryonic kidney)
HIV	Humanes Immundefizienz-Virus
HMGB1	Hochmobilitäts-Gruppe-Protein B1 (High-mobility-group-protein B1)
HO-1	Hämoxygenase-1
HUVEC	Menschliche Nabelvenenendothelzellen (Human umbilical vein endothelial cells)
ICAM-1	Interzelluläres Adhäsionsmolekül 1 (Intercellular adhesion molecule 1)
IFN-γ	Interferon-γ
IL	Interleukin
iNOS	Induzierbare NO-Synthase
IP3	Inositoltrisphosphat
LBP	Lipopolysaccharid-bindendes Protein
LPS	Lipopolysaccharide

MAP	Mitogen-aktiviertes Protein (Mitogen-activated protein)
MIF	Makrophagenmigrationsinhibierender Faktor
NADPH	Nicotinamidadenindinukleotidphosphat
NF-κB	Ein Transkriptionsfaktor (Nuclear factor 'kappa-light-chain-enhancer' of activated B-cells)
NO	Stickstoffmonoxid (Nitric oxide)
Nrf-2	Ein Transkriptionsfaktor (Nuclear factor (erythroid-derived 2)-like 2)
PAS	Perjodsäure-Schiff (Periodic acid-Schiff)
PCI	Peritoneale Kontamination und Infektion (Peritoneal contamination and infection)
PCR	Polymerase-Kettenreaktion
PCT	Procalcitonin
PI3K	Phosphoinositid-3-Kinase(n)
PKA	Proteinkinase A
PKC	Proteinkinase C
ROS	Reaktive Sauerstoffspezies (Reactive oxygen species)
SDF-1	Aus Stromazellen stammender Faktor-1 (Stromal cell-derived factor 1)
SIRS	Systemisches inflammatorisches Response-Syndrom
SOFA	Sequentielle Organversagensbewertung (Sequential organ failure assessment)
TGF-β	Transformierender Wachstumsfaktor- β (Transforming growth factor-β)
TLR4	Toll-ähnlicher Rezeptor 4 (Toll-like receptor 4)
TNF-α	Tumornekrosefaktor-α
VCAM-1	Gefäßzelladhäsionsmolekül 1 (Vascular cell adhesion molecule 1)
WHIM	Warzen-Hypogammaglobulinämie-Immundefizienz-Myelokathexis-Syndrom

1 Zusammenfassung

Aufgrund der Komplexität der Pathogenese der Sepsis und der trotz moderner Therapieverfahren immer noch sehr hohen Sterberate sind die Erforschung der pathophysiologischen Mechanismen der systemischen Inflammation und die Untersuchung kausaler Therapien von entscheidender Bedeutung. Um eine systemische Entzündung beim Menschen nachzubilden, wurden verschiedene Tiermodelle entwickelt, welche allerdings aufgrund ihrer Stärken und Schwächen kontrovers diskutiert werden. Die in der Forschung am häufigsten eingesetzten Tiermodelle wurden daher zunächst in **Manuskript I** hinsichtlich der systemischen Effekte, des Einflusses auf die Organfunktionen und der zugrundeliegenden pathophysiologischen Prozesse untersucht. Die Entzündung wurde dabei in Mäusen mittels Injektion von Lipopolysacchariden (LPS) oder einer humanen Stuhlprobe (peritoneal contamination and infection (PCI)-Modell) oder durch Ligatur und Punktion des Zökums (cecal ligation and puncture (CLP)-Modell) hervorgerufen. Es zeigte sich, dass das LPS- und das PCI-Modell einen ähnlichen zeitlichen Verlauf der systemischen Inflammation induzierten, wobei die LPS-Gabe eine insgesamt stärkere Immunreaktion auslöste: Es fand sich hierbei eine rasche Erhöhung der Serumzytokinspiegel von u.a. TNF-α und Interleukin (IL)-6, während die Blutglukosewerte sanken. Außerdem waren in den Organen ein verstärkter oxidativer Stress und eine intensive Einwanderung von Neutrophilen und Lymphozyten in die Leber und in die Milz erkennbar. Zusätzlich wurde die Biotransformationskapazität der Leber stark eingeschränkt und es war eine intensive Expression des proapoptotischen Schlüsselenzyms Caspase-3 in der Milz festzustellen. Aufgrund von Gegenregulationsmechanismen, wie der verstärkten Induktion des antiinflammatorischen Enzyms Hämoxygenase 1 (HO-1) und einer erhöhten IL-10-Sekretion, war eine Normalisierung der Vital- und Entzündungsparameter zu den späteren Zeitpunkten des Experiments festzustellen. Im Gegensatz dazu führte die CLP-Methode zu weniger stark ausgeprägten Effekten und es zeigte sich ein verzögerter Verlauf der systemischen Entzündung ohne Regeneration. Aufgrund der deutlichen Veränderung zahlreicher Vital- und Entzündungsparameter sowie der methodischen Vorteile wurde das LPS-Modell für die weiteren Untersuchungen ausgewählt und der zeitliche Endpunkt auf 24 Stunden festgesetzt, da die Effekte zu diesem Zeitpunkt am stärksten ausgeprägt waren. Als mögliche neue Zielstruktur für die Therapie der systemischen Inflammation wurde in Manuskript I zusätzlich die Expression des Chemokinrezeptors 4 (CXCR4) untersucht. Es konnte gezeigt werden,

dass dieser Rezeptor und sein natürlicher Ligand CXC-Motiv-Chemokin 12 (CXCL12) während der systemischen Entzündung in der Milz verstärkt exprimiert werden.

Aufgrund zahlreicher Hinweise in der Literatur, dass ein Antagonismus am CXCR4 die Entzündungsreaktion vorteilhaft beeinflussen könnte, wurde im **Manuskript II** mittels des CXCR4-Antagonisten AMD3100 der Einfluss einer Blockade dieses Rezeptors auf eine LPS-induzierte systemische Inflammation untersucht. Nach 24 Stunden wurden sowohl die systemischen Entzündungsparameter im Vergleich zur alleinigen LPS-Applikation und zu den Kontrolltieren als auch die Folgen für die Organfunktionen, insbesondere der Leber und Milz als zwei zentrale Organe der Immunreaktion, charakterisiert. Entgegen den Erwartungen war die zusätzliche Verabreichung mit AMD3100 nachteilig. Die Mäuse wiesen gegenüber der alleinigen LPS-Gabe einen noch stärker beeinträchtigten Gesundheitszustand auf und es fanden sich weiter erhöhte Serumspiegel von proinflammatorischen Zytokinen und von Stickstoffmonooxid. Das Blutbild der mit AMD3100 und LPS behandelten Mäuse war von einer Anämie, Thrombozytopenie, Lymphopenie und Neutrophilie geprägt. Außerdem war gegenüber der alleinigen LPS-Gabe ein erhöhter oxidativer Stress in verschiedenen Organen, ein verminderter Glykogengehalt und eine reduzierte Biotransformationskapazität der Lebern sowie eine vermehrte Einwanderung von sowohl neutrophilen Granulozyten als auch von Lymphozyten in das Lebergewebe erkennbar. Ferner führte die CXCR4-Blockade zu einer verstärkten Apoptose im Milzgewebe.

Aufgrund der in Manuskript II aufgezeigten nachteiligen Effekte von AMD3100 auf die systemische Inflammation und zur indirekten Bestätigung der dort erzielten Ergebnisse wurde in **Manuskript III** die Aktivierung der CXCR4-CXCL12-Achse mittels des hierfür synthetisierten plasmastabilen CXCL12-Analogons CTCE-0214D untersucht. Die zusätzliche Applikation von CTCE-0214D gegenüber der alleinigen LPS-Gabe verringerte die Serumspiegel der proinflammatorischen Zytokine und führte zu einer deutlichen Verbesserung der Blutzuckerwerte. Außerdem reduzierte die Substanz den oxidativen Stress in der Leber und in der Milz, verringerte die Expression von verschiedenen Zytokinen in der Leber und reduzierte das Ausmaß an apoptotischen Prozessen in den Organen. Weiterhin führte die kombinierte Gabe von LPS und CTCE-0214D gegenüber der alleinigen Verabreichung von LPS zu einer geringeren Abnahme der Biotransformationskapazität der Leber. Ferner war CTCE-0214D alleine in der Lage, das protektive Enzym HO-1 stark zu induzieren, sodass auch nach kombinierter LPS- und CTCE-0214D-Behandlung eine intensivere HO-1-Expression und -Aktivität in der Leber festgestellt wurde.

Zusammenfassend erwies sich die Verabreichung von LPS aufgrund der eindeutigen Effekte und der geringen interindividuellen Variabilität in den Vital- und Entzündungsparametern als am besten dazu geeignet, den Einfluss der CXCR4-CXCL12-Achse in der systemischen Inflammation zu untersuchen, wobei die Effekte nach 24 Stunden am ausgeprägtesten waren. Eine Aktivierung des CXCR4 wirkte dabei entzündungshemmend, antioxidativ und zytoprotektiv, wohingegen die Blockade dieses Rezeptors eine Verstärkung der Entzündungsreaktion bewirkte. Vor allem im Hinblick auf die Verminderung des oxidativen Stresses und die Verbesserung der Leberfunktion erscheint eine CXCR4-Aktivierung daher im Rahmen einer systemischen Inflammation therapeutisch als erfolgsversprechend und sollte in zukünftigen Untersuchungen weiterverfolgt werden.

2 Einleitung

2.1 Systemische Entzündung und Sepsis

2.1.1 Definition und Einordnung

Unter einer Entzündung wird eine Reaktion des Organismus auf einen Gewebeschaden verstanden, der durch Mikroorganismen oder andere Noxen (chemische/physikalische Einwirkungen, Fremdkörper etc.) verursacht werden kann. Ziel aller entzündlichen Vorgänge ist die Heilung des Gewebeschadens sowie die Elimination eingedrungener Mikroorganismen bzw. Noxen/Fremdkörper. Die Entzündung ist damit ein Ausdruck der Immunreaktion eines Organismuses (Krams et al. 2010).

Entzündliche Erkrankungen können lokal oder systemisch auftreten und lassen sich einteilen nach (Krams et al. 2010):

- ihrer klinischen Dauer (akut, protrahiert, rezidivierend, chronisch u. a.),
- ihren histologischen Charakteristika (exsudativ, nekrotisierend, granulierend, lymphozytär),
- ihrer Ätiologie (infektiös, immunologisch, physikalisch, chemisch, traumatisch, etc.).

Häufige Ursache einer Entzündung ist eine Infektion. Diese ist definiert als das Eindringen und das anschließende Vermehren eines infektiösen Agens (z.B. Bakterien, Pilze, Parasiten oder Viren) in den menschlichen oder tierischen Körper, unabhängig davon, ob es sich zu einer Krankheit entwickelt oder nicht (Barreto et al. 2006). Dabei kann eine Infektion lokal auftreten (Lokalinfektion), wie z.B. bei einer Gastritis oder einer Pneumonie, oder sich zu einer systemischen Herausforderung entwickeln (Allgemeininfektion). Bei der Allgemeininfektion gelangen Erreger in lokale Lymphknoten und vermehren sich dort. Nach einer für den jeweiligen Erreger typischen Inkubationszeit, dringen die Pathogene dann in das Blut vor und wandern in die verschiedenen Organe ein (Krams et al. 2010). Erregerspezifisch können somit einzelne Organe betroffen sein. So ist beispielsweise bei einer Tuberkulose vorrangig die Lunge befallen (Krams et al. 2010). Eine der bekanntesten Formen einer generalisierten Infektion ist die Sepsis (gemeinhin auch „Blutvergiftung“ genannt). Sie stellt die schwerste Komplikation einer systemischen Entzündung infolge einer Infektion durch Mikroorganismen dar. Der Erreger hat dabei die lokalen Abwehrmechanismen überwunden und gelangt vom Sepsisherd aus kontinuierlich oder schubweise in die Blutbahn (Krams et al. 2010).

Historisch war die Definition der Sepsis lange Zeit nicht eindeutig, da die Entstehung nicht allein auf dem Infektionsherd beruhen konnte, sondern die Reaktion der körpereigenen Immunabwehr eine weitere wichtige Rolle spielen musste. So äußerte sich Bone: „Sepsis ist definiert als eine Invasion von Mikroorganismen und/oder ihrer Toxine in den Blutstrom, zusammen mit der Reaktion des Organismus auf diese Invasion" (Bone et al. 1992). 1991 erfolgte eine Einteilung in SIRS (Systemisches inflammatorisches Response-Syndrom), Sepsis, Schwere Sepsis und Septischer Schock sowie eine Festlegung hierfür allgemeingültiger Kriterien (Bone et al. 1992). Diese erwiesen sich in der Praxis jedoch als zu unspezifisch und entsprechend nicht hilfreich. Daher überarbeitete ein Experten-Gremium aufgrund verbesserter und umfänglicherer Kenntnisse der zugrundeliegenden pathophysiologischen Mechanismen die klinische Sepsisdefinition. Die Sepsis wird seitdem als lebensbedrohliche Organdysfunktion definiert, die durch eine dysregulierte Reaktion des Organismus auf eine Infektion verursacht wird (Singer et al. 2016).

2.1.2 Symptome und Pathophysiologie

Jeder das physiologische Maß übersteigende Reiz, unabhängig von seiner Art (chemisch, physikalisch, thermisch, mechanisch, infektiös, etc.), ist in der Lage, einen Zell- und Gewebeschaden hervorzurufen, woraufhin die Zellen Entzündungsmediatoren (u.a. Prostaglandine, Zytokine, Histamin) freisetzen (Mutschler et al. 2013). Diese stehen im Zentrum jeder Entzündungsreaktion und vermögen die Reaktion zu starten, zu vermitteln und zu steuern (Mutschler et al. 2013). Wie erwähnt, lassen sich Entzündungen nach ihrem Verlauf in akute und chronische einteilen, wobei die akute Entzündung im Vordergrund dieser Arbeit stehen soll. Die typischen Anzeichen dieser treten je nach betroffenem Organ und Gewebe in unterschiedlicher Deutlichkeit auf. Nach Celsus und Galen sind die Kardinalsymptome der akuten Entzündung: Rubor (Rötung), Calor (Wärme), Tumor (Schwellung), Dolor (Schmerz) und Functio laesa (eingeschränkte Funktion) (Krams et al. 2010; Mutschler et al. 2013). Eine akute Entzündung durchläuft häufig folgende Phasen (Krams et al. 2010):

- Bildung vasoaktiver Entzündungsmediatoren
- Erhöhung der Gewebedurchblutung
- Steigerung der Kapillarpermeabilität
- Einwanderung von Leukozyten in das betroffene Gewebe

- Beseitigung der entzündungsauslösenden Gewebeschädigung und/oder der verursachenden Mikroorganismen
- Regeneration des Gewebes durch Ersatz- oder Defektheilung

Nach Bildung der zahlreichen Botenstoffe wird die Entzündungsreaktion eingeleitet. Humorale Entzündungsmediatoren, wie Kinine und Komplementfaktoren (Ward und Lentsch 1999), spielen dabei eine ebenso wichtige Rolle wie vasoaktive Botenstoffe (z.B. Prostaglandine, Bradykinin und Stickstoffmonoxid [NO]). Letztere wirken daraufhin im Entzündungsgebiet auf die Arteriolen und bewirken eine Dilatation der Gefäße (Rubor). Aufgrund der vermehrten Blutzufuhr erhöht sich der intravasale Druck im Entzündungsgebiet und der auf die Kapillarwände wirkende hydrostatische Druck wird verstärkt, wodurch es zu einem vermehrten Übertritt von Flüssigkeit in das interstitielle Gewebe kommt (Krams et al. 2010). Folgen sind Ödeme, Schwellungen (Tumor) und gegebenenfalls auch Rötungen mit Schmerzen (Rubor, Dolor). Der Zell- und Gewebeschaden kann außerdem zur Reizung und Freilegung von Schmerzfasern führen, was sich oft in der beschriebenen Fehlfunktion und in Schmerzen äußert (Functio laesa, Dolor) (Krams et al. 2010; Mutschler et al. 2013).

Zeitnah nach Einsetzen der Entzündungsreaktion steigt die Kapillarpermeabilität im Entzündungsgebiet an. Ursächlich dafür sind direkte Schädigungen der Endothelzellen. Das kapilläre Endothel lässt nun nicht nur Wasser und niedermolekulare Substanzen passieren, sondern auch höhermolekulare Proteine und es folgt die Bildung eines eiweißreichen Exsudates (Chandrasoma und Taylor 1998; Krams et al. 2010).

Durch die Verlangsamung des Blutstroms sind mehr Immunzellen, aber auch Erythrozyten und Plasmaproteine, in der Lage, durch das beschädigte Endothel ins Gewebe einzudringen (Calor, Tumor). Immunzellen wie Lymphozyten oder Granulozyten können außerdem über die vorhandenen Integrine mit endothelilalen Adhäsionsmolekülen, vor allem endothelial-leukocyte adhesion molecule 1 (ELAM-1), intercellular adhesion molecule 1 (ICAM-1) und vascular cell adhesion molecule 1 (VCAM-1) in Kontakt treten (Chandrasoma und Taylor 1998; Krams et al. 2010). Dadurch wird die aktive Diapedese eingeleitet. Neutrophile Granulozyten sind in der Regel die erste Zellpopulation im Entzündungsgebiet, besonders bei Infektionen bakteriellen Ursprungs. Später folgen Monozyten und Lymphozyten.

Durch die Aktivität der Leukozyten werden die Pathogene eliminiert und zerstörtes Gewebe abgebaut. Sofern die Bekämpfung der eingedrungenen Mikroorganismen bzw. die Beseitigung eines beschädigten Gewebeareals erfolgreich war, wird das Exsudat aufgelöst,

wobei hier Flüssigkeit und zelluläre Bestandteile über die Lymphgefäße abtransportiert werden. Im Rahmen des Entzündungsvorgangs entstandene Gewebedefekte werden durch Reparaturvorgänge beseitigt und es erfolgt eine Regeneration.

Tritt eine für das Immunsystem schwer beherrschbare Infektion auf, welche oft mit erheblichen Komplikationen verbundenen ist, liegt eine Sepsis vor (Schütt und Bröker 2011). Dieser lebensbedrohliche Zustand ist vor allem durch die in kurzen Zeitabständen ablaufenden gegenläufigen Dysregulationen des Immunsystems charakterisiert. Die septische Antwort ist eine sehr komplexe Kaskade von Ereignissen, die proinflammatorische, antiinflammatorische, zelluläre und humorale Mechanismen umfasst (Patel et al. 2003). Anfänglichem Fieber, einer erhöhten Atemfrequenz und einer Leukozytose folgt die Immunparalyse, verbunden mit Stoffwechselentgleisungen und Multiorganversagen, was mit einer Mortalität von 30-50% einhergeht (Schütt und Bröker 2011; Angus und van der Poll 2013).

Die pathogenen Erreger werden schnell von dendritischen Zellen und Makrophagen erkannt. Die daraufhin eingeleitete proinflammatorische Immunantwort kann entgleisen, woraufhin eine überschießende systemische Zytokinausschüttung (vor allem Interleukin (IL)-1, -6, -8, TNF-α) zum septischen Schock mit Todesfolge führen kann (Schütt und Bröker 2011). Die proinflammatorischen Zytokine aktivieren Endothelzellen (u.a. zur Produktion von Prostaglandinen), verursachen Flüssigkeitsaustritte ins Gewebe, damit einen Blutdruckabfall und eine Minderdurchblutung peripherer Gewebe (Kreislaufzentralisation) und schließlich einen Schockzustand mit Bewusstseinsverlust und Organversagen. Dabei sind vor allem die Niere, die Leber und die Lunge betroffen (Schütt und Bröker 2011). Kurz nach der Freisetzung der proinflammatorischen Mediatoren werden kompensatorisch antiinflammatorische Zytokine wie IL-10 und Transforming Growth Factor-β (TGF-β) gebildet und sezerniert (Holmes et al. 2003). Diese Prozesse dienen der Herunterregulierung der Synthese proinflammatorischer Mediatoren und der Wiederherstellung der Homöostase (Bone et al. 1997). Kommt es, wie bei einer Sepsis typisch, zu einer überschießenden antiinflammatorischen Reaktion, entsteht eine Immunsuppression, welche mit einer erhöhten Anfälligkeit gegenüber opportunistischen Infektionen (z.B. einer Pneumonie) verbunden ist (Bone et al. 1997; Schütt und Bröker 2011). Ist das Gleichgewicht zwischen proinflammatorischer Immunantwort und antiinflammatorischer Gegenregulation gestört, ist entweder eine überschießende Entzündungsreaktion oder eine massive Inhibition von

Abwehrprozessen die Ursache für das resultierende Multiorganversagen (Hotchkiss und Karl 2003).

2.1.3 Diagnose und Therapie

Eine frühzeitige und genaue Diagnose einer systemischen Infektion und einer Sepsis hat einen wesentlichen Einfluss auf die Überlebenschance des Patienten, da nach erfolgreicher Diagnose passende Therapiemaßnahmen eingeleitet werden können (Brunkhorst und Reinhart 2009). Gegenwärtig existiert allerdings kein Parameter, der ausschließlich zur Diagnosestellung einer systemischen Inflammation oder einer Sepsis herangezogen werden kann. Entsprechend dienen Veränderungen in klinischen und laborchemischen Parametern als Hilfestellung. Dennoch kommt es aufgrund der Vielzahl dieser Parameter oft zu ungenauen Diagnosen und die Hilfsgrößen geben keinen Aufschluss über die Ursache der Veränderung, sodass häufig nicht zwischen einer systemischen Infektion, Sepsis oder einer nichtinfektiösen Entzündungsreaktion unterschieden werden kann (Bloos und Reinhart 2014).

Zu den klinischen und laborchemischen Parametern einer entzündlichen Allgemeinreaktion gehören (Brunkhorst und Reinhart 2009; Krams et al. 2010; Reinhart et al. 2010):

- Fieber (≥ 38,0 °C, v.a. ausgelöst durch Prostaglandine, Interferone, Interleukine und TNF-α) oder Hypothermie (≤36,0 °C)
- Tachykardie mit einer Herzfrequenz ≥90/min
- Leukozytose oder Leukopenie
- Ein Anstieg der Akute-Phase-Proteine, wie des C-reaktiven Proteins (CRP), der α-Globuline und des Fibrinogens
- Ein Anstieg des Procalcitonins
- Erreger im Blut

In der Sepsisdiagnostik ist einerseits die Bestimmung der Biomarker und andererseits die Identifizierung der Erreger von entscheidender Bedeutung. Vor allem Procalcitonin (PCT), IL-6, IL-8 und das lipopolysaccharidbindende Protein (LBP) sind während der Akutphasenreaktion im Blut nachweisbar (Gruys et al. 2005). Bei schweren systemischen Infektionen wird PCT in parafollikulären Zellen der Schilddrüse und von extrathyreoidalen Geweben gebildet, wodurch der PCT-Plasmaspiegel erhöht wird (Brunkhorst und Reinhart 2009). Bei gesunden Patienten beträgt die PCT-Plasmakonzentration <0,1 ng/ml, während bei

einer schweren Sepsis diese bis auf ein Vielfaches ansteigen kann. So ist eine Sepsis bei PCT-Werten >1,0-1,5 ng/ml sehr wahrscheinlich (Brunkhorst und Reinhart 2009). Auch das proinflammatorische Zytokin IL-6 kann zur Erleichterung der Sepsisdiagnostik beitragen, da stark erhöhte IL-6-Serumkonzentrationen während einer Sepsis auftreten (Bloos und Reinhart 2014). Dieser Parameter unterliegt jedoch größeren interindividuellen Schwankungen und sollte daher nur zur Verlaufsbeurteilung herangezogen werden. Eine eher untergeordnete Rolle spielt hingegen das als allgemeiner Entzündungsmarker dienende C-reaktive Protein (CRP). Zum einen sind erhöhte Serumspiegel erst nach 4-6 Stunden und das Maximum nach 36 Stunden messbar, zum anderen tritt bei einer Vielzahl von anderen Erkrankungen ebenfalls eine erhöhte Konzentration auf (Bloos und Reinhart 2014). Seit einiger Zeit steht auch ein Laborparameter namens Presepsin zur Verfügung (Zou et al. 2014). Allerdings muss sich dieser Parameter erst noch in größeren Studien beweisen.

Die Erregeridentifizierung erfolgt mittels Polymerase-Kettenreaktion (PCR), wobei unterschieden wird zwischen der Identifizierung einer begrenzten Anzahl von Erregern und der Identifizierung aller Erreger (Bloos und Reinhart 2014). Abhängig vom Ausmaß und vom Auslöser der Infektion, ist nach erfolgreicher Diagnose eine gezielte Therapie möglich.

In der Klinik stellt der SOFA-Score („Sequential (Sepsis-Related) Organ Failure Assessment Score“) ein wesentliches Diagnosetool dar. Anhand von sechs Kriterien (Atmung, Koagulation, Leberfunktion, Herzkreislauffunktion, Glasgow Coma-Scale und Nierenfunktion) wird vor allem die Organfunktion der Patienten in den Mittelpunkt gestellt. Eine Sepsis liegt dann vor, wenn sich der SOFA-Score des Patienten akut um zwei oder mehr Punkte verschlechtert hat, da dies mit einem Sterberisiko von ungefähr 10 Prozent einhergeht. Außerdem ist eine schnelle Verdachtsdiagnose nach der neuen Leitlinie möglich, wenn zwei oder mehr der folgenden Kriterien erfüllt sind: Atemfrequenz ≥22/min, systolischer Blutdruck ≤100 mmHg, Bewusstseinsveränderung (quick (q) SOFA) (Singer et al. 2016).

Die systemische Entzündung und die Sepsis erfordern oft intensivmedizinische Behandlungsmethoden. Aufgrund der Komplexität der Erkrankung fußt die Therapie auf verschiedenen Maßnahmen (Bloos und Reinhart 2003):

- kausale Therapie mittels Antibiotikum
- chirurgische Herdsanierung
- supportive Therapie
- adjunktive Maßnahmen.

Die antibiotische Therapie muss schon vor dem definitiven Erregernachweis eingeleitet werden, da durch eine adäquate und frühzeitig begonnene Antibiotikatherapie die Mortalität und die Komplikationsrate der Sepsis gesenkt werden können (Brunkhorst und Reinhart 2009; Reinhart et al. 2010). So zeigten Brunkhorst et al., dass mit jeder Stunde Verzögerung bei der Diagnosestellung die Sterblichkeit um etwa 7 Prozent stieg. Bereits innerhalb der ersten Stunde war ein deutlicher Unterschied nachweisbar, denn mehr als 82 Prozent der Patienten, die innerhalb der ersten 30 Minuten antibiotisch behandelt worden waren, überlebten (Brunkhorst und Reinhart 2009; Martin et al. 2009). Wird hingegen kein effektives bzw. adäquates Antibiotikum verwendet, erhöht sich das Mortalitätsrisiko (Micek et al. 2005).

Zur antibiotischen Initialtherapie werden die Substanzgruppen der Penicilline, Cephalosporine und Carbapeneme empfohlen (Brunkhorst und Reinhart 2009; Reinhart et al. 2010). Unter Beachtung der lokalen Resistenzsituation sollten die Ärzte immer ein Pseudomonas-wirksames Antibiotikum auswählen (Micek et al. 2005), wobei die Fluorchinolone Ciprofloxacin und Levofloxacin nicht mehr zur Initialtherapie empfohlen werden (Reinhart et al. 2010). Ist der Erreger nachgewiesen, können die Ärzte mit einer gezielten Therapie beginnen.

Bei Vorhandensein eines Infektionsherdes muss dieser unverzüglich saniert werden, denn nur auf diesem Wege kann eine weitere Ausbreitung der Keime verhindert werden. Entsprechend sollte ein chirurgischer Eingriff erfolgen (Brunkhorst und Reinhart 2009).

Begleitet werden sollten die bisher genannten Therapieformen durch supportive Maßnahmen. Dabei sind vor allem die Beatmung, die Kreislaufstabilisierung, Nierenersatzverfahren und die enterale Ernährung von Bedeutung (Reinhart et al. 2010).

Adjuvante Therapiemaßnahmen können ebenfalls angewendet werden (Reinhart et al. 2010). Dazu zählen unter anderem sowohl Verfahren zur Toxinneutralisation als auch Maßnahmen, die der Dysregulation des Komplement-, Gerinnungs- oder Immunsystems entgegenwirken.

Allen Eingriffsmöglichkeiten zum Trotz steht derzeit kein zugelassenes Präparat für die kausale und gezielte Therapie zur Verfügung. Aufgrund der sehr hohen Mortalität und Morbidität und der sich zunehmend verschärfenden Resistenzlage der Keime gegenüber zahlreichen Antibiotika ergibt sich der Bedarf nach gezielten Therapieoptionen.

2.1.4 Die Leber in der systemischen Inflammation

Bei etwa 20% der Patienten mit Organversagen im Rahmen einer schweren Entzündungsreaktion wird eine Störung der Leberfunktion beobachtet (Bakker et al. 2004). Die Leber ist das zweitgrößte Organ des menschlichen Körpers und nimmt im Stoffwechselgeschehen des Organismus eine zentrale Stellung ein. Eine der wichtigsten Funktionen der Leber ist die Entgiftung, denn körpereigene Stoffe (z.B. Ammoniak) wandelt die Leber ebenso wie körperfremde Substanzen (z.B. Medikamente und Toxine) in inaktive, nierengängige und wasserlösliche Metabolite um (van den Berg und Gifford 2005). In der Membran des glatten endoplasmatischen Retikulums sind die meisten der für die Biotransformation wichtigen Enzymsysteme verankert. Die Oxidation ist die bedeutendste Reaktionsart der Phase I und wird überwiegend von Monooxygenasen katalysiert. Nach Verstoffwechselung wasserunlöslicher Stoffe (wie z.B. die Einführung funktioneller Gruppen), werden die entstandenen Metabolite in der Phase II an körpereigene Verbindungen (Sulfat, Glutathion, Glucuronsäure, Aminosäuren etc.) gebunden, wodurch die Wasserlöslichkeit erhöht und damit die Ausscheidbarkeit der entstandenen Produkte verbessert wird (Marquardt und Schäfer 2004). Vor allem bei septischen Patienten ist die Leber-Biotransformationskapazität von wesentlicher Bedeutung für die Entgiftung und Beseitigung von toxischen endogenen Metaboliten (z.B. von Lipiden nach Zellschädigungen) sowie von exogen verabreichten Antibiotika. Eine eingeschränkte Cytochrom P450 (CYP)-Aktivität führt zu einer geringeren Metabolisierungskapazität und -rate, sodass weniger Verbindungen über die Galle und die Nieren ausgeschieden werden können. Folglich kumulieren diese ausscheidungspflichtigen Verbindungen im Organismus, was häufig mit toxischen Auswirkungen verbunden ist und einen zusätzlich negativen Einfluss auf den bereits verschlechterten Gesundheitszustand der Patienten hat (Morgan 2001).

Ferner synthetisiert und verarbeitet die Leber ein breites Spektrum von Substanzen. Sie erzeugt und sezerniert u.a. Cholesterin und Proteine wie Albumin und Gerinnungsfaktoren (Page 2013). Darüber hinaus ist sie in der Lage, Nährstoffe wie z.B. Kohlenhydrate und Mineralien zu speichern und diese bei Bedarf dem Körper zuzuführen. Ebenso ist sie entscheidend am Energiestoffwechsel beteiligt und entsprechend für die Synthese von Lipiden, Glucose und Proteinen essentiell. Darüber hinaus dienen die lebereigenen Makrophagen, auch Kupfferzellen genannt, der Elimination von Pathogenen und dem Abbau überalterter Erythrozyten (Katz et al. 1991).

Durch die zahlreichen Funktionen der Leber wird deutlich, dass die Prognose der Sepsispatienten nachhaltig von der Funktionseinschränkung der Leber beeinflusst wird (Bakker et al. 2004; Schattenberg et al. 2006; Yan et al. 2014)). Folgen eines Leberversagens sind ein Verlust von Synthese-, Exkretions- und Entgiftungsleistungen. Während der akuten Phase einer systemischen Inflammation trägt die Leber durch ihre Synthesefunktion dazu bei, dass akute Entzündungsmediatoren, wie z.B. das CRP, α-1-Antitrypsin oder Fibrinogen, gebildet werden, um die Erreger zu bekämpfen (Vary und Kimball 1992). Im Gegenzug wird die Synthese von Albumin und Antithrombin reduziert. Diese Prozesse werden maßgeblich durch IL-6 gesteuert (Vary und Kimball 1992). Vor allem Antithrombin III wird unter physiologischen Bedingungen kontinuierlich ins Plasma abgegeben, wirkt antikoagulatorisch und besitzt an den Endothelzellen entzündungshemmende Eigenschaften (Abraham et al. 2003). Bei einem Leberversagen während einer Sepsis kann diese Protease aufgrund der eingeschränkten Synthese durch die Leber nicht mehr regulierend in die Gerinnungskaskade eingreifen, was mit einer erhöhten Thrombosegefahr einhergeht.

Etwa 80% der gewebeassoziierten Makrophagen entfallen auf die hepatischen Kupffer-Zellen, welche vor allem für die Beseitigung von Pathogenen zuständig sind (Katz et al. 1991). Infolge einer eingeschränkten Leberfunktion ist die Beseitigung der Noxen stark eingeschränkt, da eine geringere Immunantwort zu erwarten ist. Entsprechend ist der Körper anfälliger für sekundäre Infektionen (Nakatani et al. 2001).

Derzeit existiert für das Leberversagen während einer systemischen Inflammation keine effektive kausale Therapiemöglichkeit. Aufgrund der Relevanz dieses Organs ergibt sich hieraus die Notwendigkeit zur Entwicklung effektiver Therapieoptionen.

2.1.5 Die Milz in der systemischen Inflammation

Die Milz ist das größte lymphatische Organ des menschlichen Körpers. Kennzeichnend ist vor allem der starke Blutdurchfluss, denn ca. 200–300 ml/min pro 100 bis 150g Milzgewicht fließen durch das Organ (Altamura et al. 2001). Die Milz kann in zwei unterschiedliche strukturelle Funktionsbereiche unterteilt werden − die weiße und die rote Pulpa (Mebius und Kraal 2005). Die weiße Pulpa übernimmt immunologische Aufgaben, weshalb hier vor allem B- und T-Lymphozyten zu finden sind. Im Rahmen der Immunabwehr findet hier die antigeninduzierte Differenzierung und Vermehrung von B- und T-Lymphozyten statt. Dahingegen besteht die vorrangige Funktion der roten Pulpa darin, Pathogene aus dem Blut

mittels ihrer Phagozyten zu entfernen. Außerdem werden überalterte und insuffiziente Blutzellen, vor allem Erythrozyten und Thrombozyten, durch Makrophagen phagozytiert und abgebaut. Weiterhin dient die Milz als Speicherort für Erythrozyten, Leukozyten und Thrombozyten, welche bei Bedarf in die Zirkulation abgegeben werden können. Somit vereint die Milz in Struktur und Funktion zwei Organe (Mebius und Kraal 2005).

Durch die hohe Anzahl an Fresszellen und deren Aktivität in der Milz ist diese von fundamentaler Bedeutung bei der Beseitigung von Pathogenen aus dem Blutstrom. Dies äußert sich beispielsweise darin, dass nach einer Splenektomie die Gefahr für eine fulminant verlaufende Pneumokokkensepsis stark erhöht ist (Altamura et al. 2001). Außerdem besteht nach einer Splenektomie lebenslang ein erhöhtes Infektionsrisiko. Insbesondere hämatogene Infektionen mit bekapselten Bakterien, vor allem Pneumokokken, Haemophilus influenzae und Meningokokken, können in nur wenigen Stunden zu einer lebensgefährlichen Postsplenektomie-Sepsis führen (Boley et al. 1992). Folglich werden regelmäßige Schutzimpfungen sowie eine jährliche Grippeimpfung empfohlen (Rubin und Schaffner 2014).

Da nach einer Splenektomie die Filterfunktion der Milz fehlt, kann es zu einem erheblichen Anstieg der Thrombozytenzahl kommen (Thrombozytose). Es besteht somit eine erhöhte Gefahr für eine Bildung von Blutgerinnseln, welche vor allem die Portalvene verschließen können. Durchschnittlich 2-5 % der Patienten ohne Milz erleiden eine derartige lebensgefährliche Thrombose (Stamou et al. 2006).

Die Milz reagiert mit einer Größenzunahme (Splenomegalie) auf eine systemische Inflammation (Mebius und Kraal 2005). Hierbei kommt es zu einer Hypertrophie sowohl der weißen als auch der roten Pulpa, die u.a. auf einer (TNF-α- und IL-6-vermittelten) erhöhten Konzentration an High-mobility-group-protein B1 (HMGB1) im Milzgewebe beruht (Valdés-Ferrer et al. 2013). Eine stark vergrößerte Milz führt zu einer teilweise erheblich gesteigerten Elimination von Erythrozyten, Leukozyten und Thrombozyten aus dem peripheren Blut, so dass eine Zytopenie resultiert. Eine schwere Anämie kann regelmäßige Bluttransfusionen erfordern, eine Thrombozytopenie erhöht die Blutungsneigung, eine Leukozytopenie führt zu einer erhöhten Anfälligkeit für Infektionen. Da die Milz kein lebensnotwendiges Organ ist, verbleibt in diesen Fällen als einzige Therapieoption häufig nur eine Splenektomie, welche wiederum mit der bereits beschriebenen erhöhten Infektanfälligkeit verbunden ist.

2.2 Tiermodelle in der Entzündungsforschung

Wie unter 2.1.3 erwähnt, existieren etablierte Strategien zur Behandlung der systemischen Inflammation. Dennoch ist aufgrund der hohen Morbidität und Mortalität die Entwicklung neuer therapeutischer Optionen und die Identifizierung potentieller Arzneimittelkandidaten dringend erforderlich. Dafür sind tierexperimentelle Studien sehr nützlich und stellen eine Grundlage für die Charakterisierung neuer Medikamente und Therapieansätze dar (Parker und Watkins 2001). Im Wesentlichen lassen sich die Tiermodelle in der Sepsisforschung in drei Kategorien einteilen (Nemzek et al. 2008; Stortz et al. 2017):

1) Exogene Verabreichung von Toxinen
2) Exogene Verabreichung von lebenden Pathogenen
3) Chirurgische Methoden

Das perfekte Tiermodell zeichnet sich durch eine hohe Reproduzierbarkeit und eine einfache Durchführung aus. Idealerweise ist es damit möglich, den klinischen Verlauf des gewünschten Krankheitsbildes möglichst exakt nachzubilden. Jedoch gibt es signifikante Unterschiede zwischen den einzelnen Modellen bezüglich Reproduzierbarkeit, Homogenität und Nachbildung der Pathogenese einer Sepsis (Stortz et al. 2017).

2.2.1 Verabreichung von Toxinen

Dieses Entzündungsmodell wird oft in der Grundlagenforschung verwendet und beruht auf einer intravenösen oder intraperitonealen Injektion von verschiedenen Stimulantien, wie z.B. dem Bestandteil der Zellmembran gram-negativer Bakterien (Lipopolysaccharide [LPS, Endotoxin]), synthetischen Lipopeptiden oder Zymosan (Buras et al. 2005). Am häufigsten wird hier eine hohe LPS-Einmaldosis in kleine Nagetiere, wie z.B. Ratten oder Mäuse, injiziert (Rittirsch et al. 2007). Die meisten Labortiere, so auch Mäuse, sind jedoch gegen Endotoxine relativ resistent (Buras et al. 2005). So zeigten Copeland et al., dass bei Mäusen ca. 250-fach höhere LPS-Dosen notwendig sind, um eine dem klinischen Verlauf beim Menschen entsprechende Immunreaktion bzw. Zytokinantwort hervorzurufen (Copeland et al. 2005). LPS induziert eine starke Freisetzung von Zytokinen (Remick et al. 2000), was unmittelbar zum SIRS und zu einer frühen dosis-abhängigen Mortalität führen kann (Recknagel et al. 2013; Stortz et al. 2017). Die Immunantwort ist jedoch mit der menschlichen nur bedingt vergleichbar, denn die Zytokinantwort verläuft schneller und es sind höhere

Serumwerte messbar als im klinischen Geschehen (Deitch 1998; Buras et al. 2005). Das Modell eignet sich daher vermutlich vor allem zur Untersuchung der Pathophysiologie des SIRS, des endotoxischen Schocks oder der Meningokokkensepsis (Fink 2014). Dagegen liegen die Vorteile des Modells in der einfachen Handhabung und in der sehr guten Standardisierbar- und Reproduzierbarkeit. Darüber hinaus waren nach Injektion geringer LPS-Dosen in gesunde und freiwillige Patienten ähnliche pathophysiologische Veränderungen wie bei septischen Patienten nachweisbar (Fink und Heard 1990), was die Relevanz dieses Modells ebenfalls unterstreicht.

2.2.2 Verabreichung von lebenden Pathogenen

Als Alternative zu der Gabe von LPS können lebende Bakterien wie z.B. *E. coli* oder *Pseudomonas aeruginosa* appliziert werden. Dabei spielt es eine wesentliche Rolle, auf welchem Applikationsweg die Pathogene verabreicht werden, welcher Stamm und welche Art verwendet und wie viele Keime wie oft appliziert werden, denn jeder dieser Parameter beeinflusst den Verlauf maßgeblich (Nemzek et al. 2008). Der Vorteil liegt in der einfachen Standardisierbarkeit, wobei anzumerken ist, dass oft eine Immunantwort resultiert, welche jener in Folge einer hohen LPS-Gabe ähnelt (Remick und Ward 2005). Um die Nachteile zu umgehen, wurde das PCI (peritoneal contamination and infection)-Modell entwickelt. Es wird hierbei eine polymikrobielle Peritonitis durch eine intraperitoneale Injektion einer aufbereiteten, mikrobiologisch validierten humanen Stuhlsuspension induziert. Die Stuhlsuspension enthält dabei eine Anzahl verschiedener Bakterien mit (an-)aeroben und gram-positiven/negativen Eigenschaften (Gonnert et al. 2011). Entsprechend ist die Aufbereitung und Charakterisierung der Stuhlsuspension mit einem höheren experimentellen Aufwand verbunden. Vorteilhaft ist an dieser Methode, dass sich, je nach verwendeter Dosierung der Stuhlprobe und Wartezeit nach der Applikation, hochakute bis chronische Verläufe einer Sepsis mit unterschiedlichen Mortalitätsraten induzieren lassen. Außerdem ist eine gute Reproduzierbarkeit gegeben. Nach Gonnert et al. (2011) und Recknagel et al. (2013) stellt sich eine dem klinischen Verlauf beim Menschen ähnlichere systemische Inflammation ein als nach LPS-Applikation. Dennoch ist das Modell sehr jung und bedarf weiterer Untersuchungen, Validierungen und Charakterisierungen.

2.2.3 Chirurgische Methoden

Chirurgische Modelle haben in den letzten Jahrzehnten an Bedeutung gewonnen, da sie das klinische Bild einer generalisierten Infektion bzw. Sepsis gut abbilden (Stortz et al. 2017). Dabei sind verschiedene Methoden entwickelt worden, wie das Einbringen von Bakterien-imprägnierten Fibrinnetzen oder das Colon-ascendens-stent-peritonitis (CASP)-Modell (Nemzek et al. 2008). Mittlerweile als „Goldstandard“ dient allerdings das CLP-Modell, welches erstmals 1980 von Wichtermann et al. beschrieben wurde (Nemzek et al. 2008). Bei diesem Modell erfolgt eine Ligatur des Darms distal der Ileozaekalklappe. Anschließend wird eine Punktion des Zökums mit einer Kanüle durchgeführt, woraufhin Stuhl in den Peritonealraum austritt (Abb. 1). Hierbei kann die Schwere der Infektion mittels der Kanülengröße und der Anzahl der Punktionen variiert werden. Je dicker die verwendete Kanüle und je zahlreicher die Punktionen, desto mehr Darminhalt tritt aus. Ähnlich wie beim CASP-Modell kommt es zu einer abdominellen Sepsis mit einer Mischinfektion (Wichterman et al. 1980; Buras et al. 2005). Das Modell stellt den klinischen Verlauf gut dar, indem es die dynamischen Veränderungen der Herz-Kreislauf-Funktion wie beim septischen Patienten nachbildet und eine protrahierte Freisetzung von proinflammatorischen Mediatoren hervorruft (Nemzek et al. 2008). Die Nachteile dieses Modells bestehen vor allem in einer relativ schlechten Quantifizierbarkeit der exakten Menge des ausgetretenen Stuhls, der Reproduzierbarkeit und der Art der sepsisauslösenden Mikroorganismen, die aus dem Darmlumen in die Bauchhöhle übertreten (Buras et al. 2005; Gonnert et al. 2011; Stortz et al. 2017).

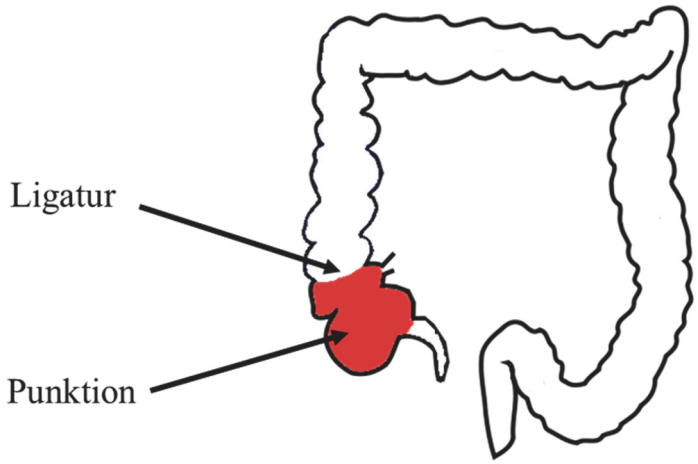

Abb.1: Schematische Darstellung des CLP Modells. Das Zaekum (rot markiert) wird ligiert und anschließend mit einer Kanüle punktiert (https://upload.wikimedia.org/wikipedia/commons/f/fa/Cieco(anatomia).png)

2.3 Der Chemokinrezeptor CXCR4 und sein Ligand CXCL12

2.3.1 Definition, Bedeutung und Vorkommen

Chemokine (abgeleitet von **chemo**taktische Zyto**kine**) sind kleine Signalproteine (8-14 kDa), die zur der großen Gruppe der Zytokine gehören (Rossi und Zlotnik 2000). Eine charakteristische strukturelle Gemeinsamkeit dieser Gruppe sind vier konservierte Cysteinreste, welche Disulfidbindungen ausbilden und somit für die jeweilige Tertiärstruktur entscheidend sind. Abhängig von der Lage der ersten beiden Cysteinreste in ihrer Proteinsequenz können sie in vier Unterklassen eingeordnet werden: die C-, C-C-, C-X-C- und C-X3-C-Chemokine, wobei das C für das jeweilige Cystein und das X für eine beliebige andere Aminosäure steht (Meiron et al. 2008). Ein sehr relevantes und gut erforschtes Chemokin, stellt das C-X-C-Motiv-Chemokin 12 dar (CXCL12, wobei L für Ligand steht). Es ist auch unter dem Namen SDF-1 (stromal cell-derived factor-1) bekannt und ist der Klasse der C-X-C-Chemokine zuzuordnen. CXCL12 wird in hoher Konzentration im Knochenmark produziert und dient hier der Rekrutierung und Verankerung von hämatopoetischen Stammzellen. Freigesetzt wird es darüber hinaus vor allem in der Lunge, in der Milz und in der Leber. Beeindruckend ist das ubiquitäre Vorkommen des Chemokins. Es lässt sich nachweisen im Knochenmark, in Lymphknoten, Leber, Lunge, Gehirn, Herz, Niere, Thymus, Magen, Bauchspeicheldrüse, Milz, Eierstock und Dünndarm (Juarez et al. 2004). CXCL12 vermittelt seine Effekte vor allem durch die Bindung an und die Aktivierung des Chemokinrezeptors CXCR4. Dieser ist ebenfalls im Organismus weit verbreitet. Neutrophile Granulozyten, Monozyten, B- und T-Lymphozyten, hämatopoetische Vorläuferzellen, dendritische Zellen, und Makrophagen tragen den Rezeptor (Nagasawa et al. 1999; Nagase et al. 2002). Darüber hinaus besitzen Zellen des Blutgefäß-Endothels, des Zentralnervensystems und des Magen-Darm-Trakts diesen Chemokinrezeptor. Neben dem CXCR4 bindet CXCL12 auch an den CXC-Motiv-Chemokinrezeptor 7 (CXCR7), wobei die physiologische Rolle des Rezeptors kontrovers diskutiert wird. Unter anderem wird eine Funktion als Chemokin-Fänger oder Chemokin-Speicher vermutet, aufgrund der fehlenden Aktivierung klassischer Signaltransduktionswege G-Protein-gekoppelter Rezeptoren (Thelen und Thelen 2008). Durch die Interaktion des CXCL12 mit seinen Rezeptoren wird eine Vielzahl sowohl physiologischer als auch pathophysiologischer Prozesse gesteuert. Als chemotaktisch wirkendes Zytokin hat es physiologisch eine Schlüsselfunktion bei der Mobilisierung und Wanderung von Stammzellen in Speicher- (wie z.B. Knochenmark) und Zielkompartimente (Ishii et al. 1999; Werner et al. 2013). Entsprechend ist die CXCR4-CXCL12-Achse in der Organogenese und Wundheilung von immenser Bedeutung. CXCR4-defiziente Mäuse zeigen

zahlreiche Defekte, vor allem in der Leukozytengenerierung und Hämatopoese, welche sich in schweren Organschäden, vor allem an Herz und Hirn, manifestieren. Ein Überleben ist deutlich erschwert (Ma et al. 1998). Die physiologische Bedeutung des Rezeptors ist darüber hinaus darin erkennbar, dass sich eine heterozygote Mutation im CXCR4-Gen (in der Region 2q21) im sogenannten Warzen-Hypogammaglobulinämie-Immundefizienz-Myelokathexis (WHIM)-Syndrom äußert (Hernandez et al. 2003). Ferner lässt sich eine Beteiligung am Wachstum und an der Metastasierung von Tumoren nachweisen, da viele Tumorzellen CXCR4-positiv sind und somit CXCL12 auch eine chemotaktische Wirkung auf die meisten Tumorzellen ausübt (Teicher und Fricker 2010). Zusätzlich fungiert der CXCR4 als Co-Rezeptor bei der Infektion von CD4-positiven T-Zellen mit HI-Viren. So konnte für CXCL12 eine hemmende Wirkung auf die Infektion der Zielzellen durch diese Viren nachgewiesen werden, welche auf eine CXCL12-induzierte Internalisierung des Rezeptors CXCR4 zurückgeführt wird (Bleul et al. 1996).

Längere Zeit galt CXCL12 als der einzige natürliche Ligand des CXCR4. Neuere Studien zeigen allerdings, dass auch Ubiquitin (Saini et al. 2010) und das Zytokin Makrophagenmigrationsinhibierender Faktor (MIF) (Bernhagen et al. 2007) in der Lage sind, den Rezeptor zu aktiveren.

2.3.2 Über den CXCR4 vermittelte Signalwege

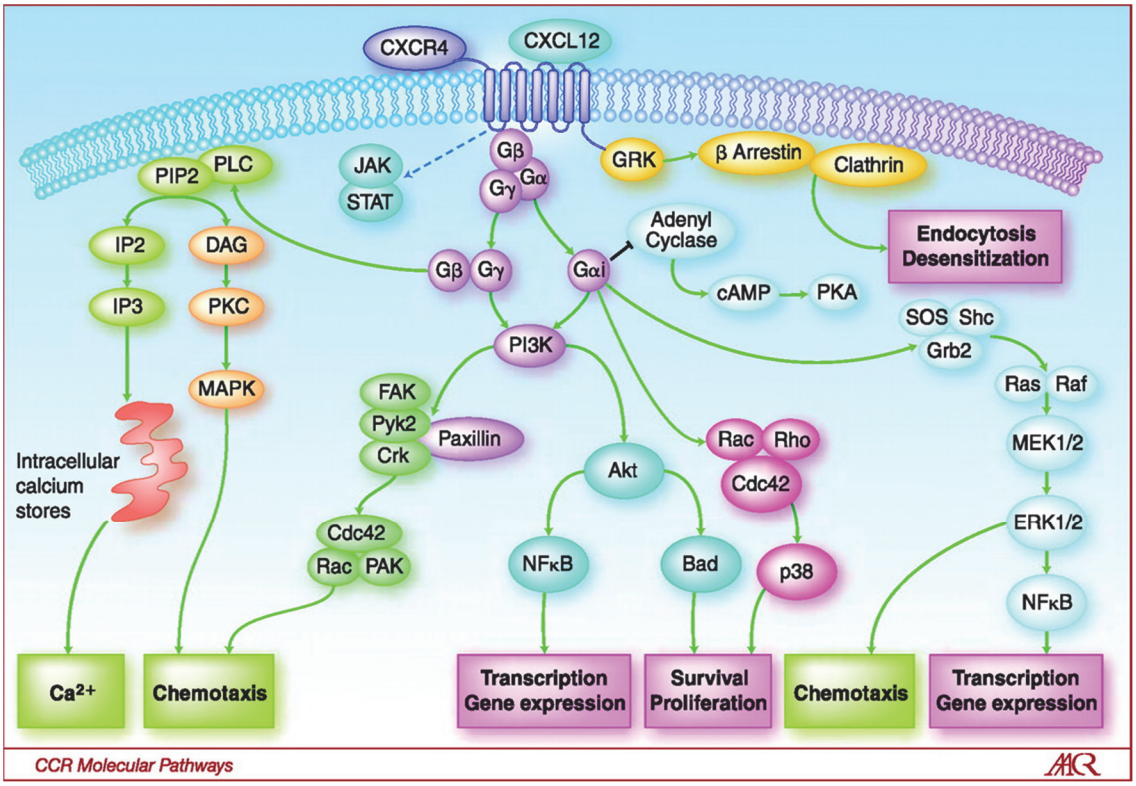

Abb.2: Schematische Darstellung möglicher Signalwege nach CXCR4-Aktivierung.

Die Bindung des CXCL12 an den CXCR4 initiiert verschiedene Signalwege, die sich unter anderem in Chemotaxis, Zellproliferation- und überleben, erhöhten intrazellulären Calciumspiegeln oder in einer verstärkten Transkription und Expression von Genen äußern (Abb. 2). Die genauen Signalwege sind mitunter gewebeabhängig und variieren zwischen den Zelltypen (Teicher und Fricker 2010).

Die CXCL12-Bindung an den CXCR4 erfolgt in zwei Schritten (Crump et al. 1997), was zu einer Konformationsänderung des Rezeptors und zu seiner Aktivierung führt. Der Rezeptor koppelt an ein G_i-Protein, was unter anderem in einer Hemmung der Adenylatzyklase und letztlich in der Aktivierung der Proteinkinase A (PKA) resultiert. Diese nimmt eine wesentliche Rolle in der Regulation des Energiestoffwechsels ein. Zusätzlich werden über die PKA spezielle Transkriptionsfaktoren aktiviert, wie das sogenannte cAMP-responsive element-binding protein (CREB). Durch einen Co-Aktivator (CREB-binding protein) wird die Transkription von Zielgenen ermöglicht, die über ein cAMP-Antwortelement (cAMP responsive element) verfügen.

Ferner wird die Phospholipase C stimuliert, welche über die sekundären Botenstoffe Inositoltrisphosphat (IP3) und Diacylglycerin (DAG) die intrazelluläre Konzentration von freien Ca^{2+}-Ionen erhöht und damit eine Reihe von Proteinkinasen aktiviert (Teicher und Fricker 2010). Außerdem wird die MAP-Kinase (mitogen-activated protein)-Kaskade und der Phosphoinositid-3-Kinase (PI3K)-Signalweg aktiviert, welche beide vor allem migratorische Prozesse sowie die Transkription und Expression von Genen initiieren.

Darüber hinaus kommt es nach der CXCR4-Aktivierung zu Phosphorylierungen an verschiedenen Stellen des C-Terminus des Rezeptors. Die Phosphorylierung wird von β-Arrestin erkannt und es erfolgt eine Internalisierung des CXCR4, woraufhin der Rezeptor lysosomal abgebaut wird oder zurück an die Plasmamembran gelangt (Busillo und Benovic 2007).

2.3.3 CXCR4 und seine Liganden in der Entzündung

Dass dem Rezeptor und seinem Liganden eine Schlüsselrolle in entzündlichen, infektiösen und immunologischen Erkrankungen zukommen könnte, zeigt das bereits beschriebene vielseitige Auftreten des Rezeptors. Ebenso konnten Triantafilou et al. nachweisen, dass der Chemokinrezeptor Teil des LPS-Erkennungsapparats ist und somit in die Aktivierung der LPS-Signaltransduktionskaskade eingreifen kann (Triantafilou et al. 2008). Ferner konnte ein Zusammenhang zwischen erhöhten CXCR4- und CXCL12-Werten im Serum und einer schwerer verlaufenden neonatalen Sepsis nachgewiesen werden (Tunc et al. 2015).

Entsprechend finden sich in der Literatur Beispiele für die Beteiligung der CXCR4-CXCL12-Achse im Entzündungsgeschehen. So führte eine erhöhte Expression von CXCL12 in entzündeten Gelenken von Patienten mit rheumatoider Arthritis zu einer Verschlechterung des Krankheitsbildes. Hier kam es sehr wahrscheinlich durch die erhöhten CXCL12-Spiegel zu einer verstärkten Rekrutierung von CXCR4-positiven Immunzellen (vorwiegend neutrophile Granulozyten, T-Zellen) in die Gelenke, was die inflammatorische Reaktion forcierte (Hansen et al. 2006). Entsprechend führte die Behandlung mittels eines gegen den Rezeptor gerichteten selektiven Peptids zu einer signifikanten Verbesserung des entzündlichen Geschehens (Tamamura et al. 2004). Bestätigt wurden diese Ergebnisse bei der Lungenentzündung bei Mensch und Maus. Hier wurde ebenfalls aufgrund einer erhöhten CXCL12-Expression im Lungengewebe eine verstärkte Einwanderung von CXCR4-positiven Zellen vom Knochenmark in die Lunge festgestellt. Analog konnte hier eine Blockade des

Rezeptors mit dem nicht-peptidischen Antagonisten AMD3100 die Entzündung unterdrücken (Gonzalo et al. 2000; Lukacs et al. 2002). Ähnliche Ergebnisse konnten bei weiteren entzündlichen Erkrankungen wie Colitis ulcerosa (Mikami et al. 2008), Lupus erythematodes (Wang et al. 2009) oder Multipler Sklerose (Calderon et al. 2006) erzielt werden. Der genaue Mechanismus der protektiven Wirkung durch den Antagonismus am CXCR4 konnte nicht vollständig geklärt werden. Dennoch gilt die Hypothese der Unterdrückung einer massiven Einwanderung von immunkompetenten und CXCR4-positiven Zellen, in Verbindung mit einer geringeren Ausschüttung proinflammatorischer Zytokine, als wahrscheinlich (Gonzalo et al. 2000; Lukacs et al. 2002; Hansen et al. 2006). Darüber hinaus wurde ein direkter Einfluss auf die Produktion von IL-6 festgestellt. Die Stimulation von Microglia und von Fibroblasten mit CXCL12 führte zu einer erhöhten IL-6-Freisetzung (Lu et al. 2009; Chen et al. 2011), was in der Leber den stärksten Stimulus zur Bildung und Sekretion von Akute-Phase-Proteinen darstellt.

Im Gegensatz dazu scheint die Aktivierung des CXCR4 bei akuten Erkrankungen wie Polytrauma oder Sepsis einen protektiven Einfluss zu haben. Eine Behandlung mit verschiedenen CXCL12-Analoga führte zu einem verbesserten Überleben, wobei die Hintergründe für diese Beobachtungen unklar blieben (Bach et al. 2012; Fan et al. 2012). Ebenso zeigte sich nach LPS-Applikation in Kombination mit AMD3100 im Zebrafisch eine erhöhte Sterberate, wobei hier ebenfalls die zugrundeliegenden Mechanismen nicht weiter hinterfragt wurden (Novoa et al. 2009).

3 Ziele der Arbeit

In der vorliegenden Arbeit stand der Einfluss der CXCR4-CXCL12-Achse auf eine schwere systemische inflammatorische Reaktion im Mittelpunkt. Insgesamt gliederte sich die Arbeit dabei in drei Teile. In **Manuskript I** wurde in einer der eigentlichen Untersuchung vorgeschalteten Studie zunächst geprüft, welches Tiermodell sich am besten dazu eignet, das antiinflammatorische und protektive Potential einer Substanz zu testen, welche (patho-) physiologischen Parameter sinnvollerweise hierzu herangezogen werden könnten und welcher Messzeitpunkt für die geplanten nachfolgenden Untersuchungen gewählt werden sollte. Ferner stand die Veränderung der CXCR4- und CXCL12-Expressionsmuster während der systemischen Entzündung im Fokus, woraus bereits eine mögliche Relevanz der Achse für den Krankheitsverlauf in der systemischen Inflammation abgeleitet werden sollte.

In **Manuskript II** wurde mit dem CXCR4-Antagonisten AMD3100 der Einfluss einer Hemmung der CXCR4-CXCL12-Achse in der systemischen Inflammation untersucht. Hierbei waren sowohl die systemischen Auswirkungen auf den Gesundheitszustand der Tiere von besonderem Interesse als auch die Folgen für die Organfunktionen, speziell von Leber und Milz als zwei zentrale Organe der Immunreaktion. Ferner stand die Untersuchung von pathophysiologischen Mechanismen wie die Veränderungen im Blutbild, die Expression von verschiedenen Zytokinen und die Einwanderung von Immunzellen, wie Neutrophile und Lymphozyten, in die Leber und Milz im Vordergrund.

Aufgrund der in Manuskript II beobachteten nachteiligen Effekte einer CXCR4-Blockade, sollte in **Manuskript III** geklärt werden, ob dagegen eine Aktivierung der CXCR4-CXCL12-Achse die systemische Inflammation verbessert und ob damit die Ergebnisse aus Manuskript II indirekt bestätigt werden können. Dabei waren ebenfalls der Gesundheitszustand der Mäuse, die systemischen Folgen und die Auswirkungen auf die Organfunktionen, insbesondere von Leber und Milz, von Interesse. Weiterhin sollte versucht werden, anhand der festgestellten Effekte einen Rückschluss auf mögliche Mechanismen zu ziehen, über welche die protektive Wirkung einer CXCR4-Aktivierung vermittelt wird.

4 Manuskripte

4.1 Manuskript I: Comprehensive comparison of the systemic effects and the influence on organ functions in three different animal models of systemic inflammation

Journal of Biomedical Science. 2017 Aug 24;24(1):60. DOI: 10.1186/s12929-017-0370-8.

Semjon Seemann, Franziska Zohles, Amelie Lupp

Status:

Eingereicht am: 27. Juni 2017

Akzeptiert am: 21. August 2017

Veröffentlicht am: 24. August 2017

Autorenschaft:

Erstautor

Beitrag der Autoren:

Semjon Seemann und Amelie Lupp haben das Projekt entwickelt, die Experimente durchgeführt, die Daten ausgewertet und das finale Manuskript geschrieben. Franziska Zohles führte ebenfalls Experimente durch. Amelie Lupp stellte darüber hinaus die Reagenzien und die analytischen Werkzeuge zur Verfügung.

Zusammenfassung

Um eine systemische Entzündung beim Menschen nachzuahmen, wurden verschiedene Tiermodelle entwickelt, welche jedoch aufgrund ihrer jeweiligen Stärken und Schwächen kontrovers diskutiert werden. In **Manuskript I** sollten deshalb die in der Forschung am weitest verbreiteten Tiermodelle einer systemischen Inflammation hinsichtlich der systemischen Effekte, des Einflusses auf die Organfunktionen und der zugrundeliegenden pathophysiologischen Prozesse untersucht werden. Die systemische Entzündung wurde in Mäusen mittels der LPS-, PCI- oder CLP-Methode induziert. Parameter wie der Gesundheitszustand der Tiere, die Körpertemperatur, die Blutglukosespiegel und die Konzentration verschiedener Zytokine wurden im Vergleich zu unbehandelten Kontrolltieren nach 2, 4, 6, 12, 24, 48 und 72 Stunden bestimmt. Zusätzlich wurden der oxidative Stress in verschiedenen Organen und als Leberfunktionsparameter der Glykogengehalt und die Biotransformationskapazität der Leber untersucht. Ferner wurden die Expression des TNF-alpha, des antioxidativ wirksamen Enzyms HO-1, des apoptotischen Schlüsselenzyms Cleaved Caspase-3 sowie verschiedene Immunzellmarker zur genaueren Charakterisierung der eingewanderten Immunzellen im Leber- und Milzgewebe mittels Immunhistochemie beurteilt. Die Ergebnisse zeigten, dass die LPS- und die PCI-Methode zu einem zeitlich ähnlichen Verlauf führte, wobei die LPS-Gabe eine stärkere Immunreaktion auslöste. In beiden Modellen kam es zu einer raschen Erhöhung der Serum-Zytokinspiegel, während der Blutglukosegehalt sank. In den Organen zeigte sich ein vermehrter oxidativer Stress und vor allem in der Milz eine deutlich erhöhte Apoptoserate. Weiterhin waren als Zeichen der Funktionseinschränkung der Lebern der Glykogengehalt und die Biotransformationskapazität stark reduziert. Zusätzlich zeigte sich eine ausgeprägte Einwanderung von Lymphozyten und Neutrophilen in die Lebern und Milzen. In den ersten 24 Stunden fanden sich bei allen Tieren in der Milz zahlreiche phagozytierte CXCR4-positive Zellen in der weißen Pulpa, wohingegen nach 72 Stunden viele immigrierte Leukozyten in der roten Pulpa zu erkennen waren. In der überwiegenden Mehrzahl der Fälle waren die Effekte nach CLP-Operation weniger stark ausgeprägt und es wurde ein verzögerter Verlauf der Entzündung festgestellt.

Zusammenfassend erwies sich das LPS-Modell am besten dazu geeignet, die Auswirkungen neuer Therapieansätze auf akute systemische Entzündungsprozesse zu untersuchen. Die Effekte waren deutlich ausgeprägt und es zeigte sich eine nur geringe Variabilität zwischen den individuellen Tieren. Ferner fanden sich die deutlichsten Veränderungen in den meisten Parametern nach 24 Stunden, weshalb der zeitliche Endpunkt für die nachfolgenden

Untersuchungen auf diesen Zeithorizont festgelegt wurde. Ebenso legen die vermehrte CXCR4-Expression sowie das veränderte CXCR4-Expressionsmuster in der Milz in allen Modellen wichtige Rolle des Rezeptors im Verlauf des Entzündungsgeschehens nahe.

Seemann *et al. Journal of Biomedical Science* (2017) 24:60
DOI 10.1186/s12929-017-0370-8

Journal of Biomedical Science

科 技 部 Ministry of Science and Technology
The cost of publication in *Journal of Biomedical Science* is borne by the Ministry of Science and Technology, Taiwan.

RESEARCH Open Access

Comprehensive comparison of three different animal models for systemic inflammation

Semjon Seemann*, Franziska Zohles and Amelie Lupp

Abstract

Background: To mimic systemic inflammation in humans, different animal models have been developed. Since these models are still discussed controversially, we aimed to comparatively evaluate the most widely used models with respect to the systemic effects, the influence on organ functions and to the underlying pathophysiological processes.

Methods: Systemic inflammation was induced in C57BL/6N mice with lipopolysaccharide (LPS) treatment, peritoneal contamination and infection (PCI), or cecal ligation and puncture (CLP). Blood glucose and circulating cytokine levels were evaluated at 0, 2, 4, 6, 12, 24, 48, and 72 h after induction of inflammation. Additionally, oxidative stress in various organs and liver biotransformation capacity were determined. Markers for oxidative stress, apoptosis, infiltrating immune cells, as well as cytokine expression patterns, were assessed in liver and spleen tissue by immunohistochemistry.

Results: Treating mice with LPS and PCI induced a very similar course of inflammation; however, LPS treatment elicited a stronger response. In both models, serum pro-inflammatory cytokine levels rapidly increased whereas blood glucose decreased. Organs showed early signs of oxidative stress, and apoptosis was increased in splenic cells. In addition, liver biotransformation capacity was reduced and there was pronounced immune cell infiltration in both the liver and spleen. Mice exposed to either LPS or PCI recovered after 72 h. In contrast, CLP treatment induced comparatively fewer effects, but a more protracted course of inflammation.

Conclusions: The LPS model of systemic inflammation revealed to be most suitable when being interested in the impact of new therapies for acute inflammation. When using the CLP model to mimic human sepsis more closely, a longer time course should be employed, as the treatment induces delayed development of systemic inflammation.

Keywords: LPS, PCI, CLP, Systemic inflammation, Oxidative stress, Cytokines

Background

Sepsis remains a significant clinical challenge in intensive care units, as it frequently results in multi-organ dysfunction and high morbidity, leading to mortality rates of approximately 50% [1]. Although there are well established strategies aimed at treating the underlying infection, the development of new therapeutic options and identification of potential drug candidates are urgently needed to prevent and combat sepsis. For these purposes, animal models can be very useful. To mimic the course of human sepsis, various rodent models have been developed. These models can be classified into three major types: exogenous administration of endotoxin [lipopolysaccharide (LPS) treatment], exogenous administration of viable pathogens [inoculation with *Escherichia coli*], and disruption of the endogenous protective barrier [cecal ligation and puncture model (CLP)] [2]. All three models have advantages and disadvantages and it is still controversial as to which of these animal models is most suitable.

The LPS animal model has several essential advantages, including technical ease and high reproducibility, particularly in the inflammatory response elicited. Shortly after LPS administration, high levels of pro-inflammatory cytokines are released and can be measured in circulating serum [3]. This leads to rapid development of systemic inflammatory response syndrome (SIRS) and subsequent

* Correspondence: semjon.seemann@yahoo.com
Institute of Pharmacology and Toxicology, Jena University Hospital, Friedrich Schiller University Jena, Drackendorfer Str. 1, 07747 Jena, Germany

dose-dependent mortality [2, 4]. However, the LPS model does not exactly reproduce the characteristic features of human sepsis, with earlier and greater cytokine responses, that are shorter in duration than in humans [5, 6]. In total, the existing data suggest that LPS can be used to study the pathophysiological processes of endotoxemia or SIRS and as a model of endotoxic shock, but not of sepsis in general [5].

To compensate for the weaknesses of the LPS model, a polymicrobial sepsis model was developed. In the peritoneal contamination and infection model (PCI), stool samples from healthy, non-vegetarian donors, which contain various aerobic and anaerobic gram-positive and gram-negative bacteria, are prepared and administered intraperitoneally. Each stool sample preparation has to be microbiologically characterized, which increases the experimental effort for this model [7]. However, the advantages of this model are high reproducibility, the more or less technical ease, and induction of polymicrobial sepsis. The authors claim that the course of systemic inflammation in the PCI model is more similar to that in humans, compared to the LPS model; however, there are only a few studies published thus far on this model [4, 7]. In addition, the relevance of the PCI model to clinical sepsis is questionable, as patients rarely have massive bacteremia [5, 8] and a single application of a high dose of bacteria causes effects close to those observed after the intravenous injection of a high dose of LPS. The clinical course runs quickly – a hypodynamic circulatory state and violent rise of serum cytokine levels are observed –, and in the absence of adequate resuscitation, the outcome is early death [9].

The most widely used sepsis model is the cecal ligation and puncture (CLP) model, which is recognized to have significant compatibility to human sepsis [10, 11]. The main advantage of the CLP model is that the peritoneum is inoculated with mixed microbial flora from the animal itself through association with devitalized tissue. After CLP induction, immune, hemodynamic, and biochemical responses similar to human sepsis are produced [12]. However, the CLP model also has disadvantages. The amount of bowel leakage is difficult to control and thus, there is a wide range of variation in the sepsis outcomes. Therefore, the CLP model is not as easy to standardize as either the LPS or PCI models. Furthermore, the intestinal flora is not uniform between animals or species and comparisons between studies should be made with caution. Additionally, variations in surgical procedures and postoperative care should also be taken into account when comparing studies. For example, the position of the suture, the size of the needle, and the number of punctures can have a huge impact on the amount of pro-inflammatory cytokines released into the peritoneum and serum and on the course of the disease [13, 14].

As comprehensive comparative data on these three models are still lacking, the present study aims to thoroughly characterize the LPS, PCI, and CLP mice models over 72 h, covering the acute phase of systemic inflammation. For this purpose, a mid-grade systemic inflammation was induced which does not cause acute lethality. Thus, there was no need to perform any antibiotic treatment or fluid resuscitation of the animals, which allowed us to investigate the natural course of the disease. The systemic immune response was evaluated by measuring serum cytokine concentrations, determining parameters of oxidative stress in various organs, and tracking immune cell emigration and immigration in spleen and liver. Liver function is critical for overall patient outcome, even more than kidney and lung function [15, 16]. Therefore, liver function parameters were also determined.

All in all, this is the first study to directly and comprehensively compare these three animal models over a time period of 72 h using non-lethal methods to investigate the systemic impact and influence on organ function resulting from exposure to inflammation. As enough data already exist comparing the animal models with the clinical course in sepsis [7, 8, 10, 17, 18], we primarily did not intend to refer our results to the situation in humans. The goal of this study was to gain a better understanding of the pathophysiological processes involved in these animal models to help researchers choose the most suitable model and to determine which parameters are useful in each model when evaluating therapeutic candidates for systemic inflammation.

Methods

Animals and experimental procedure

The study was conducted under the license of the Thuringian Animal Protection Committee (approval number: 02–044/14). The principles of laboratory animal care and the German Law on the Protection of Animals, as well as the Directive 2010/63/EU were followed. Male adult C57BL/6N mice (12-weeks-old, body weight 25–30 g; Charles River Laboratories, Sulzfeld, Germany) were used, and the animals were housed in plastic cages under standardized conditions (light-dark cycle 12/12 h, temperature 22 ± 2 °C, humidity 50 ± 10%, pellet diet Altromin 1316, water ad libitum). Mice were treated with either lipopolysaccharides [LPS] (*Escherichia coli* 0111:B4; Sigma Aldrich, Steinheim, Germany; 5 mg/kg body weight, dissolved in 0.1 ml/10 g body weight PBS), peritoneal contamination and infection [PCI] or cecal ligation and puncture [CLP] and sacrificed as described below after 2, 4, 6, 12, 24, 48 and 72 h. At the beginning of the experiment (t = 0), four control mice per treatment group were sacrificed as described. These mice did not receive any treatment. The most appropriate non-lethal LPS dose was determined in several previous (pilot) studies [19]. Polymicrobial sepsis was induced by PCI and the PCI stool batch was standardized, microbiologically validated [7] and kindly donated by apl. Prof. Dr. Ralf A. Claus,

Center for Sepsis Control and Care, Jena University Hospital, Jena, Germany. Mice received 1.5 μl/g body weight of the stool batch, dissolved in 0.1 ml/10 g body weight PBS, intraperitoneally, representing a non-lethal dose based on previous data [4, 7]. CLP was performed as previously described [20]. Briefly, anesthesia was induced with isoflurane and after the opening of the abdominal cavity through a midline incision along the linea alba, the cecum was identified, exposed and ligated with a nonabsorbable suture at half the distance between distal pole and the base of the cecum. Subsequently, the cecum was punctured using a 21G needle and gently compressed to extrude a small amount of cecal content. Also here, a mid-grade systemic inflammatory condition was intended. Afterwards, the abdominal cavity was closed again by a double suture. Since we were interested in the natural course of the disease and since we induced a mid-grade systemic inflammation making acute lethality very unlikely, in none of the three animal sepsis models antibiotic therapy or fluid resuscitation was given. To track the course of each animal model, investigations were performed at eight different time points. 0 h (which is equivalent to the control group), 2 h, 4 h, 6 h, 12 h, 24 h, 48 h and 72 h after inflammation onset, mice were sacrificed (each n = 4–6 animals per time point). At each time point, body temperatures were measured, and the condition of the animals was assessed using the Clinical Severity Score (CSS), as described previously [7]. The CSS values were assessed hourly and all efforts were made to minimize suffering of the animals. Mice which unexpectedly showed a CSS of 4 during the experimental period (which according to our experimental protocol was defined as humane endpoint) were sacrificed with an overdose of isoflurane, followed by decapitation in order to prevent further suffering. All other mice were sacrificed at the time points indicated with the same method. Brains, kidneys, livers, lungs and spleens were removed, weighed, and either fixed in 10% buffered formaldehyde or snap-frozen in liquid nitrogen for biochemical analysis. After decapitation, mice were bled completely and blood was collected in a tube (S Monovette® 1.2 ml Z Clotting activator/serum, Sarstedt, Nuembrecht, Germany) for clotting. Blood glucose levels were determined using a droplet of the whole blood with a commercially available blood glucose meter and respective test strips (BG star®, Sanofi-Aventis, Frankfurt, Germany). After 30 min, clotted blood was centrifuged at 2000 g for 10 min to obtain serum which was used for ELISA and enzymatic activity measurements. The amount of serum used for the respective assays varied between 20 μl and 50 μl. Animals that did not show any elevated levels of serum cytokines and oxidative stress in the organs were excluded from the experiment in order to make sure to have no resistant mice in the treatment groups. For histological analysis, the formalin-fixed organ samples were embedded in paraffin blocks and cut into 4-μm thin sections (n = 4–6 for each treatment group).

Interleukin (IL)-6, interleukin (IL)-10, tumor necrosis factor (TNF)-α, interferon (IFN)-γ, C-X-C motif chemokine 12 (CXCL12) and alanine aminotransferase (ALAT) assay

To determine the serum levels of IL-6, IL-10, TNF-α, IFN-γ, CXCL12 and ALAT, an IL-6 Mouse ELISA Kit (Thermo Scientific, Rockford, IL, USA), an IL-10 Mouse ELISA Kit (Thermo Scientific, Rockford, IL, USA), a mouse TNF-α Quantikine ELISA kit (R&D Systems, Minneapolis, MN, USA), a mouse IFN-γ ELISA kit (Pierce Biotechnology, Rockford, IL, USA), a mouse CXCL12/SDF-1 alpha Quantikine ELISA Kit (R&D Systems, Minneapolis, MN, USA) and a EnzyChrom™ Alanine Transaminase Assay Kit (BioAssay Systems, Hayward, CA, USA), respectively, were used according to the manufacturer's instructions.

Oxidative status in the tissues

The tissue glutathione content in its reduced (GSH) and oxidized (GSSG) forms was analyzed by homogenizing the samples with 11 volumes of 0.2 M sodium phosphate buffer (5 mM ethylenediaminetetraacetic acid [EDTA]; pH 8.0) and four volumes of 25% metaphosphoric acid. After centrifugation (12,000 g, 4 °C, 30 min), GSH content was measured in the supernatants using a colorimetric assay, as previously described [21]. The GSSG concentration was assessed fluorometrically [22]. To determine the tissue content of lipid peroxides (LPO) as thiobarbituric acid-reactive substances (TBARS), liver samples were homogenized with 19 volumes of ice-cold saline and analyzed fluorometrically, as previously described [23]. Additionally, HO-1 (heme oxygenase 1) activities were measured in the liver 9000 g supernatants (prepared as described under "biotransformation capacity") using hemin as a substrate. The amount of bilirubin formed was determined photometrically and referred to the incubation time and to the protein content of the respective 9000 g supernatants [24].

Biotransformation capacity

To obtain 9000 g supernatants for analysis, livers were homogenized with 0.1 M sodium phosphate buffer (pH 7.4) (1:2 w/v) and subsequently centrifuged at 9000 g for 20 min at 4 °C. The 9000 g supernatants were used to assess the activities of several cytochrome P450 (CYP) enzymes, and the protein content of these fractions was determined using a modified Biuret method [25]. For determination of CYP enzyme activities, the following model reactions were performed: ethoxycoumarin-O-deethylation (ECOD; [26]), ethoxyresorufin-O-deethylation (EROD; [27]), ethylmorphine-N-demethylation (EMND; [28]), meth oxyresorufin-O-demethylation (MROD; [27]), and pento xyresorufin-O-depentylation (PROD; [27]). Glutathione-S-

transferase (GST) activities were determined by photometrically measuring the resulting dinitrobenzene-glutathione conjugate, GS-DNB [29].

Histopathology and immunohistochemistry

Samples for histopathology and immunohistochemistry were prepared by cutting 4-μm sections from the paraffin blocks and floating these onto positively charged slides. Immunostaining was performed by an indirect peroxidase-labeling method, as described previously [30]. Briefly, sections were de-waxed, microwaved in 10 mM citric acid (pH 6.0) for 16 min at 600 W, and incubated with the respective primary antibodies (Table 1) at 4 °C overnight. Detection of the primary antibody was performed using either a biotinylated goat anti-rabbit, a horse anti-mouse, or a rabbit anti-goat IgG, followed by incubation with peroxidase-conjugated avidin (Vector ABC "Elite" kit, Vector, Burlingame, CA, USA). Binding of the primary antibody was visualized using 3-amino-9-ethylcarbazole (AEC) in acetate buffer (BioGenex, San Ramon, CA, USA). The sections were then rinsed, counterstained with Mayer's hematoxylin (Sigma Aldrich, Steinheim, Germany), and mounted in Vectamount™ mounting medium (Vector Laboratories, Burlingame, CA, USA). All immunohistochemical stainings were evaluated by two independent investigators. To detect the liver glycogen content, periodic-acid-Schiff staining (PAS; periodic acid, Schiff's reagent: Sigma Aldrich, Steinheim, Germany) was performed and to obtain an histological overview, hematoxylin and eosin staining (HE) of livers and spleens was done, using standard protocols [31, 32]. Identification of the specific cell types was based on their microscopic features along with the relative location of the cells in the respective tissues.

Statistical analysis

All statistical analyses and figures were computed with GraphPad Prism software, v. 6.0 (GraphPad Software, La Jolla, CA, USA). In all cases, experiments were performed with 4–6 animals per time point of each experimental group. Statistical significance was determined by using the non-parametric Kruskal-Wallis test, followed by the Mann-Whitney U test. Statistical comparisons were made versus the control of each group and are denoted as follows: LPS (asterisk, *), PCI (plus, +), CLP (diamond, #). A p value <0.05 (*,+,#) was considered as statistically significant; a p value <0.01 (**,++,##) and a p value <0.001 (***,+++,###) are further specified. Data are presented as mean ± standard deviation (SD), except for the CSS values, which are presented as medians with interquartile ranges.

Results

Measurements of health status, including blood pressure, body temperature, and body weight, are influenced by LPS, PCI, and CLP treatment

In each animal model we induced a mid-grade, non-lethal, systemic inflammatory condition to investigate the course of the disease. In the CLP model, however, one mouse after 24 h, one after 40 h and one after 70 h, had to be euthanized because of having unexpectedly reached a CSS of 4. Because these animals did not match to the allotted time points, they were not included in the further analyses. Mice receiving LPS or PCI displayed impaired health status, as evidenced by increased clinical severity scores (CSS) compared to controls (Fig. 1a). The maximum values were reached by 6–12 h after induction of infection, followed by a decline to baseline levels. After 48–72 h, there were no detectable differences in CSS values between treated mice and respective control animals. Mice

Table 1 Primary antibodies used for the immunohistochemical investigations

Primary antibody	Type, Catalogue number	Manufacturer	Dilution	Host species
CD3	monoclonal, ab16669	Abcam	1:400	Rabbit
CD8	polyclonal, sc-7188	Santa Cruz Biotechnology	1:200	Rabbit
CD68	monoclonal, ab955	Abcam	1:500	Mouse
cleaved caspase-3	monoclonal, 9661	Cell Signaling Technology	1:600	Rabbit
CXCL12	monoclonal, MAB350	R&D Systems	1:500	Mouse
CXCR4	monoclonal, 3108–1	Epitomics	1:50	Rabbit
CYP3A	polyclonal	Daiichi Pure Chemicals	1:5000	Goat
CYP2B	polyclonal	Daiichi Pure Chemicals	1:5000	Goat
CYP2E1	polyclonal	Daiichi Pure Chemicals	1:5000	Goat
F4/80	monoclonal, MCA497G	Bio-Rad Laboratories	1:200	Rat
heme oxygenase 1	polyclonal, SPA-895	Biomol GmbH	1:5000	Rabbit
iNOS	polyclonal, sc-651	Santa Cruz Biotechnology	1:500	Rabbit
TNF-α	monoclonal, sc-52746	Santa Cruz Biotechnology	1:500	Mouse

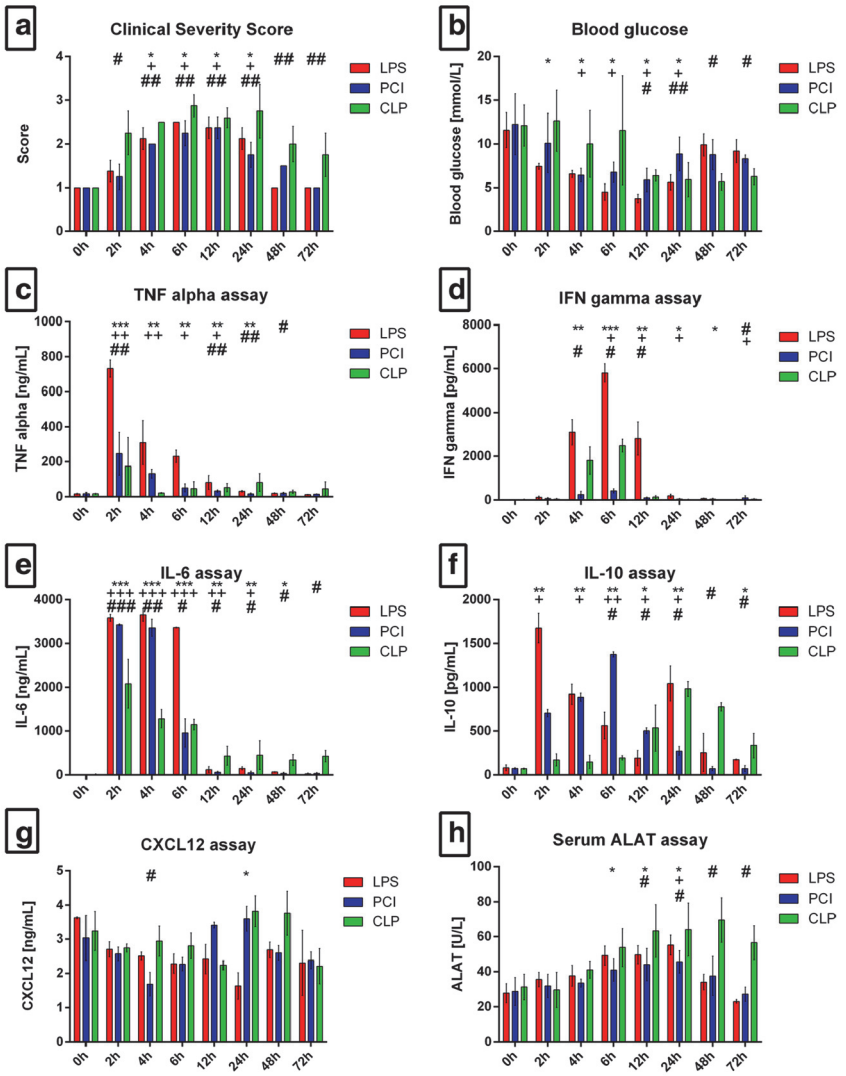

Fig. 1 General condition and systemic parameters. Mice were treated either with LPS, PCI, CLP, or were left untreated (control). 0 h (control), 2 h, 4 h, 6 h, 12 h, 24 h, 48 h and 72 h after inflammation onset, the Clinical Severity Score (**a**) was assessed and the mice were sacrificed. Blood glucose content was determined from whole blood (**b**) and serum was obtained for TNF-α, IFN-γ, IL-6, IL-10, CXCL12 and ALAT measurements (**c-h**). Data are given as mean ± standard deviation (SD) or as median with interquartile ranges (CSS), respectively; $n = 4–6$ for each group and time point. Statistical significance was determined by using the non-parametric Kruskal-Wallis test, followed by pairwise Mann-Whitney U tests. Statistical comparisons were made versus the control of each group and are denoted as follows: LPS (asterisk, *), PCI (plus, +), CLP (diamond, #). A p value <0.05 (*,+,#) was considered statistically significant; a p value <0.01 (**,++,##) and a p value <0.001 (***,+++,###) are further specified

subjected to CLP also exhibited peak CSS values after 6–12 h, but in contrast to the other two groups of animals the values remained elevated up to 72 h, indicating a protracted course of the disease without recovery (Fig. 1a).

Blood pressure and heart rate changes are of vital importance during systemic inflammation. Therefore, these parameters were measured at 24 h in order to get an impression of how these parameters are affected by the different treatment modalities. In all three animal models, blood pressure values decreased (Control: 115 ± 6 mmHg, LPS: 80 ± 8 mmHg, PCI: 90 ± 16 mmHg, CLP: 79 ± 16 mmHg) whereas the average heart rate increased (Control: 446 ± 51 bpm, LPS: 591 ± 33 bpm, PCI: 514 ± 60 bpm, CLP: 554 ± 43 bpm), in comparison to the control groups. However, there were no significant differences between the three animal models (Additional File 1).

Body temperature and weight are also affected during systemic inflammation. LPS, PCI, and CLP treatment

induced a reduction in body temperature as well as body weight in comparison to control mice. Body temperatures largely decreased between 2 and 12 h, with the greatest decrease in the CLP-treated mice (Additional File 1). After 6 h, hypothermia was observed in these animals (CLP: 30.20 ± 4.05 °C vs. control: 37.54 ± 0.50 °C, p = 0.020). The effect of the different treatment modalities on body weight was very similar, as the mice in all three animal models lost weight up to 24 h (vs. control: LPS −2.60 ± 0.78 g, p = 0.03; PCI -1.90 ± 1.48 g, p = 0.20; CLP -2.05 ± 0.90 g, p = 0.02). After 24 h, the PCI- and CLP-treated mice regained weight, whereas the LPS-treated group had still reduced weights in comparison to controls at 48 and 72 h post-treatment (Additional File 1).

Blood glucose, serum cytokine, and liver enzyme levels vary with sepsis model

To further determine the systemic consequences of LPS, PCI, and CLP treatment, we assessed glucose levels in whole blood, as well as inflammatory cytokines levels in serum. As shown in Fig. 1b, LPS- and PCI-treated mice exhibited hypoglycemia, which reached its peak 12 h post-infection. After 12 h, blood glucose levels continuously rose, eventually recovering almost to control levels. In the CLP model, hypoglycemia was also seen, but in contrast to the LPS and PCI models, blood sugar levels remained lower up to 72 h post-infection (Fig. 1b).

Inflammatory cytokine serum concentrations varied between the three animal models. LPS administration induced an elevation in tumor necrosis factor (TNF)-α levels by approximately 4500% compared to controls after only 2 h (Fig. 1c). In contrast, PCI and CLP treatment raised TNF-α concentrations only by approximately 1500% and 1000%, respectively, when compared to the controls. The further the course of the disease, the less TNF-α was measured. However, the CLP group exhibited elevated TNF-α serum levels at later time points (Fig. 1c). Similar as with TNF-α, LPS treatment had the strongest effect on serum interferon (IFN)-γ levels compared to the other models (Fig. 1d). Markedly increased levels were measured after 4, 6, and 12 h (to approximately 25,000%, 45,000%, and 22,000%, respectively) compared to control values. Whereas CLP treatment resulted in moderate increases in IFN-γ, PCI administration showed almost no effect on serum IFN-γ concentrations (Fig. 1d). Examining interleukin (IL)-6 concentrations, endotoxin administration led to an early increase in serum IL-6 levels especially at 2, 4, and 6 h post-infection (Fig. 1e). PCI-treated mice showed a similar increase in the serum levels. CLP treatment also resulted in an early elevation of the cytokine, but the increase was less than observed in the LPS or PCI model. However, after CLP treatment elevated IL-6 levels were still detectable later in the course of infection, at 72 h, when IL-6 concentrations were still approximately 5000% higher in comparison to control mice (Fig. 1e).

To investigate compensatory mechanisms, serum IL-10 concentrations were also measured. Here, the three animal models elicited varying results. LPS treatment induced a biphasic IL-10 response, with a large increase after 2 h, followed by a decrease up to 12 h, and a second elevation after 24 h (Fig. 1f). PCI treatment led to a continuous increase in IL-10 levels up to 6 h, followed by a step-by-step reduction, whereas CLP-treated mice showed a monophasic course with higher IL-10 levels at later time points.

As the CXCR4/CXCL12 axis has been shown to be of diagnostic as well as of overall importance in inflammation [19, 33, 34], the amount of serum CXCL12 was assessed. In the LPS-treated mice, CXCL12 levels continuously decreased up to 24 h after inflammation onset, followed by an increase at later time points. PCI treatment, in contrast, induced a biphasic response, with lower levels of CXCL12 after 4 h, and increased levels after 24 h, compared to control. CLP treatment led to elevated serum CXCL12 levels after 24 and 48 h (Fig. 1g).

To determine to what extent liver integrity was influenced by the three treatment modalities, serum alanine transaminase (ALAT) levels were measured. Whereas the LPS and PCI groups exhibited the highest ALAT concentrations after 24 h, CLP treatment led to a continuous increase in ALAT levels past 24 h (Fig. 1h).

LPS, PCI and CLP treatment influence tissue oxidative stress markers differentially

As oxidative stress has a substantial impact on organ function and may serve as a marker for inflammation severity, we next assessed the oxidative status of various organs through quantification of lipid peroxidation products (LPO), as well as both reduced glutathione (GSH) and oxidized glutathione (GSSG) in the brains, kidneys, livers, and lungs of treated and control mice. LPS treatment induced LPO production in brain tissue, starting at 4 h post-exposure. Neither PCI nor CLP treatment affected LPO values to a similar extent (Fig. 2a). However, LPS treatment did not influence glutathione status in the brain, as GSH and GSSG remained at constant levels throughout the course of inflammation. Likewise, PCI did not affect glutathione status. However, the CLP procedure led to decreased GSH/GSSG ratios after 48 and 72 h (Fig. 2b).

In the kidneys, LPS-treated mice exhibited the highest LPO concentrations after 24 h, whereas both PCI and CLP treatment induced maximum values at 6 h post-infection (Fig. 2c). All three treatments led to decreased GSH/GSSH ratios in the kidneys, with significantly reduced ratios at 4–24 h post-infection (Fig. 2d). Total glutathione content increased at later time points after

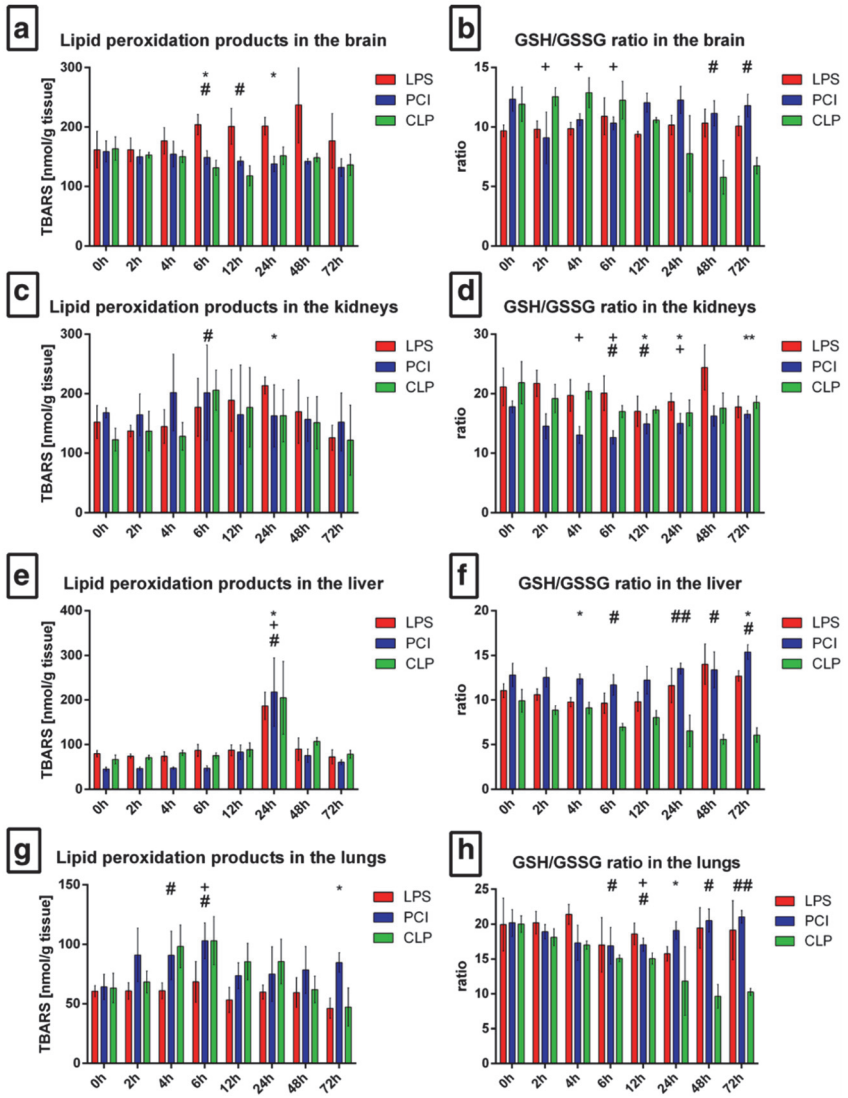

Fig. 2 Oxidative stress in different organs. At the time point indicated, mice were sacrificed and different organs were collected for the analysis of the tissue content of lipid peroxidation products as determined by thiobarbituric acid reactive substances (TBARS) (**a**, **c**, **e, g**). Additionally, the glutathione status was assessed and the GSH/GSSG ratio was calculated (**b**, **d, f, h**). Data are given as mean ± standard deviation (SD), $n = 4–6$ for each group and time point. Statistical significance was determined by using the non-parametric Kruskal-Wallis test, followed by pairwise Mann-Whitney U tests. Statistical comparisons were made versus the control of each group and are denoted as follows: LPS (asterisk, *), PCI (plus, +), CLP (diamond, #). A p value <0.05 (*,+,#) was considered statistically significant; a p value <0.01 (**,++,##) and a p value <0.001 (***,+++,###) are further specified

LPS and PCI treatment, whereas CLP-treated mice showed no differences to the controls (Additional File 2).

In the livers, no difference in LPO response was detectable between the three model groups. At 24 h, LPO levels were increased and then returned to baseline values (Fig. 2e). Glutathione status, in contrast, was diversely affected. Whereas LPS and PCI treatment induced a decrease in the ratio 4–6 h post-infection and an elevation at later time points, CLP treatment led to a step-by-step decrease in the ratio, with minimum values after 48 h (Fig. 2f). All three treatments resulted in lowered total liver glutathione content after 6–24 h. In concordance with other results, total liver glutathione in LPS- and PCI-treated mice increased at later time points, whereas the CLP procedure resulted in reduced levels even after 72 h (Additional File 2).

In the lungs, LPS administration had no effect on LPO values, whereas PCI and CLP treatment induced an increase, with maximal LPO levels observed at 6 h post-infection. The GSH/GSSG ratio in the lungs of the LPS and PCI groups was distinctly lower after 24 h or 12 h, respectively, when compared to controls. Also here, at later time points control values were reached again in the LPS and PCI models, while CLP treatment resulted in a continuous decrease in the lung GSH/GSSG ratio, reaching minimum values at 48 h (Fig. 2g and h).

Since every single mouse exhibited elevated levels of inflammatory cytokines and oxidative stress in various organs, we conclude that no mouse has been resistant to LPS, PCI and CLP treatment, respectively.

Liver function is affected in the three models of systemic inflammation

Because ALAT levels were increased in the serum of all three animal groups, liver function was further examined to gain a better understanding of the underlying processes. Hematoxylin and eosin (H&E) as well as periodic acid-Schiff (PAS) staining were performed to analyze liver tissue sections. H&E staining revealed a massive fat accumulation as well as infiltration of inflammatory cells in the livers of LPS-treated mice after 24 h (Fig. 3c and d). Although PCI- and CLP-treated mice did not show liver fat accumulation (Additional File 2), infiltrating cells were also found. However, the infiltration was less pronounced in comparison to endotoxin treatment.

When determining the liver protein content as a reference for the cytochrome P450 (CYP) model reactions, the turbidity value of each sample was assessed as an approximation of the liver fat content. In agreement with the histological data, turbidity values were increased after LPS treatment at 4–24 h only (Fig. 3c and Additional File 2).

As a measure of the liver glycogen content, PAS staining revealed a similar response in all three animal models. Treatment with LPS, PCI, and CLP led to a distinct loss of glycogen in the livers after 6 h. This effect was still present at 24 h, but levels recovered after 24 h to reach control values by 72 h in all models.

As an additional measure of oxidative stress in the livers, heme oxygenase-1 (HO-1) and inducible nitric oxide synthase (iNOS) expression were determined by immunohistochemistry. Shown in Fig. 3a, Kupffer and pit cells expressed HO-1 to a similar extent in LPS and PCI treatment groups. As the time post-treatment progressed, HO-1 expression increased, with intense expression seen after 72 h. In contrast, after CLP treatment, HO-1 expression was not affected. To substantiate these results, HO-1 activity was measured in liver 9000 g supernatants. As shown in Fig. 3b, as with HO-1 expression, there was an increase in enzyme activity progressing after LPS or PCI treatment, whereas CLP had no impact on HO-1 activity.

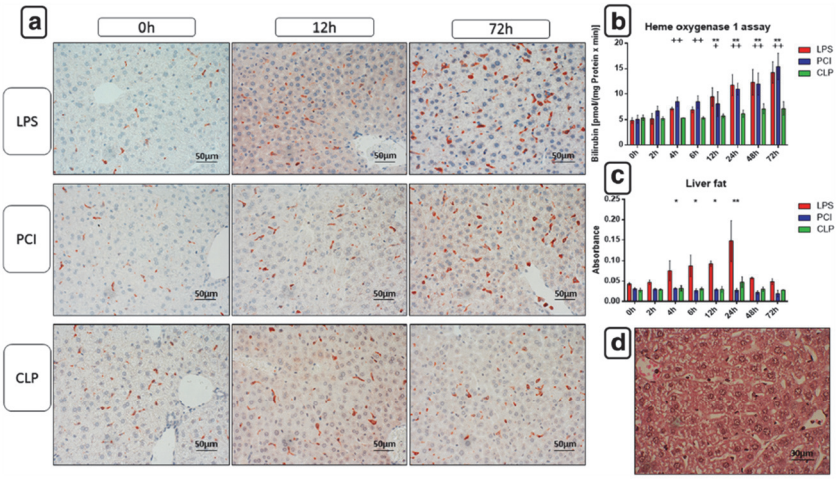

Fig. 3 Heme oxygenase-1 expression and activitiy and total fat content in the livers. At the time point indicated, mice were sacrificed and livers were collected for further biochemical and histological analysis. Representative photomicrographs from one of 4–6 different tissue samples stained for HO-1 expression at 0 h, 24 h and 72 h after LPS, PCI or CLP treatment are shown (immunohistochemistry (red-brown color), counterstaining with hematoxylin, original magnification: (**a**, 400×)). Additionally, HO-1 activities were assessed in the liver 9000 g supernatants of liver homogenates as described in the Materials and Methods section (**b**). As an approximate measurement for the fat content, the turbidity value in the 9000 g supernatants of the livers was determined (**c**) and HE stainings were performed. The photomicrograph in (**d**) shows a representative liver of an endotoxin treated mouse after 24 h, displaying large amounts of fat droplets. Data are given as mean ± standard deviation (SD), $n = 4–6$ for each group and time point. Statistical significance was determined by using the non-parametric Kruskal-Wallis test, followed by pairwise Mann-Whitney U tests. Statistical comparisons were made versus the control of each group and are denoted as follows: LPS (asterisk, *), PCI (plus, +), CLP (diamond, #). A p value <0.05 (*,+,#) was considered statistically significant; a p value <0.01 (**,++,##) and a p value <0.001 (***,+++,###) are further specified

Upon examining iNOS expression, there were no major differences between the LPS and PCI groups; however, the PCI treatment effect was less pronounced than that of LPS (Fig. 4 and Additional File 3). Administration of endotoxin led to an infiltration of iNOS-positive neutrophil granulocytes into the periportal regions of the liver lobules starting at 2 h post-infection. The largest number of infiltrating granulocytes was observed after 12 h and spread throughout the liver lobules. At later time points, few granulocytes were detectable. This effect on neutrophil migration following LPS and PCI treatment exceeded that seen after CLP treatment, where at 6 h only several neutrophils were observed, without further increases as the disease progressed (Fig. 4a, b and Additional File 3).

To gain more insight into the nature of the resident and infiltrating immune cells in the livers, sections were stained for the cell markers, CD68, F4/80, and CD3. CD68-positive cells were scarcely observed in the livers of all three treatment groups, without any significant difference to the controls. In contrast, strong F4/80 expression was seen in Kupffer and pit cells. Especially LPS and PCI challenge led to an intense increase in F4/80 expressing cells after 48 h and 72 h, an effect, which was not as pronounced after CLP treatment (Additional File 2). No observable differences were detected also in CD3 expression between the three treatment groups. Immediately after inflammation initiation, all groups had an increase in CD3+ cells throughout the liver lobules, with the maximum effect seen after 48–72 h. In the periportal regions of the liver lobules, the largest number of CD3+ lymphocytes was detectable. Here, the maximum effect was observed after 72 h.

One central parameter of liver function is its biotransformation capacity. LPS, PCI, and CLP treatment induced a significant and continuous loss in CYP enzyme activity in the liver. Twenty-four hours after infection onset, both endotoxin and PCI models had decreased activity of the CYP families 1A, 2A, 2B, and 2C (ECOD) to approximately 55% of control values, whereas CLP treatment reduced the activities to approximately 65% of controls (Fig. 5a). Similar results were measured with the individual activities of CYP1A (EROD), CYP1A2 (MROD), CYP3A (EMND), and CYP2B (PROD) (Fig. 5b and c). Notably, when treating mice with LPS and PCI, CYP activities returned to control levels after 72 h, whereas after CLP treatment, activities remained consistently reduced at later time points. These results were further confirmed by immunohistochemistry. As shown in Fig. 5d, CYP enzymes were predominantly expressed around the central veins of the liver lobules. At 12–24 h after LPS or PCI treatment, CYP expression was remarkably decreased, but returned to normal levels after 72 h. In contrast, enzyme expression remained diminished for up to 72 h with CLP treatment.

As a representative for phase 2 enzyme activities, glutathione-S-transferase (GST) activity was measured. No differences were detectable between the three treatment groups. In all animal models GST activity continuously declined during the course of the disease and remained significantly diminished at 72 h (Additional File 2).

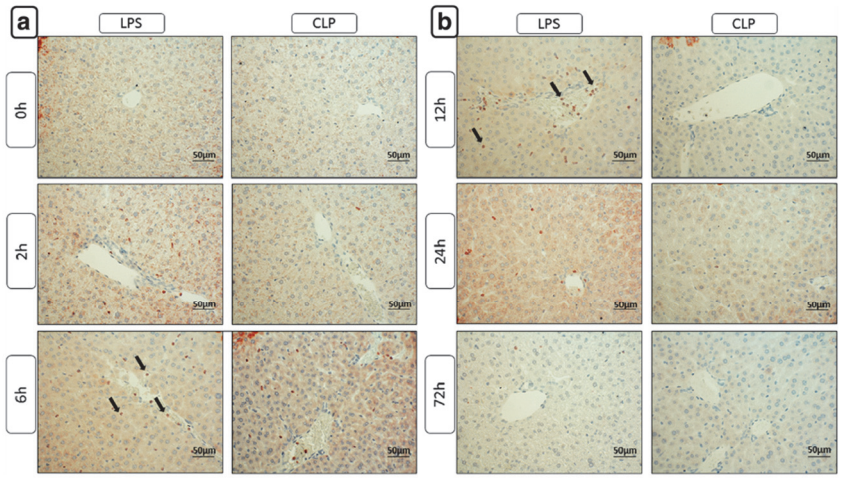

Fig. 4 Immunohistochemical evaluation of iNOS expression. At the time point indicated, mice were sacrificed and the livers were collected for immunohistochemical analysis of iNOS expression (red-brown color, counterstaining with hematoxylin). Representative photomicrographs from one of 4–6 different tissue samples each are shown (original magnification: (**a**, **b**) 400×, arrows are used to exemplarily show iNOS expressing infiltrating neutrophil granulocytes). The time points 0 h, 4 h, 12 h, 24 h and 72 h were chosen as representative time points to show the course. The staining results after PCI treatment are not depicted separately but can be found in the additional file 3 as the course was very similar to that observed after LPS administration, with the only difference, however, that less iNOS positive cells are to be seen

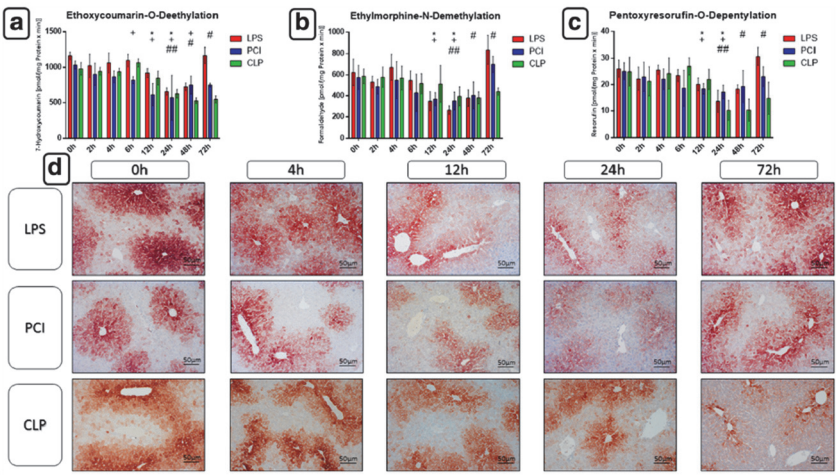

Fig. 5 Biotransformation capacity in the livers. At the time point indicated, mice were sacrificed and the livers were collected for biochemical and histological analysis. Ethoxycoumarin-O-deethylation [ECOD] (**a**), ethylmorphine-N-demethylation [EMND] (**b**) and pentoxyresorufin-O-depentylation [PROD] (**c**) activities in 9000 g supernatants are shown exemplarily. Data are given as mean ± standard deviation (SD), $n = 4–6$ for each group and time point. Statistical significance was determined by using the non-parametric Kruskal-Wallis test, followed by pairwise Mann-Whitney U tests. Statistical comparisons were made versus the control of each group and are denoted as follows: LPS (asterisk, *), PCI (plus, +), CLP (diamond, #). A p value <0.05 (*,+,#) was considered statistically significant; a p value <0.01 (**,++,##) and a p value <0.001 (***,+++,###) are further specified. **d**: CYP 3A2 isoforms expressions in liver tissue as determined by immunohistochemistry (red-brown color, counterstaining with hematoxylin). Representative photomicrographs from one of 4–6 different liver tissue samples are shown (original magnification: 400×). 0 h, 4 h, 12 h, 24 h and 72 h were chosen as representative time points to depict the course

Splenic morphology and histology is influenced differentially in the sepsis models

The spleen functions to clear senescent erythrocytes and maintain a blood reserve, and plays a significant role in the immune system. Therefore, we next investigated its response to the different inflammatory challenge models. LPS and PCI treatments caused a time-dependent splenomegaly. In comparison to controls, LPS and PCI challenge significantly increased splenic weights by approximately 100% and 125%, respectively, after 72 h. CLP treatment, however, did not affect splenic weight (Fig. 6a). Histological examination revealed an increased number of erythrocytes in the red pulp after 4 h, along with mild edema in the LPS and PCI models, whereas the impact of CLP was not that evident (Fig. 6d and Additional File 3). Additionally, iNOS positive neutrophils were detected in the red pulp at 24 h post-LPS administration and post-PCI (Fig. 6e and Additional File 3). After 24 and after 48 h, neutrophils were also detectable in the white pulp of endotoxic mice. However, this infiltration was not observed in the other two animal models.

Splenic oxidative status was also determined by measuring the content of reduced and oxidized glutathione. GSH/GSSG ratios, as well as total glutathione, increased 4 h after LPS or PCI challenge (Fig. 6b and c). At later time points, however, there were no differences observed in total glutathione content, whereas the GSH/GSSG ratio in endotoxin-treated mice was decreased in comparison to controls, indicating higher oxidative stress (Fig. 6b and c).

Apoptosis plays an important role in inflammation. Therefore, we determined the amount and distribution of apoptotic cells by immunohistochemical analysis of the cleaved form of the pro-apoptotic enzyme, caspase-3. As depicted in Fig. 7, the majority of cells expressing cleaved caspase-3 was located in the white pulp. LPS challenge upregulated this expression at 12 and 24 h noticeably, in comparison to controls and the other treatment groups. CLP treatment induced the appearance of tingible body macrophages as soon as 2 h post-treatment, with cleaved caspase-3 expression peaking already after 4–6 h, indicating early apoptotic events.

To compare our previous findings [33] and the serum CXCL12 concentrations of the present investigation with the splenic chemokine expression, splenic sections were stained for CXCR4 and CXCL12. In control animals, CXCR4 was expressed on macrophages and lymphocytes in the red and white pulp, and on lymphocytes in the marginal zone of lymphoid follicles. Early after LPS treatment, CXCR4+ cells were present in the follicles inside tingible body macrophages. Similar observations were made after PCI and CLP treatment, with maximal staining reached at 12–24 h post-infection. After 72 h, endotoxin and PCI treated mice exhibited a large number of CXCR4+ cells in the red pulp, particularly around the vessels, with a similar but less degree of staining seen with CLP treatment (Fig. 8).

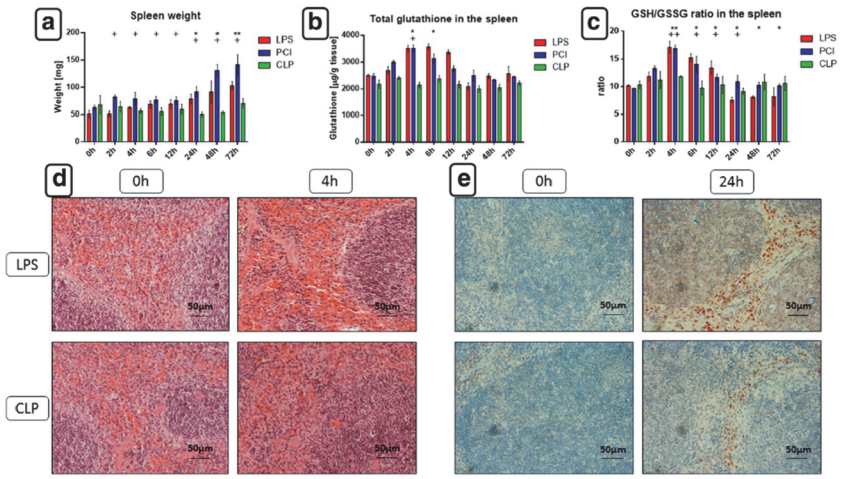

Fig. 6 Spleen weights, glutathione status, histomorphology and iNOS expression in the spleen. At the time point indicated, mice were sacrificed and the spleens were collected for further analysis. (**a**) Spleen weights. (**b, c**) Total glutathione content and GSH/GSSG ratio in the spleen tissue. Data are given as mean ± standard deviation (SD), $n = 4–6$ for each group and time point. Statistical significance was determined by using the non-parametric Kruskal-Wallis test, followed by pairwise Mann-Whitney U tests. Statistical comparisons were made versus the control of each group and are denoted as follows: LPS (asterisk, *), PCI (plus, +), CLP (diamond, #). A p value <0.05 (*,+,#) was considered statistically significant; a p value <0.01 (**,++,##) and a p value <0.001 (***,+++,###) are further specified. (**d**) HE staining showing a large amount of erythrocytes in the red pulp of endotoxic mice after 4 h and a less pronounced effect after CLP. (**e**) iNOS expression in the spleens, 24 h after LPS and CLP treatment (immunohistochemistry [red-brown color], counterstaining with hematoxylin). Representative photomicrographs from one of 4–6 different tissue samples each are shown (original magnification: 400×)

To examine the cell populations having immigrated into the red pulp of the spleens after 72 h in greater detail (remarkable immune cell immigration was only visible after 48–72 h), additional immunohistochemical stainings were performed. Here, the differences between the three treatment groups were secondary to us. However, by using CXCL12 as a marker for immune cells, we observed a significant amount of CXCL12-expressing monocytes in the red pulp 72 h after LPS challenge. PCI and CLP treatment, in contrast, did not induce CXCL12 expression to a similar extent (Fig. 9c). As stated previously, iNOS+ cells were present in the red pulp after 24 h of LPS treatment. Although weaker staining was observed, iNOS+ neutrophils remained after 72 h. Additionally, a distinct set of CD68+, but F4/80-negative cells were found in the red pulp. As depicted in Fig. 9a,

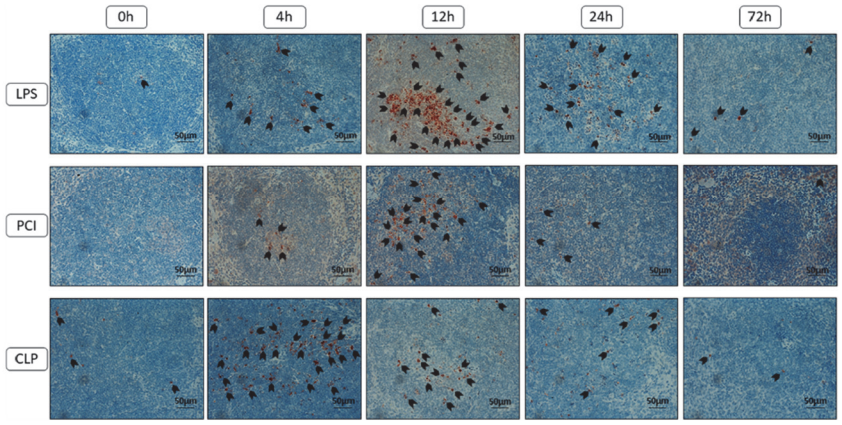

Fig. 7 Cleaved caspase-3 expression in the spleens. At the time point indicated, mice were sacrificed and the spleens were collected for immunohistological analysis. Representative photomicrographs from one of 4–6 different tissue samples stained for cleaved caspase-3 expression are shown (red-brown color, counterstaining with hematoxylin; original magnification: 400×). 0 h, 4 h, 12 h, 24 h and 72 h were chosen as representative time points to depict the course. Furthermore, arrowheads were added to obtain an overview about the amount of cells expressing the enzyme

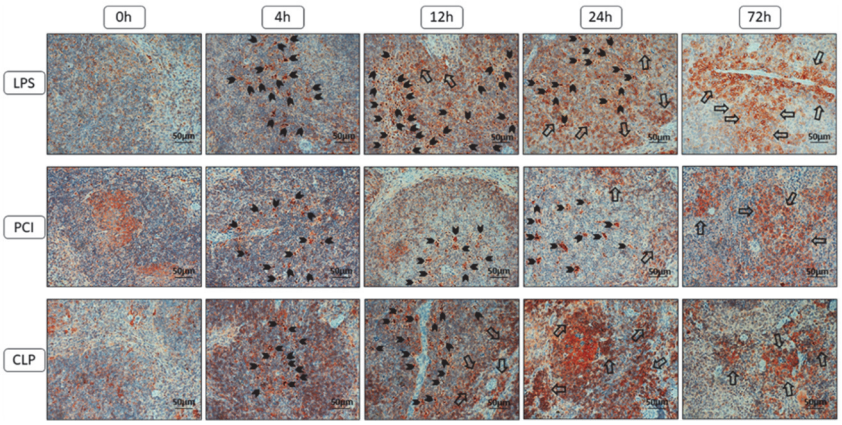

Fig. 8 CXCR4 expression in the spleens. At the time point indicated, mice were sacrificed and the spleens were collected for immunohistological analysis. Representative photomicrographs from one of 4–6 different tissue samples stained for CXCR4 expression are shown (red-brown color, counterstaining with hematoxylin; original magnification: 400×). 0 h, 4 h, 12 h, 24 h and 72 h were chosen as representative time points to depict the course. Additionally, arrowheads were added to mark the CXCR4 positive cells that were engulfed by the tingible body macrophages and larger arrows were used to show the infiltrating immune cells exhibiting membrane-bound CXCR4 expression at later time points

CD68+ cells were also observed in the white pulp of the spleens of LPS-treated mice, but not in the other models. CD8+ cells were observed in both the red and the white pulp 72 h after LPS administration. In spleens of PCI and CLP-treated mice, the red pulp also had CD8 + cells, although to a lesser extent than in LPS-treated animals. Notably, cells in the red pulp were not predominantly CD3+ (Fig. 9b). Finally, TNF-α was strongly expressed in the cell population which had immigrated into the red pulp after 72 h, with more pronounced staining after LPS administration as compared to either PCI or CLP treatment.

Discussion

The objective of this study was to comparatively assess the time courses of different pathophysiological parameters in three commonly used animal sepsis models, LPS, PCI, and CLP. The models showed both similarities as well as distinct differences, with the most common notable differences observed between the CLP treatment group and the LPS/PCI models. LPS- and PCI-treated animals had similar courses of systemic inflammation and measurable outcomes. Since the levels of pro-inflammatory cytokines and oxidative stress were elevated in every single mouse, we conclude that the systemic inflammation was successfully

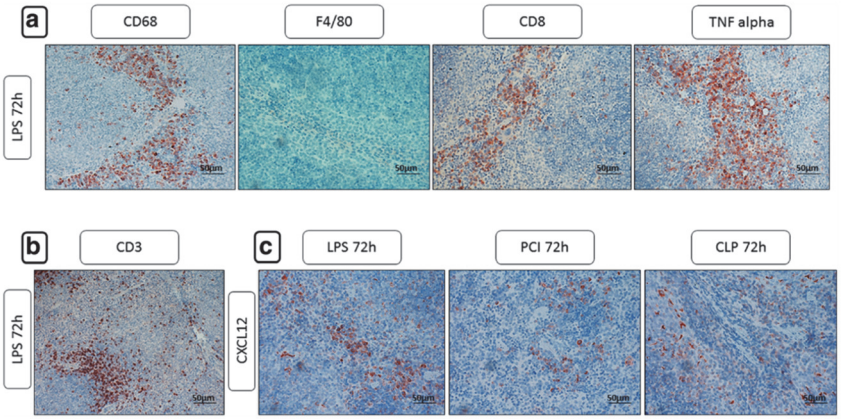

Fig. 9 CD68, F4/80, CD8, TNF-α, CD3 and CXCL12 expression in the spleens after 72 h. At the time point indicated, mice were sacrificed and the spleens were collected for immunohistological analysis. Representative photomicrographs from one of 4–6 different tissue samples stained 72 h after inflammation onset for CD68, F4/80, CD8, TNF-α, CD3 and CXCL12 expression are shown (red-brown color, counterstaining with hematoxylin; original magnification: 400×)

induced and that mice were not resistant to LPS, PCI or CLP treatment.

Although a non-lethal systemic inflammation model was intended, following CLP treatment three mice had to be sacrificed before the end of the experiment due to having reached a CSS of 4, demonstrating a disadvantage of this experimental model. Standardization is known to be difficult with CLP methodology and is dependent on the technique used and the experience of the surgeon. Indeed, in the current study, the CLP group had the largest standard deviations in most outcome measurements. In addition, mice that had received CLP treatment exhibited impaired health status at the later time points investigated, indicating a protracted course of systemic inflammation. These results are in agreement with several other studies, suggesting that CLP treatment induces a delayed course of disease [3, 35]. In contrast, LPS and PCI treatment induced an acute inflammatory condition that progressed quickly, but also resolved rapidly, as after 72 h, mice returned to a healthy status. Since negative outcomes after LPS and PCI treatment have been reported to occur mainly during the first 72 h [36, 37], it is very likely that all mice will survive in the long-term. In contrast, on the basis of our findings and on literature data, we expect only few mice to further survive CLP treatment post-72 h [20]. As a result of an acute and severe systemic inflammation, mice in all models consumed less food and water, leading to a significant, but transient weight loss, albeit to a lesser extent in the CLP group, confirming previous results [38]. Additionally, LPS and CLP administration resulted in hypothermia, as in other studies [38]. This was probably a result of the rapid induction of the disease state and the large surface-area-to-volume ratio of these small animals [18].

In addition to general health status, there were significant differences in the kinetics and magnitude of the serum cytokine release between the three animal models. LPS and PCI treatment induced early peak cytokine responses of TNF-α and IL-6 with a rapid decrease in values thereafter. In contrast, a previously published study reported that PCI treatment caused only a negligible TNF-α response and a delayed release profile for IL-6, increasing over several hours [4]. This apparent discrepancy could be explained by the higher PCI dose used in the literature study (thus making fluid resuscitation necessary), as the authors aimed to induce mortality after 48 h. The PCI model is a relatively new model and, consequently, inter-laboratory differences have to be considered. With respect to human sepsis, IL-6 levels have been shown to reflect the severity of disease and to correlate with mortality [39], and the persistence of IL-6 and TNF-α rather than the peak levels have been shown to correlate with disease severity [40], suggesting that the CLP model is most comparable to human sepsis with respect to cytokine response.

The exogenous administration of LPS is associated with a massive toll-like receptor 4 (TLR4) activation, leading to a significant cytokine response. Presumably, the application of a polymicrobial suspension does not trigger TLR4 activation directly to the extent seen with LPS, but our results also indicate that the bacteria and their components evoked rapid onset of inflammation. Accordingly, in our investigation the differences seen between the LPS and PCI group with respect to the course of inflammatory cytokine release were not very conspicuous. CLP treatment, in contrast, is associated with a comparably slow release of bacteria into the bloodstream, thus showing a slower but protracted course of the disease.

All animal models resulted in reduced blood glucose levels and low liver glycogen reserves early after inflammation onset, which is in accordance with previous investigations [41, 42]. However, the glucose kinetics of all animal models used do not represent the clinical course in human sepsis, which has to be regarded as a disadvantage of these models. TNF-α, on the one hand, is well known to activate NF-κB, which in turn leads to a strong induction of cyclooxygenase-2 (COX-2) expression. Prostaglandins on their part (progressively more produced after COX-2 induction) have been shown to stimulate glycogenolysis in the liver [43]. On the other hand, TNF-α and IL-1β have been demonstrated to induce hypoglycemia [44]. Therefore, as LPS treatment, followed by PCI and CLP, had the largest impact on glucose levels, TNF-α kinetics may serve as an explanation for the differences observed in the glucose values over time between the three animal models. Additionally, the acute inflammatory process caused by LPS administration may have led to rapid glucose consumption, further contributing to the rapid decline in blood glucose values in this model.

In septic patients, the liver biotransformation capacity is of essential importance for the detoxification and elimination of toxic endogenous metabolites as well as exogenously administered antibiotic therapies. Lower CYP activity leads to a reduction in metabolized compounds that can be then excreted via bile and the kidneys, leading to an accumulation of these compounds and toxic effects, exerting a negative impact on the already reduced health condition of the patients [45]. TNF-α and IL-6 play a pivotal role in impairment of liver function by decreasing the biotransformation capacity [46, 47]. Both LPS and PCI treatments induced early increases in TNF-α and IL-6 serum levels, followed by a maximal loss in CYP enzyme activity and expression at 12–24 h. Also here, after 72 h baseline values were reached again. In contrast, CLP-treated mice exhibited decreased CYP activity and expression at later time points, following the prolonged release of TNF-α and

IL-6 in this model. As CLP treatment decreased CYP activities at later time points, the prolonged impairment of health status in these animals may be, at least in part, explained by the reduced ability to detoxify endogenous substances, generated as a result of the inflammatory condition.

Pro-inflammatory cytokine expression leads to increased generation of reactive oxygen species (ROS) via impairment of mitochondrial integrity and function and increased nicotinamide adenine dinucleotide phosphate (NADPH)-oxidase expression and activity [48, 49]. Elevated serum TNF-α, IL-6, and IFN-γ levels could have led to the decreased GSH/GSSG and increased LPO values seen in all models and in most organs investigated in this study. These parameters are indirect indicators of increased oxidative stress due to elevated production of ROS. While the glutathione system serves as an important anti-oxidative means of the body with, however, a limited capacity, LPO are the result of an excessive oxidative stress which had overwhelmed the overall antioxidant capacity of the organism and had caused (besides a damage of other macromolecules) a degradation of cellular membranes. The severity of oxidative stress may have been additionally augmented by the diminished total glutathione content of both the liver and the other organs investigated (Additional File 2), indicating a reduced capacity to produce glutathione and export this important antioxidant to other tissue sites. This may have been caused either by cytokine-mediated downregulation of glutathione synthesizing/recycling enzymes or by direct damage of liver cells, as indicated by elevated serum ALAT values in all three animal models.

Whereas the GSH/GSSG ratio and total glutathione content in LPS- and PCI-treated organs returned to baseline at later time points, in the CLP model, values progressively decreased with the course of treatment in all organs investigated. These observations were paralleled by serum ALAT levels. The activities remained increased at 48 and 72 h after CLP treatment, whereas LPS- and PCI treated-mice displayed normal ALAT values at the end of the experimental time course. TNF-α, IFN-γ, and IL-6 serum levels (and therefore probably ROS levels) were increased at later time points after CLP, which differed from LPS and PCI treatment. ROS have been shown to negatively impact biotransformation capacity [50]. Accordingly, in contrast to the LPS and PCI models, liver CYP expression and activity in CLP-treated mice also remained lower at later time points, as mentioned above.

Perhaps the increased activity and expression of HO-1 after LPS and PCI treatment has contributed to the observed recovery in these models. Targeted overexpression of HO-1 has been demonstrated to have beneficial effects in various experimental animal models of inflammation [51]. Moreover, previous investigations have shown that HO-1 attenuates TNF-α and ROS levels [52], which agrees with our results after LPS and PCI treatment. Additionally, HO-1-deficient mice have been shown to be more susceptible to polymicrobial sepsis, underlining the protective role of this enzyme [51, 53]. As CLP treatment did not affect the expression and activity of this anti-oxidative and anti-inflammatory enzyme, this might have been a contributing factor to the protracted and delayed disease seen in this model. Moreover, the sustained increase in ALAT levels underlines the limited liver function at later time points in the CLP model. Increased GSH and HO-1 levels might have contributed to the recovery seen in the LPS- and PCI-treated mice by triggering compensatory mechanisms [54].

As TNF-α and IFN-γ have been previously shown to be able to strongly upregulate inducible nitric oxide synthase (iNOS) [55], we stained iNOS in the livers and spleens. We found an evident amount of positive neutrophils having immigrated into the liver and splenic tissue after LPS treatment, which has also been reported by others [17]. This infiltration, although to a lesser extent, was also observed after PCI treatment, whereas the CLP procedure resulted in only few neutrophils in the liver tissue. Previous studies have shown that pro-inflammatory cytokines enhance the expression of cell adhesion molecules after bacterial infection [56]. Accordingly, more neutrophils could have entered the tissue due to an increased amount of adhesion molecules in the vessels. Lower amounts of pro-inflammatory cytokines were expressed in the PCI treatment group compared to the LPS group, and even less after CLP treatment. Therefore, fewer cells may have migrated as a result of lower cytokine levels in these models.

Previous studies have shown that high doses of LPS may trigger cell death pathways [57]. However, we did not see a significant expression of cleaved caspase-3 in the liver, regardless of treatment. In our study lower doses of LPS and fecal slurry were administered, which may not have been high enough to illicit an apoptotic response in the liver. Nevertheless, the livers of LPS-treated mice showed remarkable amounts of fat accumulation and periportal inflammatory cell infiltration, suggesting the massive TLR4 activation to be relevant for these effects. In contrast to the liver, however, increased cleaved caspase-3 expression was detectable in the spleen. Again, the increased production of TNF-α, IL-6, and IFN-γ, as well as high mobility group box-1 (HMGB-1) might have been responsible for this effect [35, 58]. Interestingly, CLP-treated mice displayed the highest cleaved caspase-3 expression early after treatment. This may be a result of an endotoxin and TNF-α-independent pathway, as has been proposed previously [59].

Interestingly, splenomegaly occurred after LPS and PCI treatment, but CLP had no impact on spleen mass. This is in agreement with a previous study that revealed septic spleens to exhibit increased weights 2–4 weeks after CLP onset [35]. The massive splenic erythrocyte accumulation in endotoxin and PCI-treated mice more than likely contributed to spleen enlargement. This is further supported by our previous report that detected a decreased hematocrit in LPS-treated mice after 24 h [19]. LPS and PCI challenge has led to a redistribution of erythrocytes into the spleen, which may indicate damage to the red blood cells. Infiltrating immune cells, predominantly monocytes and neutrophils, could also have contributed to increased splenic weights. CXCR4, CXCL12, TNF-α, iNOS, CD68, and CD8+ cells were detected in the red pulp of LPS and PCI-treated mice after 72 h. Based on histological appearance, we believe that these cells were predominantly monocytes and neutrophils, which had entered the tissue, perhaps to start the recovery process following the onset of inflammation.

As chemokines are of great importance for migration, and as we observed immune cell infiltration into the tissues, the chemokine receptor CXCR4 expression was examined. Here, our previous observations were confirmed, that CXCR4+ cells undergo apoptosis in the white pulp and are engulfed by macrophages, which then appear as tingible body macrophages [33]. Especially LPS- and PCI-treated mice exhibited a large amount of CXCR4+ cells in the red pulp after 72 h. Other authors have shown that LPS induces a reduction in CXCR4 surface expression in a dose- and time-dependent manner in peripheral neutrophils and monocytes [60]. In the current study, these findings can be explained by increased emigration of these cells out of the circulation and into the tissues. Consistent with this, CXCL12 levels were decreased in the serum, suggesting lower retention of CXCR4+ cells in the blood and an increase in CXCR4+ cells in the tissues. Additionally, in the literature treatment with TNF-α, IFN-γ, IL-1β and LPS has been shown to downregulate CXCL12 and CXCR4 expression in human brain microvessel endothelial cells [61], suggesting TLR4 activation (along with the subsequent pro-inflammatory cytokine release) to be the major activator. This might be a reason why we have observed noticeable effects after LPS or PCI treatment only.

To evaluate the anti-inflammatory response, we measured the serum levels of IL-10, as a prototypic anti-inflammatory cytokine. Consistent with our other results and with findings in the literature [62], CLP treatment induces anti-inflammatory mechanisms late in the course of disease. The early IL-10 induction after LPS and PCI treatment may have contributed to the early recovery observed in these two animal models, as IL-10 has been shown to suppress the production of TNF-α, IL-1, IL-6, and IL-8 [63, 64]. Presumably, the acute inflammatory stimulus in LPS or PCI treated mice has triggered the early IL-10 release.

Conclusions

In summary, the present study demonstrates that non-lethal, systemic inflammation induced by LPS and PCI treatment influences organ functions, cytokine responses, oxidative stress levels, and overall health status differently in comparison to the CLP procedure. The LPS and PCI models induced rapid onset of inflammation, including an early increase in serum pro-inflammatory cytokines and oxidative stress in organ tissues, a rapid decrease in blood glucose values and biotransformation capacity, immune cell infiltration from the circulation into the liver and spleen, and apoptosis in the spleen. LPS administration exhibited the strongest inflammatory effects of all of the models tested. Interestingly, LPS- and PCI-treated mice recovered by 72 h, probably through the induction of protective mechanisms, such as HO-1 upregulation. CLP treatment induced a protracted course of disease with impairment of health status persisting through the end of the experiment.

This study demonstrates that it is essential to be aware of differences in models of systemic inflammation to ensure that experimental aims are addressed appropriately. This includes an evaluation of the time period to be investigated when testing new anti-inflammatory drugs, for example. In assessing the impact on acute inflammation, the LPS model is the most suitable, as systemic effects are easily identifiable and measureable. In addition, LPS is easy to administer and the model is highly reproducible. Certainly, injection of LPS does not exactly reproduce the course of human sepsis, while CLP serves as the “gold standard” in this respect. However, with this model the time period has to be chosen long enough as the treatment induces a delayed course of inflammation. In conclusion, each model has benefits which must be weighed with the experimental parameters to be investigated and the overall aim of each individual study.

Additional files

Additional file 1: Blood pressure, heart rate, body weight and body temperature. At the time point indicated, mice were sacrificed and body weights as well as body temperatures were determined. Additionally, blood pressure values and heart rates were assessed after 24 h. Data are given as mean ± standard deviation (SD); n = 4–6 for each group and time point. Statistical significance was determined by using the non-parametric Kruskal-Wallis test, followed by pairwise Mann-Whitney U tests. Statistical comparisons were made versus the control of each group and are denoted as follows: LPS (asterisk, *), PCI (plus, +), CLP (diamond, #). A p value <0.05 (*,+,#) was considered statistically significant; a p value <0.01 (**,++,##) and a p value <0.001 (***,+++,###) are further specified. (TIFF 422 kb)

Additional file 2: Total glutathione concentration in different organs, glutathione-S-transferase activities and F4/80 expression in the livers. At the time point indicated, mice were sacrificed and different organs were collected for the analysis of the total glutathione content (**a-d**). Furthermore, glutathione-S-transferase (GST) activities were determined in the 9000 g liver supernatants (**e**). Data are given as mean ± standard deviation (SD); $n = 4–6$ for each group and time point. Statistical significance was determined by using the non-parametric Kruskal-Wallis test, followed by pairwise Mann-Whitney U tests. Statistical comparisons were made versus the control of each group and are denoted as follows: LPS (asterisk, *), PCI (plus, +), CLP (diamond, #). A p value <0.05 (*,+,#) was considered statistically significant; a p value <0.01 (**,++,##) and a p value <0.001 (***,+++,###) are further specified. The photomicrographs in (**f**) show representative livers after 48 h, displaying large amounts F4/80 positive cells after LPS and PCI treatment. In (**g**), HE stainings of PCI- and CLP-treated mice after 24 h are shown as a supplement to Fig. 3d. PCI and CLP treatment caused almost no fat accumulation in the livers. (TIFF 1084 kb)

Additional file 3: iNOS expression in the livers and spleens as well as HE staining in the spleens of PCI-treated mice. At the time point indicated, mice were sacrificed and livers and spleens were collected for immunohistochemical analysis. (**a**) Course of iNOS expression (red-brown color, counterstaining with hematoxylin; original magnification: 400×) in the livers of PCI-treated mice as supplements to Fig. 4a and b. Arrows exemplarily show the infiltrating neutrophils. (**b**) HE-stained spleens 24 h after PCI treatment (original magnification: 400×). (**c**) iNOS expression patterns after PCI treatment at 24 h (original magnification: 400×) as a supplemental to Fig. 6e. (TIFF 1827 kb)

Abbreviations

ALAT: Alanine aminotransferase; CD: Cluster of differentiation; CLP: Cecal ligation and puncture; CSS: Clinical severity score; CXCL12: CXC motif chemokine 12; CXCR4: CXC chemokine receptor type 4; CYP: Cytochrome P450; ECOD: Ethoxycoumarin-O-deethylation; EMND: Ethylmorphine-N-demethylation; EROD: Ethoxyresorufin-O-deethylation; GSH: Reduced glutathione; GSSG: Oxidized glutathione; GST: Glutathione-S-transferase; HO-1: Heme oxygenase 1; IL: Interleukin; iNOS: Inducible nitric oxide synthase; LPO: Lipid peroxides; LPS: Lipopolysaccharides; MROD: Methoxyresorufin-O-demethylation; PCI: Peritoneal contamination and infection; PROD: Pentoxyresorufin-O-depentylation; SIRS: Systemic inflammatory response syndrome; TBARS: Thiobarbituric acid-reactive substances; TLR4: Toll-like receptor 4; TNF: Tumor necrosis factor

Acknowledgements

The authors would like to thank apl. Prof. Dr. Ralf A. Claus and his working group from the Department of Anaesthesiology and Intensive Care / Center for Sepsis Control and Care, Jena University Hospital, for donating, standardizing and microbiologically validating the PCI stool batch.

Funding

This research did not receive any specific grant from any funding agency in the public, commercial or not-for-profit sector.

Availability of data and materials

All datasets, on which the conclusions of the manuscript rely on, are presented in the paper.

Authors' contributions

SS and AL designed the research study. SS, FZ and AL performed the research. SS and AL analyzed the data. SS and AL wrote the paper. SS, FZ and AL approved the final manuscript.

Ethics approval and consent to participate

The study was conducted under the licence of the Thuringian Animal Protection Committee (Approval number: 02–044/14). The principles of laboratory animal care and the German Law on the Protection of Animals as well as the Directive 2010/63/EU were followed.

Consent for publication

Not applicable.

Competing interests

The authors declare that there is no conflict of interest that could be perceived as prejudicing the impartiality of the research reported.

Publisher's Note

Springer Nature remains neutral with regard to jurisdictional claims in published maps and institutional affiliations.

Received: 27 June 2017 Accepted: 21 August 2017
Published online: 24 August 2017

References

1. Martin G, Brunkhorst FM, Janes JM, Reinhart K, Sundin DP, Garnett K, Beale R. The international PROGRESS registry of patients with severe sepsis: Drotrecogin alfa (activated) use and patient outcomes. Crit Care. 2009;13:R103. 10.1186/cc7936.
2. Stortz JA, Raymond SL, Mira JC, Moldawer LL, Mohr AM, Efron PA. Murine models of sepsis and trauma: can we bridge the gap? ILAR J. 2017:1–16. 10.1093/ilar/ilx007.
3. Remick DG, Newcomb DE, Bolgos GL, Call DR. Comparison of the mortality and inflammatory response of two models of sepsis: Lipopolysaccharide vs. cecal ligation and puncture. Shock. 2000;13:110–6.
4. Recknagel P, Gonnert FA, Halilbasic E, Gajda M, Jbeily N, Lupp A, et al. Mechanisms and functional consequences of liver failure substantially differ between endotoxaemia and faecal peritonitis in rats. Liver Int. 2013;33:283–93. 10.1111/liv.12012.
5. Deitch EA. Animal models of sepsis and shock: a review and lessons learned. Shock. 1998;9:1–11.
6. Buras JA, Holzmann B, Sitkovsky M. Animal models of sepsis: setting the stage. Nat Rev Drug Discov. 2005;4:854–65. 10.1038/nrd1854.
7. Gonnert FA, Recknagel P, Seidel M, Jbeily N, Dahlke K, Bockmeyer CL, et al. Characteristics of clinical sepsis reflected in a reliable and reproducible rodent sepsis model. J Surg Res. 2011;170:e123–34. 10.1016/j.jss.2011.05.019.
8. Fink MP, Heard SO. Laboratory models of sepsis and septic shock. J Surg Res. 1990;49:186–96.
9. Remick DG, Ward PA. Evaluation of endotoxin models for the study of sepsis. Shock. 2005;24(Suppl 1):7–11.
10. Dejager L, Pinheiro I, Dejonckheere E, Libert C. Cecal ligation and puncture: the gold standard model for polymicrobial sepsis? Trends Microbiol. 2011;19:198–208. 10.1016/j.tim.2011.01.001.
11. Hubbard WJ, Choudhry M, Schwacha MG, Kerby JD, Rue LW, Bland KI, Chaudry IH. Cecal ligation and puncture. Shock. 2005;24(Suppl 1):52–7.
12. Wichterman KA, Baue AE, Chaudry IH. Sepsis and septic shock–a review of laboratory models and a proposal. J Surg Res. 1980;29:189–201.
13. Ruiz S, Vardon-Bounes F, Merlet-Dupuy V, Conil J-M, Buleon M, Fourcade O, et al. Sepsis modeling in mice: ligation length is a major severity factor in cecal ligation and puncture. Intensive Care Med Exp. 2016;4:22. 10.1186/s40635-016-0096-z.
14. Ebong S, Call D, Nemzek J, Bolgos G, Newcomb D, Remick D. Immunopathologic alterations in murine models of sepsis of increasing severity. Infect Immun. 1999;67:6603–10.
15. Yan J, Li S, Li S. The role of the liver in sepsis. Int Rev Immunol. 2014;33:498–510. 10.3109/08830185.2014.889129.
16. Nesseler N, Launey Y, Aninat C, Morel F, Malledant Y, Seguin P. Clinical review: the liver in sepsis. Crit Care. 2012;16:235. 10.1186/cc11381.
17. Copeland S, Warren HS, Lowry SF, Calvano SE, Remick D. Acute inflammatory response to endotoxin in mice and humans. Clin Diagn Lab Immunol. 2005;12:60–7. 10.1128/CDLI.12.1.60-67.2005.
18. Nemzek JA, Hugunin KMS, Opp MR. Modeling sepsis in the laboratory: merging sound science with animal well-being. Comp Med. 2008;58:120–8.
19. Seemann S, Lupp A. Administration of AMD3100 in endotoxemia is associated with pro-inflammatory, pro-oxidative, and pro-apoptotic effects in vivo. J Biomed Sci. 2016;23:68. 10.1186/s12929-016-0286-8.
20. Rittirsch D, Huber-Lang MS, Flierl MA, Ward PA. Immunodesign of experimental sepsis by cecal ligation and puncture. Nat Protoc. 2009;4:31–6. 10.1038/nprot.2008.214.
21. ELLMAN GL. Tissue sulfhydryl groups. Arch Biochem Biophys. 1959;82:70–7.
22. Hissin PJ, Hilf R. A fluorometric method for determination of oxidized and reduced glutathione in tissues. Anal Biochem. 1976;74:214–26.
23. Yagi T, Day RS. Differential sensitivities of transformed and untransformed murine cell lines to DNA cross-linking agents relative to repair of O6-methylguanine.

Mutation Research/DNA Repair Reports. 1987;184:223–7. 10.1016/0167-8817(87)90020-4.
24. Yoshida T, Kikuchi G. Sequence of the reaction of heme catabolism catalyzed by the microsomal heme oxygenase system. FEBS Lett. 1974; 48:256–61.
25. Lubet RA, Mayer RT, Cameron JW, Nims RW, Burke M, Wolff T, Guengerich F. Dealkylation of pentoxyresorufin: a rapid and sensitive assay for measuring induction of cytochrome(s) P-450 by phenobarbital and other xenobiotics in the rat. Arch Biochem Biophys. 1985;238:43–8. 10.1016/0003-9861(85)90138-9.
26. Aitio A. A simple and sensitive assay of 7-ethoxycoumarin deethylation. Anal Biochem. 1978;85:488–91. 10.1016/0003-2697(78)90245-2.
27. Pohl RJ, Fouts JR. A rapid method for assaying the metabolism of 7-ethoxyresorufin by microsomal subcellular fractions. Anal Biochem. 1980; 107:150–5. 10.1016/0003-2697(80)90505-9.
28. Kleeberg U, Klinger W. Sensitive formaldehyde determination with Nash's reagent and a 'tryptophan reaction. J Pharmacol Methods. 1982;8:19–31.
29. Habig WH, Pabst MJ, Jakoby WB. Glutathione S-transferases. The first enzymatic step in mercapturic acid formation. J Biol Chem. 1974;249:7130–9.
30. Lupp A, Danz M, Müller D. Morphology and cytochrome P450 isoforms expression in precision-cut rat liver slices. Toxicology. 2001;161:53–66. 10.1016/s0300-483x(01)00333-x.
31. Fischer AH, Jacobson KA, Rose J, Zeller R. Hematoxylin and eosin staining of tissue and cell sections. CSH Protoc. 2008;2008:pdb.prot4986. doi:10.1101/pdb.prot4986.
32. McManus JFA. Histological and Histochemical uses of periodic acid. Stain Technol. 2009;23:99–108. 10.3109/10520294809106232.
33. Seemann S, Lupp A. Administration of a CXCL12 analog in Endotoxemia is associated with anti-inflammatory, Anti-Oxidative and Cytoprotective Effects In Vivo. PLoS One. 2015;10:e0138389. 10.1371/journal.pone.0138389.
34. Tunc T, Cekmez F, Cetinkaya M, Kalayci T, Fidanci K, Saldir M, et al. Diagnostic value of elevated CXCR4 and CXCL12 in neonatal sepsis. J Matern Fetal Neonatal Med. 2015;28:356–61. 10.3109/14767058.2014.916683.
35. Valdes-Ferrer SI, Rosas-Ballina M, Olofsson PS, Lu B, Dancho ME, Ochani M, et al. HMGB1 mediates splenomegaly and expansion of splenic CD11b+ Ly-6C(high) inflammatory monocytes in murine sepsis survivors. J Intern Med. 2013;274:381–90. 10.1111/joim.12104.
36. Gröger M, Rennert K, Giszas B, Weiß E, Dinger J, Funke H, et al. Monocyte-induced recovery of inflammation-associated hepatocellular dysfunction in a biochip-based human liver model. Sci Rep. 2016;6:21868. 10.1038/srep21868.
37. Lechner AJ, Velasquez A, Knudsen KR, Johanns CA, Tracy TF, Matuschak GM. Cholestatic liver injury increases circulating TNF-alpha and IL-6 and mortality after Escherichia Coli endotoxemia. Am J Respir Crit Care Med. 1998;157: 1550–8. 10.1164/ajrccm.157.5.9709067.
38. Ebong SJ, Call DR, Bolgos G, Newcomb DE, Granger JI, O'Reilly M, Remick DG. Immunopathologic responses to non-lethal sepsis. Shock. 1999;12:118–26.
39. Vianna RCS, Gomes RN, Bozza FA, Amancio RT, Bozza PT, David CMN, Castro-Faria-Neto HC. Antibiotic treatment in a murine model of sepsis: impact on cytokines and endotoxin release. Shock. 2004;21:115–20. 10.1097/01.shk.0000111828.07309.21.
40. Pinsky MR, Vincent JL, Deviere J, Alegre M, Kahn RJ, Dupont E. Serum cytokine levels in human septic shock. Relation to multiple-system organ failure and mortality. Chest. 1993;103:565–75.
41. Osuchowski MF, Craciun FL, Schuller E, Sima C, Gyurko R, Remick DG. Untreated type 1 diabetes increases sepsis-induced mortality without inducing a prelethal cytokine response. Shock. 2010;34:369–76. 10.1097/SHK.0b013e3181dc40a8.
42. Oguri S, Motegi K, Iwakura Y, Endo Y. Primary role of interleukin-1 and interleukin-1 in Lipopolysaccharide-induced hypoglycemia in mice. Clin Vaccine Immunol. 2002;9:1307–12. 10.1128/CDLI.9.6.1307-1312.2002.
43. Casteleijn E, Kuiper J, van Rooij HC, Kamps JA, Koster JF, van Berkel TJ. Endotoxin stimulates glycogenolysis in the liver by means of intercellular communication. J Biol Chem. 1988;263:6953–5.
44. Raetzsch CF, Brooks NL, Alderman JM, Moore KS, Hosick PA, Klebanov S, et al. Lipopolysaccharide inhibition of glucose production through the toll-like receptor-4, myeloid differentiation factor 88, and nuclear factor kappa b pathway. Hepatology. 2009;50:592–600. 10.1002/hep.22999.
45. Morgan ET. Regulation of cytochrome p450 by inflammatory mediators: why and how? Drug Metab Dispos. 2001;29:207–12.
46. Zhou M, Maitra SR, Wang P. The potential role of transcription factor aryl hydrocarbon receptor in downregulation of hepatic cytochrome P-450 during sepsis. Int J Mol Med. 2008;21:423–8.
47. Jacob A, Zhou M, Wu R, Wang P. The role of hepatic cytochrome P-450 in sepsis. Int J Clin Exp Med. 2009;2:203–11.
48. Shoji Y, Uedono Y, Ishikura H, Takeyama N, Tanaka T. DNA damage induced by tumour necrosis factor-alpha in L929 cells is mediated by mitochondrial oxygen radical formation. Immunology. 1995;84:543–8.
49. Kim Y-S, Morgan MJ, Choksi S, Liu Z-G. TNF-induced activation of the Nox1 NADPH oxidase and its role in the induction of necrotic cell death. Mol Cell. 2007;26:675–87. 10.1016/j.molcel.2007.04.021.
50. Carlson TJ, Billings RE. Role of nitric oxide in the cytokine-mediated regulation of cytochrome P-450. Mol Pharmacol. 1996;49:796–801.
51. Chung SW, Liu X, Macias AA, Baron RM, Perrella MA. Heme oxygenase-1-derived carbon monoxide enhances the host defense response to microbial sepsis in mice. J Clin Invest. 2008;118:239–47. 10.1172/JCI32730.
52. Tamion F, Richard V, Renet S, Thuillez C. Protective effects of heme-oxygenase expression against endotoxic shock: inhibition of tumor necrosis factor-alpha and augmentation of interleukin-10. J Trauma. 2006;61:1078–84. 10.1097/01.ta.0000239359.41464.ef.
53. Hassaan PS, Mehanna RA, Dief AE. The potential role of Hemopexin and Heme Oxygenase-1 inducer in a model of sepsis. Physiology Journal. 2015; 2015:1–10. 10.1155/2015/208485.
54. Lu SC. Regulation of glutathione synthesis. Mol Asp Med. 2009;30:42–59. 10.1016/j.mam.2008.05.005.
55. Kirkeboen KA, Strand OA. The role of nitric oxide in sepsis–an overview. Acta Anaesthesiol Scand. 1999;43:275–88.
56. Soderquist S. Vikerfors. Adhesion molecules (E-selectin, intercellular adhesion molecule-1 (ICAM-1) and vascular cell adhesion molecule-1 (VCAM-1)) in sera from patients with Staphylococcus Aureus bacteraemia with or without endocarditis. Clin Exp Immunol. 1999;118: 408–11. 10.1046/j.1365-2249.1999.01081.x.
57. Hong J-Y, Lebofsky M, Farhood A, Jaeschke H. Oxidant stress-induced liver injury in vivo: role of apoptosis, oncotic necrosis, and c-Jun NH2-terminal kinase activation. Am J Physiol Gastrointest Liver Physiol. 2009;296:G572–81. 10.1152/ajpgi.90435.2008.
58. Zhou M, Wu R, Dong W, Leong J, Wang P. Accelerated apoptosis contributes to aging-related hyperinflammation in endotoxemia. Int J Mol Med. 2010;25:929–35.
59. Hiramatsu M, Hotchkiss RS, Karl IE, Buchman TG. Cecal ligation and puncture (CLP) induces apoptosis in thymus, spleen, lung, and gut by an endotoxin and TNF-independent pathway. Shock. 1997;7:247–53.
60. Kim HK, Kim J-E, Chung J, Han K-S, Cho H-I. Surface expression of neutrophil CXCR4 is down-modulated by bacterial endotoxin. Int J Hematol. 2007;85: 390–6. 10.1532/IJH97.A30613.
61. Liu KKY, Dorovini-Zis K. Regulation of CXCL12 and CXCR4 expression by human brain endothelial cells and their role in CD4+ and CD8+ T cell adhesion and transendothelial migration. J Neuroimmunol. 2009;215:49–64. 10.1016/j.jneuroim.2009.08.003.
62. Osuchowski MF, Welch K, Siddiqui J, Remick DG. Circulating cytokine/inhibitor profiles reshape the understanding of the SIRS/CARS continuum in sepsis and predict mortality. J Immunol. 2006;177:1967–74. 10.4049/jimmunol.177.3.1967.
63. Fiorentino DF, Zlotnik A, Mosmann TR, Howard M, O'Garra A. IL-10 inhibits cytokine production by activated macrophages. J Immunol. 1991;147:3815–22.
64. Waal Malefyt R de, Abrams J, Bennett B, Figdor CG, Vries JE de. Interleukin 10(IL-10) inhibits cytokine synthesis by human monocytes: an autoregulatory role of IL-10 produced by monocytes. J Exp Med 1991;174:1209–1220.

4.2 Manuskript II: Administration of AMD3100 in endotoxemia is associated with pro-inflammatory, pro-oxidative, and pro-apoptotic effects in vivo

Journal of Biomedical Science. 2016 Oct 3;23(1):68. DOI: 10.1186/s12929-016-0286-8.

Semjon Seemann, Amelie Lupp

Status:

Eingereicht am: 23. Mai 2016

Akzeptiert am: 27. September 2016

Veröffentlicht am: 03. Oktober 2016

Autorenschaft:

Erstautor

Beitrag der Autoren:

Semjon Seemann und Amelie Lupp haben das Projekt entwickelt, die Experimente durchgeführt, die Daten ausgewertet und das finale Manuskript geschrieben. Amelie Lupp stellte die Reagenzien und die analytischen Werkzeuge zur Verfügung.

Zusammenfassung

Der Chemokinrezeptor CXCR4 zeichnet sich im adulten Organismus durch sein ubiquitäres Vorkommen aus und ist vor allem auf Zellen des Immunsystems exprimiert. Sowohl zahlreiche Literaturdaten als auch die Ergebnisse von Manuskript I deuten darauf hin, dass dieser Rezeptor und sein natürlicher Ligand CXCL12 einen entscheidenden Einfluss auf entzündliche Erkrankungen nehmen können. Das Ziel des **Manuskripts II** war es daher, die Auswirkungen einer CXCR4-Blockade auf die systemische Entzündung näher zu charakterisieren und ihre Folgen sowohl für den Gesamtorganismus als auch für die Organfunktionen zu bewerten. Hierzu wurde Mäusen entweder nur das entsprechende Lösungsmittel (Kontrollen), nur LPS, nur der CXCR4-Antagonist AMD3100 oder LPS plus AMD3100 intraperitoneal verabreicht. Vierundzwanzig Stunden später wurden der Gesundheitszustand und die Körpertemperatur der Tiere erfasst sowie zahlreiche Blut- und Serumparameter und der oxidative Stress in verschiedenen Organen gemessen. Weiterhin wurde die Leberfunktion anhand des Glykogengehalts und der Biotransformationskapazität bestimmt. Schließlich wurde mithilfe der Immunhistochemie und des Immunoblottings im Leber- und Milzgewebe die Expression des antioxidativ wirksamen Enzyms HO-1, des proapoptotischen Enzyms Cleaved Caspase-3 sowie verschiedene Immunzellmarker analysiert. Die zusätzliche Behandlung mit AMD3100 während der systemischen Entzündung führte zu einer verstärkten inflammatorischen Reaktion. Die Mäuse wiesen gegenüber der alleinigen LPS-Gabe einen stärker beeinträchtigten Gesundheitszustand und weiter erhöhte Serumspiegel von TNF-α, IFN-γ und Stickstoffmonoxid auf. Ferner war das Blutbild der Mäuse aufgrund der AMD3100- und LPS-Gabe von einer Anämie, Thrombozytopenie, Lymphopenie und Neutrophilie geprägt. Weiterhin verstärkte die CXCR4-Blockade den oxidativen Stress, reduzierte den Glykogengehalt und die Biotransformationskapazität in den Lebern und führte zu einer vermehrten Einwanderung von sowohl neutrophilen Granulozyten als auch von Lymphozyten in die Leber. In der Milz waren eine verringerte Lymphozytenzahl und eine erhöhte Apoptoserate festzustellen. Ferner verminderte AMD3100 alleine die Expression und Aktivität der HO-1. Die Daten zeigen, dass sich eine CXCR4-Blockade mittels AMD3100 in der akuten systemischen Entzündung proinflammatorisch, prooxidativ und proapoptotisch äußert und dass sowohl der allgemeine Gesundheitszustand der Tiere als auch die Leberfunktion erheblich beeinträchtigt werden.

Seemann and Lupp *Journal of Biomedical Science* (2016) 23:68
DOI 10.1186/s12929-016-0286-8

Journal of Biomedical Science

科 技 部 Ministry of Science and Technology
The cost of publication in *Journal of Biomedical Science* is borne by the Ministry of Science and Technology, Taiwan.

RESEARCH Open Access

Administration of AMD3100 in endotoxemia is associated with pro-inflammatory, pro-oxidative, and pro-apoptotic effects in vivo

Semjon Seemann* and Amelie Lupp

Abstract

Background: Chemokine receptor 4 (CXCR4) is a multifunctional G protein-coupled receptor that is activated by its natural ligand, C-X-C motif chemokine 12 (CXCL12). As a likely member of the lipopolysaccharide (LPS)-sensing complex, CXCR4 is involved in pro-inflammatory cytokine production and exhibits substantial chemo-attractive activity for various inflammatory cells. Here, we aimed to characterize the effects of CXCR4 blockade in systemic inflammation and to evaluate its impact on organ function. Furthermore, we investigated whether CXCR4 blockade exerts deleterious effects, thereby substantiating previous studies showing a beneficial outcome after treatment with CXCR4 agonists in endotoxemia.

Methods: The CXCR4 antagonist AMD3100 was administered intraperitoneally to mice shortly after LPS treatment. After 24 h, health status was determined and serum tumor necrosis factor alpha (TNF alpha), interferon gamma (IFN gamma), and nitric oxide (NO) levels were measured. We further assessed oxidative stress in the brain, kidney, and liver as well as liver biotransformation capacity. Finally, we utilized immunohistochemistry and immunoblotting in liver and spleen tissue to determine cluster of differentiation 3 (CD3), CD8, CD68, and TNF alpha expression patterns, and to assess the presence of various markers for apoptosis and oxidative stress.

Results: Mice treated with AMD3100 displayed impaired health status and showed enhanced serum levels of TNF alpha, IFN gamma and NO levels in endotoxemia. This compound also amplified LPS-induced oxidative stress in all tissues investigated and decreased liver biotransformation capacity in co-treated animals. Co-treatment with AMD3100 further inhibited expression of nuclear factor (erythroid-derived 2)-like 2 (Nrf-2), heme oxygenase-1 (HO-1), and various cytochrome P450 enzymes, whereas it enhanced expression of CD3, inducible nitric oxide synthase, and TNF alpha, as well as the total number of neutrophils in liver tissue. Spleens from co-treated animals contained large numbers of erythrocytes and neutrophils, but fewer CD3+ cells, and demonstrated increased apoptosis in the white pulp.

Conclusions: AMD3100 administration in a mouse model of endotoxemia further impaired health status and liver function and mediated pro-inflammatory, pro-oxidative, and pro-apoptotic effects. This suggests that interruption of the CXCR4/CXCL12 axis is deleterious in acute inflammation and confirms previous findings showing beneficial effects of CXCR4 agonists in endotoxemia, thereby more clearly elucidating the role of CXCR4 in inflammation.

Keywords: CXCR4, AMD3100, CXCL12, Endotoxemia, Oxidative stress

* Correspondence: semjon.seemann@yahoo.com
Institute of Pharmacology and Toxicology, Jena University Hospital, Friedrich Schiller University Jena, Drackendorfer Str. 1, 07747 Jena, Germany

Background

Chemokine receptor 4 (CXCR4) is a multifunctional G protein-coupled receptor, activated by its natural ligand C-X-C motif chemokine 12 (CXCL12) as well as by macrophage migration inhibitory factor (MIF) and ubiquitin [1, 2]. Both CXCR4 and CXCL12 perform important biological functions during embryonic development and hematopoiesis and have pleiotropic roles in the immune system and during tissue repair processes [3]. The fundamental importance of CXCR4 has been demonstrated by the fact that mice lacking this receptor are unable to survive due to critical defects in leukocyte generation and hematopoiesis, leading to embryonic and neonatal fatalities, as well as defects in heart and brain development [4]. CXCL12 also exhibits substantial chemo-attractive activity for various cells, such as monocytes and T cells, both of which play critical roles in inflammatory processes [5, 6].

CXCR4 was previously found to be involved in the production of pro-inflammatory cytokines, such as interleukin 6 (IL-6), which is increased after CXCR4 activation in microglia, human oral cancer cells, and fibroblasts [7–9]. The authors attributed this observation to a substantial activation of phosphatidylinositol-4,5-bisphosphate 3-kinase (PI3K), nuclear factor 'kappa-light-chain-enhancer' of activated B-cells (NF-kB), and activator protein 1 (AP-1). Additionally, CXCR4 activation with CXCL12 increased TNF alpha mRNA and protein levels in primary astrocytes in vitro [10].

Despite these observations, the role of the CXCR4/CXCL12 axis in inflammatory diseases remains controversial and is not well characterized. Several authors have reported beneficial outcomes after treatment with various CXCR4 antagonists in models of rheumatoid arthritis, colitis, and lupus erythematodes [11–13]. Because elevated levels of CXCL12 were present in the affected tissue, blockade of CXCR4 resulted in a decreased infiltration with CXCR4+ cells, such as T cells and neutrophils, leading to a mitigation of the inflammatory conditions. In contrast, previous investigations from our group and others revealed a beneficial outcome after administration of a CXCR4 agonist in the lipopolysaccharides (LPS)-induced model of inflammation in vivo [14–16].

As a well-established animal model for systemic inflammation and septic shock, administration of LPS in mice can be used to study the anti-inflammatory potential of various drugs. LPS binds the lipopolysaccharide binding protein (LBP) and interacts with a receptor complex formed by CD14 (cluster of differentiation 14), MD-2 (myeloid differentiation protein-2), and toll-like receptor 4 (TLR4), which then activates TLR4-mediated signal transduction. This leads to increased NF-kB activation and enhanced production of proteases, reactive oxygen species (ROS), and nitrogen species (NOS) [17]. Pro-inflammatory cytokines are also produced, leading to an increased oxidative burst and decreased biotransformation capacity of the liver [18]. In regard to the numerous medications sepsis patients are usually treated with, the preservation of the biotransformation capacity is of substantial importance.

CXCR4 has been shown to be a component of the LPS-sensing complex, suggesting that treatment with CXCR4 agonists or antagonists could modulate TLR4 signaling [19]. However, little is known regarding the precise effects of CXCR4 blockade in endotoxemia. Therefore, in this study, we further aimed to unravel the systemic impact of such a blockade on LPS-induced organ damage, by treating mice with a combination of the CXCR4 antagonist AMD3100 and LPS. We hypothesized that several effects might only become visible by antagonizing the receptor, rather than administering a CXCR4 agonist, enabling us to understand the impact of CXCR4 in endotoxemia. We focused mainly on the health status of treated mice and specifically, whether a CXCR4 blockade would worsen endotoxemia, as suggested previously [14–16]. We further measured the effect of AMD3100 on production of pro-inflammatory cytokines, induction of oxidative stress in different tissues, and the liver biotransformation capacity. We focused on the liver and spleen as two crucial organs to determine the in vivo significance of the CXCR4/CXCL12 axis. Consequently, we intended to understand the impact of CXCR4 in endotoxemia more precisely and to explore its influence in inflammation from another perspective.

Methods

Animals and experimental procedure

The study was conducted under the license of the Thuringian Animal Protection Committee (approval number: 02–044/14). The principles of laboratory animal care and the German Law on the Protection of Animals, as well as the Directive 2010/63/EU were followed. Male adult C57BL/6 N mice (12-weeks-old, body weight 25–30 g; Charles River Laboratories, Sulzfeld, Germany) were used, and the animals were housed in plastic cages under standardized conditions (light-dark cycle 12/12 h, temperature 22 ± 2 °C, humidity 50 ± 10 %, pellet diet Altromin 1316, water ad libitum). A total of 30 mice were randomly divided into four groups: control, LPS, AMD3100 ($n = 7$ each), and AMD3100 plus LPS ($n = 9$). LPS (*Escherichia coli* 0111:B4, Sigma Aldrich, Steinheim, Germany) was injected intraperitoneally (5 mg/kg body weight, dissolved in phosphate-buffered saline [PBS]) and AMD3100 (5 mg/kg body weight, Tocris Bioscience, Bristol, UK) was administered in

PBS intraperitoneally 2 h after endotoxemia onset. The most appropriate LPS dose, as well as the final time point, were determined in pilot studies, and the AMD3100 dose was selected based on previous publications [20, 21]. At 24 h post-LPS treatment, body temperatures were measured, and the condition of the animals was assessed using the Clinical Severity Score (CSS), as described previously [22]. Afterwards, the mice were sacrificed using isoflurane anesthesia, and their brains, kidneys, livers, and spleens were removed, weighed, and either fixed in 10 % buffered formaldehyde or snap-frozen in liquid nitrogen for biochemical analysis or immunoblotting, respectively. Additionally, whole blood was collected, and blood sugar levels were determined using a commercially available blood glucose meter and respective test strips (BG star®, Sanofi-Aventis, Frankfurt, Germany). Subsequently, serum was obtained and used for enzyme-linked immunosorbent assay (ELISA) and enzymatic activity measurements. For histological analysis, the formalin-fixed organ samples were embedded in paraffin blocks and cut into 4-μm thin sections ($n = 7$ for each treatment group).

IFN gamma, TNF alpha, aspartate aminotransferase (ASAT), alanine aminotransferase (ALAT), nitric oxide (NO), urea, and creatinine assays

To determine the serum levels of IFN gamma, TNF alpha, ASAT, ALAT, and NO, a mouse IFN gamma ELISA kit (Pierce Biotechnology, Rockford, IL, USA), a mouse TNF-alpha Quantikine ELISA kit (R&D Systems, MA, USA), the EnzyChrom™ Aspartate Transaminase Assay Kit, the EnzyChrom™ Alanine Transaminase Assay Kit (both BioAssay Systems, Hayward, CA, USA) and the Nitrate/Nitrite Colorimetric Assay Kit (Cayman Chemical Company, Michigan, USA), respectively, were used according to the manufacturer instructions. Creatinine was determined by means of the Jaffé reaction. Briefly, in a strongly alkaline medium, picric acid is added to the sample. Under these conditions, it reacts with creatinine to form an orange-red complex, which can be measured photometrically at 492 nm. Serum urea was measured using the commercially available colorimetric Urea Assay Kit (Sigma-Aldrich Chemie GmbH, Steinheim, Germany), which utilizes coupled enzyme reactions involving urease and glutamate dehydrogenase, resulting in a product that can be detected at 570 nm.

Oxidative status in the tissues

The tissue glutathione content in its reduced (GSH) and oxidized (GSSG) forms was analyzed by homogenizing the samples with 11 volumes of 0.2 M sodium phosphate buffer (5 mM ethylenediaminetetraacetic acid [EDTA]; pH 8.0) and four volumes of 25 % metaphosphoric acid. After centrifugation (12000 g, 4 °C, 30 min), GSH content was measured in the supernatants using a colorimetric assay, as previously described [23]. The GSSG concentration was assessed fluorometrically [24]. To determine the tissue content of lipid peroxides (LPO) as thiobarbituric acid-reactive substances (TBARS), liver samples were homogenized with 19 volumes of ice-cold saline and analyzed fluorometrically, as previously described [25].

Biotransformation capacity

To obtain 9000 g supernatants for analysis, livers were homogenized with 0.1 M sodium phosphate buffer (pH 7.4) (1:2 w/v) and subsequently centrifuged at 9000 g for 20 min at 4 °C. The 9000 g supernatants were used to assess the activities of several cytochrome P450 (CYP) enzymes, and the protein content of these fractions was determined using a modified Biuret method [26]. For determination of CYP enzyme activities, the following model reactions were performed: ethoxycoumarin-O-deethylation (ECOD; [27]), ethoxyresorufin-O-deethylation (EROD; [28]), methoxyresorufin-O-demethylation (MROD; [28]), p-nitrophenol-hydroxylation (PNPH; [29]), and pentoxyresorufin-O-dependentylation (PROD; [28]).

Histopathology and immunohistochemistry

Samples for histopathology and immunohistochemistry were prepared by cutting 4-μm sections from the paraffin blocks and floating these onto positively charged slides. Immunostaining was performed by an indirect peroxidase-labeling method, as described previously [30]. Briefly, sections were de-waxed, microwaved in 10 mM citric acid (pH 6.0) for 16 min at 600 W, and incubated with the respective primary antibodies (Table 1) at 4 °C overnight. Detection of the primary antibody was performed using either a biotinylated goat anti-rabbit, a horse anti-mouse, or a rabbit anti-goat IgG, followed by incubation with peroxidase-conjugated avidin (Vector ABC "Elite" kit, Vector, Burlingame, CA, USA). Binding of the primary antibody was visualized using 3-amino-9-ethylcarbazole (AEC) in acetate buffer (BioGenex, San Ramon, CA, USA). The sections were then rinsed, counterstained with Mayer's hematoxylin (Sigma Aldrich, Steinheim, Germany), and mounted in Vectamount™ mounting medium (Vector Laboratories, Burlingame, CA, USA). Additionally, TUNEL (TdT-mediated dUTP-biotin nick end labeling) staining was performed using the In Situ Cell Death Detection Kit, POD (Roche Diagnostics, Mannheim, Germany), according to the manufacturer instructions. All immunohistochemical stainings were evaluated by two independent investigators. To detect the liver glycogen content, periodic-acid-Schiff staining (PAS; periodic acid, Schiff's reagent: Sigma Aldrich, Steinheim, Germany) was performed, using standard protocols [31]. Identification of the specific cell types was based on their

Table 1 Primary antibodies used for immunohistochemistry (IHC) and immunoblotting (IB)

Primary antibody	Type, Catalogue number	Manufacturer	Dilution IHC/IB	Host species
CD3	polyclonal, sc-20047	Santa Cruz Biotechnology	1:500/1:200	Mouse
CD8	polyclonal, sc-7188	Santa Cruz Biotechnology	1:200/-	Rabbit
CD68/ED1	monoclonal, MCA341R	AbDSerotec	1:50/-	Mouse
cleaved caspase-3	monoclonal, 9661	Cell Signaling Technology	1:600/1:1000	Rabbit
CYP3A	polyclonal	Daiichi Pure Chemicals	1:5000/1:10000	Goat
CYP2B	polyclonal	Daiichi Pure Chemicals	1:5000/1:10000	Goat
CYP2E1	polyclonal	Daiichi Pure Chemicals	1:5000/1:10000	Goat
heme oxygenase 1	polyclonal, SPA-895	Biomol GmbH	1:5000/1:10000	Rabbit
iNOS	polyclonal, sc-651	Santa Cruz Biotechnology	1:500/-	Rabbit
Nrf-2	polyclonal, sc-722	Santa Cruz Biotechnology	-/1:500	Rabbit
TNF alpha	monoclonal, sc-52746	Santa Cruz Biotechnology	1:500/-	Mouse
VEGF	monoclonal, sc-7269	Santa Cruz Biotechnology	1:500/-	Mouse

microscopic features along with the relative location of the cells in the respective tissues.

Immunoblotting

Frozen liver and spleen samples ($n = 4$ from all treatment groups) were weighed and added (1:4) to detergent buffer (50 mM Tris-HCl, pH = 7.4, 150 mM NaCl, 5 mM EDTA, 10 mM NaF, 10 mM disodium pyrophosphate, 1 % Nonidet P-40, 0.5 % sodium deoxycholate, 0.1 % sodium dodecyl sulfate [SDS]) in the presence of protease and phosphatase inhibitors (Complete Mini and PhosSTOP; Roche Diagnostics, Mannheim, Germany). The samples were then sonicated for 10 s and gently inverted for 1 h at 4 °C before centrifugation for 30 min at 14800 g at 4 °C. Next, samples were diluted with SDS sample buffer (62.5 mM Tris-HCl, pH = 7.6, 2 % SDS, 20 % glycerol, 100 mM dithiothreitol, 0.005 % bromophenol blue), heated to 95 °C for 10 min, cooled to room temperature, and subsequently subjected to 10 % SDS-polyacrylamide gel electrophoresis (SDS-PAGE) and blotted onto polyvinylidene fluoride (PVDF) membranes. Liver blots were incubated with anti-CYP3A2, anti-CYP2B1, anti-CYP2E1, or anti-heme oxygenase-1 antibodies, whereas spleen blots were incubated with anti-cleaved caspase-3, anti-Nrf-2, or anti-CD3 antibodies, followed by incubation with peroxidase-conjugated anti-rabbit or anti-mouse secondary antibodies (Santa Cruz Biotechnology, Heidelberg, Germany; dilution 1:5000) and enhanced chemiluminescence detection (Thermo Scientific, Rockford, USA). β-actin, used as a loading control, was detected using a monoclonal mouse antibody (sc-47778, Santa Cruz Biotechnology, Heidelberg, Germany). All experiments were performed in quadruplicate.

Blood cell quantification in the peripheral blood and in liver and spleen

At 24 h post-LPS treatment, blood was collected from all mice and transferred to vials containing EDTA in order to prevent clotting. The samples were then analyzed using a Sysmex pocH-100iV Diff hematology analyzer. Additionally, iNOS-positive neutrophils in the livers and in the spleens of all mice were counted in 10 independent visual fields each at a magnification of 630× or 200×, respectively, using a light microscope.

Statistical analysis

All statistical analyses and figures were computed with GraphPad Prism software, v. 6.0 (GraphPad Software, La Jolla, CA, USA). In all cases, experiments were performed with seven animals per experimental group, except for the immunoblots, which were carried out in duplicate, with four animals per experimental group. Statistical significance was determined by using the one-way analysis of variance (ANOVA) and the Tukey post-hoc test, except for the CSS and the different blood cell types, which were analyzed by the non-parametric Kruskal-Wallis test, followed by the Mann-Whitney U test. A p value <0.05 (*) was considered as statistically significant; a p value <0.01 (**) and a p value <0.001 (***) are further specified. Data are presented as mean ± standard error of the mean (SEM), except for CSS and for the quantification of the different blood cell types, which are presented as medians, with interquartile ranges.

Results

Mortality, health status, weight development, and body temperatures

To assess the effect of CXCR4 blockade on LPS-mediated injury, male adult C57BL/6 N mice were treated intraperitoneally with LPS, AMD3100, AMD3100 plus LPS, or PBS (control) ($n = 7$ for all groups except AMD3100 plus LPS, where $n = 9$). We first conducted preliminary investigations to confirm the appropriate LPS dose and found that 5 mg/kg body weight

was suitable in terms of causing no mortality within 24 h. However, in our LPS plus AMD3100 group, two out of the nine mice died, and these animals were not used for further analysis.

The remaining animals were evaluated 24 h after LPS treatment, and we found that those receiving LPS displayed an impaired health status as compared to controls, which was even more severe after co-administration of AMD3100 and LPS, as evidenced by increased CSSs, in comparison to the control and LPS-treated mice (Fig. 1a). Specifically, co-treated mice showed less activity, moved notably slower and with more difficulty, slept more often, and exhibited a ruffled fur, as compared to the other groups of animals. Further, these mice consumed less food and water than even the mice treated with LPS alone, which, *inter alia*, led to a weight loss (Fig. 1b). Treatment of the animals with LPS alone or with AMD3100 alone led to reduced body temperatures when compared with the control mice. In accordance with the other data, an additive effect was observed in animals receiving both AMD3100 and LPS (Fig. 1c).

Blood count, blood glucose, serum TNF alpha, IFN gamma, NO, creatinine, and urea levels

Administration of LPS led to a decreased hematocrit and reduced the amount of platelets and white blood cells, when compared to the control group. However, the additional AMD3100-mediated CXCR4 blockade reduced all these parameters even further. In contrast, the neutrophil count in the peripheral blood was enhanced after endotoxin challenge, whereas animals co-treated with AMD3100 and LPS contained slightly fewer circulating cells in comparison to the LPS group. Additionally, AMD3100 alone was able to cause neutrophilia, when compared to the PBS treatment control (Fig. 2a-e). To further determine the systemic effect of a CXCR4 blockade, we assessed the amount of glucose in whole blood, as well as the levels pro-inflammatory cytokines and NO in the serum. After 24 h, endotoxin treatment induced hypoglycemia, whereas co-administration of AMD3100 and LPS reduced blood glucose levels even further (Fig. 1d). Moreover, administration of LPS triggered an elevation of serum TNF alpha and IFN gamma levels by about 250 and 30 %, respectively, as compared to the control group. AMD3100 in conjunction with LPS further increased the serum levels of both cytokines in endotoxic mice by more than 35 and 12 %, respectively (Fig. 1e and f). LPS challenge also induced higher serum NO levels, indicating increased oxidative stress, and CXCR4 blockade further amplified these effects, thereby leading to the highest NO levels observed (Fig. 1g). Finally, blocking CXCR4 in endotoxemia produced higher serum creatinine levels, as compared to the control or to the LPS groups. In contrast, serum urea levels were decreased after LPS and (even more distinctly) after AMD3100 plus LPS challenge (Additional file 1 b, c). For all parameters investigated, other than neutrophil count, no relevant influence of AMD3100 alone was detectable.

Oxidative stress in different tissues

Due to the increased serum NO levels in mice treated with LPS and LPS plus AMD3100, we assessed the oxidative status in different organs. Therefore, we quantified the lipid peroxidation products (LPO), as well as the levels of reduced (GSH) and oxidized glutathione (GSSG) in the brains, kidneys, and livers of treated and control mice. We found that 24 h after endotoxemia onset, increased oxidative stress was detectable in all organs investigated. In the brains, LPS induced an elevated production of LPO, while co-administration of AMD3100 and LPS produced even higher levels (Fig. 3a). In parallel, the GSH/GSSG ratio was decreased due to a reduced amount of GSH (Fig. 3b). Interestingly, AMD3100 treatment alone also increased LPO production and produced an enlarged GSH/GSSG ratio. The oxidative states in the kidneys and in the livers were found to be very similar (Fig. 3c-f). These results demonstrate that endotoxin induces ROS production, which is indirectly measureable by the increased LPO content and the impaired glutathione status, and critically, co-treatment with AMD3100 worsens these effects even further. The liver, in particular, was strongly affected, as this organ showed approximately 35 % higher LPO values and 15 % less total glutathione content in animals co-treated with LPS and AMD3100, as compared to the LPS group.

Liver

To better understand the underlying cause(s) of oxidative stress observed in the different organs investigated, we used immunoblotting and immunohistochemistry. Here, we focused on the anti-oxidative enzymes, HO-1 and Nrf-2. As shown in Fig. 3g, our immunoblots revealed that HO-1 was induced after LPS challenge. In contrast, AMD3100 treatment alone led to a decrease in HO-1 expression, and after co-administration of AMD3100 and LPS, a further reduction was observed. These data were confirmed by our immunohistochemical analysis (Fig. 4a-e). Here, HO-1 expression could be detected mainly in Kupffer and in some pit cells, an effect that was clearly visible after LPS challenge. Again, we see that AMD3100 alone caused a distinct decrease in HO-1 expression in comparison to both LPS-treated and control animals, and after co-administration of AMD3100 and LPS, HO-1 expression was almost completely abolished. For Nrf-2, immunoblot analysis revealed an up-regulation after LPS administration,

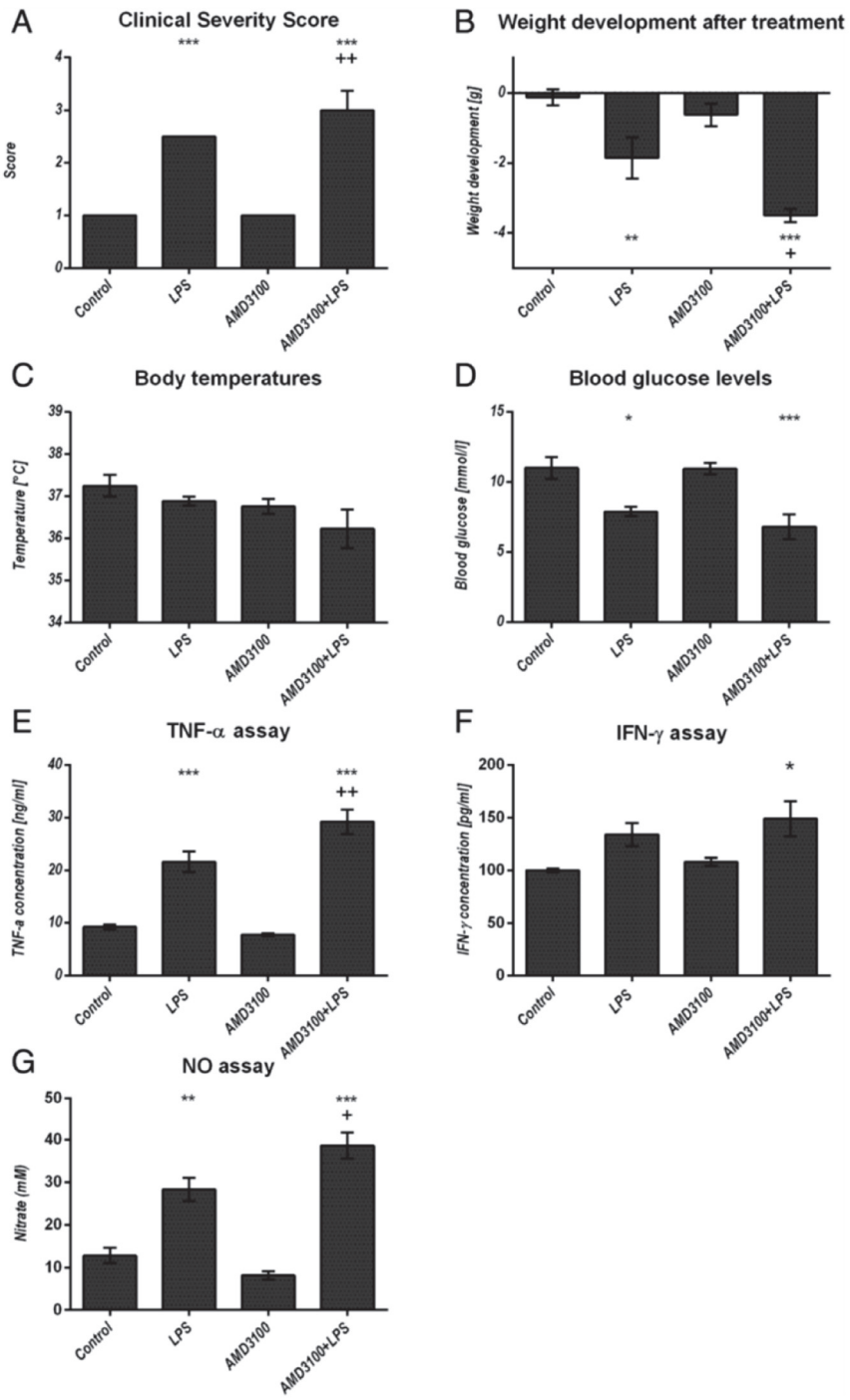

Fig. 1 (See legend on next page.)

(See figure on previous page.)
Fig. 1 General condition and systemic parameters. C57BL/6 N mice were treated either with LPS (5 mg/kg body weight), AMD3100 (5 mg/kg body weight), with both substances or with the solvent PBS (control). 24 h after LPS administration, the Clinical Severity Score (**a**), the body weight (**b**) and the body temperature (**c**) were assessed and the mice were sacrificed. Blood glucose content was determined from whole blood (**d**) and serum was obtained for TNF alpha, interferon (IFN) gamma and nitric oxide (NO) measurements (**e**-**g**). Data are given as mean ± standard error of the mean (SEM) or as median with interquartile ranges (CSS), respectively; n = 7 for each group. Statistical significant differences between the different treatment groups were determined by using the one-way analysis of variance (ANOVA) and the Tukey post hoc test, except for the CSS, which was analyzed by the non-parametric Kruskal-Wallis test followed by the Mann-Whitney-*U* test. They are indicated as follows: *, $p < 0.05$; **, $p < 0.01$; ***, $p < 0.001$ vs. control animals; $^{+}$, $p < 0.05$; $^{++}$, $p < 0.01$; $^{+++}$, $p < 0.001$ vs. LPS treatment

whereas co-treatment with AMD3100 and endotoxin led to a decreased Nrf-2 expression in the tissue (Fig. 3g).

To further determine how CXCR4 blockade could influence liver integrity, we measured the serum levels of ALAT and ASAT, ALAT, however, representing a more specific indicator of liver inflammation. In comparison to the control, LPS challenge caused an increase in ASAT values by about 20 %. However, AMD3100 alone was also able to induce ASAT levels to a comparable extent, and an additive effect was observed after combined treatment with AMD3100 and LPS (Fig. 4j). Similarly, endotoxin treatment augmented the serum concentrations of ALAT by about 100 % in comparison to the control, and the additional CXCR4 blockade caused a further increase in ALAT levels by about 20 % (Fig. 4k), indicating severe hepatocellular damage.

In light of these results and in order to gain a more detailed understanding of liver function in treated animals, we first performed periodic acid-Schiff staining as a measure for liver glycogen content (Fig. 4e-h). Exposure to LPS produced a massive loss of glycogen in the livers, although some glycogen reserves were still detectable. However, the additional CXCR4 blockade was able to remove all glycogen reserves from hepatocytes, and the livers from co-treated mice showed structural changes, which could be attributed to slight edema and intense fat accumulation. When determining the liver protein content as a reference for the CYP model reactions, we additionally assessed the turbidity value of each sample and used this as an approximation of the liver fat content. In concordance with our histological data, AMD3100 caused an additional fat accumulation in endotoxin-treated mice (Fig. 4l). While the samples of LPS treated mice were more turbid than the controls by about 110 %, the additional CXCR4 blockade provoked an additional 220 % increase. In parallel, a significant loss in liver protein content was observed. Whereas LPS provoked a decrease by about 9 %, co-treatment caused a >15 % loss, when compared with the control mice receiving PBS only (see Additional file 1 a).

Another crucial parameter for assessing liver function is the biotransformation capacity. As expected from our previous investigations on the effects of CTCE0214D in endotoxemia, we found that LPS caused a distinct loss in the activity of several CYP enzymes in the liver. Notably, whereas endotoxin decreased the activities of CYP1A, 2A, 2B, and 2C (ECOD) to approximately 70 % of the control values, the co-treatment further reduced all activities by about 25 % (Fig. 5a). Similar results were obtained when measuring the activities of CYP1A (EROD), CYP1A2 (MROD), CYP2B (PROD), and CYP1E (PNPH) (exemplary depicted in Fig. 5b and c). In comparison to LPS alone, additional administration of the CXCR4 antagonist further diminished CYP activities by approximately 30, 40, 25, and 30 %, respectively, when compared to the LPS group. Similar results were obtained in the corresponding Western blot analyses. Here, our data indicate that endotoxin treatment reduced expression of CYP2B, CYP2E1, and CYP3A in liver tissue (Fig. 5d), and the addition of AMD3100 led to a further decline in CYP enzyme expression; CYP2B isoforms, in particular, were strongly affected. These results were further confirmed by our immunohistochemical findings. As shown in Fig. 5e, the CYP enzymes are predominantly expressed around the central veins. However, 24 h after LPS challenge, CYP expression was notably decreased, and after co-administration of AMD3100, a further decrease was observed (Fig. 5f and g).

In order to further clarify the mechanisms underlying these effects, we performed additional immunohistochemical stainings. Specifically, in accordance with the massive oxidative stress observed in the livers of mice treated with AMD3100 plus LPS, iNOS stainings revealed several iNOS-overexpressing neutrophil granulocytes that had apparently entered the tissue. This effect distinctly exceeded that seen after treatment with LPS alone (Fig. 2f and 5h, i). Similar results were observed in the corresponding staining for vascular endothelial growth factor (VEGF). While some VEGF-positive granulocytes were seen in the periportal regions of mice that had received LPS alone (Fig. 6a), after co-treatment with AMD3100 and endotoxin, a larger number of granulocytes were observed infiltrating the liver tissue and spreading throughout the liver lobules (Fig. 6b).

To approximate the amount of T cells in the tissue, we used CD3 as a marker because of its presence at all

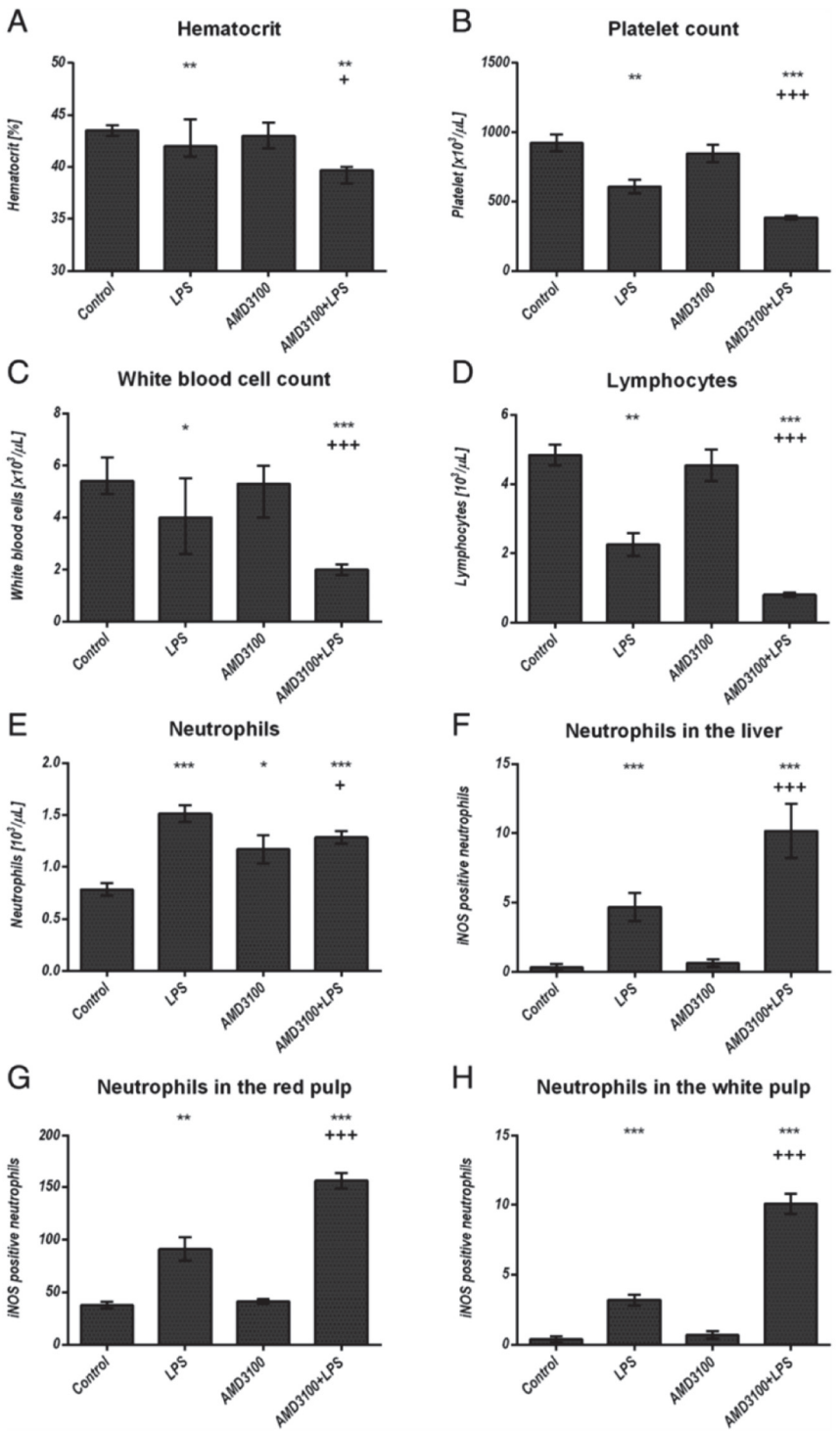

Fig. 2 (See legend on next page.)

(See figure on previous page.)
Fig. 2 Blood cell quantification in the peripheral blood and in the organs. C57BL/6 N mice were treated either with LPS (5 mg/kg body weight), AMD3100 (5 mg/kg body weight), with both substances or with the solvent PBS (control). 24 h after LPS administration, the mice were sacrificed and the blood as well as the livers and spleens were collected. 50 μl of each blood sample were analyzed by using the Sysmex pocH-100iV Diff hematology analyzer for hematocrit, platelet, white blood cell, lymphocyte and neutrophil count (**a**-**e**). Liver (**f**) and spleen sections (**g**-**h**) of each mouse were stained by means of immunohistochemistry for iNOS expression and iNOS positive neutrophils were counted in ten independent visual fields each at a magnification of 630× or 200×, respectively, using a microscope. Data are given as median with interquartile ranges; n = 7 for each group. Statistical significant differences between the different treatment groups were determined by using the non-parametric Kruskal–Wallis followed by the Mann-Whitney-*U* test and indicated as follows: *, $p < 0.05$; **, $p < 0.01$; ***, $p < 0.001$ vs. control animals; $^{+}$, $p < 0.05$; $^{++}$, $p < 0.01$; $^{+++}$, $p < 0.001$ vs. LPS treatment

stages of T-cell development (Fig. 6c-f). While some CD3+ Kupffer and pit cells were scattered throughout the liver lobules in all treatment groups, after LPS treatment, additional CD3+ lymphocytes and granulocytes were detectable in the periportal regions, some of which had already entered the tissue (Fig. 6d). Again, in comparison to the LPS group, CXCR4 blockade with AMD3100 further enhanced the amount of CD3+ cells present throughout the liver lobules. Figure 6f shows several CD3+ granulocytes and lymphocytes infiltrating the liver after co-treatment with LPS and AMD3100.

We then aimed to determine the liver cell population responsible for the production of the elevated TNF alpha serum levels observed in endotoxemia, particularly after co-treatment with AMD3100 and LPS. Therefore, we performed TNF alpha stainings in the liver tissue from all treatment groups (Fig. 6g-j). As clearly evident from Fig. 6j, sinusoidal endothelial cells are the major source of TNF alpha production. Besides some Kupffer and pit cells, these endothelial cells very strongly express this pro-inflammatory cytokine when the livers are co-challenged with AMD3100 and LPS for 24 h. Though to a much lesser extent, endotoxin itself was also able to induce TNF alpha expression, whereas the livers of control and AMD3100-treated animals exhibit only few TNF alpha-positive cells.

Spleen

The spleen is crucial for removing damaged red blood cells and bacteria from the bloodstream. Therefore, we were interested in how this organ responds to LPS, as well as to the AMD3100 plus LPS challenge. We found that LPS causes splenomegaly, as the spleen weights were significantly increased by about 40 % after 24 h of treatment, in comparison to those from the control group (Fig. 7a). Histological examination of the spleen further revealed an increased number of erythrocytes in the red pulp and a modest accumulation of neutrophils, along with a mild edema in the white pulp after LPS treatment. Critically, administration of the CXCR4 blockade with AMD3100 intensified all these effects, and 24 h post-treatment, the spleen weights from these animals were about 20 % higher than those from mice treated with LPS alone.

We next sought to determine the distribution of CD3+ cells in the spleen, in order to determine how these results compare to our data from the liver. We observed a large number of T-lymphocytes surrounding the periarteriolar lymphoid sheaths in the white pulp of spleens from control animals, and from mice treated with AMD3100 alone (Figs. 7c and e). In comparison, endotoxin challenge led to a massive efflux of CD3+ cells from the white pulp (Fig. 7d). Again, this effect was much more pronounced after CXCR4 blockade with AMD3100, and here, nearly no CD3+ lymphocytes were detectable in the spleen tissue (Fig. 7f). In combination with our findings from the liver, these results indicate that under inflammatory conditions, CD3+ cells seem to leave the spleen and to migrate to other organs, such as the liver.

To further substantiate our immunohistochemical data, we then performed additional immunoblotting experiments. As shown in Fig. 7b, administration of LPS caused a distinct reduction in CD3 expression in the spleen tissue, as compared to the control and to the AMD3100-only treatment. This effect was more pronounced after additional CXCR4 blockade with AMD3100. In parallel, we also examined the presence of CD8+ and CD68+ cells in the spleen tissue by immunohistochemistry. Here, in comparison to the control and to the AMD3100-only treatment, a clear increase in the number of CD8+ and CD68+ cells could be seen in the white pulp in spleens from LPS-challenged mice, and again, after combined treatment with AMD3100 and LPS, this effect was more pronounced.

Because apoptotic processes are of substantial importance in endotoxemia, we subsequently determined the amount, and the distribution of cells undergoing apoptosis using TUNEL staining (Figs. 8a-d, and i). We found that 24 h post-treatment, endotoxin caused an elevated apoptosis in the white pulp. In particular, tingible body macrophages appeared to be the main locus of cell death, and co-treatment with AMD3100 further exacerbated these effects. By assessing the expression of cleaved caspase-3 with immunohistochemistry and immunoblotting (Fig. 7b), we were able to confirm these observations, as the CXCR4 blockade amplified the appearance of this pro-apoptotic enzyme. Finally, when

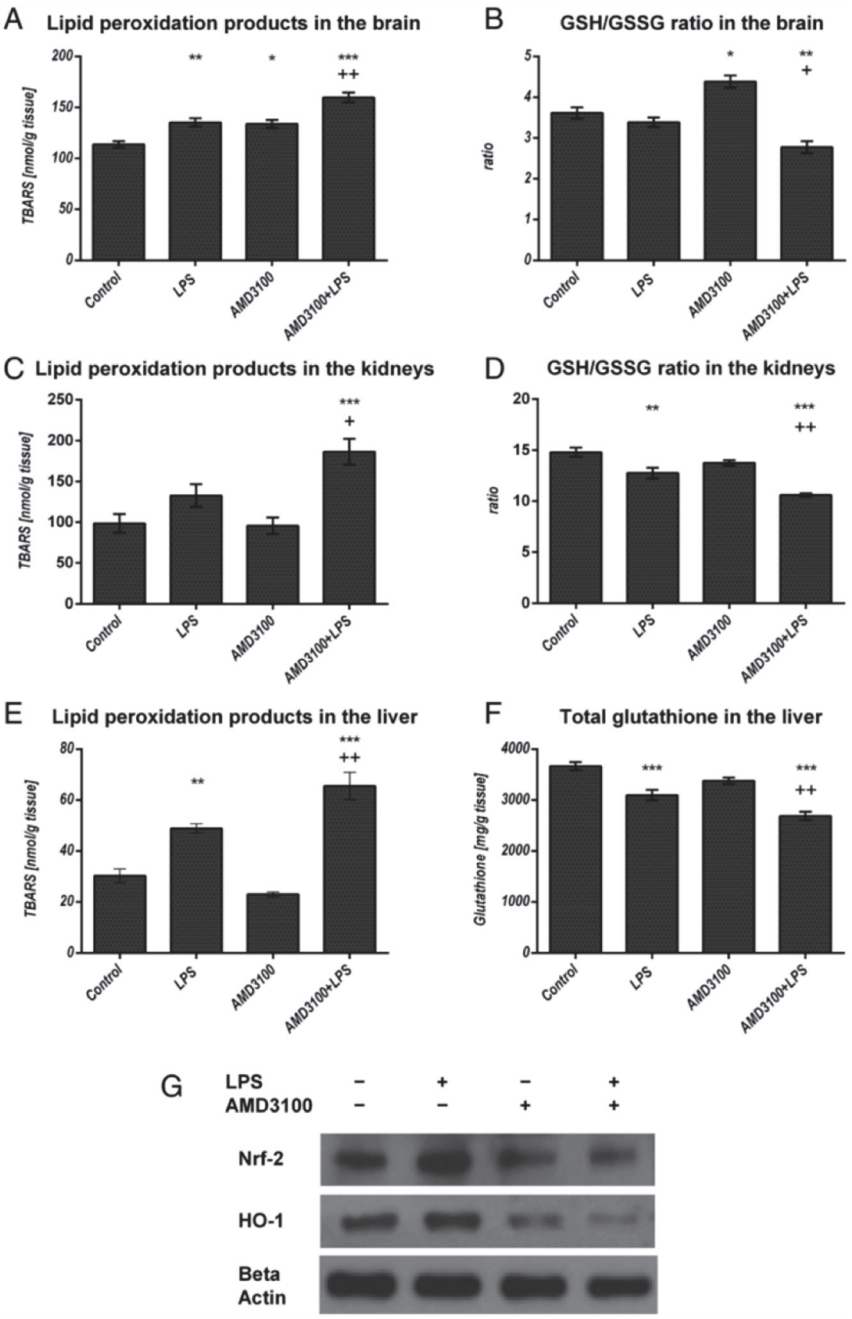

Fig. 3 Oxidative stress in different organs. C57BL/6 N mice were treated either with LPS (5 mg/kg body weight), AMD3100 (5 mg/kg body weight), with both substances or with the solvent PBS (control). 24 h after LPS administration, the mice were sacrificed and different organs were collected for the analysis of the tissue content of lipid peroxidation products as determined by thiobarbituric acid reactive substances (TBARS) (**a**, **c**, **e**). As additional parameters, the GSH/GSSG ratio in the brain and kidneys (**b**, **d**) and the total glutathione content in the liver (**f**) are depicted. Data are given as mean ± standard error of the mean (SEM), n = 7 for each group. Statistical significant differences between the different treatment groups were determined by using the one-way analysis of variance (ANOVA) and the Tukey post hoc test and are indicated as follows: *, $p < 0.05$; **, $p < 0.01$; ***, $p < 0.001$ vs. control animals; $^{+}$, $p < 0.05$; $^{++}$, $p < 0.01$; $^{+++}$, $p < 0.001$ vs. LPS treatment. In (**g**) representative examples of n = 4 independent immunoblot analyses of Nrf-2 and HO-1 expression in the liver are shown

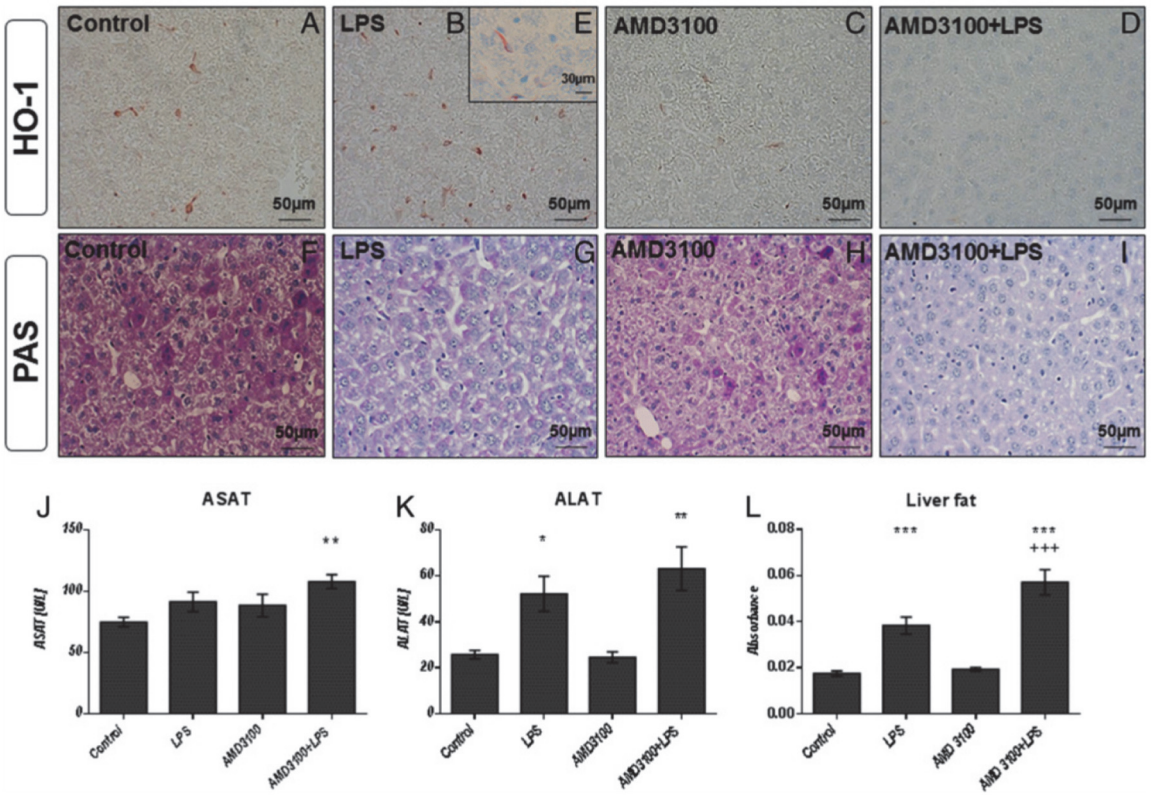

Fig. 4 Heme oxygenase-1 expression, serum ASAT, ALAT levels, glycogen and total fat content in the livers. C57BL/6 N mice were treated either with LPS (5 mg/kg body weight), AMD3100 (5 mg/kg body weight), with both substances or with the solvent PBS (control). 24 h after LPS administration, the mice were sacrificed and blood and livers were collected for further biochemical and histological analysis. (**a**-**i**): Representative photomicrographs from one of seven different tissue samples stained for HO-1 expression are shown (immunohistochemistry (red-brown color), counterstaining with hematoxylin, original magnification: (**a**-**d**, **f**-**i**) 400×, (**c**) 630×). The photomicrograph in (**e**) shows a single Kupffer cell at a higher magnification (630×). As an approximate measurement for the fat content, we determined the turbidity value in the 9000 g supernatants of the livers (**l**). **j** and **k** depict the serum concentrations of ASAT and ALAT of all treatment groups. Data are given as mean ± standard error of the mean (SEM); $n = 7$ for each group. Statistical significant differences between the different treatment groups were determined by using the one-way analysis of variance (ANOVA) and the Tukey post hoc test and are indicated as follows: *, $p < 0.05$; **, $p < 0.01$; ***, $p < 0.001$ vs. control animals; $^{+}$, $p < 0.05$; $^{++}$, $p < 0.01$; $^{+++}$, $p < 0.001$ vs. LPS treatment; #, $p < 0.05$; ##, $p < 0.01$; ###, $p < 0.001$ vs. AMD3100 administration

determining iNOS expression, we detected several neutrophil granulocytes in both the red and the white pulp of co-treated mice (Figs. 2g-h and 8e-h, and j). Critically, although LPS alone enhanced the amount of iNOS-positive granulocytes in the red pulp, in comparison to control treatment, the additional CXCR4 blockade with AMD3100 amplified this effect in the red pulp and induced additional iNOS expression in the white pulp. Treatment with AMD3100 alone had no effect on iNOS expression in the spleen.

Discussion

In contrast to other studies, which focused mainly on the general outcome of the animals and on the migration of several inflammatory cell populations in different inflammation models, we were primarily interested in the precise effects of CXCR4 blockade in endotoxemia. In particular, we focused on the systemic impact, as well as the influence on organ function. Furthermore, we intended to confirm previous investigations, which utilized different CXCR4 agonists [15, 16, 32], and in particular, our preceding study, in which we found that the CXCL12 analog CTCE-0214D exerted protective effects. Also, we aimed to indirectly show that CTCE-0214D signals through CXCR4 and to further unravel whether an interruption of the CXCR4/CXCL12 axis results in a deleterious outcome in endotoxemia.

Here, our findings demonstrate a devastating impact of AMD3100 in endotoxemia. This is consistent with our previous study, in which almost all parameters were improved after administration of the CXCL12 analog CTCE-0214D [14]. From these results, we concluded

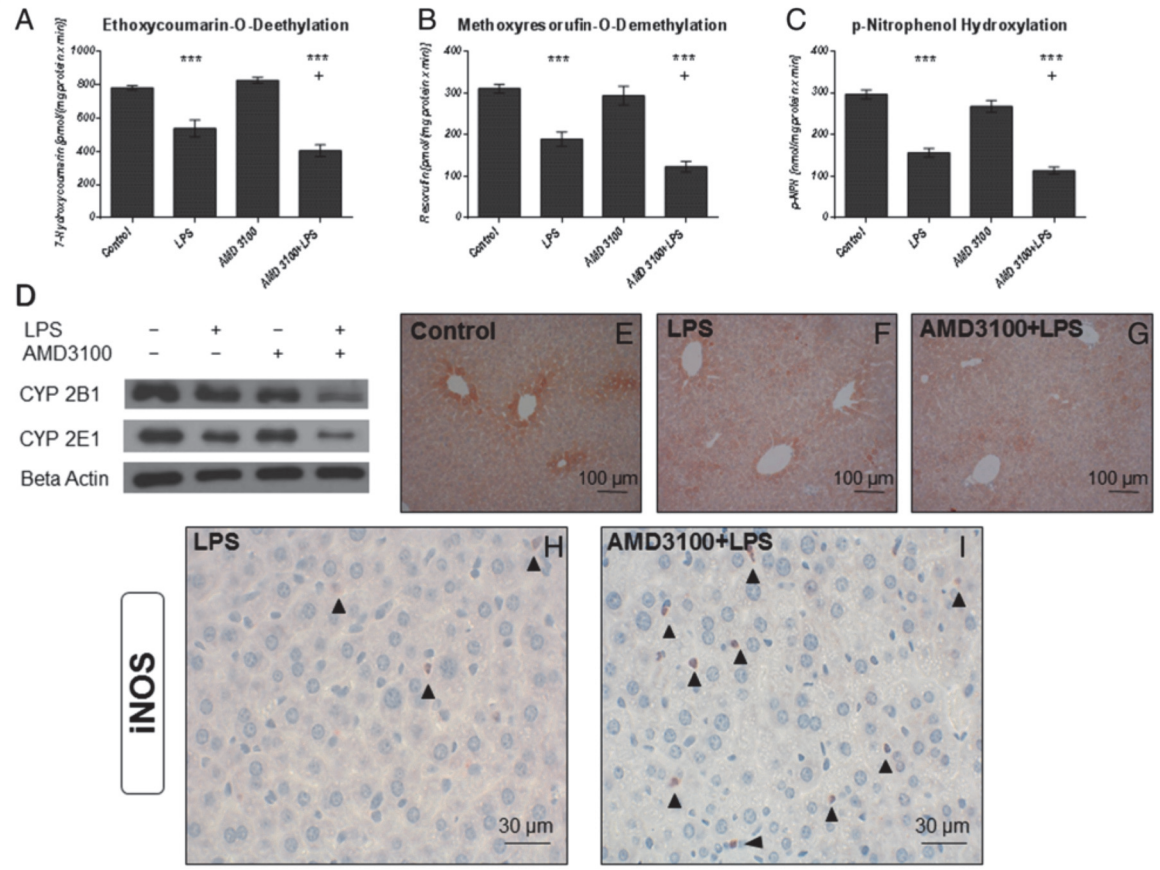

Fig. 5 Biotransformation capacity and iNOS expression in the livers. C57BL/6 N mice were treated either with LPS (5 mg/kg body weight), AMD3100 (5 mg/kg body weight), with both substances or with the solvent PBS (control). 24 h thereafter, the mice were sacrificed and the livers were collected for biochemical and histological analysis. Ethoxycoumarin-O-deethylation [ECOD] (**a**), methoxyresorufin-O-demethylation [MROD] (**b**) and p-nitrophenol-hydroxylation [PNPH] (**c**) activities in 9000 g supernatants are shown exemplarily. Data are given as mean ± standard error of the mean (SEM); n = 7 for each group. Statistical significant differences between the different treatment groups were determined by using the one-way analysis of variance (ANOVA) and the Tukey post hoc test and are indicated as follows: *, $p < 0.05$; **, $p < 0.01$; ***, $p < 0.001$ vs. control animals; $^{+}$, $p < 0.05$; $^{++}$, $p < 0.01$; $^{+++}$, $p < 0.001$ vs. LPS treatment. **d**: CYP2B and CYP2E1 expression in liver tissue as determined by immunoblotting. Representative examples of n = 4 independent immunoblots are depicted. **e** and **g**: CYP 2B isoforms expression in liver tissue as determined by immunohistochemistry (red-brown color, counterstaining with hematoxylin). Representative photomicrographs from one of seven different liver tissue samples are shown (original magnification: 200×). **h** and **i**: iNOS expression in liver tissue as determined by immunohistochemistry (red-brown color, counterstaining with hematoxylin). Representative photomicrographs from one of seven different liver tissue samples are shown (magnification: 630×, arrowheads: iNOS expressing infiltrating neutrophil granulocytes)

that this analog exerts its effects through CXCR4, and thus, CXCR4 exhibits a massive impact on systemic inflammation. This is also in good agreement with other investigations showing that CTCE-0214D and ubiquitin increase survival and diminish pro-inflammatory cytokine levels in vivo. Also, in line with our results, administration of AMD3100 in combination with LPS was associated with an increased mortality in zebrafish [33] and specific CXCL12 inhibitors revealed to be deleterious during sepsis induced by cecal ligation and puncture (CLP) [34].

CXCL12 and its receptor are mandatory for the migration of several cells, including monocytes, neutrophils, and hematopoietic progenitor cells. Delano et al. showed that mobilization of neutrophils to the sites of infection is CXCR4/CXCL12-dependent and that an interruption of the CXCR4/CXCL12 axis impaired bacterial clearance [34]. In addition, Guan et al. demonstrated that the CXCL12 analog, CTCE-0214D, recruits polymorphonuclear leukocytes (PMN) to the site of infection and enhances their phagocytic activity, thereby improving bacterial clearance in CLP-induced sepsis [32]. AMD3100 was also shown to promote inflammatory cell egress, simultaneously inhibiting their recruitment to sites of injury [35]. In addition, AMD3100 appeared to

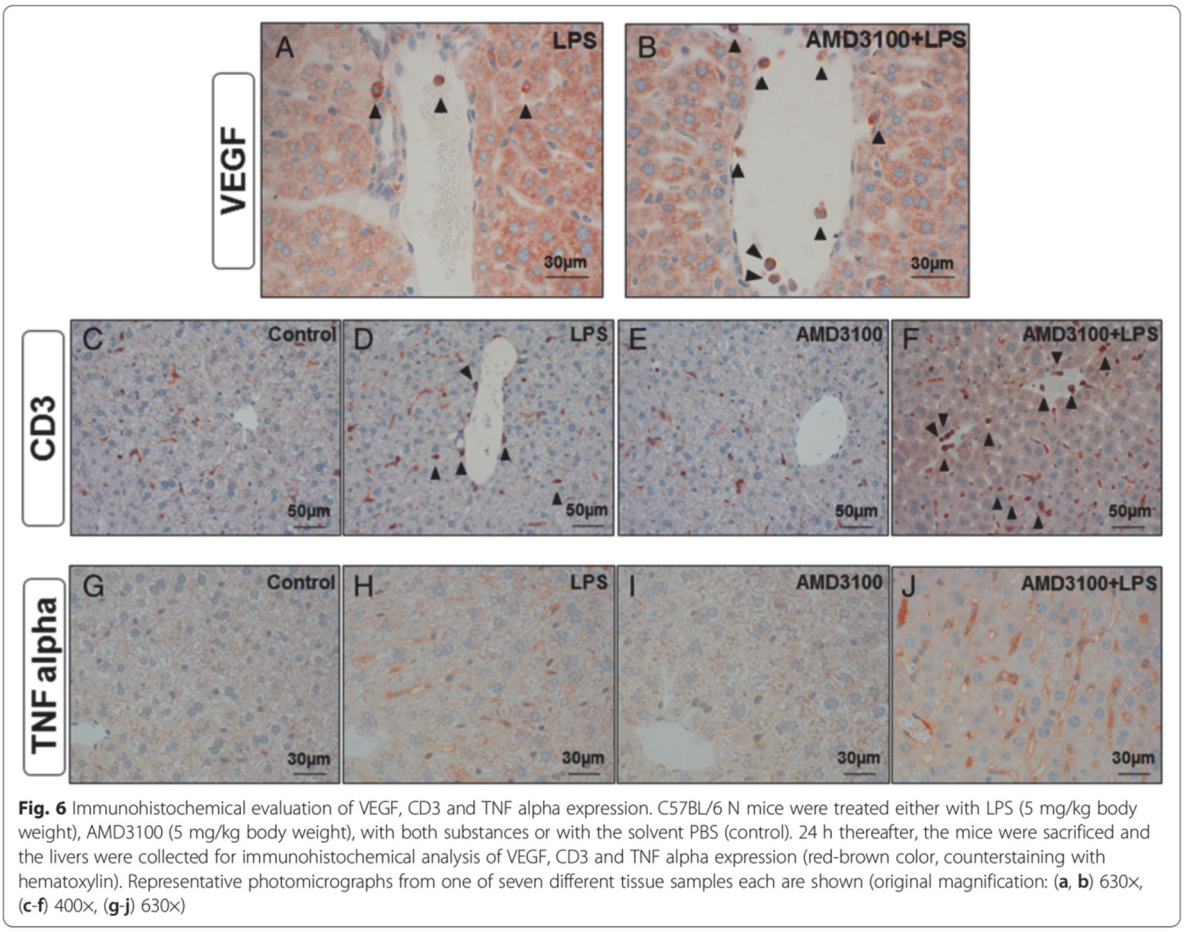

Fig. 6 Immunohistochemical evaluation of VEGF, CD3 and TNF alpha expression. C57BL/6 N mice were treated either with LPS (5 mg/kg body weight), AMD3100 (5 mg/kg body weight), with both substances or with the solvent PBS (control). 24 h thereafter, the mice were sacrificed and the livers were collected for immunohistochemical analysis of VEGF, CD3 and TNF alpha expression (red-brown color, counterstaining with hematoxylin). Representative photomicrographs from one of seven different tissue samples each are shown (original magnification: (**a**, **b**) 630×, (**c**-**f**) 400×, (**g**-**j**) 630×)

cause a preferential release of neutrophils from the lungs, while inhibiting their return to the bone marrow for elimination from the blood [36], indicating that CXCR4 blockade can negatively influence physiological defense mechanisms. These findings may serve as possible explanations for our observations, as we detected a larger number of neutrophil granulocytes in the livers and spleens of mice treated with AMD3100 plus LPS, in comparison to LPS-only treated animals. This suggests that neutrophils entered the tissues and their return to the bone marrow was likely blocked by the interrupted CXCR4/CXCL12 signaling. This hypothesis is also supported by the severe apoptosis observed in the white pulp of the spleen, as the large (unnecessary and nonfunctional) cell amount is probably answered by an increased cell death.

Furthermore, we identified fewer CD3+ cells in the spleens, but evidently more CD3+ cells in the livers of AMD3100 plus LPS co-treated mice, as compared to the LPS-only treated controls, suggesting that CXCR4 blockade "shifts" pro-inflammatory cells to the livers to provoke an inflammatory condition. Investigations by Tsuchiya et al. revealed CXCR4 conditional knock-out mice to exhibit increased numbers of CD3+ cells in the liver when inducing a chronic liver disease with CCl4 [37], whereas others were not able to detect such signs of inflammation in the liver when blocking CXCR4 [35]. Besides, we detected a reduced number of lymphocytes in the bloodstream after 24 h, suggesting severe disease progression, which seems to be a critical challenge for the immune system. An enhanced degree of apoptosis, mainly in the thymus and spleen, as well as the intensified immigration of lymphocytes into the tissues, may serve as possible explanations. This also applies to the neutrophil count in the blood. As we observed more neutrophils in the organs, we hypothesize that CXCR4 blockade promotes their migration from the bloodstream. This is supported by the observation that LPS and AMD3100 alone induce neutrophilia when compared to the control mice. However, these results warrant further investigations. Altogether, we assume that migration plays a predominant role in the observed

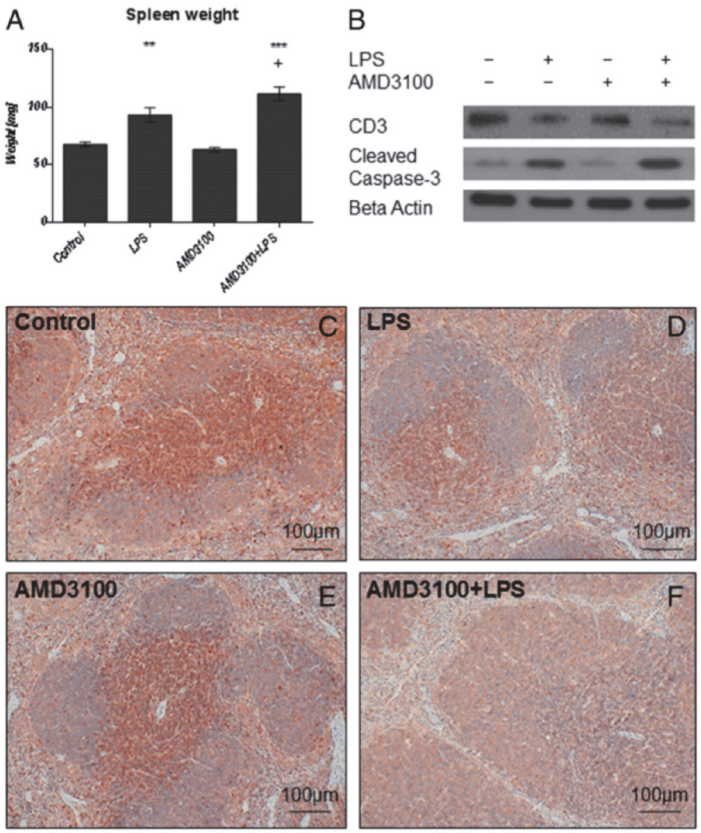

Fig. 7 Spleen weights and CD3 and cleaved caspase-3 expression in the spleen. C57BL/6 N mice were treated either with LPS (5 mg/kg body weight), AMD3100 (5 mg/kg body weight), with both substances or with the solvent PBS (control). 24 h thereafter, the mice were sacrificed and the spleens were collected for further analysis. **a**: Spleen weights. Data are given as mean ± standard error of the mean (SEM); $n = 7$ for each group. Statistical significant differences between the different treatment groups were determined by using the one-way analysis of variance (ANOVA) and the Tukey post hoc test and are indicated as follows: *, $p < 0.05$; **, $p < 0.01$; ***, $p < 0.001$; $^{+}$, $p < 0.05$; $^{++}$, $p < 0.01$; $^{+++}$, $p < 0.001$ vs. LPS. **b**: CD3 and cleaved caspase-3 expression in the spleen as determined by immunoblotting. Representative immunoblots of $n = 4$ independent analyses are shown. **c**-**f**: cleaved caspase-3 expression in the spleen as determined by immunohistochemistry (red-brown color, counterstaining with hematoxylin). Representative photomicrographs from one of seven different tissue samples each are shown (original magnification: 200×)

phenotypes, as more CD68+ and CD8+ cells were found in the spleens of co-treated mice, suggesting macrophages and cytotoxic T cells to immigrate after AMD3100 administration in endotoxemia.

It is important to note that the complexity of the CXCR4/CXCL12 axis has previously been clearly demonstrated. For example, a study found that both a three-fold increase in neutrophils, known to be injurious, and a two-fold increase in hematopoietic stem cells, known to be protective, occurred simultaneously at 36 h post-injury. Here, the authors hypothesized that the neutrophilic predominance may have mitigated any potential beneficial effects from the hematopoietic stem cells [35, 38]. These findings may help to explain the seemingly contradictory results obtained in different studies, such as a beneficial impact of a CXCR4 blockade in autoimmune diseases and a deleterious influence in ischemia and acute inflammation [14, 39].

In accordance with previous investigations, which found that CXCR4 agonists reduce serum levels of pro-inflammatory cytokines in endotoxemia [14–16], we detected increased levels of serum TNF alpha and IFN gamma after CXCR4 blockade. Also Bach et al. detected increased TNF alpha levels in polytrauma after AMD3100 and LPS challenge [40]; however, the exact cause of these observations remains unknown. As previously stated, CXCR4 may influence TLR4 signaling and consequently lead to increased inflammatory responses. However, whether an activation or blockade is beneficial remains unclear and seems to depend on the cell line, the in vitro stimulus, and on the type of inflammation in vivo [19, 41]. As in other experiments, we attempted to

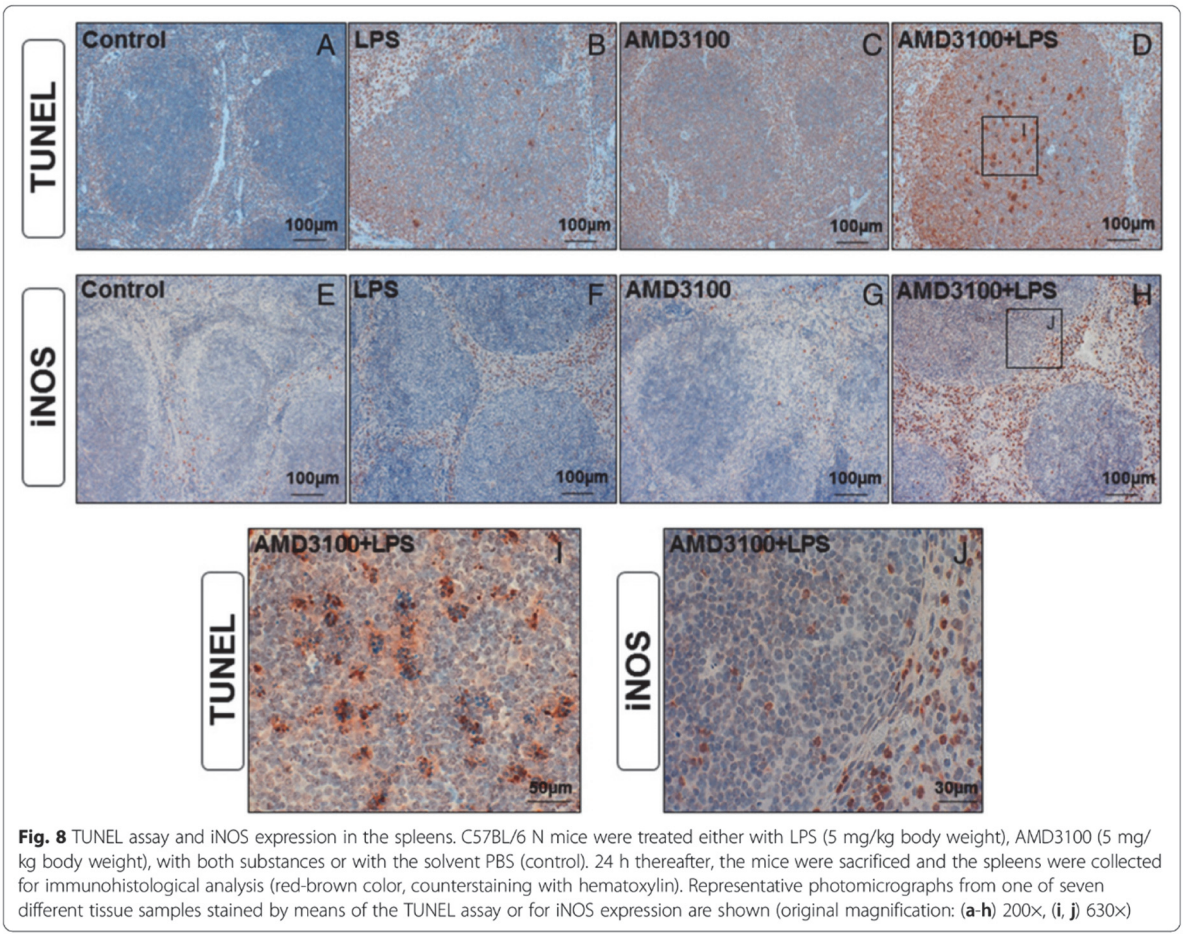

Fig. 8 TUNEL assay and iNOS expression in the spleens. C57BL/6 N mice were treated either with LPS (5 mg/kg body weight), AMD3100 (5 mg/kg body weight), with both substances or with the solvent PBS (control). 24 h thereafter, the mice were sacrificed and the spleens were collected for immunohistological analysis (red-brown color, counterstaining with hematoxylin). Representative photomicrographs from one of seven different tissue samples stained by means of the TUNEL assay or for iNOS expression are shown (original magnification: (**a**-**h**) 200×, (**i**, **j**) 630×)

elucidate if THP-1 monocytes and macrophages are affected after challenge with LPS alone, or in combination with AMD3100 or CXCL12. However, we were unable to detect any impact on TNF alpha secretion (Additional file 1 d, e). We therefore hypothesize that a direct role for CXCR4 in TLR4 signaling is secondary, and that migration likely plays the predominant role. The infiltrating neutrophils and T lymphocytes may have contributed to the observed deleterious conditions, as they are able to produce large amounts of pro-inflammatory cytokines. However, we discovered that, besides the infiltrating cells, endothelial cells in the liver are the major source of TNF alpha production. Whether these cells are directly activated by LPS, or are stimulated by a previous activation, e.g., from Kupffer cells or neutrophils, warrants further investigation. Up until now, there have been few studies focusing on endothelial cells as a source of pro-inflammatory cytokine production. In one case, it was found that HUVECs stimulated with IL-1 alpha produced a moderate amount of TNF alpha, whereas LPS did not induce TNF alpha secretion [42]. This underscores the complexity of the CXCR4/CXCL12 axis in inflammatory diseases.

We further found that AMD3100 in combination with endotoxin caused massive oxidative stress, particularly in the brains, kidneys, and livers, which can lead to a severe damage of several cell structures, including lipids and membranes, proteins, and DNA [43]. As mentioned, we detected several neutrophils in the livers of co-treated mice that likely contributed to the increased TNF alpha and IFN gamma production. Both cytokines have been reported to generate ROS via mitochondria and NADPH oxidase and are able to heavily upregulate iNOS [44, 45]. We confirmed these observations in our study, as we identified several neutrophils in the livers of the co-treated mice expressing iNOS. Correspondingly, we measured elevated serum NO levels that may have contributed to the massive oxidative stress in all organs investigated. Furthermore, NO is known to be involved in hypotension, cardiodepression, and vascular

hyporeactivity in septic shock [46]. Therefore, it may have negatively influenced the general well-being of the mice, as evidenced by their decreased health status.

Interestingly, immunoblot and immunohistochemistry analysis further revealed reduced HO-1 levels after AMD3100 challenge in endotoxemia. The protective effects of HO-1 have been clearly demonstrated, as HO-1-deficient mice were found to be more susceptible to microbial sepsis [47]. HO-1 functions as an anti-oxidative and anti-inflammatory enzyme, and several authors have reported decreased TNF alpha and ROS levels after its activation [48]. In endotoxemia, oxidative stress plays a critical role, and attenuation of a central enzyme, such as HO-1, is likely to have detrimental effects. Here, our findings are in agreement with our previous study, which found that the CXCL12 analog CTCE-0214D induced the HO-1 expression and activity in the liver [14]. Furthermore, co-treatment with AMD3100 and LPS further diminished the levels of Nrf-2 in the liver, suggesting CXCR4 blockade to be pro-oxidative, as activation of Nrf-2 results in the induction of many cytoprotective proteins, such as NAD(P)H quinone oxidoreductase 1, glutamate-cysteine ligase, and HO-1 [49].

As we further measured a decreased biotransformation capacity in livers from mice treated with AMD3100 plus LPS, as compared to the LPS-only group, their ability to detoxify and eliminate LPS-induced secondary products, such as reactive oxygen species, was even more restricted. Consequently, the fewer CYP families are active, the fewer proteins are protected from degradation. Furthermore, biotransformation capacity is of critical importance, as septic patients are frequently treated with several drugs, such as antibiotics. Therefore, we postulate that CXCR4 blockade could further impair a patient's overall outcome by enhancing the side effects from multiple medications. Again, with AMD3100, we detected results that are consistent with our previous study, in which we showed that CTCE-0214D treatment improved the biotransformation capacity and the oxidative status in the liver in endotoxemia. Together, these results suggest that modulation of CXCR4 is of critical importance in this disease.

In addition to biotransformation capacity, treatment with AMD3100 in conjunction with LPS induced liver damage by causing fat accumulation and slight edema, along with increased serum ALAT and ASAT levels. These findings are in good agreement with a recent study, in which AMD3100 was used in combination with CCl4 [35]. Here, the mice showed a trend towards increased liver necrosis at 36 h, while ALAT and ASAT levels were slightly, but not significantly, enhanced. From these results, the authors concluded that there may be a trend towards increased hepatic inflammation when administering AMD3100 in combination with CCl4. Furthermore, the decreased liver glycogen content and the reduced blood glucose levels indicate a massive glucose consumption. Kupffer and endothelial cells are the major producers of various prostaglandins, which have been shown to trigger glycogenolysis in the liver [50, 51]. In addition, TNF alpha decreased gluconeogenesis in hepatocytes isolated from 10-day-old rats [52], suggesting an excessive activation of inflammatory cells to be responsible for the alteration of the glucose homeostasis.

In order to further determine the impact of CXCR4 blockade on the kidneys, we measured the concentrations of urea and creatinine in the serum (Additional file 1 b, c). We postulate that the reduced serum urea levels seen after LPS treatment, and that become more pronounced after co-treatment with AMD3100, are attributable to impaired liver function, as the liver produces the majority of urea. Only in cases where kidney function is limited to 30 % or less, do serum urea levels increase, and thus, this parameter may serve as a measure for kidney damage. Consequently, our data also suggest that liver function is more severely affected than kidney function in endotoxemia. However, after AMD3100 plus LPS administration, serum creatinine was significantly enhanced, suggesting that kidney function is slightly impaired, at least in this instance.

As reported, co-administration of AMD3100 and LPS caused splenomegaly, mainly due to an increased number of erythrocytes and neutrophils in the red pulp and a slight edema, as well as the occurrence of some neutrophils in the white pulp. Splenomegaly is a well-known response to LPS challenge, in which nonfunctional erythrocytes and white blood cells are degraded. Apparently, CXCR4 blockade resulted in more cells in need of elimination that subsequently entered the spleen tissue, resulting in a more severe inflammation and an impaired health status. Correspondingly, we observed massive apoptosis in the white pulp after co-administration of AMD3100 and LPS. Further, cleaved caspase-3 expression was strongly increased, confirming a role for apoptosis. These observations are in accordance with our previous investigations, in which the CXCL12 analog was able to mitigate apoptosis in the white pulp, once again suggesting CXCR4 modulation is of critical importance in endotoxemia.

Conclusions

In summary, in the present investigation, we demonstrated that CXCR4 blockade with AMD3100 exerts deleterious effects in multiple facets of endotoxemia. Specifically, we found that AMD3100 treatment in conjunction with LPS further worsened the health status, augmented pro-inflammatory cytokine expression, increased oxidative stress, and induced apoptosis in different organs, as compared to LPS alone. Further, this

blockade mediated an additional decrease in liver biotransformation capacity, as well as a reduction in HO-1 expression. We also observed an increased immigration of several inflammatory cell populations into the tissues in mice co-treated with AMD3100 plus LPS, which likely contributed to the devastating overall outcome observed in these animals. The present results are consistent with previous findings, in which different CXCR4 agonists were found to exert beneficial effects in endotoxemia in vivo. In addition, by detecting effects with the CXCR4 antagonist, AMD3100, that are in direct contrast to those observed with the CXCL12 analog, CTCE-0214D, in endotoxemia, we can hypothesize that treatment with CTCE-0214D exerts its protective effects mainly via CXCR4. Collectively, these data enhance our understanding of the CXCR4/CXCL12 axis in inflammatory diseases and help to clarify the rare, and sometimes contradictory studies, in this field.

Additional file

Additional file 1: Protein content in the liver, serum creatinine and urea levels and TNF alpha assay in THP-1 monocytes as well as macrophages. C57BL/6 N mice were treated either with LPS (5 mg/kg body weight), AMD3100 (5 mg/kg body weight), with both substances or with the solvent PBS (control). 24 h thereafter, the mice were sacrificed and the livers were collected for the determination of the protein content in the 9000 g supernatants by using the Biuret method (A). Also, the blood was obtained and serum creatinine as well as serum urea levels were measured (B, C). Data are given as mean ± standard error of the mean (SEM); $n = 7$ for each group. Statistical significant differences between the different treatment groups were determined by using the one-way analysis of variance (ANOVA) and the Tukey post hoc test and are indicated as follows: *, $p < 0.05$; **, $p < 0.01$; ***, $p < 0.001$ vs. control animals; $^{+}$, $p < 0.05$; $^{++}$, $p < 0.01$; $^{+++}$, $p < 0.001$ vs. LPS treatment. THP-1 cells were cultured in RPMI 1640 supplemented with 10 % fetal bovine serum and 100 nM penicillin/streptomycin (all Capricorn Scientific, Ebsdorfergrund, Germany) and were cultured at a density of about 1.0×10^6/ml at 5 % CO_2 at 37 °C. To obtain THP-1 macrophages, cells were differentiated with PMA (phorbol 12-myristate 13-acetate; Sigma-Aldrich, St. Louis, MO) at a concentration of 40 ng/ml for three days. For the experiments, the cells were pretreated with AMD3100 or CXCL12, respectively, 30 min before LPS was added. After additional 12 h, the media were collected and analyzed for TNF alpha concentration by using a TNF alpha ELISA Kit (Thermo Fisher Scientific, Massachusetts, USA) (D, E). Data are given as mean ± standard error of the mean (SEM); $n = 3$ independent experiments. (PDF 169 kb)

Abbreviations

AP-1: Activator protein 1; CD3/6/8/14/55/68: Cluster of differentiation 3/6/8/14/55/68; CLP: Cecal ligation and puncture; CXCL12: CXC motif chemokine 12; CXCR4: CXC chemokine receptor type 4; CYP: Cytochrome P450; GSH: Reduced glutathione; GSSG: Oxidized glutathione; HEK cells: Human embryonic kidney cells; HO-1: Heme oxygenase 1; HUVEC: Human umbilical vein endothelial cell; IFN gamma: Interferon gamma; IgG: Immunoglobulin G; IL: Interleukin; LPO: Lipid peroxides; LPS: Lipopolysaccharides; MD-2: Myeloid differentiation protein-2; MIF: Macrophage migration inhibitory factor; NF-kB: Nuclear factor 'kappa-light-chain-enhancer' of activated B-cells; NO: Nitric oxide; Nrf-2: Nuclear factor (erythroid-derived 2)-like 2; PBS: Phosphate-buffered saline; PI3K: Phosphatidylinositol-4,5-bisphosphate 3-kinase; PVDF: Polyvinylidene fluoride; ROS: Reactive oxygen species; SDS: Sodium dodecyl sulfate; TLR4: Toll-like receptor 4; TNF alpha: Tumor necrosis factor alpha; TUNEL: TdT-mediated dUTP-biotin nick end labeling; VEGF: Vascular endothelial growth factor

Acknowledgments

The authors would like to thank apl. Prof. Dr. Ralf Claus from the Department of Anaesthesiology and Intensive Care, Jena University Hospital, for enabling the use of the Sysmex pocH-100iV Diff hematology analyzer.

Funding

This research did not receive any specific grant from any funding agency in the public, commercial or not-for-profit sector.

Availability of data and materials

All datasets, on which the conclusions of the manuscript rely on, are presented in the paper.

Authors' contributions

SS and AL designed the research study. SS and AL performed the research. SS and AL analyzed the data. SS and AL wrote the paper. SS and AL approved the final manuscript.

Competing interests

The authors declare that there is no conflict of interest that could be perceived as prejudicing the impartiality of the research reported.

Consent for publication

Not applicable.

Ethics approval and consent to participate

The study was conducted under the licence of the Thuringian Animal Protection Committee (Approval number: 02–044/14). The principles of laboratory animal care and the German Law on the Protection of Animals as well as the Directive 2010/63/EU were followed.

Received: 23 May 2016 Accepted: 27 September 2016
Published online: 03 October 2016

References

1. Saini V, Marchese A, Majetschak M. CXC chemokine receptor 4 is a cell surface receptor for extracellular ubiquitin. J Biol Chem. 2010;285:15566–76. doi:10.1074/jbc.M110.103408.
2. Bernhagen J, Krohn R, Lue H, Gregory JL, Zernecke A, Koenen RR, et al. MIF is a noncognate ligand of CXC chemokine receptors in inflammatory and atherogenic cell recruitment. Nat Med. 2007;13:587–96. doi:10.1038/nm1567.
3. Karin N. The multiple faces of CXCL12 (SDF-1alpha) in the regulation of immunity during health and disease. J Leukoc Biol. 2010;88:463–73. doi:10.1189/jlb.0909602.
4. Ma Q, Jones D, Borghesani PR, Segal RA, Nagasawa T, Kishimoto T, et al. Impaired B-lymphopoiesis, myelopoiesis, and derailed cerebellar neuron migration in CXCR4- and SDF-1-deficient mice. Proc Natl Acad Sci. 1998;95:9448–53. doi:10.1073/pnas.95.16.9448.
5. Oberlin E, Amara A, Bachelerie F, Bessia C, Virelizier JL, Arenzana-Seisdedos F, et al. The CXC chemokine SDF-1 is the ligand for LESTR/fusin and prevents infection by T-cell-line-adapted HIV-1. Nature. 1996;382:833–5. doi:10.1038/382833a0.
6. Bleul CC, Farzan M, Choe H, Parolin C, Clark-Lewis I, Sodroski J, Springer TA. The lymphocyte chemoattractant SDF-1 is a ligand for LESTR/fusin and blocks HIV-1 entry. Nature. 1996;382:829–33. doi:10.1038/382829a0.
7. Lu DY, Tang CH, Yeh WL, Wong KL, Lin CP, Chen YH, et al. SDF-1alpha up-regulates interleukin-6 through CXCR4, PI3K/Akt, ERK, and NF-kappaB-dependent pathway in microglia. Eur J Pharmacol. 2009;613:146–54. doi:10.1016/j.ejphar.2009.03.001.
8. Tang CH, Chuang JY, Fong YC, Maa MC, Way TD, Hung CH. Bone-derived SDF-1 stimulates IL-6 release via CXCR4, ERK and NF-kappaB pathways and promotes osteoclastogenesis in human oral cancer cells. Carcinogenesis. 2008;29:1483–92. doi:10.1093/carcin/bgn045.
9. Chen HT, Tsou HK, Hsu CJ, Tsai CH, Kao CH, Fong YC, Tang CH. Stromal cell-derived factor-1/CXCR4 promotes IL-6 production in human synovial fibroblasts. J Cell Biochem. 2011;112:1219–27. doi:10.1002/jcb.23043.
10. Han Y, He T, Huang PCA, Ransohoff RM. TNF-alpha mediates SDF-1 alpha-induced NF-kappa B activation and cytotoxic effects in primary astrocytes. J Clin Invest. 2001;108:425–35. doi:10.1172/JCI12629.
11. Tamamura H, Fujisawa M, Hiramatsu K, Mizumoto M, Nakashima H, Yamamoto N, et al. Identification of a CXCR4 antagonist, a T140 analog, as

an anti-rheumatoid arthritis agent. FEBS Lett. 2004;569:99–104. doi:10.1016/j.febslet.2004.05.056.
12. Mikami S, Nakase H, Yamamoto S, Takeda Y, Yoshino T, Kasahara K, et al. Blockade of CXCL12/CXCR4 axis ameliorates murine experimental colitis. J Pharmacol Exp Ther. 2008;327:383–92. doi:10.1124/jpet.108.141085.
13. Wang A, Fairhurst A, Tus K, Subramanian S, Liu Y, Lin F, et al. CXCR4/CXCL12 hyperexpression plays a pivotal role in the pathogenesis of lupus. J Immunol. 2009;182:4448–58. doi:10.4049/jimmunol.0801920.
14. Seemann S, Lupp A. Administration of a CXCL12 Analog in Endotoxemia Is Associated with Anti-Inflammatory, Anti-Oxidative and Cytoprotective Effects In Vivo. PLoS One. 2015;10:e0138389. doi:10.1371/journal.pone.0138389.
15. Fan H, Wong D, Ashton SH, Borg KT, Halushka PV, Cook JA. Beneficial effect of a CXCR4 agonist in murine models of systemic inflammation. Inflammation. 2012;35:130–7. doi:10.1007/s10753-011-9297-5.
16. Majetschak M, Cohn SM, Nelson JA, Burton EH, Obertacke U, Proctor KG. Effects of exogenous ubiquitin in lethal endotoxemia. Surgery. 2004;135:536–43. doi:10.1016/j.surg.2003.09.006.
17. Park BS, Lee JO. Recognition of lipopolysaccharide pattern by TLR4 complexes. Exp Mol Med. 2013;45:e66. doi:10.1038/emm.2013.97.
18. Jacob A, Zhou M, Wu R, Wang P. The role of hepatic cytochrome P450 in sepsis. Int J Clin Exp Med. 2009;2:203–11.
19. Triantafilou M, Lepper PM, Briault CD, Ahmed MA, Dmochowski JM, Schumann C, Triantafilou K. Chemokine receptor 4 (CXCR4) is part of the lipopolysaccharide "sensing apparatus". Eur J Immunol. 2008;38:192–203. doi:10.1002/eji.200636821.
20. Jujo KMII, Sekiguchi H, Klyachko E, Misener S, Tanaka T, et al. CXC-chemokine receptor 4 antagonist AMD3100 promotes cardiac functional recovery after ischemia/reperfusion injury via endothelial nitric oxide synthase-dependent mechanism. Circulation. 2013;127:63–73. doi:10.1161/CIRCULATIONAHA.112.099242.
21. Broxmeyer HE, Orschell CM, Clapp DW, Hangoc G, Cooper S, Plett PA, et al. Rapid mobilization of murine and human hematopoietic stem and progenitor cells with AMD3100, a CXCR4 antagonist. J Exp Med. 2005;201:1307–18. doi:10.1084/jem.20041385.
22. Gonnert FA, Recknagel P, Seidel M, Jbeily N, Dahlke K, Bockmeyer CL, et al. Characteristics of clinical sepsis reflected in a reliable and reproducible rodent sepsis model. J Surg Res. 2011;170:e123–34. doi:10.1016/j.jss.2011.05.019.
23. Ellman GL. Tissue sulfhydryl groups. Arch Biochem Biophys. 1959;82:70–7. doi:10.1016/0003-9861(59)90090-6.
24. Hissin PJ, Hilf R. A fluorometric method for determination of oxidized and reduced glutathione in tissues. Anal Biochem. 1976;74:214–26. doi:10.1016/0003-2697(76)90326-2.
25. Yagi T, Day RS. Differential sensitivities of transformed and untransformed murine cell lines to DNA cross-linking agents relative to repair of O6-methylguanine. Mutat Res/DNA Repair Rep. 1987;184:223–7. doi:10.1016/0167-8817(87)90020-4.
26. Lubet RA, Mayer RT, Cameron JW, Nims RW, Burke M, Wolff T, Guengerich F. Dealkylation of pentoxyresorufin: A rapid and sensitive assay for measuring induction of cytochrome(s) P-450 by phenobarbital and other xenobiotics in the rat. Arch Biochem Biophys. 1985;238:43–8. doi:10.1016/0003-9861(85)90138-9.
27. Aitio A. A simple and sensitive assay of 7-ethoxycoumarin deethylation. Anal Biochem. 1978;85:488–91. doi:10.1016/0003-2697(78)90245-2.
28. Pohl RJ, Fouts JR. A rapid method for assaying the metabolism of 7-ethoxyresorufin by microsomal subcellular fractions. Anal Biochem. 1980;107:150–5. doi:10.1016/0003-2697(80)90505-9.
29. Chang TK, Crespi CL, Waxman DJ. Spectrophotometric analysis of human CYP2E1-catalyzed p-nitrophenol hydroxylation. Methods Mol Biol. 2006;320:127–31. doi:10.1385/1-59259-998-2:127.
30. Lupp A, Danz M, Müller D. Morphology and cytochrome P450 isoforms expression in precision-cut rat liver slices. Toxicology. 2001;161:53–66. doi:10.1016/s0300-483x(01)00333-x.
31. McManus JFA. Histological and Histochemical Uses of Periodic Acid. Stain Technol. 2009;23:99–108. doi:10.3109/10520294809106232.
32. Guan S, Guo C, Zingarelli B, Wang L, Halushka PV, Cook JA, Fan H. Combined treatment with a CXCL12 analogue and antibiotics improves survival and neutrophil recruitment and function in murine sepsis. Immunology. 2014. doi:10.1111/imm.12382.
33. Novoa B, Bowman TV, Zon L, Figueras A. LPS response and tolerance in the zebrafish (Danio rerio). Fish Shellfish Immunol. 2009;26:326–31. doi:10.1016/j.fsi.2008.12.004.
34. Delano MJ, Kelly-Scumpia KM, Thayer TC, Winfield RD, Scumpia PO, Cuenca AG, et al. Neutrophil mobilization from the bone marrow during polymicrobial sepsis is dependent on CXCL12 signaling. J Immunol. 2011;187:911–8. doi:10.4049/jimmunol.1100588.
35. Saiman Y, Jiao J, Fiel MI, Friedman SL, Aloman C, Bansal MB. Inhibition of the CXCL12/CXCR4 chemokine axis with AMD3100, a CXCR4 small molecule inhibitor, worsens murine hepatic injury. Hepatol Res. 2015;45:794–803. doi:10.1111/hepr.12411.
36. Devi S, Wang Y, Chew WK, Lima R, A-Gonzalez N, Mattar CN, et al. Neutrophil mobilization via plerixafor-mediated CXCR4 inhibition arises from lung demargination and blockade of neutrophil homing to the bone marrow. J Exp Med. 2013;210:2321–36. doi:10.1084/jem.20130056.
37. Tsuchiya A, Imai M, Kamimura H, Takamura M, Yamagiwa S, Sugiyama T, et al. Increased susceptibility to severe chronic liver damage in CXCR4 conditional knock-out mice. Dig Dis Sci. 2012;57:2892–900. doi:10.1007/s10620-012-2239-8.
38. Mark AL, Sun Z, Warren DS, Lonze BE, Knabel MK, Melville WGM, et al. Stem cell mobilization is life saving in an animal model of acute liver failure. Ann Surg. 2010;252:591–6. doi:10.1097/SLA.0b013e3181f4e479.
39. Dai S, Yuan F, Mu J, Li C, Chen N, Guo S, et al. Chronic AMD3100 antagonism of SDF-1alpha-CXCR4 exacerbates cardiac dysfunction and remodeling after myocardial infarction. J Mol Cell Cardiol. 2010;49:587–97. doi:10.1016/j.yjmcc.2010.07.010.
40. Bach 4th HH, Saini V, Baker TA, Tripathi A, Gamelli RL, Majetschak M. Initial assessment of the role of CXC chemokine receptor 4 after polytrauma. Mol Med. 2012;18:1056–66. doi:10.2119/molmed.2011.00497.
41. Kishore SP, Bungum MK, Platt JL, Brunn GJ. Selective suppression of Toll-like receptor 4 activation by chemokine receptor 4. FEBS Lett. 2005;579:699–704. doi:10.1016/j.febslet.2004.12.047.
42. Imaizumi T, Itaya H, Fujita K, Kudoh D, Kudoh S, Mori K, et al. Expression of Tumor Necrosis Factor- in Cultured Human Endothelial Cells Stimulated With Lipopolysaccharide or Interleukin-1. Arterioscler, Thrombo, Vasc Biol. 2000;20:410–5. doi:10.1161/01.ATV.20.2.410.
43. Valko M, Leibfritz D, Moncol J, Cronin MT, Mazur M, Telser J. Free radicals and antioxidants in normal physiological functions and human disease. Int J Biochem Cell Biol. 2007;39:44–84. doi:10.1016/j.biocel.2006.07.001.
44. Kim YS, Morgan MJ, Choksi S, Liu ZG. TNF-induced activation of the Nox1 NADPH oxidase and its role in the induction of necrotic cell death. Mol Cell. 2007;26:675–87. doi:10.1016/j.molcel.2007.04.021.
45. Totemeyer S, Sheppard M, Lloyd A, Roper D, Dowson C, Underhill D, et al. IFN-gamma enhances production of nitric oxide from macrophages via a mechanism that depends on nucleotide oligomerization domain-2. J Immunol. 2006;176:4804–10.
46. de Cruz SJ, Kenyon NJ, Sandrock CE. Bench-to-bedside review: the role of nitric oxide in sepsis. Expert Rev Respir Med. 2009;3:511–21. doi:10.1586/ers.09.39.
47. Chung SW, Liu X, Macias AA, Baron RM, Perrella MA. Heme oxygenase-1-derived carbon monoxide enhances the host defense response to microbial sepsis in mice. J Clin Invest. 2008;118:239–47. doi:10.1172/jci32730.
48. Tamion F, Richard V, Renet S, Thuillez C. Protective effects of heme-oxygenase expression against endotoxic shock: inhibition of tumor necrosis factor-alpha and augmentation of interleukin-10. J Trauma. 2006;61:1078–84. doi:10.1097/01.ta.0000239359.41464.ef.
49. Ma Q. Role of nrf2 in oxidative stress and toxicity. Annu Rev Pharmacol Toxicol. 2013;53:401–26. doi:10.1146/annurev-pharmtox-011112-140320.
50. Kuiper J, de Rijke YB, Zijlstra FJ, van Waas MP, van Berkel TJ. The induction of glycogenolysis in the perfused liver by platelet activating factor is mediated by prostaglandin D2 from Kupffer cells. Biochem Biophys Res Commun. 1988;157:1288–95.
51. Kmiec Z. Cooperation of liver cells in health and disease. Adv Anat Embryol Cell Biol. 2001;161:III–XIII. 1-151.
52. Goto M, Yoshioka T, Battelino T, Ravindranath T, Zeller WP. TNFalpha decreases gluconeogenesis in hepatocytes isolated from 10-day-old rats. Pediatr Res. 2001;49:552–7. doi:10.1203/00006450-200104000-00018.

4.3 Manuskript III: Administration of a CXCL12 analog in endotoxemia is associated with anti-inflammatory, anti-oxidative and cytoprotective effects in vivo

PLoS One. 2015 Sep 16;10(9):e0138389. DOI: 10.1371/journal.pone.0138389.

Semjon Seemann, Amelie Lupp

Status:

Eingereicht am: 13. Juli 2015

Akzeptiert am: 28. August 2015

Veröffentlicht am: 16. September 2015

Autorenschaft:

Erstautor

Beitrag der Autoren:

Semjon Seemann und Amelie Lupp haben das Projekt entwickelt, die Experimente durchgeführt, die Daten ausgewertet und das finale Manuskript geschrieben. Amelie Lupp stellte die Reagenzien und die analytischen Werkzeuge zur Verfügung.

Zusammenfassung

Aufgrund des in Manuskript II beschriebenen negativen Einflusses einer CXCR4-Blockade mittels AMD3100, ergab sich als Konsequenz, ein CXCL12-Analogon in der akuten systemischen Entzündung zu untersuchen. Zielstellung des **Manuskripts III** war folglich, parallel zum Manuskript II, die systemischen Effekte einer CXCR4-Stimulation aufzudecken, die Auswirkungen auf die LPS-induzierten Organschäden zu untersuchen und die Hypothese zu bestätigen, dass eine Aktivierung der CXCR4-CXCL12-Achse einen positiven Einfluss haben könnte. Aufgrund der sehr geringen Halbwertszeit von freiem CXCL12 von nur wenigen Sekunden wurde die Synthese des plasmastabilen peptidischen CXCL12-Analogons CTCE-0214D in Auftrag gegeben. Diese Substanz wurde kurz vor der LPS-Gabe den Mäusen subkutan injiziert und das Experiment wurde analog zu Manuskript II durchgeführt und nach 24 Stunden beendet. Die Behandlungsgruppen gliederten sich in eine Kontrollgruppe mit Lösungsmittelgabe, eine Gruppe, die nur das LPS appliziert bekam, eine Gruppe, der nur das CTCE-0214D verabreicht wurde und in eine Gruppe von Mäusen, die sowohl LPS als auch CTCE-0214D injiziert bekamen. Wie in Manuskript II wurden der Gesundheitszustand der Mäuse, die Körpertemperatur, verschiedene Blut- und Serumparameter, der oxidative Stress in den Organen sowie der Glykogengehalt und die Biotransformationskapazität in den Lebern bestimmt. Ferner wurden mittels Immunhistochemie verschiede Marker für oxidativen Stress, für apoptotische Prozesse sowie die Zytokinexpression und Immunzellmarker in den Lebern und Milzen ermittelt. CTCE-0214D verringerte die TNF-α-, IFN-γ- und Blutzuckerwerte im Vergleich zur LPS-Gruppe deutlich. Außerdem reduzierte die Substanz den oxidativen Stress im Leber- und Milzgewebe und erhöhte den Glykogengehalt und die Biotransformationskapazität der Lebern deutlich. Darüber hinaus verminderte CTCE-0214D die Expression von CXCR4, CXCL12 und NF-κB in den Organen und führte zu einer geringeren Apoptoserate in der Milz. CTCE-0214D alleine war außerdem in der Lage die HO-1 stark zu induzieren. Zusammenfassend wirkte sich die Gabe des CXCL12-Analogons entzündungshemmend, antioxidativ und zytoprotektiv aus und stellt somit eine vielversprechende neue Behandlungsmöglichkeit akuter systemischer Entzündungen dar. Vor allem im Zusammenhang mit einer mit der systemischen Entzündung einhergehenden Leberfunktionsstörung und übermäßigen Produktion freier Radikale erscheint die CXCR4-Aktivierung therapeutisch erfolgsversprechend und sollte weiterverfolgt werden.

PLOS | ONE

RESEARCH ARTICLE

Administration of a CXCL12 Analog in Endotoxemia Is Associated with Anti-Inflammatory, Anti-Oxidative and Cytoprotective Effects *In Vivo*

Semjon Seemann*☯, Amelie Lupp☯

Institute of Pharmacology and Toxicology, Jena University Hospital, Friedrich Schiller University Jena, Jena, Germany

☯ These authors contributed equally to this work.
* semjon.seemann@yahoo.com

OPEN ACCESS

Citation: Seemann S, Lupp A (2015) Administration of a CXCL12 Analog in Endotoxemia Is Associated with Anti-Inflammatory, Anti-Oxidative and Cytoprotective Effects *In Vivo*. PLoS ONE 10(9): e0138389. doi:10.1371/journal.pone.0138389

Editor: Partha Mukhopadhyay, National Institutes of Health, UNITED STATES

Received: July 13, 2015

Accepted: August 28, 2015

Published: September 16, 2015

Data Availability Statement: All relevant data are within the paper and its Supporting Information files.

Funding: This research did not receive any specific grant from any funding agency in the public, commercial or not-for-profit sector.

Competing Interests: The authors have declared that no competing interests exist.

Abstract

Background

The chemokine receptor CXCR4 is a multifunctional receptor which is activated by its natural ligand C-X-C motif chemokine 12 (CXCL12). As CXCR4 is part of the lipopolysaccharide sensing complex and CXCL12 analogs are not well characterized in inflammation, we aimed to uncover the systemic effects of a CXCL12 analog in severe systemic inflammation and to evaluate its impact on endotoxin induced organ damages by using a sublethal LPS dose.

Methods

The plasma stable CXCL12 analog CTCE-0214D was synthesized and administered subcutaneously shortly before LPS treatment. After 24 hours, mice were sacrificed and blood was obtained for TNF alpha, IFN gamma and blood glucose evaluation. Oxidative stress in the liver and spleen was assessed and liver biotransformation capacity was determined. Finally, CXCR4, CXCL12 and TLR4 expression patterns in liver, spleen and thymus tissue as well as the presence of different markers for apoptosis and oxidative stress were determined by means of immunohistochemistry.

Results

CTCE-0214D distinctly reduced the LPS mediated effects on TNF alpha, IFN gamma, ALAT and blood glucose levels. It attenuated oxidative stress in the liver and spleen tissue and enhanced liver biotransformation capacity unambiguously. Furthermore, in all three organs investigated, CTCE-0214D diminished the LPS induced expression of CXCR4, CXCL12, TLR4, NF-κB, cleaved caspase-3 and gp91 phox, whereas heme oxygenase 1 expression and activity was induced above average. Additionally, TUNEL staining revealed anti-apoptotic effects of CTCE-0214D.

Conclusions

In summary, CTCE-0214D displayed anti-inflammatory, anti-oxidative and cytoprotective features. It attenuated reactive oxygen species, induced heme oxygenase 1 activity and mitigated apoptosis. Thus, the CXCR4/CXCL12 axis seems to be a promising target in the treatment of acute systemic inflammation, especially when accompanied by a hepatic dysfunction and an excessive production of free radicals.

Introduction

Administration of bacterial endotoxin represents a well-established animal model to investigate systemic inflammation and is frequently used to study the host's innate immune response [1]. One of the main structures that play an important role in the innate immune system is represented by the toll-like receptors (TLR) necessary for the recognition of several pathogen-associated molecular patterns. Exposure of mammals to LPS leads, in particular, to an increased release of pro-inflammatory cytokines through TLR4-signaling. LPS hereby binds the lipopolysaccharide binding protein and interacts with a receptor complex formed by CD14 (cluster of differentiation 14), MD-2 (myeloid differentiation protein-2) and TLR4, which then results in TLR4 transduced signals that in turn lead to an increased expression of NF-κB, proteases and reactive oxygen and nitrogen species [2]. In septic and acute inflammatory diseases, widespread activation of TLR4 has been detected by different authors leading to the conclusion that TLR4 activation has to be limited [3]. It is known that other extracellular proteins—such as heat shock proteins (HSP 70 and HSP 90), CD55 and the chemokine receptor 4 (CXCR4) are able to influence TLR4 signaling, thus representing an interesting target to prevent TLR4 activation [4,5]. Concerning CXCR4, its importance has been demonstrated by showing that it is part of the "LPS-sensing apparatus" [6], suggesting that intervention with CXCR4 agonists or antagonists could result in reduced TLR4 signaling. Furthermore, intervention with a CXCR4 ligand could weaken LPS effects which are triggered by LPS binding to CXCR4 directly. Naturally, CXCR4 is activated by its ligand CXCL12, also known as stromal cell-derived factor 1 (SDF-1), which represents a multifunctional cytokine. CXCL12 is constitutively expressed by various cells and tissues, and exhibits chemo-attractive activity for monocytes, bone marrow neutrophils, and early stage B cell precursors [7,8]. It is also a highly efficient and potent chemoattractant for T cells, as well as a co-stimulator of their activation [9]. Moreover, CXCR4 deficient mice are not able to survive [10]. This impressively demonstrates the physiological importance of the CXCR4/CXCL12 axis. Recently, the diagnostic value has been shown in neonatal sepsis, where elevated CXCR4 and CXCL12 levels were accompanied by increased sepsis severity [11]. The involvement of the CXCR4/CXCL12 axis in autoimmune and inflammatory diseases is undisputed as treating rheumatoid arthritis, inflammatory bowel disease or lupus erythematodes with CXCR4-antagonists revealed beneficial outcomes [12–14]. As it turned out, CXCR4 and CXCL12 occurred above average in the affected tissue, so inhibition of the CXCR4/CXCL12 axis resulted in lower inflammatory responses—probably because less CXCR4 positive cells entered the tissue. In contrast, activation of the CXCR4 seemed to have positive effects on such systemic and acute diseases as sepsis or polytrauma and, there is evidence that in vivo treatment with CXCL12 analogs results in improved survival [15,16]. Nevertheless, the existing data concerning the role of the CXCR4/CXCL12 axis in inflammatory diseases remains contradictious and up to now, no further investigations were carried out to determine what exact effects a CXCL12 analog exerts in endotoxemia systemically and in the

organs. We are the first to investigate the impact of a CXCL12 analog on a sublethal dose of endotoxin as we tested the plasma stable derivative of CXCL12, CTCE-0214D, and its influence on LPS induced organ damages. In contrast to others, we did not aim to investigate the impact of CTCE-0214D on the mortality rate as there are already data available which prove a beneficial influence of the CXCL12 analog CTCE-0214 in vivo both without and with co-treatment with other drugs [15,17,18]. Hence, we applied a sublethal dose of endotoxin, because we aimed to understand the effects mediated through the CXCL12 analog and to confirm the previously shown positive impact on septic shock. We focused on liver, spleen and thymus function to evaluate a possible beneficial impact of the treatment and to gain an idea concerning the underlying processes and effects. In addition, we were interested in the CXCR4/CXCL12 expression patterns and how these were changed during disease progression.

Material and Methods

CTCE-0214D

As CXCL12 is known to have a short half-life, we designed the plasma stable peptide CTCE-0214D in analogy to the peptide CTCE-0214 originally developed by Chemokine Therapeutics. CTCE-0214D was custom synthesized by Centic Biotec, Heidelberg, Germany. By using a four-glycine linker, the N-terminal region (residues 1–14) was connected to the C-terminal region (residues 55–66) of CXCL12, while (in contrast to CTCE-0214) the last amino acid (asparagine) was substituted by aspartate to avoid license problems. As previously shown, slight deviations in C terminal regions barely affect affinity to and activation of the CXCR4 [19,20]. The analogue is cyclized between the amino acid residues at the positions 20 and 24 by an isopeptide bond. To achieve plasma stability, the two cysteins were replaced by alanine and phenylalanine, respectively. The amino acid sequence of the peptide as one-letter code is as follows: KPVSLSYRAPFRFF-GGGG-LKWIQEYLEKALD.

Animals and experimental procedure

The study was conducted under the licence of the Thuringian Animal Protection Committee (Reg-Nr.: 02-044/14). The principles of laboratory animal care and the German Law on the Protection of Animals as well as the Directive 2010/63/EU were followed. Male adult C57BL/6N mice (12-weeks-old, body weight 25–30 g; Charles River Laboratories, Sulzfeld, Germany) were used. The animals were housed in plastic cages under standardized conditions (light-dark cycle 12/12 h, temperature 22 ± 2°C, humidity 50 ± 10%, pellet diet Altromin 1316, water ad libitum). A total of 28 mice was randomly divided into four groups (n = 7 each): Control, LPS, CTCE-0214D and CTCE-0214D plus LPS. LPS (E. coli 0111:B4, Sigma Aldrich, Steinheim, Germany) was injected intraperitoneally (5 mg/kg body weight), whereas CTCE-0214D (20 mg/kg body weight) was administered in 0.9% saline shortly before endotoxemia onset subcutaneously. The most appropriate LPS dose was determined in a pilot study, in which we administered 1 mg/kg, 5 mg/kg or 10 mg/kg body weight LPS, respectively. As 5 mg/kg body weight LPS caused no mortality and the LPS effect was strong enough to detect possible beneficial effects after co-treatment with potential drugs, we chose this dosage for our further investigations. The dose of CTCE-0214D was selected based on previous publications, which investigated the CXCL12 analog CTCE-0214 in vivo [15, 21,22]. As we aimed a prolonged effect of the CXCL12 analog, we administered CTCE-0214D subcutaneously and chose a higher concentration than the minimum effective dose of 10 mg/kg body weight. The study design was chosen as the subcutaneous administration results in a delayed release and thereby in a prolonged effect, as the drug has to be initially absorbed, whereas the intraperitoneal LPS injection causes an immediate inflammatory response. 24 hours after LPS treatment, body temperature

was measured and the mice's condition was assessed by using the Clinical Severity Score (CSS) described previously [23]. Afterwards, the mice were sacrificed in isoflurane anesthesia and their liver, spleen and thymus were removed, weighed and either fixed in 10% buffered formaldehyde or snap-frozen in liquid nitrogen for biochemical analysis. Additionally, whole-blood was collected and blood sugar levels were determined using a commercially available blood glucose meter and respective test strips (BG star®, Sanofi-Aventis, Frankfurt, Germany). Subsequently, serum was obtained and used for ELISA measurements. To perform histological analysis, the formalin-fixed organ samples were embedded in paraffin blocks and cut into 4 μm thin sections (n = 7 for each treatment group).

IFN-γ, TNF-α, aspartate aminotransferase (ASAT) and alanine aminotransferase (ALAT) assays

To determine the serum levels of interferon-γ, TNF-α, ASAT and ALAT, mouse IFN-γ ELISA kit (Pierce Biotechnology, Rockford, IL, USA), mouse TNF-alpha Quantikine ELISA kit (R&D Systems, MA, USA), EnzyChrom™ Aspartate Transaminase Assay Kit or EnzyChrom™ Alanine Transaminase Assay Kit (both BioAssay Systems, Hayward, CA, USA), respectively, were used according to the manufacturer's instructions.

Oxidative status in the tissues

The tissue content of glutathione in its reduced (GSH) and oxidized (GSSG) form was analyzed by homogenizing the samples with eleven volumes of 0.2 M sodium phosphate buffer (5 mM EDTA; pH 8.0) and four volumes of 25% metaphosphoric acid. After centrifugation (12000g, 4°C, 30 min) GSH content was measured in the supernatants using a colorimetric assay as previously described [24]. The GSSG concentration was assessed fluorometrically [25]. To determine the tissue content of lipid peroxides (LPO) as thiobarbituric acid reactive substances (TBARS), liver samples were homogenized with 19 volumes of ice-cold saline and analyzed fluorometrically [26]. Additionally, HO-1 (heme oxygenase 1) activities were measured in the liver 9000g supernatants (prepared as described under"biotransformation capacity") using hemin as a substrate. The amount of bilirubin formed was determined photometrically and referred to the incubation time and to the protein content of the respective 9000g supernatants [27].

Biotransformation capacity

To obtain 9000g supernatants, the livers were homogenized with 0.1 M sodium phosphate buffer (pH 7.4) (1:2 w/v) and subsequently centrifuged at 9000g for 20 minutes at 4°C. Activities of all biotransformation reactions were assessed in these 9000g supernatants and referred to the protein content of this fraction which was determined with a modified Biuret method [28]. For assessment of cytochrome P450 (CYP) enzyme activities, the following model reactions were performed: benzyloxyresurofin-O-debenzylation (BROD; [29]), ethoxycoumarin-O-deethylation (ECOD; [30]), ethoxyresorufin-O-deethylation (EROD; [31]), ethylmorphine-N-demethylation (EMND; [32]), methoxyresorufin-O-demethylation (MROD; [31]), p-nitrophenol-hydroxylation (PNPH; [33]), pentoxyresorufin-O-depentylation (PROD; [31]). Glutathione-S-transferase (GST) activities were determined by photometrically measuring the resulting dinitrobenzene-glutathione conjugate, GS-DNB [34].

Histopathology and immunohistochemistry

Four-μm-sections were prepared from the paraffin blocks and floated onto positively charged slides. Immunostaining was performed by an indirect peroxidase labeling method as described

previously [35]. Briefly, sections were dewaxed, microwaved in 10 mM citric acid (pH 6.0) for 16 min at 600 W and then incubated with the respective primary antibodies (Table 1) at 4°C overnight. Detection of the primary antibody was performed using either a biotinylated goat anti-rabbit IgG, rabbit anti-goat IgG or horse anti-mouse IgG, respectively, followed by an incubation with peroxidase-conjugated avidin (Vector ABC "Elite" kit, Vector, Burlingame, CA, USA). Binding of the primary antibody was visualized using 3-amino-9-ethylcarbazole (AEC) in acetate buffer (BioGenex, San Ramon, CA, USA). The sections were then rinsed, counterstained with Mayer's hematoxylin and mounted in Vectamount™ mounting medium (Vector Laboratories, Burlingame, CA, USA). Additionally, TUNEL (TdT-mediated dUTP-biotin nick end labeling) staining was performed by using the In Situ Cell Death Detection Kit, POD (Roche Diagnostics, Mannheim, Germany) according to manufacturer's instructions. All immunohistochemical stainings were evaluated by two independent investigators. In the case of a discrepancy in the scoring between the two investigators a final decision was achieved by consensus. In spleen and thymus, the occurrence was assessed as follows: 0: negative; 1: seldom; 2: frequent; 3: diffuse. Additionally, the intensity of staining was evaluated as follows: 0: no staining; 1: mild; 2: moderate; 3: strong. In the livers, occurrence and staining intensity of Kupffer and pit cells were determined using the same rating. To detect the glycogen content in the livers, periodic-acid-Schiff staining (PAS; periodic acid, Schiff's reagent: Sigma Aldrich, Steinheim, Germany) was performed by using standard protocols [36]. Identification of the specific cell types was based on their microscopic features along with the relative location of the cells in the respective tissues.

Statistical Analysis

All statistical analyses and figures were computed with GraphPad Prism 6.0 software (GraphPad Software, La Jolla, CA, USA). All experiments were performed with seven animals per experimental group and statistical significance was determined by using the one-way analysis of variance (ANOVA) and the Tukey post hoc test. A p value of less than 0.05 (*) was considered as statistically significant; a p value of less than 0.01 (**) and a p value of less than 0.001 (***) are denoted separately. Data are given as mean ± standard error of the mean (SEM).

Results

Blood glucose, body temperature and general condition

To examine the systemic influence of the CXCL12 analog, blood sugar levels, body temperatures and body and organ weights of all animals were determined. Additionally, the general condition of the mice was assessed by using the Clinical Severity Score. 24 hours after treatment, blood glucose levels of LPS challenged mice were significantly reduced by more than

Table 1. Primary antibodies used for the immunohistochemical investigations.

Primary antibody	Type, Catalogue number	Manufacturer	Dilution	Host species
CXCR4	monoclonal, 3108–1	Epitomics	1:50	Rabbit
CXCL12	monoclonal, MAB350	R&D Systems	1:500	Mouse
TLR4	polyclonal, sc-12511	Santa Cruz Biotechnology	1:500	Goat
NF-κB	monoclonal, sc-8008	Santa Cruz Biotechnology	1:500	Mouse
cleaved caspase-3	monoclonal, 9661	Cell Signaling Technology	1:600	Rabbit
gp91 phox	polyclonal, sc-5827	Santa Cruz Biotechnology	1:500	Goat
Heme oxygenase 1	polyclonal, SPA-895	Biomol GmbH	1:5000	Rabbit

doi:10.1371/journal.pone.0138389.t001

50% when compared to control animals, whereas CTCE-0214D plus LPS treated mice showed only a slight, but non-significant reduction of the values by about 20% when compared to the control group. However, in comparison to the LPS group, concomitant administration of CTCE-0214D to LPS treatment caused an increase in the blood glucose levels by more than 60% ($p \leq 0.01$). Mice receiving CTCE-0214D alone showed no relevant difference in blood glucose levels to the control group (Fig 1).

After 24 hours, endotoxic mice displayed a reduced body temperature in comparison to the control animals (36.2±0.2°C vs. 37.2±0.3°C, $p = 0.09$) and to the CTCE 0214D plus LPS group (37.1±0.3°C, vs. LPS, $p = 0.14$). In accordance with these results, the CSS was improved after CTCE-0214D plus LPS treatment as compared to mice which had received LPS only (1.9±0.4 vs. 2.5±0, $p \leq 0.001$). No relevant influence of CTCE-0214D alone was detectable. In contrast to the effects seen on body temperature and on general condition, the CXCL12 analog had no impact on LPS induced body weight reduction (both treatment groups approximately -3.0g).

TNF-α and IFN-γ serum levels

To investigate the impact of CTCE-0214D on endotoxemia, we measured serum cytokine levels at sacrifice. Compared to the control group, administration of LPS caused an elevation of serum TNF-α by about 330%, whereas CTCE-0214D was able to reduce the LPS-induced increase in serum TNF-α levels by more than 30%. Similar results were found when serum INF-γ concentrations were determined. In comparison to the control group, the LPS challenge provoked an increase by about 160%, while CTCE-0214D plus LPS co-administration resulted in not significantly elevated serum INF-γ concentrations. In comparison to the LPS treated animals, the CTCE-0214D plus LPS group showed almost two-fold lower serum IFN-γ levels ($p = 0.02$). In both ELISAs, no relevant influence of CTCE-0214D alone was detectable (Fig 1).

Liver: Oxidative stress, biotransformation capacity, cytokines and apoptosis

As the aminotransferases ASAT and ALAT are part of the diagnostic evaluation to determine liver health, we measured the serum levels of both enzymes (S2 Fig), however ALAT represents a more specific indicator of liver inflammation than ASAT. Endotoxin caused a massive increase in the serum concentration of both enzymes when compared to the control group (ASAT: 63.0±7.4 U/L vs. 98.3±9.0 U/L, $p = 0.005$; ALAT: 35.7±4.6 U/L vs. 85.7±16.5; $p = 0.002$). CTCE-0214D was able to decrease the enzyme activities throughout. The ASAT activities were reduced by about 15% when compared to the LPS group, whereas the ALAT activities showed a significant reduction of about 60% ($p = 0.002$). Remarkably, the ALAT activities of the control and of the CTCE-0214D plus LPS group are at the same level (35.7±4.6 U/L vs. 33.6±4.8 U/L, $p = 0.98$). To determine whether CTCE-0214D may attenuate LPS induced ROS production in liver tissue, the content of lipid peroxidation products (LPO) as well as the glutathione status was measured. Furthermore, we were interested in CYP and glutathione-S-transferase activities, which are known to be down regulated by endotoxin [37,38]. 24 hours after induction of endotoxemia, the livers of LPS treated mice had a more than 10 fold higher LPO concentration compared to control animals. Moreover, endotoxin caused a decrease in the total glutathione content to approximately 75% of the control level, whereas the GSH/GSSG ratio showed only a slight reduction. CTCE-0214D was able to diminish the LPS effects significantly. In doing this, the CXCL12 analog reduced the LPO content almost by half (vs. LPS $p = 0.005$) and was able to significantly increase the total glutathione content (vs. LPS $p = 0.003$)—corresponding to almost 90% of the control level. By increasing the reduced glutathione concentration by approximately 20% in regard to LPS ($p \leq 0.001$), the GSH/GSSG ratio

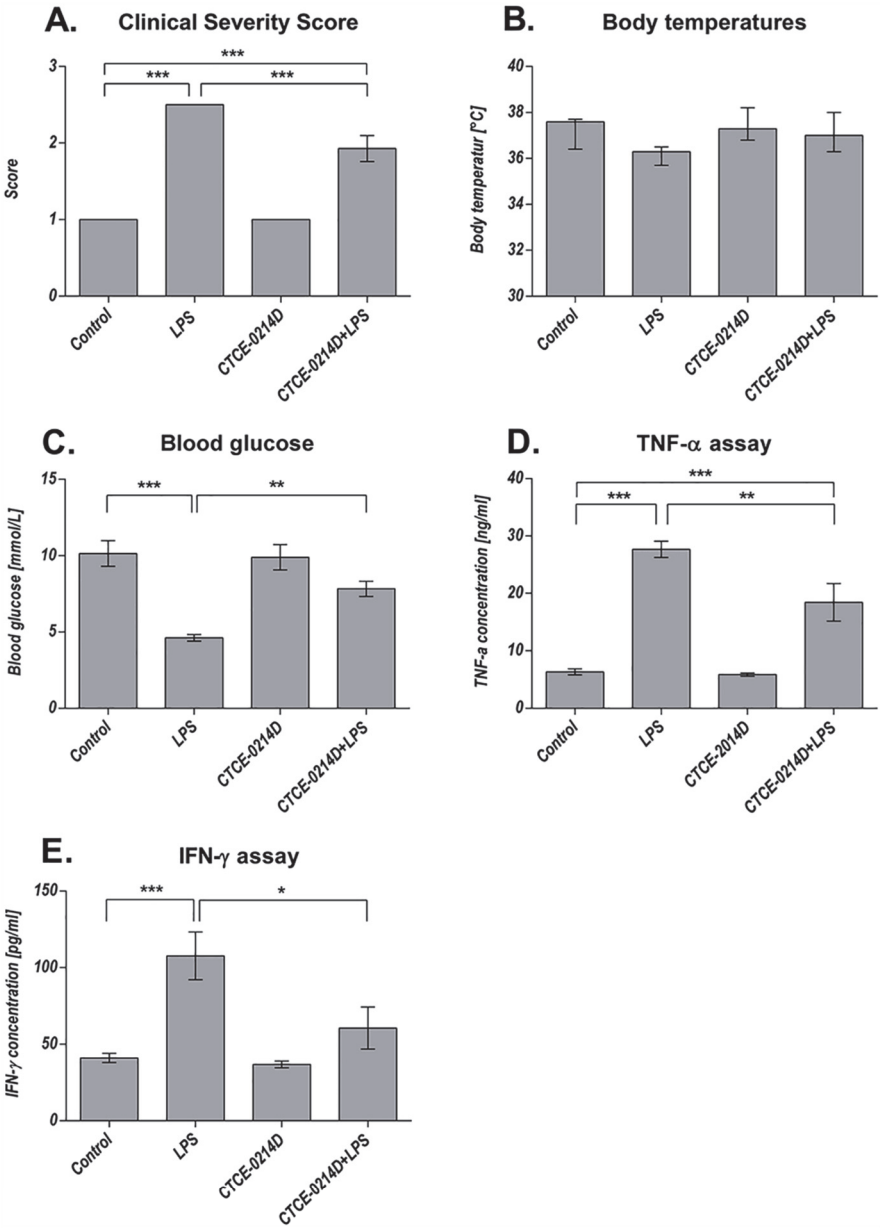

Fig 1. Clinical Severity Score, body temperatures, blood glucose, serum TNF-α and IFN-γ levels. 24 hours after LPS administration, the Clinical severity score was improved after CTCE-0214D plus LPS treatment as compared to mice which had received LPS only (A, 1.9±0.4 vs. 2.5±0, $p \leq 0.001$). In addition, endotoxic mice showed reduced body temperatures in comparison to the control (B, 36.2±0.2°C vs. 37.2±0.3°C, $p = 0.09$) and to the CTCE 0214D plus LPS group (37.1±0.3°C, vs. LPS $p = 0.14$). Moreover, a decrease of blood glucose levels (C) by about 50% when compared to the control group was seen (4.6±0.2 mmol/L vs. 10.1±0.9 mmol/L, $p \leq 0.001$). The CTCE-0214D plus LPS group showed a blood sugar level of 7.8±0.5 mmol/L, which is equivalent to an elevation by more than 65% when compared to endotoxin treatment only ($p \leq 0.01$). In addition, no significance was detectable in comparison to the control group. Serum TNF-α concentrations (D) were significantly reduced after co-administration of CTCE-0214D and LPS (27.7±1.4 ng/mL vs. 18.5±3.3 ng/mL, $p \leq 0.01$), while LPS caused an increase of more than 330% in comparison to the control group (6.6±0.5 ng/mL, $p \leq 0.001$). Similar results were achieved when determining serum

IFN-γ levels (E). Compared to the control, the LPS challenge provoked an increase of approximately 160% (107.7±15.6 pg/mL vs. 41.1±3.0 pg/mL, $p \leq 0.001$), while CTCE0214D plus LPS co-administration did not result in significantly elevated serum INF-γ concentrations (60.5±13.8 pg/mL vs. 41.1±3.0 pg/mL, $p = 0.58$). Statistical significance ($p \leq 0.05$) was determined by using the one-way analysis of variance (ANOVA) and the Tukey post hoc test. Data are given as mean ± standard error of the mean (SEM), n = 7; *, $p \leq 0.05$; **, $p \leq 0.01$; ***, $p \leq 0.001$.

doi:10.1371/journal.pone.0138389.g001

was enhanced significantly ($p \leq 0.001$)—once again underlining CTCE-0214D's protective effects (Fig 2). In accordance with these results, the endotoxin-induced activity loss of several CYP families was attenuated. By determining CYP1A, 2A, 2B, 2C (ECOD) or CYP1A, 2A, 2B, 2C, 3A (BROD) activities, respectively, CTCE-0214D's protective effect was underlined impressively when compared to LPS treatment. Especially, when activities of specific CYP families were ascertained, LPS turned out to impair CYP1A activities to approximately 40% of the control values, whereas there was no significant difference in the values between CTCE-0214D plus LPS and saline treated mice. Similar results were observed when measuring activities of CYP1A2, CYP3A, CYP2B and CYP1E. In comparison to LPS alone, co-administration of the CXCL12-analog and endotoxin increased CYP activities by approximately 35%, 70%, 90% and 120%, yet being significantly decreased when compared to control levels. Fittingly, we witnessed increased glutathione-s-transferase activities of about 20% when comparing the CTCE-0214D plus LPS to the LPS group (Fig 3).

To gain further information on the actions of CTCE-0214D in endotoxemia, we used Periodic acid-Schiff and immunohistochemial stainings. Exposure to LPS evoked an impressive loss of glycogen content in the livers, whereas the livers of CTCE-0214D plus LPS treated mice showed no difference to the control group at all (Fig 4A–4C). Moreover, many Kupffer and pit cells were perceivable after the LPS challenge, while the CXCL12 analog caused a reduction in these cells. Immunohistochemically, differences were noticeable in the amount and staining intensity of Kupffer and pit cells. Almost all hepatocytes were stained non-specifically. The administration of endotoxin led to an increased expression of CXCR4, NF-κB, cleaved caspase-3 and gp91 phox in Kupffer and pit cells (Table 2). Throughout, a staining of these target structures was seldom found in the livers of CTCE-0214D plus LPS treated mice. In fact, there was often no obvious difference recognizable when compared to the control group (Table 2). Suitably, CTCE-0214D's protective features were visible when observing HO-1 expression (Fig 4D–4H). While the antioxidant enzyme was evidently up-regulated after LPS exposure, CTCE-0214D plus LPS treatment caused the highest HO-1 expression in Kupffer and pit cells. In addition, it should be mentioned that the animals treated with CTCE-0214D only already showed a higher HO-1 expression throughout in comparison to the control group (Table 2 and Fig 4D–4H). In parallel to the immunohistochemical stainings also the HO-1 activity was measured in the liver 9000g supernatants. LPS, CTCE-0214D and CTCE-0214D plus LPS administration increased the HO-1 activity by approximately 90%, 120% and 210%, respectively, when compared to the control group. The combined CTCE-0214D plus LPS treatment revealed the highest HO-1 activity levels, which were additionally significantly elevated in comparison to the values of the LPS or CTCE-0214D group, respectively (Fig 4I).

Spleen: Oxidative stress, CXCR4/CXCL12 axis, TLR4, apoptosis and HO-1

To determine the influence of the CXCL12 analog on the oxidative status, we measured the glutathione level in splenic tissue. While the total glutathione content was almost similar throughout, the GSH/GSSG ratio of CTCE-0214D plus LPS treated mice was enhanced when compared to endotoxic ones, an effect, which was mainly due to significantly reduced GSSG concentrations (Fig 2).

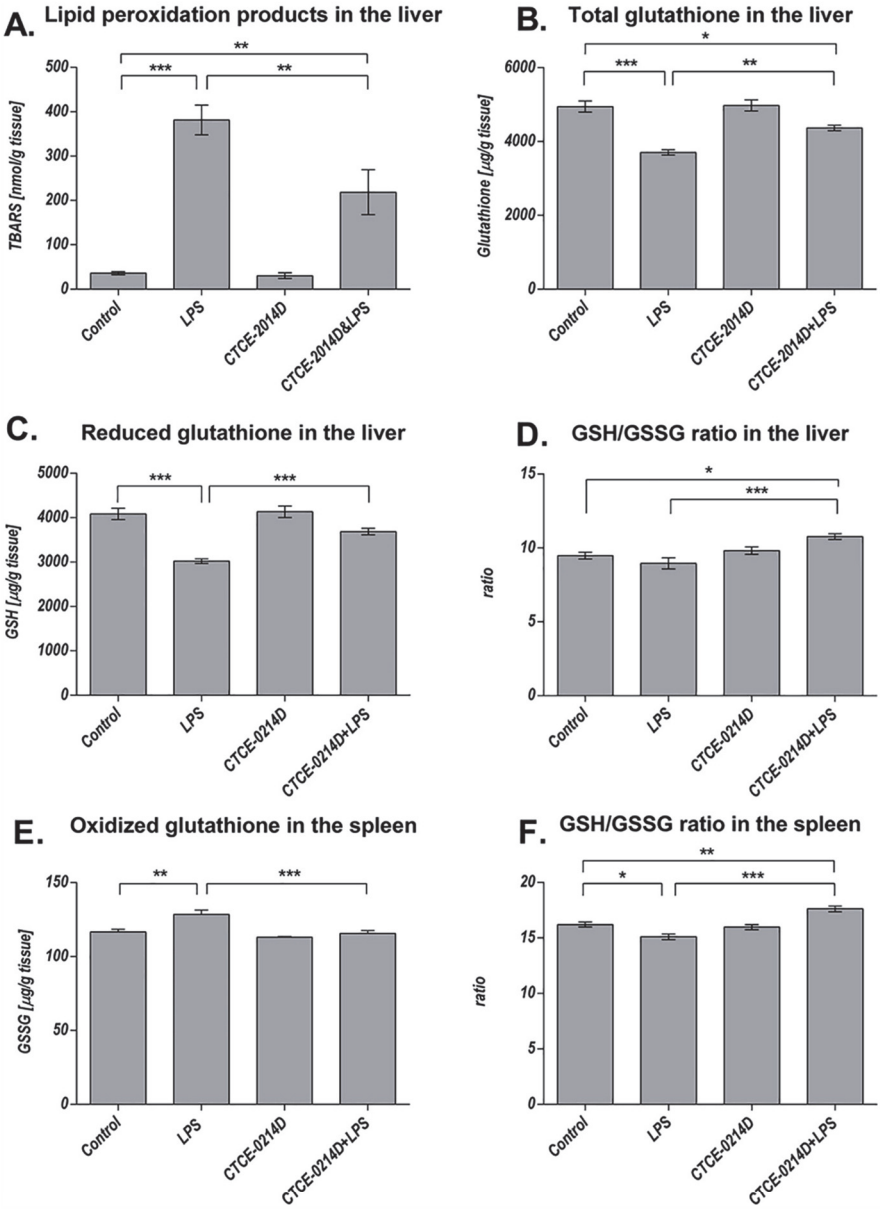

Fig 2. Oxidative stress in the liver and spleen. Tissue content of lipid peroxidation products as determined by thiobarbituric acid reactive substances (TBARS) in the livers of all animal groups 24 hours after treatment (A). CTCE-0214D reduced TBARS elevated due to endotoxemia to almost the half. As further parameters, total glutathione content (B), reduced glutathione levels (GSH, C) and the GSH/GSSG ratio were evaluated (D). In comparison to the control group, endotoxin caused a decrease in the total as well as reduced glutathione content and minimized the GSH/GSSG ratio, while co-administration of CTCE-0214D was able to mitigate all LPS effects significantly. Endotoxin caused a significantly reduced GSH/GSSG ratio in the spleen, whereas CTCE-0214D was able to increase the ratio which was attributable mainly to reduced GSSG levels. Statistical significance ($p \leq 0.05$) was determined by using the one-way analysis of variance (ANOVA) and the Tukey post hoc test. Data are given as mean ± standard error of the mean (SEM), n = 7; *, $p \leq 0.05$; **, $p \leq 0.01$; ***, $p \leq 0.001$.

doi:10.1371/journal.pone.0138389.g002

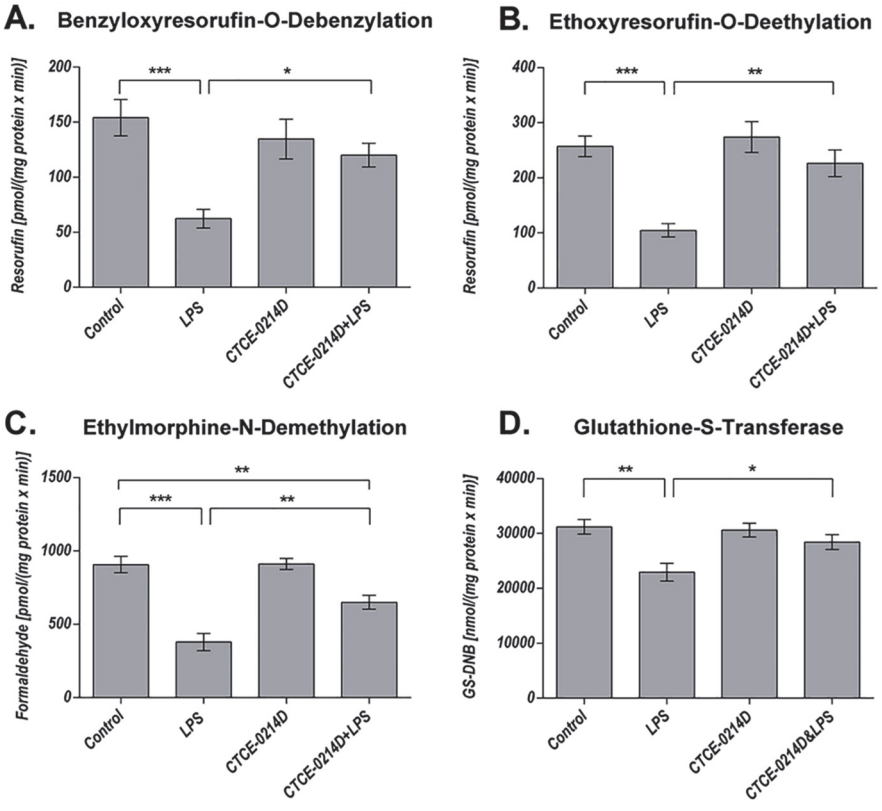

E.

Model reaction	CYP	Control	LPS	CTCE-0214D	CTCE-0214D+LPS
BROD	*1A,2A,2B,2C,3A*	154.1±16.4	62.3±8.4***	134.7±18.1	120.1±10.7^{+}
ECOD	*1A,2A,2B,2C*	477.4±25.0	243.3±26.9***	466.1±34.2	358.4±9.2*,$^{+}$
EMND	*3A*	907.5±55.6	379.6±58.8***	911.9±37.5	649.8±46.9**,$^{++}$
EROD	*1A*	257.1±18.8	104.6±12.1***	274.2±28.0	226.4±24.1^{++}
MROD	*1A2*	739.5±46.0	339.9±29.0***	683.3±43.6	456.2±17.6***
PNPH	*1E*	184.9±17.2	44.6±6.9***	144.2±13.2	98.3±11.1***,$^{+}$
PROD	*2B*	13.6±1.5	5.4±1.2***	15.3±1.2	8.0±0.7*
GST		31220±1329	22940±1619**	30608±1235	28429±1342^{+}

Fig 3. Biotransformation capacity. Benzyloxyresorufin-O-debenzylation [BROD] (A), ethoxyresorufin-O-deethylation [EROD] (B), ethylmorphine-N-demethylation [EMND] (C) and glutathione-S-transferase (D, as 1-chloro-2,4-dinitrobenzene conjugation) activities in 9000g supernatants are shown exemplarily. LPS impaired BROD activities to approximately 40% of the control values, whereas enzyme activities of CTCE-0214D plus LPS treated mice were elevated by more than 90% when compared to endotoxin administration alone. Moreover, no significant difference was detectable between CTCE-0214D plus LPS or saline treated mice. Furthermore, CTCE-0214D plus LPS treated mice revealed significantly elevated EROD activities when compared to LPS treatment, whereas no significance to the control group was detectable. Co-administration of CTCE-0214D and LPS ameliorated endotoxins effects on EMND activities (elevation by about 70%), the activity, however, still being significantly decreased when compared to control. Furthermore, increased glutathione-S-transferase activities were observed when comparing the CTCE-0214D plus LPS to the LPS group. Statistical significance ($p \leq 0.05$) was determined by using the one-way analysis of variance (ANOVA) and the Tukey post hoc test. Data are given as mean ± standard error of the mean (SEM), n = 7; *, $p \leq 0.05$; **, $p \leq 0.01$; ***, $p \leq 0.001$. In (E), the results of all performed model reactions are presented in pmol/(mg protein x min), except PNPH and GST, which are given in nmol/(mg protein x min). Statistical significance was determined and marked as mentioned, with the addition that significance to the LPS group was marked separately; $^{+}$, $p \leq 0.05$; $^{++}$, $p \leq 0.01$; $^{+++}$, $p \leq 0.001$ vs. LPS.

doi:10.1371/journal.pone.0138389.g003

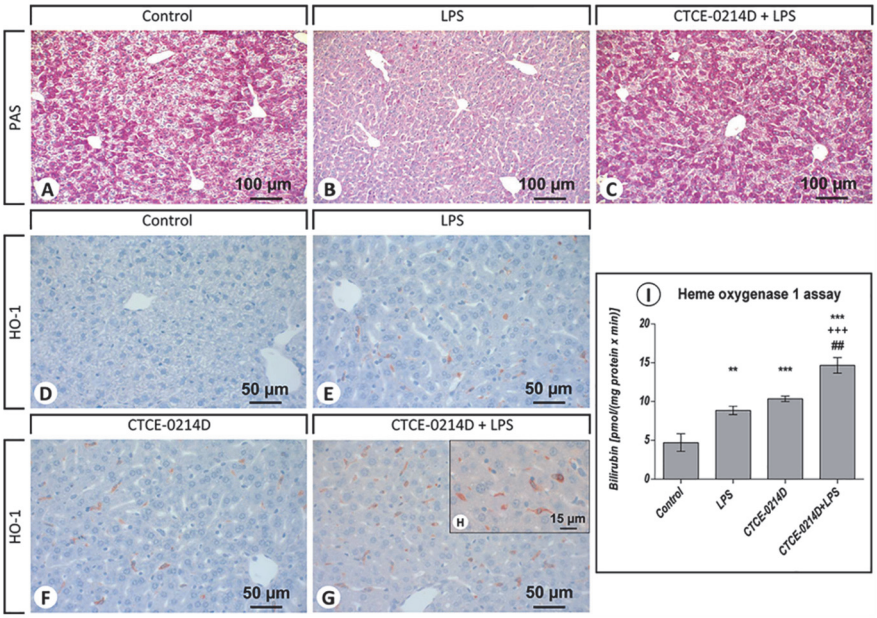

Fig 4. Periodic acid-Schiff (PAS) staining and immunohistochemical staining of heme oxygenase 1 in the livers. Representative photomicrographs from one of seven different tissue samples are shown (magnification: (A-C) 200x, (D-G) 400x, (H) 630x). For reasons of clarity, the PAS staining of the CTCE-0214D group is not shown as there were no differences to be observed when compared to the control. Exposure to LPS (B) evoked an impressive loss of glycogen content in the livers, whereas the livers of CTCE-0214D plus LPS treated mice (C) showed no difference to the control group (A) at all. LPS exposure (E) enhanced HO-1 occurrence in Kupffer and pit cells, whereas CTCE-0214D on its own (F) was able to induce HO-1 above average. Combined CTCE-0214D plus LPS administration (G) resulted in maximum HO-1 levels. The photomicrograph in (H) shows single Kupffer and pit cells, respectively, at a higher magnification (630x). To quantify the HO-1 activity in the liver, we performed an assay in the 9000g supernatants (I). LPS, CTCE-0214D and CTCE-0214D plus LPS administration increased the HO-1 activity by approximately 90%, 120% and 210%, respectively, when compared to the control group. The combined CTCE-0214D plus LPS treatment revealed the highest HO-1 activity levels, which were additionally significantly elevated in comparison to the values of the LPS or CTCE-0214D group, respectively. Statistical significance ($p \leq 0.05$) was determined by using the one-way analysis of variance (ANOVA) and the Tukey post hoc test. Data are given as mean ± standard error of the mean (SEM), n = 7; *, $p \leq 0.05$; **, $p \leq 0.01$; ***, $p \leq 0.001$ vs. control; $^{+}$, $p \leq 0.05$; $^{++}$, $p \leq 0.01$; $^{+++}$, $p \leq 0.001$ vs. LPS; #, $p \leq 0.05$; ##, $p \leq 0.01$; ###, $p \leq 0.001$ vs. CTCE-0214D.

doi:10.1371/journal.pone.0138389.g004

Immunohistochemistry revealed a correlation concerning the occurrence of CXCR4 and its ligand CXCL12 (Fig 5). After saline treatment, CXCR4 appeared on macrophages and lymphocytes in the red and white pulp, wherein in lymphoid follicles its presence was principally limited to lymphocytes in the marginal zone. After LPS treatment, CXCR4 positive cells were noticed only rarely in the red pulp, but the stronger the course of the disease, the more of these CXCR4 positive cells were found to be located in the white pulp. Accordingly, the CTCE-0214D plus LPS group displayed fewer CXCR4 positive cells in the splenic tissue (Table 2 and Fig 5A–5C and 5G). When focusing on CXCL12 staining in the spleens of saline treated animals, we ascertained particularly splenocytes in the white and red pulp and plasma cells in the red pulp to produce CXCL12 (Fig 5D). Obviously, endotoxin caused a widespread occurrence of CXCL12 all over the spleen (Fig 5E and 5H). While a staining of plasma cells, splenocytes and endothelial vascular cells appeared in the red pulp, an immunoreactivity of splenocytes and tingible body macrophages occurred predominantly in the white pulp (Table 2 and Fig 5D–5F and 5H). The more CXCL12 positive cells appeared in the spleen, the more CXCR4 positive cells were detectable. Especially the tingible body macrophages (CXCL12 positive) and the engulfed lymphocytes in their cell bodies (CXCR4 positive) support this hypothesis.

Table 2. Immunohistochemical staining of CXCR4, CXCL12, TLR4, NF-κB, cleaved caspase-3, gp91 phox, heme oxygenase 1 and the TUNEL assay.

Staining	Treatment Group	Liver		Spleen				Thymus			
		Kupffer and pit cells		*Red pulp*		*White pulp*		*Cortex*		*Medulla*	
		Occ	*Int*	*Occ*	*Int*	*Occ*	*Int*	*Occ*	*Int*	*Occ*	*Int*
CXCR4	*Control*	1	1	1	1	1	1	2	1	2	1
	LPS	2	2	1	1	3	3	3	2	1	2
	CTCE-0214D	1	1	1	1	1	1	2	1	2	1
	CTCE-0214D+LPS	1	1	1	1	2	1	2	1	2	2
CXCL12	*Control*	2	2	1	2	2	2	1	2	2	2
	LPS	2	2	3	2	3	3	2	3	1	1
	CTCE-0214D	2	2	1	2	2	2	1	2	2	1
	CTCE-0214D+LPS	2	2	2	2	2	2	2	3	2	2
TLR4	*Control*	1	1	1	1	1	1	1	1	1	1
	LPS	2	2	2	1	3	3	2	1	1	1
	CTCE-0214D	1	1	1	1	1	1	1	1	1	1
	CTCE-0214D+LPS	1	1	1	1	2	1	1	1	1	1
NF-κB	*Control*	1	1	2	2	3	1	3	1	3	1
	LPS	2	2	2	2	3	3	3	3	3	1
	CTCE-0214D	1	1	2	2	3	1	3	1	3	1
	CTCE-0214D+LPS	1	1	1	2	3	1	3	1	3	1
cleaved	*Control*	0	0	1	2	1	2	1	2	1	3
caspase-3	*LPS*	2	2	1	2	3	3	3	3	1	3
	CTCE-0214D	0	0	1	2	1	2	1	2	1	3
	CTCE-0214D+LPS	1	1	1	2	1	2	1	2	1	3
gp91 phox	*Control*	1	1	1	1	0	0	1	1	1	1
	LPS	2	2	2	1	2	1	3	2	2	1
	CTCE-0214D	1	1	1	1	0	0	1	1	1	1
	CTCE-0214D+LPS	1	2	1	1	1	1	2	2	2	1
Heme	*Control*	0	0	1	1	0	0	1	1	1	1
oxygenase 1	*LPS*	2	2	2	1	2	2	1	1	1	1
	CTCE-0214D	2	2	2	2	0	0	1	1	1	1
	CTCE-0214D+LPS	3	3	3	2	2	2	1	1	1	1
TUNEL	*Control*	0	0	0	0	1	2	1	1	1	3
	LPS	2	2	1	2	3	3	3	3	1	3
	CTCE-0214D	0	0	0	0	1	2	1	1	1	3
	CTCE-0214D+LPS	1	1	0	0	1	2	1	1	1	3

Presented are the results in the tissues of liver, spleen and thymus of all treatment groups (each n = 7). Occurrence (Occ) was assessed as following: 0: negative; 1: seldom; 2: frequent; 3: diffuse. Additionally, the intensity of staining was evaluated as follows: 0: no staining; 1: mild; 2: moderate; 3: strong.

doi:10.1371/journal.pone.0138389.t002

Continuing, TLR4 distribution in splenic tissue was confined primarily to the white pulp, whereas cells of the red pulp displayed almost no membrane-bound staining (Fig 6A–6C). Especially splenocytes and lymphocytes of septic spleens were identified to show an intensive TLR4 expression (Fig 6A–6C). Furthermore, when CTCE-0214D was administered in endotoxemia, lympho- and splenocytes in lymphoid follicles of the white pulp were found to exhibit decreased NF-κB activities (Fig 6E). In contrast to LPS and CTCE-0214D plus LPS administration, saline treated mice revealed a ubiquitous expression of the nuclear factor—particularly

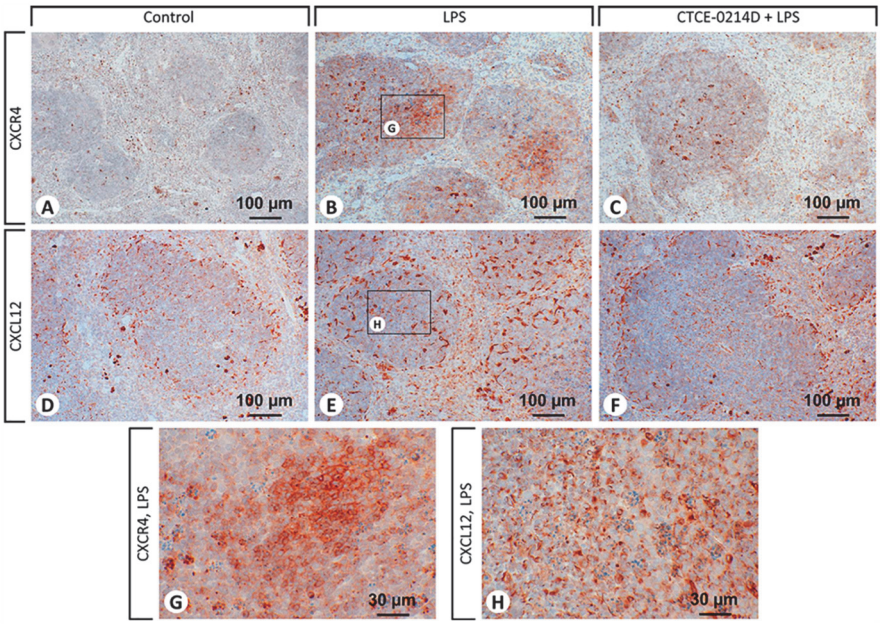

Fig 5. Immunohistochemical staining of CXCR4 and CXCL12 in the spleens. Representative photomicrographs from one of seven different tissue samples are shown (magnification: 200x). For reasons of clarity, the CTCE-0214D group is not shown as there were no differences to be observed when compared to the control. After saline treatment (A), CXCR4 appeared on macrophages and on lymphocytes in the red and in the white pulp, wherein in lymphoid follicles its presence was predominantly limited to lymphocytes in the marginal zone. Several cells in the red pulp are stained non-specifically (clearly distinguishable from the specific staining because of a granular appearance of the staining). LPS challenge (B) caused various CXCR4 positive cells to appear in the white pulp. The additional administration of CTCE-0214D diminished the amount of CXCR4 positive cells in the tissue to a minimum (C). CXCL12 staining in the spleen of saline treated animals (D) revealed that particularly splenocytes in the white and in the red pulp as well as plasma cells in the red pulp produced CXCL12. LPS treatment caused an increased CXCL12 expression in plasma cells, splenocytes and endothelial vascular cells in the red pulp, whereas in the white pulp predominantly splenocytes and tingible body macrophages became positive. Co-administration of CTCE-0214D to the endotoxin (F) evidently reduced the appearance of CXCL12. In the photomicrographs of (G) and (H) the tingible body macrophages (CXCL12 positive) and the engulfed lymphocytes in their cell bodies (CXCR4 positive) are depicted at a higher magnification (630x).

doi:10.1371/journal.pone.0138389.g005

when compared to the red pulp (Table 2 and Fig 6D–6F). Examination of the spleens from septic mice revealed cells in the white pulp to express cleaved caspase-3 above average (Fig 6H and 6J). Besides a few spleno- and lymphocytes, especially tingible body macrophages showed an increased cleaved caspase-3 expression and were found unambiguously more often in LPS-challenged mice in contrast to other treatment groups. In the white as well as in the red pulp, CTCE-0214D reduced the appearance of cleaved caspase-3 to a minimum (Table 2 and Fig 6G–6J). The TUNEL assay confirmed the results, as spleens of CTCE-0214D plus LPS treated mice revealed a significantly reduced amount of cells undergoing apoptosis (Fig 7). In contrast, endotoxin induced a massive cell death, especially in the white pulp (Fig 7A–7C and 7G). Furthermore, the red pulp of LPS challenged mice clearly showed a higher perfusion which was detectable by the more frequent appearance of erythrocytes.

Also, macrophages and splenocytes in the white pulp of endotoxic mice were observed to express gp91 phox above average, whereas macrophages and neutrophil granulocytes in the red pulp showed similar expression levels in all treatment groups. In addition to its effects on the glutathione content, the beneficial features of CTCE-0214D were further underlined by the fact that LPS-induced gp91 phox activities in macrophages were ameliorated (Table 2).

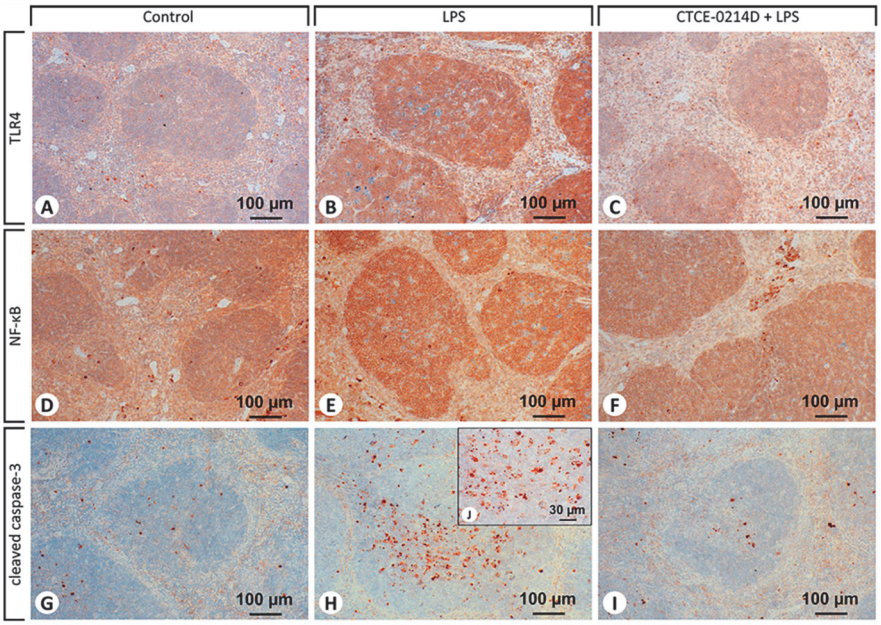

Fig 6. Immunohistochemical staining of TLR4, NF-κB and cleaved caspase-3 in the spleens. Representative photomicrographs from one of seven different tissue samples are shown (magnification: (A-I) 200x, (J) 630x). For reasons of clarity, the CTCE-0214D group is not shown as there were no differences to be observed when compared to the control. TLR4 occurred primarily in the white pulp, whereas cells of the red pulp displayed almost no membrane-bound staining. Especially after LPS treatment (B), spleno- and lymphocytes were identified to show an intensive TLR4 expression. Co-administration of CTCE-0214D to LPS clearly decreased the staining intensity of NF-κB, as lympho—and splenocytes in lymphoid follicles of the white pulp displayed diminished NF-κB levels (F). Nevertheless, the nuclear factor occurred ubiquitously in the spleens of all groups. Besides a few spleno- and lymphocytes, especially tingible body macrophages showed advanced cleaved caspase-3 activity and were found unambiguously more often in LPS-challenged mice (H,J). Co-administration of CTCE-0214D plus LPS reduced the appearance of cleaved caspase-3 to a minimum (I).

doi:10.1371/journal.pone.0138389.g006

Suitably, the results of the HO-1 staining further underline the fact that administration of a CXCL12 analog is associated with anti-oxidative effects during inflammation. Similar to the staining results obtained in the liver, HO-1 expression was the highest after co-administration of CTCE-0214D plus LPS (Table 2). Especially macrophages in the red pulp and tingible body macrophages in the white pulp exhibited high enzyme activities. CTCE-0214D itself was able to induce HO-1 in macrophages and in granulocytes in the red pulp, while LPS treatment consistently caused the lowest expression of HO-1 in the red pulp. In the white pulp of LPS treated mice, HO-1 occurred predominantly on tingible body macrophages to a similar extent as after CTCE-0214D plus LPS co-treatment (Table 2).

Thymus: CXCR4/CXCL12 axis, NF-κB and apoptosis

With respect to the CXCR4/CXCL12 axis, thymus immunohistochemistry revealed the same results as were seen in the spleen (Table 2). While tingible body macrophages expressed large amounts of CXCL12, CXCR4 occurred predominantly on the engulfed lymphocytes inside or in those located in close proximity. Furthermore, we recognized thymocytes in the medulla of the thymus as well as macrophages and endothelial cells in the cortex to be the major CXCL12 producers (not shown).

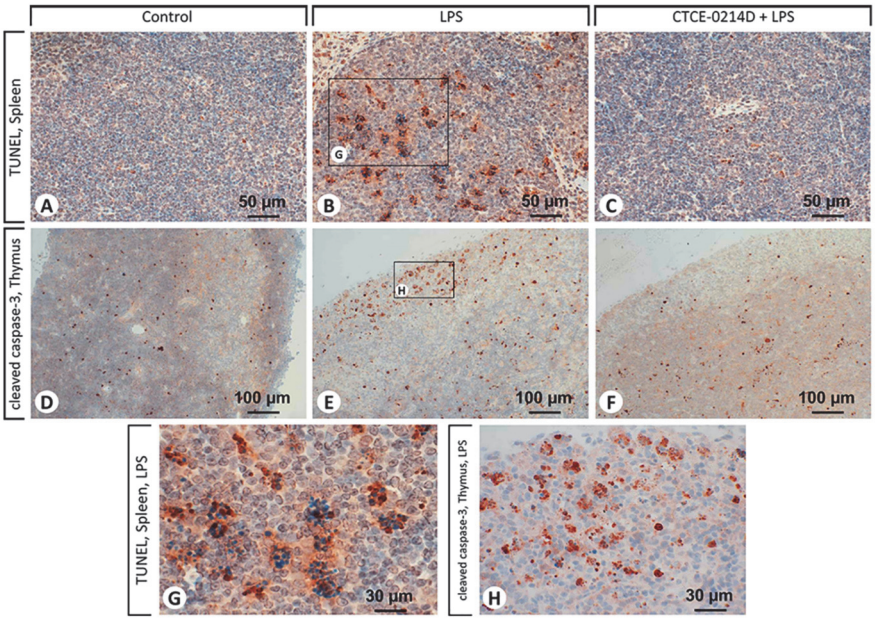

Fig 7. TUNEL assay in the spleens and immunohistochemical staining of the cleaved caspase-3 in the thymi. Representative photomicrographs from one of seven different tissue samples are shown (magnification: (A-C) 400x, (D-F) 200x, (G,H) 630x). For reasons of clarity, the CTCE-0214D group is not shown as there were no differences to be observed when compared to the control group. Whereas endotoxin induced cell death in both the white and red pulp (B), CTCE-0214D was able to significantly diminish the amount of cells undergoing apoptosis (C), which is particularly evident in the white pulp. In the thymi of the LPS group, endotoxin caused a massive appearance of cleaved caspase-3 in the cortex (E), whereas the medulla did not significantly differ from the other treatment groups. CTCE-0214D decreased the cleaved caspase-3 expression in the cortical regions to control level and caused a raise in the amount of lymphocytes (F), especially when compared to the LPS group. The magnifications in (G) and (H) reveal the tingible body macrophages in the white pulp to be the main locus of apoptotic cell death.

doi:10.1371/journal.pone.0138389.g007

Moreover, almost every cell in the cortex of the thymus of LPS treated mice exhibited a high expression of NF-κB. In contrast to the other treatment groups, after LPS administration the medulla was additionally characterized by fewer lympho- and thymocytes, so consequently, a minimized NF-κB occurrence was observed. In addition, we were able to detect an atrophy of the cortical regions. The thymus of mice treated with CTCE-0214D plus LPS, however, also revealed an atrophy in cortex, but the medulla appeared to be enlarged as a result of more lympho- and thymocytes present in this region. Furthermore, co-administration of CTCE-0214D and LPS attenuated the NF-κB expression in cortical regions to control-like levels (not shown).

By using immunohistochemistry, we were able to perceive the influence of CTCE-0214D on the thymus, since a substantial raise in the amount of lymphocytes and a decrease in cleaved caspase-3 expression in the tissue was seen when compared to the LPS group. 24 hours after treatment, cleaved caspase-3 showed a remarkably high expression in the cortical regions of the thymi of septic mice, whereas the presence of this marker in the medulla did not differ from the other treatment groups. Very similar to the spleen, many tingible body macrophages were also recognized in the thymus tissue after LPS treatment, the cells engulfed being the main locus of apoptosis simultaneously. CTCE-0214D decreased the cleaved caspase-3 expression in the cortex to control level, while its presence in the medulla was not affected substantially (Table 2 and Fig 7D–7F and 7H). In accordance with these results, the TUNEL assay

revealed the thymic cortex of LPS treated mice to be the main locus of apoptosis. We detected endotoxin to cause a massive cell death there, whereas CTCE-0214D was able to significantly mitigate apoptosis (Table 2).

Discussion and Conclusions

It has been previously shown that by blocking the CXCR4/CXCL12 axis with synthetic antagonists during sepsis, the release of neutrophils from the bone marrow was prevented. This was accompanied by a 5 fold increase in peritoneal bacteria forming units in comparison to CLP (cecal ligation and puncture) treatment. Consequently, the mortality increased by about 40% [39]. Accordingly, when treating zebrafish with AMD 3100, a specific inhibitor of CXCR4, LPS treatment associated mortality was increased [40]. This finding is in good agreement with our results, as we were also able to observe a worsening of endotoxemia symptoms when additionally treating mice with AMD3100. In this case, significantly increased levels of serum TNF-α as well as lipid peroxidation products in the livers were seen, when compared to the control or LPS group, respectively. In addition, a significant loss of body weight was observed which was accompanied by reduced protein, total glutathione and CYP activity levels in the livers of co-treated mice (S1 Fig). On the other hand, the administration of exogenous CXCL12 was shown to induce a clear reduction in parasitemia after malarial infection in mice [41]. As CXCL12 is known to be highly expressed in the bone marrow of healthy animals to host CXCR4 positive cells, there is some evidence that the gradient is inverted in infectious diseases [39,17]. Our results support this hypothesis as we were able to show a higher content of CXCL12 producing cells in spleens of LPS challenged mice. Moreover, a larger amount of CXCR4 positive cells was detectable and the more CXCL12 appeared on tingible body macrophages the more CXCR4 positive cells were noticeable. Probably, the tingible body macrophages attract dysfunctional lymphocytes to remove them as a part of the host immune response to the endotoxin challenge. CTCE-0214D reduced the amount of tingible body macrophages in spleen and thymus indicating that the removal of pathogens was evidently more successful at the time of sacrifice. Consequently, exogenous CXCL12 administration appears to be a possibility to support the organism to mobilize functional CXCR4 positive cells to the local sites of infection, which is essential for survival. Our findings are in accordance with the recently described superiority of the combined treatment with CTCE-0214 and imipenem, in which neutrophil recruitment to the site of infection and bacterial clearance were improved in mice [17].

Additionally, we were able to detect an evidently reduced TLR4 appearance in spleens of mice treated with CTCE-0214D plus LPS. In the acute phase, endotoxic mice show a high expression of TLR4 which is known to be a physiological answer to a pathogen challenge and is predominantly caused by endotoxin and IFN-γ [42,43]. Consequently, LPS is able to activate receptor signaling which is accompanied by the enhanced activation of transcription factors like NF-κB. Considered along with the obviously diminished appearance of NF-κB in the liver, spleen and thymus, CTCE-0214D seems to distinctly attenuate TLR4 signaling. In addition, as LPS has been shown previously to directly activate CXCR4 [6], CTCE-0214D could antagonize LPS binding. Suitably, CXCL12 has been shown to suppress NF-κB activation in response to LPS stimulation in transfected HEK cells [44]. This is in accordance with the observed reduction of serum TNF-α levels, which may be a consequence of receptor antagonism or inhibition of NF-κB activation. This hypothesis is further supported by the decreased NF-κB and TNF-α production after administering ubiquitin in lethal endotoxemia, while ubiquitin was recently identified to be a CXCR4 agonist [45]. NF-κB plays a pivotal role in host immune response and functions as a key regulator by controlling cell proliferation, differentiation, apoptosis and immune and stress responses. Especially cyclooxygenase-2 (COX-2) is a well-known product

of NF-κB activation. Produced by COX-2 induction, prostaglandins were formerly shown to stimulate glycogenolysis in the liver. Considered along with the enhanced metabolic activities in inflammation, which require many resources, the administration of endotoxin results in hypoglycemia [46,47]. Correspondingly, in the present investigation histological assessment revealed the livers of endotoxic mice to exhibit almost no glycogen reserves, while CTCE-0214D plus LPS treatment inhibited endotoxin effects completely. Suitably, activation of CXCR4 significantly enhanced blood glucose levels. Along with body temperature and general condition, blood glucose levels are of diagnostic value in identifying septic diseases [48], once again emphasizing CTCE-0214D's beneficial influence as the CXCL12 analog improved all parameters. Moreover, massive NF-κB activity results in the excessive production of pro-inflammatory cytokines such as TNF-α and IL-6. In particular, both are thought to play pivotal roles in endotoxemia by decreasing the biotransformation capacity in the liver to a minimum [37,49]. We determined CTCE-0214D to attenuate serum TNF-α levels, which is in good accordance to previous investigations concerning CTCE-0214 [15]. As a result, CTCE-0214D evidently improved phase 1 (CYP) and phase 2 (GST) enzyme activities. By doing so, CTCE-0214D probably improved the ability to detoxify LPS-induced secondary products such as reactive oxygen species. In addition, while septic patients are frequently treated with several drugs such as multiple antibiotics, the patients' biotransformation capacity is of relevant importance to detoxify and eliminate the resulting metabolites. As CTCE-0214D significantly recovered the biotransformation capacity, it could improve the patients' overall outcome as it may contribute to reduce the side effects caused by the multiple medications. Additionally, the more CYP families are active, the more proteins are protected from degradation [50]. Especially, reduced glutathione is of massive importance because of its diverse functions including detoxification, modulation of cell proliferation and antioxidant defense [51]. GSH has also been implicated in the modulation of cell death and is essential for cell survival as the GSH-depleted γ-glutamylcysteine synthetase knock-out mice died of massive apoptotic cell death [52,53]. As we were able to ascertain a beneficial glutathione status in both liver and spleen, this is probably one reason why CTCE-0214D exerts anti apoptotic effects. Furthermore, CXCL12 has been shown to inhibit cortical neuron apoptosis by increasing the ratio of Bcl-2/Bax after traumatic brain injury [54] and, also, pancreatic β cell survival was promoted by the activation of the pro-survival kinase Akt after CXCL12 administration [55]. Considered along with the reduced serum TNF-α and ROS levels in liver and spleen, CTCE-0214D probably provides its anti-apoptotic features in several distinct ways which may explain the massive reduction of apoptotic cells and the decreased expression of the cleaved caspase-3 witnessed in all organs.

Especially in the liver, endotoxin caused massive oxidative stress, which can be an important mediator of damage to cell structures, including lipids and membranes, proteins, and DNA [56]. CTCE-0214D, however, diminished LPS effects evidently which, in turn, is probably a result of several processes taking place simultaneously. Of key relevance is the attenuated occurrence of NF-kB, probably caused by attenuated TLR4 signaling. During inflammatory processes, the expression of phagocytic NADPH oxidase (gp91 phox) is dependent on, and induced by, NF-κB. Upon stimulation by growth factors and cytokines, the oxidase generates superoxide and other ROS by using NADPH [57]. Under normal circumstances, a mild activity of the NADPH oxidase is essential to eliminate bacteria and fungi. Endotoxin, however, was capable of amplifying the NADPH oxidase occurrence in the liver, spleen and thymus, while organs of mice treated with CTCE-0214D exhibited a moderate expression. Another potential reason for the observed reduction of ROS levels is probably due to the decreased serum TNF-α and IFN-γ levels as the cytokines have already been reported several times to generate ROS via mitochondria and NADPH oxidase [58,59]. Furthermore, in addition to NF-κB, both cytokines are able to heavily upregulate the inducible nitric oxide synthase (iNOS). Consequently,

CTCE-0214D seems likely to attenuate iNOS´ ability to produce nitric oxide (NO). Besides producing cell toxic peroxynitrite, NO may contribute to hypotension, cardiodepression and vascular hyporeactivity in septic shock [60].

Finally, we demonstrated that CTCE-0214D is able to increase HO-1 activity in the liver as well as its expression in the liver and spleen. Once again, CTCE-0214D underlines its protective features as targeted overexpression of HO-1 has been shown to have beneficial effects in various experimental animal models of inflammation, a finding supported by the fact that HO-1 deficient mice are more susceptible to polymicrobial sepsis [61]. Moreover, previous investigations confirmed HO-1 to clearly attenuate TNF-α, ROS and NADPH oxidase levels [62,63] which is in good agreement with our results.

In summary, in the present investigation we were able to demonstrate that the CXCL12 analog CTCE-0214D displayed anti-inflammatory, anti-oxidative and cytoprotective features and thus was able to attenuate LPS-induced effects distinctly throughout. In contrast, blocking the CXCR4 with AMD3100 revealed to be disadvantageous and worsened the disease. As we are the first to reveal exact effects of CXCR4 activation, our results suggest the CXCR4/CXCL12 axis to be a promising target not only for the treatment of endotoxemia but also for the management of other acute inflammatory diseases. Especially when accompanied by an impaired liver function and an excessive production of free radicals, CXCL12 analogs represent a new treatment option to prevent and mitigate the disease progression.

Supporting Information

S1 Fig. Blockade of the CXCR4/CXCL12 axis with AMD3100 in endotoxemia. Male adult C57BL/6N mice (12-weeks-old, body weight 25–30 g; Charles River Laboratories, Sulzfeld, Germany) were used. The animals were housed in plastic cages under standardized conditions (light-dark cycle 12/12 h, temperature 22 ± 2°C, humidity 50 ± 10%, pellet diet Altromin 1316, water ad libitum). A total of 28 mice was randomly divided into four groups (n = 7 each): Control, LPS, AMD3100 and AMD3100 plus LPS. LPS (E. coli 0111:B4, Sigma Aldrich, Steinheim, Germany) was injected intraperitoneally (5mg/kg body weight), whereas AMD3100 (5 mg/kg body weight) was administered in PBS shortly after endotoxemia onset intraperitoneally. 24 hours after LPS treatment, mice were weighed and sacrificed in isoflurane anesthesia. Blood serum and livers were obtained and used for biochemical analysis. After combined treatment with AMD3100 plus LPS, significantly increased levels of serum TNF-α as well as lipid peroxidation products in the livers of mice when compared to the control or LPS group, respectively, were observed. In addition, a significant loss of body weight was observed which was accompanied by reduced protein, total glutathione and CYP activity levels in the livers of the co-treated mice. Statistical significance ($p \leq 0.05$) was determined by using the one-way analysis of variance (ANOVA) and the Tukey post hoc test. Data are given as mean ± standard error of the mean (SEM), n = 7; *, $p \leq 0.05$; **, $p \leq 0.01$; ***, $p \leq 0.001$ vs. control; $^{+}$, $p \leq 0.05$; $^{++}$, $p \leq 0.01$; $^{+++}$, $p \leq 0.001$ vs. LPS. These results clearly indicate that a blockade of the CXCR4/CXCL12 axis in endotoxemia is disadvantageous and worsens the disease. Undoubtedly, the chemokine receptor CXCR4 plays an important role in endotoxemia, and hence its activation becomes a promising treatment option not only for handling endotoxemia but also for other acute inflammatory diseases, especially when accompanied by an impaired liver function. The study was conducted under the licence of the Thuringian Animal Protection Committee. The principles of laboratory animal care and the German Law on the Protection of Animals as well as the Directive 2010/63/EU were followed.
(PDF)

S2 Fig. Aspartate aminotransferase (ASAT) and alanine aminotransferase (ALAT) activities in the serum. LPS caused a massive increase in the serum concentration of both enzymes when compared to the control group (ASAT: 63.0±7.4 U/L vs. 98.3±9.0 U/L, p = 0.005; ALAT: 35.7±4.6 U/L vs. 85.7±16.5 U/L; p = 0.002). However, CTCE-0214D was able to decrease the enzyme activities throughout. The ASAT activities (A) were reduced by about 15% when compared to the LPS group (p = 0.5), whereas the ALAT activities (B) showed a significant reduction by about 60% (p = 0.002). Remarkably, the ALAT activities of the control and of the CTCE-0214D plus LPS group are at the same level (35.7±4.6 U/L vs. 33.6±4.8 U/L, p = 0.98). As ALAT represents a more specific indicator of liver inflammation than ASAT, these findings underline the protective effects of CTCE-0214D on the livers impressively.
(PDF)

Author Contributions

Conceived and designed the experiments: SS AL. Performed the experiments: SS AL. Analyzed the data: SS AL. Contributed reagents/materials/analysis tools: SS AL. Wrote the paper: SS AL.

References

1. Alexander C, Rietschel ET. Bacterial lipopolysaccharides and innate immunity. J Endotoxin Res. 2001; 7: 167–202. PMID: 11581570
2. Park BS, Lee J. Recognition of lipopolysaccharide pattern by TLR4 complexes. Exp Mol Med. 2013. doi: 10.1038/emm.2013.97
3. Wittebole X, Castanares-Zapatero D, Laterre PF. Toll-like receptor 4 modulation as a strategy to treat sepsis. Mediators Inflamm. 2010. doi: 10.1155/2010/568396
4. Triantafilou M, Miyake K, Golenbock DT, Triantafilou K. Mediators of innate immune recognition of bacteria concentrate in lipid rafts and facilitate lipopolysaccharide-induced cell activation. J Cell Sci. 2002; 115: 2603–11. PMID: 12045230
5. Vabulas RM, Wagner H, Schild H. Heat shock proteins as ligands of toll-like receptors. Curr Top Microbiol Immunol. 2002; 270: 169–84. PMID: 12467251
6. Triantafilou M, Lepper PM, Briault CD, Ahmed MA, Dmochowski JM, Schumann C, et al. Chemokine receptor 4 (CXCR4) is part of the lipopolysaccharide "sensing apparatus". Eur J Immunol. 2008; 38: 192–203. PMID: 18081034
7. Karin N. The multiple faces of CXCL12 (SDF-1alpha) in the regulation of immunity during health and disease. J Leukoc Biol. 2010; 88: 463–73. doi: 10.1189/jlb.0909602 PMID: 20501749
8. D'Apuzzo M, Rolink A, Loetscher M, Hoxie JA, Clark-Lewis I, Melchers F, et al. The chemokine SDF-1, stromal cell-derived factor 1, attracts early stage B cell precursors via the chemokine receptor CXCR4. Eur J Immunol. 1997; 27: 1788–93. PMID: 9247593
9. Nanki T, Lipsky PE. Stimulation of T-Cell activation by CXCL12/stromal cell derived factor-1 involves a G-protein mediated signaling pathway. Cell Immunol. 2001; 214: 145–54. PMID: 12088413
10. Ma Q, Jones D, Borghesani PR, Segal RA, Nagasawa T, Kishimoto T, et al. Impaired B-lymphopoiesis, myelopoiesis, and derailed cerebellar neuron migration in CXCR4- and SDF-1-deficient mice. Proc Natl Acad Sci USA. 1998; 95: 9448–53. PMID: 9689100
11. Tunc T, Cekmez F, Cetinkaya M, Kalayci T, Fidanci K, Saldir M, et al. Diagnostic value of elevated CXCR4 and CXCL12 in neonatal sepsis. J Matern Fetal Neonatal Med 2014; 22: 1–6.
12. Tamamura H, Fujisawa M, Hiramatsu K, Mizumoto M, Nakashima H, Yamamoto N, et al. Identification of a CXCR4 antagonist, a T140 analog, as an anti-rheumatoid arthritis agent. FEBS Lett. 2004; 569: 99–104. PMID: 15225616
13. Mikami S, Nakase H, Yamamoto S, Takeda Y, Yoshino T, Kasahara K, et al. Blockade of CXCL12/CXCR4 axis ameliorates murine experimental colitis. J Pharmacol Exp Ther. 2008; 327: 383–92. doi: 10.1124/jpet.108.141085 PMID: 18716065
14. Wang A, Fairhurst AM, Tus K, Subramanian S, Liu Y, Lin F, et al. CXCR4/CXCL12 hyperexpression plays a pivotal role in the pathogenesis of lupus. J Immunol. 2009; 182: 4448–58. doi: 10.4049/jimmunol.0801920 PMID: 19299746

15. Fan H, Wong D, Ashton SH, Borg KT, Halushka PV, Cook JA. Beneficial effect of a CXCR4 agonist in murine models of systemic inflammation. Inflammation. 2012; 35: 130–7. doi: 10.1007/s10753-011-9297-5 PMID: 21274742

16. Bach HH 4th, Saini V, Baker TA, Tripathi A, Gamelli RL, Majetschak M. Initial assessment of the role of CXC chemokine receptor 4 after polytrauma. Mol Med. 2012; 18: 1056–66. doi: 10.2119/molmed.2011.00497 PMID: 22634721

17. Guan S, Guo C, Zingarelli B, Wang L, Halushka PV, Cook JA, et al. Combined treatment with a CXCL12 analogue and antibiotics improves survival and neutrophil recruitment and function in murine sepsis. Immunology. 2014. doi: 10.1111/imm.12382

18. Fan H, Goodwin AJ, Chang E, Zingarelli B, Borg K, Guan S, et al. Endothelial progenitor cells and a stromal cell-derived factor-1α analogue synergistically improve survival in sepsis. Am J Respir Crit Care Med. 2014. doi: 10.1164/rccm.201312-2163OC

19. Xu L, Li Y, Sun H, Li D, Hou T. Structural basis of the interactions between CXCR4 and CXCL12/SDF-1 revealed by theoretical approaches. Mol Biosyst. 2013; 9: 2107–17. doi: 10.1039/c3mb70120d PMID: 23702796

20. Huang X, Shen J, Cui M, Shen L, Luo X, Ling K, et al. Molecular dynamics simulations on SDF-1alpha: binding with CXCR4 receptor. Biophys J. 2003; 84: 171–84. PMID: 12524273

21. Glawe JD, Mijalis EM, Davis WC, Barlow SC, Gungor N, McVie R, et al. SDF-1-CXCR4 differentially regulates autoimmune diabetogenic T cell adhesion through ROBO1-SLIT2 interactions in mice. Diabetologia. 2013; 56: 2222–30. doi: 10.1007/s00125-013-2978-x PMID: 23811810

22. Perez LE, Alpdogan O, Shieh JH, Wong D, Merzouk A, Salari H, et al. Increased plasma levels of stromal-derived factor-1 (SDF-1/CXCL12) enhance human thrombopoiesis and mobilize human colony-forming cells (CFC) in NOD/SCID mice. Exp Hematol. 2004; 32: 300–7. PMID: 15003316

23. Gonnert FA, Recknagel P, Seidel M, Jbeily N, Dahlke K, Bockmeyer CL, et al. Characteristics of clinical sepsis reflected in a reliable and reproducible rodent sepsis model. J Surg Res. 2011; 170: 123–34.

24. Ellman GL. Tissue sulfhydryl groups. Arch Biochem Biophys. 1959; 82: 70–7. PMID: 13650640

25. Hissin PJ, Hilf R. A fluorometric method for determination of oxidized and reduced glutathione in tissues. Anal Biochem. 1976; 74: 214–26. PMID: 962076

26. Yagi T, Day RS 3rd. Differential sensitivities of transformed and untransformed murine cell lines to DNA cross-linking agents relative to repair of O6-methylguanine. Mutat Res. 1987; 184: 223–7. PMID: 3670325

27. Yoshida T, Kikuchi G. Sequence of the reaction of heme catabolism catalyzed by the microsomal heme oxygenase system. FEBS Lett. 1974; 48: 256–61 PMID: 4154870

28. Klinger W, Müller D. The influence of age on the protein concentration in serum, liver and kidney of rats determined by various methods. Z Versuchstierkd. 1974; 16: 149–53. PMID: 4854887

29. Lubet RA, Mayer RT, Cameron JW, Nims RW, Burke MD, Wolff T, et al. Dealkylation of pentoxyresorufin: a rapid and sensitive assay for measuring induction of cytochrome(s) P-450 by phenobarbital and other xenobiotics in the rat. Arch Biochem Biophys. 1985; 238: 43–8. PMID: 3985627

30. Aitio A. A simple and sensitive assay of 7-ethoxycoumarin deethylation. Anal Biochem. 1978; 85: 488–91. PMID: 565602

31. Pohl RJ, Fouts JR. A rapid method for assaying the metabolism of 7-ethoxyresorufin by microsomal subcellular fractions. Anal Biochem. 1980; 107: 150–5. PMID: 6776841

32. Kleeberg U, Klinger W. Sensitive formaldehyde determination with Nash's reagent and a 'tryptophan reaction'. J Pharmacol Methods. 1982; 8: 19–31. PMID: 7121014

33. Chang TK, Crespi CL, Waxman DJ. Spectrophotometric analysis of human CYP2E1-catalyzed p-nitrophenol hydroxylation. Methods Mol Biol. 2006; 320: 127–31. PMID: 16719383

34. Habig WH, Pabst MJ, Jakoby WB. Glutathione S-transferases. The first enzymatic step in mercapturic acid formation. J Biol Chem. 1974; 249: 7130–9. PMID: 4436300

35. Lupp A, Danz M, Müller D. Morphology and cytochrome P450 isoforms expression in precision-cut rat liver slices. Toxicology. 2001; 161: 53–66. PMID: 11295255

36. McManus JF. Histological and histochemical uses of periodic acid. Stain Technol. 1948; 23: 99–108. PMID: 18867618

37. Jacob A, Zhou M, Wu R, Wang P. The role of hepatic cytochrome P-450 in sepsis. Int J Clin Exp Med. 2009; 2: 203–11. PMID: 19918313

38. Choi SH, Kim SG. Lipopolysaccharide inhibition of rat hepatic microsomal epoxide hydrolase and glutathione S-transferase gene expression irrespective of nuclear factor-kappaB activation. Biochem Pharmacol. 1998; 56: 1427–36. PMID: 9827574

39. Delano MJ, Kelly-Scumpia KM, Thayer TC, Winfield RD, Scumpia PO, Cuenca AG, et al. Neutrophil mobilization from the bone marrow during polymicrobial sepsis is dependent on CXCL12 signaling. J Immunol. 2011; 187: 911–8. doi: 10.4049/jimmunol.1100588 PMID: 21690321

40. Novoa B, Bowman TV, Zon L, Figueras A. LPS response and tolerance in the zebrafish (Danio rerio). Fish Shellfish Immunol. 2009; 26: 326–31. doi: 10.1016/j.fsi.2008.12.004 PMID: 19110060

41. Garnica MR, Souto JT, Silva JS, de Andrade HF Jr. Stromal cell derived factor 1 synthesis by spleen cells in rodent malaria, and the effects of in vivo supplementation of SDF-1alpha and CXCR4 receptor blocker. Immunol Lett. 2002; 83: 47–53. PMID: 12057854

42. Yan ZQ. Regulation of TLR4 expression is a tale about tail. Arterioscler Thromb Vasc Biol. 2006; 26: 2582–4. PMID: 17110607

43. Bosisio D, Polentarutti N, Sironi M, Bernasconi S, Miyake K, Webb GR, et al. Stimulation of toll-like receptor 4 expression in human mononuclear phagocytes by interferon-gamma: a molecular basis for priming and synergism with bacterial lipopolysaccharide. Blood. 2002; 99: 3427–31. PMID: 11964313

44. Kishore SP, Bungum MK, Platt JL, Brunn GJ. Selective suppression of Toll-like receptor 4 activation by chemokine receptor 4. FEBS Lett. 2005; 579: 699–704. PMID: 15670831

45. Majetschak M, Cohn SM, Nelson JA, Burton EH, Obertacke U, Proctor KG. Effects of exogenous ubiquitin in lethal endotoxemia. Surgery. 2004; 135: 536–43. PMID: 15118591

46. Casteleijn E, Kuiper J, Van Rooij HC, Kamps JA, Koster JF, Van Berkel TJ. Endotoxin stimulates glycogenolysis in the liver by means of intercellular communication. J Biol Chem. 1988; 263: 6953–5. PMID: 3284878

47. Raetzsch CF, Brooks NL, Alderman JM, Moore KS, Hosick PA, Klebanov S, et al. Lipopolysaccharide inhibition of glucose production through the Toll-like receptor-4, myeloid differentiation factor 88, and nuclear factor kappa b pathway. Hepatology. 2009; 50: 592–600. doi: 10.1002/hep.22999 PMID: 19492426

48. Reinhart K, Bauer M, Riedemann NC, Hartog CS. New approaches to sepsis: molecular diagnostics and biomarkers. Clin Microbiol Rev. 2012; 25: 609–34. doi: 10.1128/CMR.00016-12 PMID: 23034322

49. Zhou M, Maitra SR, Wang P. The potential role of transcription factor aryl hydrocarbon receptor in downregulation of hepatic cytochrome P-450 during sepsis. Int J Mol Med. 2008; 21: 423–8. PMID: 18360687

50. Morgan ET. Regulation of cytochrome p450 by inflammatory mediators: why and how? Drug Metab Dispos. 2001; 29: 207–12. PMID: 11181485

51. Lu SC. Regulation of glutathione synthesis. Mol Aspects Med. 2009; 30: 42–59. doi: 10.1016/j.mam.2008.05.005 PMID: 18601945

52. Dalton TP, Chen Y, Schneider SN, Nebert DW, Shertzer HG. Genetically altered mice to evaluate glutathione homeostasis in health and disease. Free Radic Biol Med. 2004; 37: 1511–26. PMID: 15477003

53. Muyderman H, Wadey AL, Nilsson M, Sims NR. Mitochondrial glutathione protects against cell death induced by oxidative and nitrative stress in astrocytes. J Neurochem 2007; 102: 1369–82. PMID: 17484727

54. Mao W, Yi X, Qin J, Tian M, Jin G. CXCL12 inhibits cortical neuron apoptosis by increasing the ratio of Bcl-2/Bax after traumatic brain injury. Int J Neurosci. 2014; 124: 281–90. doi: 10.3109/00207454.2013.838236 PMID: 23984821

55. Yano T, Liu Z, Donovan J, Thomas MK, Habener JF. Stromal cell derived factor-1 (SDF-1)/CXCL12 attenuates diabetes in mice and promotes pancreatic beta-cell survival by activation of the prosurvival kinase Akt. Diabetes. 2007; 56: 2946–57. PMID: 17878289

56. Valko M, Leibfritz D, Moncol J, Cronin MT, Mazur M, Telser J. Free radicals and antioxidants in normal physiological functions and human disease. Int J Biochem Cell Biol. 2007; 39: 44–84. PMID: 16978905

57. Anrather J, Racchumi G, Iadecola C. NF-kappa B regulates phagocytic NADPH oxidase by inducing the expression of gp91phox. J Biol Chem. 2006; 281: 5657–67. PMID: 16407283

58. Shoji Y, Uedono Y, Ishikura H, Takeyama N, Tanaka T. DNA damage induced by tumour necrosis factor-alpha in L929 cells is mediated by mitochondrial oxygen radical formation. Immunology. 1995; 84: 543–8. PMID: 7790027

59. Kim YS, Morgan MJ, Choksi S, Liu ZG. TNF-induced activation of the Nox1 NADPH oxidase and its role in the induction of necrotic cell death. Mol Cell. 2007; 26: 675–87. PMID: 17560373

60. De Cruz SJ, Kenyon NJ, Sandrock CE. Bench-to-bedside review: the role of nitric oxide in sepsis. Expert Rev Respir Med. 2009; 3: 511–21. doi: 10.1586/ers.09.39 PMID: 20477340

61. Chung SW, Liu X, Macias AA, Baron R, Perrella MA. Heme oxygenase-1-derived carbon monoxide enhances the host defense response to microbial sepsis in mice. J Clin Invest. 2008; 118: 239–47. PMID: 18060048

62. Tamion F, Richard V, Renet S, Thuillez C. Protective effects of heme-oxygenase expression against endotoxic shock: inhibition of tumor necrosis factor-alpha and augmentation of interleukin-10. J Trauma. 2006; 61: 1078–84. PMID: 17099512

63. Datla SR, Dusting GJ, Mori TA, Taylor CJ, Croft KD, Jiang F. Induction of heme oxygenase-1 in vivo suppresses NADPH oxidase derived oxidative stress. Hypertension. 2007; 50: 636–42. PMID: 17679649

5 Diskussion

5.1 Auswahl des bestgeeigneten Tiermodells

Um das am meisten geeignete Tiermodell zur Bestimmung des Einflusses der CXCR4-CXCL12-Achse auf den Verlauf einer systemischen Entzündung zu finden, wurden in Manuskript I das LPS-, das PCI- und das CLP-Modell als die in der Forschung am häufigsten verwendeten Tiermodelle vergleichend untersucht. Ziel war es dabei, herauszufinden, welches Tiermodell die Untersuchung des antiinflammatorischen und protektiven Potentials einer Substanz zulässt, welche (patho-) physiologischen Parameter sinnvollerweise herangezogen werden könnten und welcher Messzeitpunkt gewählt werden sollte, um nachfolgend den Einfluss der CXCR4-CXCL12-Achse mittels der Applikation verschiedener Liganden zu überprüfen. Dabei fanden sich zwischen den Tiermodellen innerhalb des untersuchten Zeitraums sowohl einige Gemeinsamkeiten in den Vitalparametern als auch wesentliche Unterschiede bezüglich der Entzündungsparameter, des oxidativen Stresses und des Migrationsverhaltens verschiedener Leukozytenpopulationen. Am deutlichsten waren die Differenzen zwischen der CLP-Gruppe und dem LPS- bzw. PCI-Modell ausgeprägt, wohingegen letztere sich nicht wesentlich unterschieden.

Eine Gemeinsamkeit aller Modelle bestand darin, dass alle Methoden zu einem verschlechterten Gesundheitszustand führten und somit, unabhängig vom auslösenden Stimulus, eine systemische Inflammation induzierten (Manuskript I). Ferner zeigten sich Gemeinsamkeiten bezüglich der bestimmten Vitalparameter der Mäuse. So waren in allen drei Modellen sowohl der systolische als auch der diastolische Blutdruck erniedrigt und die Herzfrequenz erhöht (Anhang Supplemental Data Manuskript I). Diese Veränderungen deuten darauf hin, dass alle Methoden einen schockähnlichen Zustand induzierten. So wird im Zuge eines Kreislaufschocks reflektorisch vermehrt Adrenalin gebildet und ins Blut freigesetzt, welches die Herzfrequenz erhöht (Bonanno 2011). Außerdem entsteht bei einem septisch-toxischen Schock häufig ein Endothelzellschaden, welcher einen Flüssigkeitsaustritt aus den Kapillaren in das Gewebe mit nachfolgendem relativem Blutvolumenmangel nach sich zieht (Riede et al. 2009). Darüber hinaus tritt aufgrund des Kreislaufschocks während der systemischen Inflammation eine Zentralisation des Blutes ein, um die Versorgung lebenswichtiger Organe, wie Herz und Gehirn, sicherzustellen (Riede et al. 2009). Der Blutdruck der Mäuse wurde am Schwanz der Tiere gemessen, welcher vermutlich aufgrund der Zentralisation des Blutes in allen Gruppen ähnlich schlecht durchblutet war. Dies könnte

ein zusätzlicher Grund dafür gewesen sein, dass bezüglich dieser Parameter keine wesentlichen Unterschiede zwischen den drei Modellen verzeichnet werden konnten.

Weiterhin kam es in allen Gruppen zu einer Hypoglykämie (Manuskript I) sowie zu einem schnellen Verbrauch der Glykogenreserven der Leber. Diese Effekte könnten Resultat einer deutlichen Steigerung des Energieumsatzes sein. Energiefordernde Prozesse sind hierbei vor allem die vermehrte Synthese von Abwehrproteinen, das Abräumen der Nekrosen und der eingedrungenen Pathogene in den Organen sowie der Wiederaufbau von zerstörtem Gewebe (Müller-Werdan et al. 2005). Weitere Gründe für die beobachtete Hypoglykämie könnten, neben einer verminderten hepatischen Gluconeogenese, erhöhte TNF-α und IL-1β-Serumwerte, welche über ihre Signalwege einen hohen Glukoseverbrauch induzieren, darstellen (Maitra et al. 2000; Preyra und Worster 2003; Raetzsch et al. 2009). Die Bedeutung des Glukose-Haushalts wird darin deutlich, dass eine Hypoglykämie das Mortalitätsrisiko bei Sepsis-Patienten nachweislich erhöht (Ssekitoleko et al. 2011; Park et al. 2012). Die Mäuse der CLP-Gruppe wiesen im Gegensatz zur LPS- und PCI-Therapie, deren Blutzuckerwerte sich bis zum Ende des Experiments wieder erholten, durchgehend niedrige Werte auf (Manuskript I), was unter anderem dazu beigetragen haben könnte, dass einzelne Tiere unerwartet verstarben.

Trotz aller Gemeinsamkeiten überwogen die Unterschiede zwischen den Modellen. Obwohl die Methoden derart justiert wurden, dass jeweils eine nicht-letale systemische Entzündungsreaktion induziert wurde, starben drei Mäuse aus der CLP-Gruppe. Dies zeigt einen wesentlichen Nachteil dieses experimentellen Modells auf, denn die Standardisierbarkeit ist im Vergleich zum LPS- oder PCI-Modell deutlich eingeschränkt. Ebenso wiesen nahezu alle evaluierten Parameter nach CLP-Operation die größten Standardabweichungen auf, was ebenfalls auf eine stark eingeschränkte Reproduzierbarkeit und Standardisierbarkeit hindeutet. Diese Probleme werden auch in der Literatur hervorgehoben (Dejager et al. 2011; Fink 2014). Weiterhin kann sowohl die Nadelgröße als auch die Anzahl der Punktionen die Schwere und den Verlauf der Sepsis stark beeinflussen. Entsprechend wurde gezeigt, dass die Menge an proinflammatorischen Zytokinen, die nach CLP-Operation ins Peritoneum und ins Serum freigesetzt wird, von der Nadelgröße abhängt (Ebong et al. 1999; Ruiz et al. 2016). Einerseits ergibt sich hierüber die Möglichkeit, die Schwere der systemischen Inflammation zu steuern, andererseits setzt dies eine große Erfahrung und ein präzises Arbeiten des Chirurgen voraus.

Ferner ergaben die Untersuchungen, dass die CLP-Methode einen protrahierten Krankheitsverlauf induziert, wohingegen das LPS- und das PCI-Modell zu einem rascher auftretenden und schwereren Krankheitsverlauf, nachfolgend aber auch zu einer beginnenden Regeneration innerhalb des untersuchten Zeitraums von 72 Stunden, führen. So fanden sich im Gegensatz zu den beiden anderen Tiermodellen nach CLP-Operation insbesondere zu den späteren Zeitpunkten erhöhte Serumspiegel proinflammatorischer Zytokine (Manuskript I), ein vermehrter oxidativer Stress in den Organen und eine verringerte Biotransformationskapazität der Leber. Auch Remick et al. und Valdés-Ferrer et al. konnten beim Vergleich der LPS- und CLP-Methode einen ähnlich unterschiedlichen Verlauf der von ihnen untersuchten Parameter zeigen (Remick et al. 2000; Valdés-Ferrer et al. 2013).

Zwischen dem LPS- und dem PCI-Modell waren dagegen nur geringe Unterschiede festzustellen. Allerdings zeigten Recknagel et al. in einer vorangegangenen Studie, dass die PCI-Methode eine vergleichsweise geringe TNF-α-Antwort induzierte und ein verzögertes IL-6-Freisetzungsprofil bewirkte (Recknagel et al. 2013). Dieser Widerspruch könnte durch die in der genannten Studie verwendete höhere PCI-Dosis erklärt werden, da die Autoren eine Mortalität nach 48 Stunden gewährleisten wollten. Außerdem wurde eine Flüssigkeitssubstitution durchgeführt, welche entsprechend Einfluss auf den natürlichen Verlauf der Entzündung hat, da sie eine supportive Therapiemaßnahme darstellt. Hinzu kommt, dass das PCI-Modell relativ neu ist und daher auch Inter-Labor-Unterschiede berücksichtigt werden sollten.

Die beobachteten Differenzen zwischen den drei Tiermodellen in den untersuchten Parametern, allen voran im oxidativen Stress in den Organen, in der Biotransformationskapazität der Leber und in der Zellimmigration in Leber und Milz (Manuskript I), lassen sich vermutlich auf die hervorgerufenen unterschiedlichen Zytokinprofile zurückführen. Wie erwähnt, führten die LPS- und die PCI-Gabe zu einer raschen und starken Ausschüttung von TNF-α und IL-6 (Manuskript I). Sowohl beide Zytokine als auch IFN-γ leiten die Produktion von reaktiven Sauerstoffspezies (ROS) ein, indem sie die Produktion und Aktivität von NF-κB steigern, die mitochondriale Integrität beeinträchtigen und die Aktivität der Nicotinamid-Adenin-Dinukleotidphosphat (NADPH)-Oxidase verstärken (Shoji et al. 1995; Kim et al. 2007). Die erhöhten Serumzytokinkonzentrationen könnten somit zu dem oxidativen Stress, insbesondere dem verminderten Glutathiongehalt und den erhöhten Lipidperoxidationprodukten, geführt haben (Manuskript I). Darüber hinaus sind TNF-α und IL-6 entscheidende Mediatoren, welche zu

einer verminderten Biotransformationskapazität der Leber beitragen (Morgan 2001; Jacob et al. 2009). Die zu späteren Zeitpunkten nach CLP-Operation festgestellten erhöhten Serumzytokinspiegel könnten entsprechend zu den im Vergleich zu den beiden anderen Modellen weiterhin signifikant erniedrigten CYP-Aktivitäten beigetragen haben.

In Bezug auf den klinischen Verlauf wurde in der Literatur gezeigt, dass vor allem die IL-6-Serumwerte die Schwere der systemischen Entzündung widerspiegeln und dass die Höhe der IL-6-Konzentration mit der Mortalität korreliert (Pinsky et al. 1993; Vianna et al. 2004). Außerdem besteht ein Zusammenhang zwischen der Persistenz von IL-6 und TNF-α im Blut und der Schwere der Erkrankung (Pinsky et al. 1993), was darauf hindeutet, dass das CLP-Modell in Bezug auf die Immunreaktion am ehesten mit der menschlichen Sepsis vergleichbar ist. Trotz aller methodischer Probleme stellt dies einen wesentlichen Vorteil des Modells dar.

Ferner zeigten vorangegangene Studien, dass vor allem IL-1β, IL-6 und TNF-α die Expression von Zelladhäsionsmolekülen, wie z.B. ICAM-1, nach bakterieller Infektion verstärken (Soderquist et al. 1999; Wung et al. 2005; Nathan 2006). Die massivste Zytokinfreisetzung war in den vorliegenden Untersuchungen nach LPS-Gabe zu beobachten, gefolgt von der PCI- und der CLP-Methode. Dementsprechend war festzustellen, dass nach LPS-Verabreichung mehr Neutrophile in das Gewebe immigrierten als bei der PCI- oder CLP-Methode (Manuskript I), was in der vermutlich erhöhten Anzahl an Adhäsionsmolekülen der Endothelzellen begründet liegen mag. Chosay et al. konnten darüber hinaus ebenfalls zeigen, dass die Gabe von LPS zu einer im Vergleich zur Kontrollgruppe verstärkten Immigration von Neutrophilen in die Gewebe führt (Chosay et al. 1997).

Die LPS- bzw. PCI-behandelten Mäuse erholten sich überwiegend nach 48 und 72 Stunden wieder, was anhand verschiedener Vital- und Entzündungsparameter auf Referenzniveau erkennbar war, wohingegen nach CLP-Operation keine Genesung erkennbar war. Diese Diskrepanzen könnten u.a. durch eine starke Freisetzung von IL-10 zustande gekommen sein, da nach LPS-Gabe bzw. nach PCI schon zu frühen Zeitpunkten erhöhte Werte im Serum messbar waren (Manuskript I). IL-10 fungiert als ein stark anti-inflammatorisches Zytokin und vermag u.a. die Synthese von TNF-α, IL-1β, IL-6 und IFN-γ in u.a. Monozyten und dendritischen Zellen zu hemmen. Gleichzeitig induziert es die Synthese entzündungshemmender Moleküle, wie z.B. IL-1-Rezeptor (Bazzoni et al. 2010; Moore et al. 2001). Darüber hinaus mag der erhöhte Glutahtion (GSH)-Gehalt in den Organen den Genesungsprozess nach LPS-Gabe bzw. nach PCI beschleunigt haben. GSH hat vielfältige Funktionen im Körper. Es besitzt antioxidative, antiinflammatorische und antiapoptotische

Eigenschaften (Dalton et al. 2004; Lu 2009). Ferner ließ sich nach Anwendung der CLP-Methode keine Induktion der HO-1 feststellen, wohingegen die LPS-Verabreichung und die PCI dieses Enzym aktivierten (Manuskript I). Die Relevanz wird dadurch deutlich, dass sich eine gezielte Überexpression der HO-1 in verschiedenen experimentellen Tiermodellen antiinflammatorisch und protektiv auswirkte (Kang et al. 2013; Luo et al. 2014). Bestätigung finden diese Befunde darin, dass HO-1-defiziente Mäuse anfälliger für eine polymikrobielle Sepsis sind (Chung et al. 2008). Darüber hinaus zeigen weitere Studien, dass das antiinflammatorische Enzym die TNF-α-Serumkonzentration nachhaltig zu senken und die IL-10-Serumkonzentration deutlich zu steigern vermag (Tamion et al. 2006).

Einen einzigen Grund für die Unterschiede zwischen den Tiermodellen auszumachen, ist aufgrund der Komplexität nicht möglich. Dennoch bewirkt die exogene Verabreichung von LPS bekanntermaßen eine massive Toll-like receptor 4 (TLR4)-Aktivierung, welche wiederum zu der beobachteten signifikanten Zytokinreaktion führt (Underhill und Ozinsky 2002). Vermutlich löst die Injektion einer polymikrobiellen Suspension (wie beim PCI-Modell) die TLR4-Aktivierung nicht in demselben Ausmaß aus. Die Zusammensetzung der Suspension deutet darauf hin, dass eine TLR4-Aktivierung durch die gramnegativen Bakterien (LPS ist ein Bestandteil der Zellwand) stattfindet, jedoch auch andere Rezeptoren des angeborenen Immunsystems zur Erkennung der u.a. grampositiven Bakterien beitragen (Underhill und Ozinsky 2002). Dennoch zeigen die Ergebnisse, dass die Bakterien und ihre Komponenten einen schnellen Eintritt der Entzündungsreaktion hervorrufen. Entsprechend liegen die geringfügigen Unterscheide im Verlauf und die etwas stärker ausgeprägten Effekte nach Endotoxin-Gabe vermutlich in der Zusammensetzung der Injektionslösungen begründet. Die CLP-Methode ist dagegen mit einer vergleichsweise langsamen Freisetzung von Bakterien mit unterschiedlichen Eigenschaften in den Blutkreislauf verbunden, was einen verzögerten, aber langwierigen Verlauf der Erkrankung hervorruft.

Die Ergebnisse verdeutlichen, dass die methodischen Nachteile der CLP-Methode, insbesondere die geringe Standardisierbar- und Reproduzierbarkeit, den Vorteil der eventuellen stärkeren klinischen Relevanz überwogen. Außerdem stellte der protrahierte Entzündungsverlauf eine Herausforderung dar, indem signifikante Effekte kaum bzw. erst zum Ende des Experiments deutlich sichtbar wurden. Demzufolge ist die Evaluation einer neuen antiinflammatorischen Substanz erschwert, da diese über einen längeren Zeitraum wirken und entsprechend eine längere Halbwertszeit aufweisen bzw. öfters appliziert werden müsste. Eine Modifizierung der Methode hin zur Induktion einer schwereren systemischen

Inflammation, um deutlichere Effekte bereits früher zu sehen, wäre mit einer höheren Mortalität verbunden und würde eine Beantwortung der eigentlichen Fragestellung, die methodisch bedingten Unterschiede in den Effekten zu vergleichen, nicht ermöglichen. Der verzögerte Verlauf deutet außerdem darauf hin, dass längere Versuchszeiträume (>72 Stunden) benötigt werden, was die klinische Relevanz etwas einschränkt, da während eines solch langen Zeitraumes höchstwahrscheinlich zusätzliche chirurgische, adjunktive und supportive Maßnahmen eingeleitet werden. Das PCI-Modell besticht durch die Induktion einer polymikrobiellen Entzündung. Jedoch erwiesen sich die Ergebnisse als nahezu identisch mit jenen nach LPS-Applikation, wobei einige Effekte schwächer ausgeprägt waren. Aufgrund des methodisch höheren Aufwands (vor allem in der Präparation der Stuhlsuspension), den bislang geringen Erfahrungen mit dieser Methode und der entsprechend spärlichen Datenlage in der Literatur, rückte dieses Modell in den vorliegenden Untersuchungen in den Hintergrund. Obwohl der klinische Verlauf einer Sepsis nicht ideal nachgestellt werden kann, erwies sich das LPS-Modell dennoch als das geeignetste Tiermodell. Die Methode ist sehr gut reproduzierbar, besitzt den geringsten methodischen Aufwand und hat zudem einen historisch langen Anwendungshorizont, wodurch viele Vergleichsdaten vorliegen. Darüber hinaus waren die beobachteten Effekte in den vorliegenden Untersuchungen eindeutig und zeigten ihr Maximum nahezu immer nach 12-24 Stunden. Entsprechend ergab sich hieraus, dass einerseits das LPS-Modell und andererseits der Zeitpunkt nach 24 Stunden zur Ermittlung des Einflusses des CXCR4 und seiner Liganden auf das Entzündungsgeschehen am idealsten sind.

5.2 Migrationsverhalten verschiedener Leukozytenpopulationen in die Leber und Milz

Wie unter 2.2.3 erwähnt, erwies sich der Antagonismus am CXCR4 bei einigen entzündlichen Erkrankungen als vorteilhaft, da eine Einwanderung von CXCR4-kompetenten Entzündungszellen ins Gewebe und eine damit verbundene Zytokinfreisetzung unterbunden wurde. Die Tatsache, dass bei einem septischen Schock und in den ersten Stunden einer schweren Sepsis überwiegend durch einen Zytokinsturm erhebliche Zell- und Organschäden entstehen, führte zu der Intention, die massive Freisetzung der proinflammatorischen Mediatoren durch einen CXCR4-Antagonismus zu blockieren. Die Verabreichung von AMD3100, einem spezifischen CXCR4-Inhibitor, erwies sich allerdings in den vorliegenden

Untersuchungen als unvorteilhaft – die Entzündung wurde verschärft (Manuskript II). Im Gegensatz dazu führte die Applikation des plasmastabilen CXCL12-Analogons CTCE-0214D zu einer wesentlichen Verbesserung der durch LPS induzierten systemischen Inflammation (Manuskript III). Diese Beobachtungen können u.a. mit dem Migrationsverhalten verschiedener Entzündungszellen erklärt werden.

Wie erwähnt, sind das Chemokin CXCL12 und sein Rezeptor CXCR4 für die Migration von Monozyten, Neutrophilen und hämatopoetischen Vorläuferzellen sehr entscheidend. Entsprechend konnten Delano et al. nachweisen, dass die Mobilisierung von Neutrophilen aus dem Knochenmark und weiteren Speicherorten in die Peripherie und an die Infektionsorte CXCR4-CXCL12-abhängig ist und dass eine Unterbindung der CXCR4-CXCL12-Interaktion die Beseitigung der Pathogene im Blut und in den Organen erheblich beeinträchtigt (Delano et al. 2011). Nach Eindringen des Erregers in den Organismus ist die schnelle Bekämpfung von entscheidender Bedeutung, um eine Ausbreitung zu verhindern. Während die CXCR4-Blockade im Entzündungsgeschehen die Mobilisierung von immunkompetenten Zellen zu hemmen scheint, ist die unterstützende Aktivierung der CXCR4-CXCL12-Achse mit einer verstärkten Rekrutierung von u.a. Neutrophilen verbunden. Folgerichtig konnte gezeigt werden, dass die Gabe eines plasmastabilen CXCL12-Analogons bei einer CLP-induzierten Sepsis in Mäusen zahlreiche Neutrophile in die Peripherie und an den Infektionsort mobilisierte (Delano et al. 2011; Guan et al. 2014). Darüber hinaus wurde eine verstärkte phagozytotische Aktivität und daraus folgend eine effizientere Beseitigung der Pathogene beobachtet, was sich vor allem in der Blutbahn und auch in der Lunge protektiv auswirkte (Guan et al. 2014). Zusätzlich wurde gezeigt, dass CXCL12 die Migration von natürlichen Killerzellen in die Organe fördert und somit zur Beseitigung der Pathogene beiträgt (Goda et al. 2006). Zusammenfassend deutet vieles darauf hin, dass die schnelle Rekrutierung von CXCR4-positiven Zellen in der akuten systemischen Entzündung erfolgversprechend zu sein scheint und die exogene Verabreichung von CXCL12-Analoga vorteilhaft ist, um funktionelle CXCR4-positive Zellen schnell an die Infektionsorte zu dirigieren, wohingegen eine CXCR4-Blockade die physiologischen Abwehrmechanismen negativ beeinflussen kann. Die in dieser Arbeit vorgestellten Ergebnisse (Manuskript III) stimmen mit dem kürzlich beschriebenen positiven Einfluss der kombinierten Behandlung mit dem CXCL12-Analogon CTCE-0214 und Imipenem überein, bei der die Mobilisierung von Neutrophilen an den Infektionsort verstärkt und die bakterielle Clearance bei Mäusen verbessert wurden (Guan et al. 2014).

Weiterhin konnte gezeigt werden, dass die exogene CXCL12-Zufuhr eine deutliche Reduktion der Parasitenanzahl in Mäusen nach einer Malariainfektion zur Folge hatte (Garnica et al. 2002). CXCL12 ist physiologisch bedeutend im Knochenmark von gesunden Tieren und Menschen exprimiert und hält als Chemokin mit seiner hohen Konzentration viele CXCR4-positive Zellen dort fest. In der Peripherie ist dagegen unter physiologischen Bedingungen nur eine geringe CXCL12-Konzentration nachzuweisen. Dieser Gradient scheint jedoch in der systemischen Entzündung bzw. in Infektionskrankheiten invertiert zu sein, d.h. die Peripherie hat aufgrund des hohen Gehalts an CXCL12 eine chemotaktische bzw. „lockende“ Wirkung auf CXCR4-exprimierende Zellen (Delano et al. 2011; Guan et al. 2014). Die hier vorliegenden Ergebnisse stützen diese Erkenntnisse, da vermehrt CXCL12-produzierende Zellen in den Milzen nach LPS-Gabe aufzufinden waren (Manuskript III). Darüber hinaus fanden sich verstärkt CXCR4-positive Zellen in den Milzen und je mehr Sternhimmelmakrophagen in der weißen Pulpa CXCL12 exprimierten, desto mehr CXCR4-kompetente Zellen immigrierten und waren in den Organschnitten nachweisbar. Wahrscheinlich ziehen die Sternhimmelmakrophagen u.a. Lymphozyten an, um die hohe Zellmenge etwas zu verringern. Dafür spricht auch die in der weißen Pulpa vermehrt stattfindende Apoptose. CTCE-0214D reduzierte die Menge der Sternhimmelmakrophagen in der Milz und im Thymus, was darauf hinweist, dass einerseits weniger Zellen immigrierten und andererseits das ganze Entzündungsgeschehen weniger stark ausgeprägt war. Folglich scheint die exogene Verabreichung von CXCL12-Analoga bzw. von CXCR4-Agonisten eine Möglichkeit zu sein, den Organismus zu unterstützen, um funktionelle CXCR4-positive Zellen schnell zu mobilisieren.

Da durch die Gabe von AMD3100 in der systemischen Entzündung die schnelle Rekrutierung von CXCR4-positiven Immunzellen eingeschränkt zu sein scheint, ist eine adäquate Immunantwort nach einer Infektion nur bedingt möglich. Entsprechend können Noxen (wie z.B. LPS) Zellschädigungen und eine starke Immunreaktion hervorrufen. Durch die erhöhte TNF-α-, IL-6-, IL-1β- und IFN-γ-Freisetzung, findet u.a. eine verstärkte Expression von Adhäsionsmolekülen statt, welche zur beschriebenen verstärkten Einwanderung von Neutrophilen in Leber und Milz (Manuskript II) führt (Collins et al. 1995). In der Milz war ferner eine verstärkte Apoptose in der weißen Pulpa zu verzeichnen, was u.a. eine Reaktion auf die immens erhöhte Zellzahl darstellt. Außerdem trugen die in der Milz und im Thymus verstärkt beobachtete Apoptose nach LPS- bzw. AMD- plus LPS-Gabe und die damit einhergehende geringere Anzahl an Lymphozyten maßgeblich dazu bei, dass eine Leukozytopenie im Blut nach AMD3100+LPS-Verabreichung nachweisbar war (Manuskript

II). Der antiapoptotische Effekt nach CTCE-0214D-Gabe zeigt sich hiermit auch nicht weniger relevant, da Lymphozyten von maßgeblicher Bedeutung im Rahmen der Immunantwort sind. Allerdings war nach zusätzlicher AMD3100-Gabe eine Umverteilung der Lymphozyten zu beobachten, sodass weniger Zellen in den Milzen von AMD3100+LPS-behandelten Mäusen nachweisbar waren, wohingegen die Leber eine vermehrte Lymphozyten-Anzahl aufwies (Manuskript II). Dieser Befund deutet auf eine Verschiebung der Zellpopulation zum Ort der verstärkten Entzündung hin. Dazu passend zeigten Untersuchungen von Tsuchiya et al., dass CXCR4-Knockout-Mäuse, eine erhöhte Anzahl von Cluster of differentiation 3 (CD3)-positiven Lymphozyten in der Leber aufwiesen (Tsuchiya et al. 2012).

Da AMD3100 eine kurze Halbwertszeit von ca. dreieinhalb Stunden besitzt (Hendrix et al. 2000), sind die ermittelten Daten nach 24 Stunden differenziert zu betrachten. Die in der Peripherie im Gegensatz zu Kontrolle festgestellte Neutrophilie nach AMD3100+LPS-Gabe mag durch eine (verstärkte) Gegenregulation nach Abklingen der Wirkung des AMD3100 aufgetreten sein. Da aufgrund der CXCR4-Blockade weniger Neutrophile zur Beseitigung der Pathogene mobilisiert werden konnten, mag es zu einer stärkeren Zell- und Organschädigung gekommen sein, welche wiederum verstärkt Neutrophile anlockt, wenn die hemmende Wirkung des AMD3100 aufgrund der kurzen Halbwertszeit nachlässt. Die nach alleiniger AMD3100-Gabe festgestellte geringfügige Neutrophilie nach 24 Stunden könnte durch eine Freisetzung von Neutrophilen aus den Lungen induziert worden sein, da gleichzeitig eine Rückkehr der CXCR4-positiven Zellen ins Knochenmark zur Elimination aus dem Blut gehemmt wurde (Devi et al. 2013). Im Entzündungsgeschehen ist dieser Zusammenhang allerdings mit Vorsicht zu betrachten und wohl untergeordnet, da der CXCL12-Gradient in der systemischen Entzündung, wie beschrieben, invertiert zu sein scheint.

Insgesamt scheint der Einfluss der CXCR4-CXCL12-Achse auf die akute systemische Inflammation sehr komplex zu sein. So fanden Saiman et al. keine Anzeichen einer Entzündung in der Leber nach CXCR4-Blockade in Kombination mit einer Tetrachlorkohlenstoff-Gabe (Saiman et al. 2015). Zudem zeigte die Studie, dass nach AMD3100-Verabreichung sowohl die dreifache Menge an Neutrophilen im Blut und in der Leber als auch die doppelte Menge an hämatopoetischen Stammzellen in der Leber nach 36 Stunden nachweisbar waren. Die Autoren vermuten, dass die verstärkte Aktivität der Neutrophilen potentielle positive Effekte der hämatopoetischen Stammzellen abgeschwächt haben könnte (Broxmeyer et al. 2005; Saiman et al. 2015). Diese Erkenntnisse können dazu

beitragen, die scheinbar widersprüchliche Datenlage bezüglich einer Aktivierung bzw. Hemmung der CXCR4-CXCL12-Achse in entzündlichen Erkrankungen (siehe Kapitel 2.3.3) zu erklären. So mag die schnelle Rekrutierung von CXCR4-positiven Zellen in die Peripherie und an die Entzündungsorte während einer rheumatoiden Arthritis oder eines Lupus erythematodes nicht vorteilhaft sein, sodass sich der Agonismus am CXCR4 nachteilig auswirken sollte. Durch eine CXCR4-Blockade werden nur wenige Entzündungszellen aus den Speicherorten in die Peripherie entlassen und entsprechend ist die Immigration in die Organe vermindert. Hierin könnte der positive Einfluss von CXCR4-Antagonisten in Autoimmunerkrankungen begründet liegen. Außerdem befinden sich die Noxen und Auslöser der Autoimmunkrankheiten oft in den Organen und nicht im Blutstrom, weshalb eine schnelle Mobilisierung von Neutrophilen ins periphere Blut zur Beseitigung der Pathogene nicht notwendig zu sein scheint und eher im Gegenteil eine potentielle Immigration der Entzündungszellen ermöglichen würde.

5.3 Systemische Effekte und die Auswirkungen auf die Organfunktionen

Die CXCR4-Hemmung mit AMD3100 führte zu einer deutlichen Freisetzung proinflammatorischer Zytokine (Manuskript II). Verantwortlich dafür sind vermutlich die verstärkt eingewanderten Neutrophilen und Lymphozyten, welche diese Zytokine im Rahmen der Immunantwort produzieren. Im Gegensatz dazu führte die Gabe des CXCL12-Analogos CTCE-0214D zu einer merklichen Reduktion der Serumspiegel dieser Mediatoren (Manuskript III). Ebenso waren in der Perjodsäure-Schiff (PAS)-Färbung nach CTCE-0214D-Behandlung weniger Entzündungszellen in der Leber nach 24 Stunden zu erkennen (Manuskript III). Fan et al. zeigten bereits, dass das CXCL12-Analogon CTCE-0214 in der Lage ist, die TNF-α und IL-6-Serumspiegel in Nagern zu senken, und weitere Untersuchungen in Schweinen nach Polytrauma bestätigten dies (Bach et al. 2012; Fan et al. 2012). Die zugrundeliegenden Mechanismen, weitere systemische Effekte und auch mögliche Einflüsse auf die Organe waren allerdings nicht Bestandteil dieser Untersuchung. Neben den beschriebenen Migrationsprozessen mögen sowohl molekulare als auch weitere zelluläre Prozesse zu den beobachteten Effekten beigetragen haben.

Die Aktivierung der CXCR4-CXCL12-Achse mittels CTCE-0214D führte bei der in der vorliegenden Untersuchung erzeugten akuten systemischen Entzündung zu einer

verminderten TLR4-Expression in den Organen, wohingegen LPS-behandelte Mäuse ein verstärktes TLR4-Vorkommen zeigten (Manuskript III). Endotoxin ist dafür bekannt, den TLR4-Rezeptor zu aktivieren und über Transkriptionsfaktoren wie NF-κB die Produktion zahlreicher Zytokine zu induzieren. Unter dem Einfluss von CTCE-0214D war hingegen eine geringere Expression von NF-κB in Leber, Milz und Thymus zu verzeichnen, was eine verminderte TLR4-Signaltransduktion nach CXCR4-Aktivierung nahelegt. Dazu passend konnte durch in-vitro-Versuche gezeigt werden, dass CXCL12 die NF-κB-Aktivierung nach LPS-Stimulation in transfizierten HEK-Zellen unterdrückt (Kishore et al. 2005). Darüber hinaus scheint der CXCR4 ein Teil des LPS-Erkennungsapparats zu sein und als eine Art Co-Rezeptor zu fungieren (Triantafilou et al. 2008). Außerdem vermag LPS den CXCR4 direkt zu aktivieren und somit weitere entzündliche Prozesse einzuleiten (Triantafilou et al. 2008). Entsprechend könnte ein Ligand am CXCR4 die direkte Bindung von LPS an den CXCR4 unterbinden oder eine Rezeptorkonfirmationsänderung bewirken, was den Krankheitsverlauf positiv beeinflussen könnte. Ob ein Agonist oder ein Antagonist den protektiven Effekt ausübt, ist in der Literatur stark umstritten. Ebenso ist dies auch abhängig von der Zelllinie und deren Eigenschaften (Kishore et al. 2005; Triantafilou et al. 2008). Die hier vorgelegten Ergebnisse nach CTCE-0214D-Gabe zeigen eine Reduktion der Serum-TNF-α-Spiegel (Manuskript III), was die Folge einer Rezeptormodulation und einer indirekten NF-κB-Hemmung sein kann. In der Literatur konnte ferner gezeigt werden, dass der kürzlich entdeckte CXCR4-Agonist Ubiquitin im Rahmen einer LPS-induzierten systemischen Inflammation die NF-κB- und TNF-α-Produktion nachhaltig senken konnte (Majetschak et al. 2004). Um diesen Erkenntnissen genauer nachzugehen, wurden THP-1-Monozyten und -Makrophagen, welche beide den CXCR4 und den TLR4 exprimieren, kombiniert und alleine mit LPS, AMD3100 und CXCL12 in vitro stimuliert. Jedoch hatte weder der Antagonismus, noch der Agonismus am CXCR4 einen relevanten Einfluss auf die ausgeschüttete Zytokinmenge (Anhang Supplemental Data Manuskript II). Weitere Untersuchungen an Jurkat- und HepG2-Zellen blieben ebenso erfolglos. Diese Ergebnisse sind widersprüchlich zu den wenigen Literaturdaten. Jedoch sollte beachtet werden, dass in den genannten Studien oft artifizielle Zellmodelle verwendet wurden und (vor allem in HEK-Zellen) mehrere Transfektionen dem eigentlichen Versuch vorgeschaltet waren, was die eigentliche Relevanz und Aussagekraft einschränkt. Zusätzlich sprechen die hier vorgelegten Ergebnisse (Manuskript II und III) eher dafür, dass die Migration von Immunzellen eine zentralere Rolle spielt und ein direkter Einfluss von LPS auf die CXCR4-Signalwege eher von untergeordneter Bedeutung ist.

NF-κB spielt eine zentrale Rolle bei der Immunantwort des Wirts und fungiert als Schlüsselregulator u.a. durch die Kontrolle der Zellproliferation, der Apoptose und vieler Immun- und Stressreaktionen (Morgan und Liu 2011). Besonders die Cyclooxygenase-2 (COX-2) ist ein bekanntes Produkt nach NF-κB-Aktivierung. Durch die COX-2 gebildet, stimulieren Prostaglandine eine Glykogenolyse in der Leber (Casteleijn et al. 1988). Die nach CTCE-0214D festgestellte geringere NF-κB-Expression mag auf diesem Wege zu dem deutlich höheren Glykogengehalt in der Leber beigetragen haben. Hierzu passt der Befund, dass nach CXCR4-Blockade eine deutlich stärkere Glykogendepletion im Vergleich zur alleinigen LPS-Gabe zu beobachten war (Manuskript II). Ferner war eine verstärkte Hypoglykämie nach CXCR4-Hemmung durch AMD3100 festzustellen, wohingegen die Verabreichung von CTCE-0214D die Blutzuckerwerte signifikant verbesserte (Manuskript III). Der schlechte Allgemeinzustand der Tiere nach der CXCR4-Blockade erforderte viele Ressourcen, um der Entzündung und dem oxidativen Stress entgegenzuwirken, wohingegen nach CTCE-0214D-Gabe ein besserer Allgemeinzustand der Tiere zu verzeichnen war und entsprechend weniger Energiereserven verbraucht werden mussten, was durch den höheren Blutzucker signalisiert wird. Da bereits eine Hypoglykämie ein erhöhtes Mortalitätsrisiko bedingt (Park et al. 2012), ist der hierüber vermittelte Einfluss von CTCE-0214D auf den Allgemeinzustand der Tiere von wesentlicher Bedeutung.

Die Hauptquelle der TNF-α-Produktion in der Leber nach 24 Stunden waren Endothelzellen, wobei sich die TNF-α-Expression der Zellen durch die AMD3100-vermittelte CXCR4-Blockade erheblich intensivierte (Manuskript II). Jedoch bleibt unklar, ob diese Zellen direkt durch LPS angeregt oder indirekt über eine vorherige Aktivierung von z.B. Kupffer-Zellen, Neutrophilen oder Lymphozyten stimuliert wurden. Bisher gab es nur wenige Studien, die sich auf Endothelzellen als Quelle der entzündungsfördernden Zytokine konzentrierten. Dennoch konnte festgestellt werden, dass mit IL-1α stimulierte human umbilical vein endothelial cells (HUVECs) eine moderate Menge an TNF-α erzeugten, während LPS keine TNF-α-Sekretion induzierte (Imaizumi et al. 2000). In Verbindung mit der Tatsache, dass die typischen TNF-α-Produzenten Monozyten, Neutrophile und Lymphozyten sind, spricht daher einiges für eine indirekte Aktivierung der Endothelzellen.

Weiterhin wiesen AMD3100+LPS-behandelte Mäuse einen massiv erhöhten oxidativen Stress in den Gehirnen, Nieren und Lebern auf (Manuskript II). Wie erwähnt, immigrierten viele Neutrophile in die Leber, welche vermutlich zur erhöhten TNF-α- und IFN-γ-Produktion beigetragen haben. Beide Zytokine sind in der Lage, ROS über Mitochondrien und über die

NADPH-Oxidase zu erzeugen und die induzierbare NO-Synthase (iNOS) stark zu stimulieren (Tötemeyer et al. 2006; Kim et al. 2007). Entsprechend waren erhöhte Serum-NO-Spiegel nach CXCR4-Blockade messbar, welche zum vermehrten oxidativen Stress beigetragen haben und den im vorangegangenen Experiment (Anhang Supplemental Data Manuskript I) gemessenen niedrigen Blutdruck nach LPS-Gabe erklären würden. Beides beeinflusst das allgemeine Wohlbefinden der Mäuse negativ, was mit dem schlechteren Allgemeinzustand der Tiere übereinstimmt. Ferner reduzierte CTCE-0214D die Expression der NADPH-Oxidase. Unter normalen Umständen ist eine milde Aktivität der NADPH-Oxidase essentiell, um Pathogene wie Bakterien und Pilze zu eliminieren. Eine überschießende Reaktion geht hingegen mit erhöhtem oxidativen Stress, Organschäden und einem möglichen Organversagen einher (Kim et al. 2007).

Eine potentielle Erklärung für die positiven Ergebnisse nach CXCR4-Aktivierung und den nachteiligen Auswirkungen nach CXCR4-Antagonismus könnte die unterschiedliche Regulation der HO-1 sein. Wie beschrieben, ist eine gezielte Überexpression des antiinflammatorisch und antioxidativ wirkenden Enzyms protektiv und steigert das Überleben in Nagern. Der CXCR4-Rezeptor scheint den vorliegenden Ergebnissen zufolge einen wesentlichen Einfluss auf die Expression und Aktivität dieses Enzyms zu haben, da ein Antagonismus zu einer geringeren Aktivität und Expression in der Leber führte (Manuskript II), wohingegen ein Agonismus das Enzym induzierte (Manuskript III). HO-1 ist in der Lage, die TNF-α- und ROS-Produktion zu senken, was mit den entsprechend niedrigeren TNF-α- und ROS-Spiegeln nach CTCE-0214D-Gabe übereinstimmt. Interessant ist, dass AMD3100 alleine die HO-1-Aktivität signifikant senken konnte, während CTCE-0214D eine Induktion des Enzyms bewirkte. Dies deutet auf einen entscheidenden Einfluss des CXCR4 hin. Möglich erscheint eine Induktion der PKCζ über einen CXCR4-abhängigen Weg (Maru 2016). Darüber hinaus führte die Blockade mit AMD3100 zu einer geringeren Nuclear factor (erythroid-derived 2)-like 2 (Nrf-2)-Expression in der Leber (Manuskript II). Nrf-2 stellt einen protektiven Transkriptionsfaktor dar, welcher die Expression zahlreicher zytoprotektiver Enzyme wie NAD(P)H-Chinon-Oxidoreduktase 1, Glutamat-Cystein-Ligase und HO-1 erhöht (Ma 2013). Somit scheint AMD3100 über eine geringere Nrf-2-Aktivierung die HO-1-Produktion zu inhibieren. Dazu passend zeigten Dinić et al., dass CXCL12 pankreatische β-Zellen vor oxidativem Stress durch eine Nrf2-induzierte Zunahme der Katalase-Expression und -Aktivität schützt (Dinić et al. 2016).

Ferner mag der erhöhte Gehalt an reduziertem Glutathion aufgrund seiner zytoprotektiven und antioxidativen Wirkung nicht unwesentlich zur besseren Situation der mit CTCE-0214D behandelten Mäusen beigetragen haben (Manuskript III). GSH ist darüber hinaus entscheidend für das Überleben der Zellen. So wiesen γ-Glutamylcysteinsynthetase-Knockout-Mäuse durch die nur eingeschränkt mögliche GSH-Neusynthese einen ausgeprägten GSH-Mangel auf und verstarben aufgrund einer massiv einsetzenden Apoptose (Dalton et al. 2004; Muyderman et al. 2007). Neben dem positiven Glutathionstatus war in der Milz nach CXCR4-Aktivierung eine deutlich geringere Apoptoserate nachweisbar. Der verringerte Zelltod der Leukozyten führte zu einem kompetenteren Immunsystem mitsamt effektiverer Antwort. Welche Mechanismen genau verantwortlich waren, bedarf weiterer Untersuchungen. Dennoch sollte eine direkte CXCR4-Beteiligung in Erwägung gezogen werden, da die Apoptose in den Milzen nach CXCR4-Blockade mit AMD3100 verstärkt wurde (Manuskript II). Möglicherweise erhöht CXCL12 das Verhältnis des antiapoptotischen B-cell lymphoma 2 (Bcl-2) gegenüber dem proapoptotischen Bax, wie es bereits nach einem Hirntrauma nachgewiesen werden konnte (Mao et al. 2014). Infrage kommt auch eine Aktivierung des PI3K/Akt-Signalwegs. So wurde nach CXCL12-Verabreichung ein verbessertes Überleben der Insulin produzierenden β-Zellen des Pankreas in Mäusen beobachtet (Yano et al. 2007). Dennoch ist der antiapoptotische Einfluss über mehrere Signalwege am wahrscheinlichsten, denn die erwähnt niedrigeren TNF-α- und ROS-Spiegel nach CXCR4-Aktivierung haben ihrerseits sehr wahrscheinlich durch eine verringerte Induktion apoptotischer Prozesse zum Gesamtbild beigetragen.

Wie bereits ausgeführt, spielen v.a. TNF-α und IL-6 eine zentrale Rolle, indem sie die Biotransformationskapazität der Leber reduzieren. Die Aktivierung der CXCR4-CXCL12-Achse reduzierte die Zytokinproduktion und entsprechend waren merklich höhere CYP-Aktivitäten nachweisbar (Manuskript III). Mäuse, welche hingegen mit AMD3100 behandelt worden waren, wiesen dagegen verringerte CYP-Aktivitäten auf (Manuskript II), was zu dem deutlich schlechteren Allgemeinzustand nach LPS-Gabe beigetragen haben wird, da die CYP-Enzyme nur eingeschränkt in der Lage waren, ausscheidungspflichtige Moleküle zu metabolisieren. Darüber hinaus ist die Neusynthese der Steroidhormone von verschiedenen CYP-Enzymen abhängig (Monostory und Dvorak 2011). Entsprechend könnte ein verminderter Aufbau der Hormone zu einer insuffizienten Immunantwort beigetragen haben. Weiterhin ist die Biotransformationskapazität auch deshalb von entscheidender Bedeutung, weil septische Patienten häufig mit mehreren Medikamenten wie Antibiotika behandelt werden. Eine CXCR4-Blockade wäre daher im klinischen Verlauf wahrscheinlich ungünstig,

da die Nebenwirkungen der über die Leber verstoffwechselten Medikamente verstärkt zum Tragen kommen würden (Jacob et al. 2009).

Neben der reduzierten Biotransformationskapazität waren in der Leber nach der CXCR4-Blockade mit AMD3100 weitere Schädigungen erkennbar. Histologisch zeigte sich eine intensive Fettansammlung, und auch ein geringfügiges Ödem war erkennbar. Auch die Serum-Alanin-Aminotransferase (ALAT)- und -Aspartat-Aminotransferase (ASAT)-Aktivitäten als Indikatoren für einen Leberzellschaden wurden durch AMD3100 weiter erhöht. Dazu passend konnte CTCE-0214D die nach LPS-Gabe gestiegenen Leberparameter deutlich senken, wodurch der protektive Einfluss noch zusätzlich verdeutlicht wird (Anhang Supplemental Data Manuskript III). Diese Ergebnisse reihen sich in die aktuelle Literatur ein, in welcher der Einfluss von AMD3100 auf eine chronische Leberentzündung getestet wurde (Saiman et al. 2015). Hier war ein Trend zu einer verstärkten Leberzellnekrose nach 36 Stunden erkennbar, während die ALAT- und ASAT-Werte leicht, aber nicht signifikant erhöht wurden. Die Autoren schlussfolgerten, dass es tendenziell zu einem schwereren Verlauf der Leberentzündung kommt, wenn zusätzlich AMD3100 verabreicht wird.

Neben der Leber- war auch die Nierenfunktion nach CXCR4-Antagonisierung verstärkt beeinträchtigt. Als Indikatoren dienten sowohl die Harnstoff- als auch die Kreatininkonzentration im Serum (Anhang Supplemental Data Manuskript II). Der Harnstoffgehalt war nach der Behandlung mit AMD3100 deutlich reduziert. Diese Beobachtungen sind jedoch sehr wahrscheinlich eher auf die beeinträchtigte Lebersyntheseleistung als auf die verringerte Nierenfunktion zurückzuführen, da die Leber den Hauptteil des Harnstoffs produziert (Mezey 1982). Nur in den Fällen, in denen die glomeruläre Filtrationsrate auf 50% oder weniger fällt, steigen die Harnstoffspiegel des Serums deutlich an, weshalb dieser Parameter sodann als Maß für schwere Nierenschäden dienen kann (Baum et al. 1975). Bezüglich des Serumkreatinins waren nach CXCR4-Blockade ebenfalls im Vergleich zur alleinigen LPS-Verabreichung signifikant erhöhte Werte feststellbar, die auf eine Beeinträchtigung der Nierenfunktion hinweisen. Dennoch ist bei diesem Parameter eine vorsichtige Betrachtung geboten, da er von vielen (auch nicht mit der Niere in Zusammenhang stehenden) Faktoren beeinflusst wird, wie z.B. Alter, Geschlecht, Muskelmasse oder Ernährungsstatus (Edelstein 2008). Folglich deuten die Ergebnisse darauf hin, dass die Synthesefunktion der Leber sowohl nach alleiniger LPS- als auch nach kombinierter LPS- und AMD3100-Gabe maßgeblich beeinflusst wurde, die Nieren jedoch

wohl nur einen mäßigen Schaden davontrugen. Passend dazu zeigten sich in den Nieren histologisch, abgesehen von einem milden Ödem, keine größeren Veränderungen.

In der Milz war nach der CXCR4-Blockade vor allem eine vermehrte Splenomegalie zu verzeichnen. Histologisch waren nach AMD3100+LPS-Gabe insbesondere eine große Anzahl an Erythrozyten und Neutrophilen in der roten Pulpa neben einem leichten Ödem erkennbar. Außerdem zeigten sich einige Entzündungszellen in der weißen Pulpa, was durch die genannte dort verstärkt stattfindende Apoptose zu erklären ist. Wie unter 2.1.5 beschrieben, ist die Hypertrophie der Pulpa u.a. TNF-α- und IL-6-vermittelt (Valdés-Ferrer et al. 2013). Damit könnte die nach AMD3100-Gabe beobachtete Splenomegalie erklärt werden, wohingegen die CXCR4-Aktivierung zu keiner Organvergrößerung führte. Anscheinend führte die CXCR4-Blockade verstärkt dazu, dass geschädigte, der Eliminierung bedürftige Immunzellen in das Milzgewebe einwanderten, woraufhin eine massive Apoptose stattfand (Manuskript II). Die beobachtete Anämie und Thrombozytopenie nach CXCR4-Blockade (Manuskript II) ist ebenso u.a. mit der Splenomegalie zu erklären, da die Beseitigung dysfunktionaler Blutzellen vor allem in der Milz stattfindet.

6 Schlussfolgerungen und Ausblick

Die Ergebnisse verdeutlichen, dass die Verabreichung von LPS die eindeutigsten Veränderungen in den Vital- und Entzündungsparametern nach 24 Stunden zur Folge hatte. Für die Untersuchung eines protektiven Einflusses einer neuen Substanz und zur Untersuchung (patho-)physiologischer Abläufe, eignet sich dieses Modell daher am besten, um eine potentielle Verbesserung des Gesundheitszustandes zu erkennen. Insbesondere der Verlauf einer akuten sytemischen Entzündung ließ sich mit dem LPS-Model gut nachbilden. Ferner zeigte sich in allen Tiermodellen, dass der Chemokinrezeptor 4 und sein Ligand während der Entzündungsreaktion ihre Expressionsmuster verändern, sodass auf einen relevanten Einfluss während der Immunreaktion geschlussfolgert werden kann.

Die Unterstützung der CXCR4-CXCL12-Achse mittels eines Agonisten verbesserte die systemische Entzündung in der akuten Phase deutlich, während eine Unterbrechung des Signalweges sich als unvorteilhaft herausstellte. Die CXCR4-Blockade ging u.a. einher mit einem verschlechterten Allgemeinzustand, einer verstärkten Expression proinflammatorischer Zytokine, einem erhöhten Niveau an oxidativem Stress und einer vermehrten Apoptose in den Organen. Ferner vermittelte die Blockade eine zusätzliche Abnahme der Leber-Biotransformationskapazität sowie eine Reduktion der HO-1-Expression. CTCE-0214D wirkte hingegen entzündungshemmend, antioxidativ und zytoprotektiv. Einiges deutet darauf hin, dass eine Verminderung migratorischer Prozesse die protektive Wirkung hervorruft und eine direkte Beeinflussung des TLR4-Signalings in diesem Zusammenhang eher von untergeordneter Bedeutung ist. Die in der Folge geringere Anzahl an Neutrophilen und Lymphozyten in den Organen bedingt eine verminderte Ausschüttung proinflammatorischer Zytokine, welche bei der Regulation vieler der gemessenen Parameter eine Schlüsselfunktion einnehmen und somit von zentraler Bedeutung sind.

Die Ergebnisse legen nahe, dass die Gabe von CTCE-0214D auch in anderen akuten systemisch-entzündlichen Erkrankungen von Vorteil sein kann. Entsprechend bieten sich weitere Einsatzgebiete im Bereich der Infektiologie an. Der Verlauf einer Meningokokken-Sepsis erinnert stark an den Ablauf der systemischen Inflammation nach LPS-Gabe, weshalb die Untersuchung eines CXCR4-Agonisten hier naheliegend ist. Ferner würden weitere Untersuchungen zum Einfluss auf die Überlebensrate der Tiere eine sinnvolle Ergänzung darstellen, um den protektiven Effekt zu untermauern. Außerdem wäre damit ein weiterer

Grundstein für die Untersuchung eines CXCR4-Agonisten in einem dem Menschen ähnlicheren Tier, wie z.B. dem Schwein, gelegt.

Die genauen zellulären Mechanismen, über welche CTCE-0214D seine protektive Wirkung entfaltet, konnten in der vorgelegten Arbeit nicht vollumfänglich eruiert werden, was perspektivisch dennoch erstrebenswert ist, um ein tieferes Verständnis für die beobachteten Effekte zu erhalten. Dabei sollte jedoch unbedingt auf die Wahl einer geeigneten Zelllinie geachtet werden, welche einerseits den CXCR4, den CXCR7 und den TLR4 exprimiert und andererseits in einem physiologisch relevanten Zusammenhang zur Fragestellung steht. Ferner ist es molekular gesehen interessant, den Einfluss des CXCR7 zu untersuchen und zu analysieren, ob dieser eine Art „Scavenger-Funktion“ für überschüssiges CXCL12 ausübt oder seinerseits über andere Signalwege protektive oder schädliche Prozesse einleitet. Hierbei gilt es allerdings zu beachten, dass nur wenige Antagonisten für den CXCR7 zur Verfügung stehen und die Möglichkeiten in Bezug auf eine selektive Aktivierung des Rezeptors noch geringer sind. Dennoch wäre bezüglich der Aktivierung des CXCR7 eine molekulare Untersuchung mit AMD3100 interessant, da in einem vorherigen Experiment gezeigt werden konnte, dass AMD3100 als allosterischer Agonist am CXCR7 agiert (Kalatskaya et al. 2009). Auch in Bezug auf das Migrationsverhalten der verschiedenen Immunzellen bleiben einige Fragen offen. Idealerweise würde sich eine zeitabhängige Untersuchung des peripheren Blutbildes nach CXCR4-Aktivierung und -Deaktivierung anbieten. Somit könnte eine eindeutige Verteilung der Zellpopulationen im Blut nachgewiesen werden. Ein nächster Schritt würde in ausführlichen histologischen und FACS-Analysen der Organe bestehen, um einen Eindruck zu erhalten, inwieweit Neutrophile und Lymphozyten in Abhängigkeit von der Zeit in die Organe einwandern. Entsprechend bietet sich auch die Untersuchung der Speicherorgane Knochenmark und Lunge an. Eine Garantie, die Prozesse vollumfänglich abzugreifen, ist dennoch nicht gegeben, da unklar ist, inwieweit weitere Zytokine, wie z.B. CXCL1, CXCL2 und CXCL5, welche ihre Effekte überwiegend über CXCR2 vermitteln (Kolaczkowska und Kubes 2013), zu dem Gesamtbild beitragen. Generell besteht die Schwierigkeit einer eindeutigen und vollumfänglichen Aufklärung der Zusammenhänge in dem ubiquitären Vorkommen des Rezeptors CXCR4 und seines Liganden. Die Untersuchung molekularer Prozesse in einzelnen Zelllinien bzw. in einem einzelnen Organ erscheint insofern erschwert, als dass die physiologische Relevanz aufgrund der vielfältigen (Gegen-) Regulationsmechanismen unklar bleibt. Die beobachteten Effekte sind als Summeneffekte zu betrachten und geben häufig nur einen Hinweis darauf, welcher von vielen parallel ablaufenden Prozessen den überwiegenden Einfluss gehabt haben könnte. Für diese

weitergehenden Fragestellungen liefern die vorliegenden Untersuchungen und deren Ergebnisse eine wesentliche Grundlage.

7 Literatur- und Quellenverzeichnis

Abraham E, Reinhart K, Opal S, Demeyer I, Doig C, Rodriguez AL, Beale R, Svoboda P, Laterre PF, Simon S, Light B, Spapen H, Stone J, Seibert A, Peckelsen C, Deyne C de, Postier R, Pettilä V, Sprung CL, Artigas A, Percell SR, Shu V, Zwingelstein C, Tobias J, Poole L, Stolzenbach JC, Creasey AA. 2003. Efficacy and safety of tifacogin (recombinant tissue factor pathway inhibitor) in severe sepsis. A randomized controlled trial. JAMA, 290(2):238–247.

Altamura M, Caradonna L, Amati L, Pellegrino NM, Urgesi G, Miniello S. 2001. Splenectomy and sepsis. The role of the spleen in the immune-mediated bacterial clearance. Immunopharmacology and immunotoxicology, 23(2):153–161.

Angus DC, van der Poll T. 2013. Severe sepsis and septic shock. The New England journal of medicine, 369(9):840–851.

Bach HH, Saini V, Baker TA, Tripathi A, Gamelli RL, Majetschak M. 2012. Initial assessment of the role of CXC chemokine receptor 4 after polytrauma. Molecular medicine, 18:1056–1066.

Bakker J, Grover R, McLuckie A, Holzapfel L, Andersson J, Lodato R, Watson D, Grossman S, Donaldson J, Takala J. 2004. Administration of the nitric oxide synthase inhibitor NG-methyl-L-arginine hydrochloride (546C88) by intravenous infusion for up to 72 hours can promote the resolution of shock in patients with severe sepsis. Results of a randomized, double-blind, placebo-controlled multicenter study. Critical care medicine, 32(1):1–12.

Barreto ML, Teixeira MG, Carmo EH. 2006. Infectious diseases epidemiology. Journal of epidemiology and community health, 60(3):192–195.

Baum N, Dichoso CC, Carlton CE. 1975. Blood urea nitrogen and serum creatinine. Physiology and interpretations. Urology, 5(5):583–588.

Bazzoni F, Tamassia N, Rossato M, Cassatella MA. 2010. Understanding the molecular mechanisms of the multifaceted IL-10-mediated anti-inflammatory response. Lessons from neutrophils. European journal of immunology, 40(9):2360–2368.

Bernhagen J, Krohn R, Lue H, Gregory JL, Zernecke A, Koenen RR, Dewor M, Georgiev I, Schober A, Leng L, Kooistra T, Fingerle-Rowson G, Ghezzi P, Kleemann R, McColl SR,

Bucala R, Hickey MJ, Weber C. 2007. MIF is a noncognate ligand of CXC chemokine receptors in inflammatory and atherogenic cell recruitment. Nature medicine, 13(5):587–596.

Bleul CC, Farzan M, Choe H, Parolin C, Clark-Lewis I, Sodroski J, Springer TA. 1996. The lymphocyte chemoattractant SDF-1 is a ligand for LESTR/fusin and blocks HIV-1 entry. Nature, 382(6594):829–833.

Bloos F, Reinhart K. 2003. Aktuelle Aspekte zur supportiven und adjuvanten Therapie der Sepsis. Aktuelle Ernährungsmedizin, 28(3):186–190.

Bloos F, Reinhart K. 2014. Rapid diagnosis of sepsis. Virulence, 5(1):154–160.

Boley SJ, Kaleya RN, Brandt LJ. 1992. Mesenteric venous thrombosis. The Surgical clinics of North America, 72(1):183–201.

Bonanno FG. 2011. Physiopathology of shock. Journal of emergencies, trauma, and shock, 4(2):222–232.

Bone RC, Balk RA, Cerra FB, Dellinger RP, Fein AM, Knaus WA, Schein RM, Sibbald WJ. 1992. Definitions for sepsis and organ failure and guidelines for the use of innovative therapies in sepsis. The ACCP/SCCM Consensus Conference Committee. American College of Chest Physicians/Society of Critical Care Medicine. Chest, 101(6):1644–1655.

Bone RC, Grodzin CJ, Balk RA. 1997. Sepsis. A new hypothesis for pathogenesis of the disease process. Chest, 112(1):235–243.

Broxmeyer HE, Orschell CM, Clapp DW, Hangoc G, Cooper S, Plett PA, Liles WC, Li X, Graham-Evans B, Campbell TB, Calandra G, Bridger G, Dale DC, Srour EF. 2005. Rapid mobilization of murine and human hematopoietic stem and progenitor cells with AMD3100, a CXCR4 antagonist. The Journal of experimental medicine, 201(8):1307–1318.

Brunkhorst FM, Reinhart K. 2009. Diagnose und kausale Therapie der Sepsis. Der Internist, 50(7):810–816.

Buras JA, Holzmann B, Sitkovsky M. 2005. Animal models of sepsis. Setting the stage. Nature reviews. Drug discovery, 4(10):854–865.

Busillo JM, Benovic JL. 2007. Regulation of CXCR4 signaling. Biochimica et biophysica acta, 1768(4):952–963.

Calderon TM, Eugenin EA, Lopez L, Kumar SS, Hesselgesser J, Raine CS, Berman JW. 2006. A role for CXCL12 (SDF-1alpha) in the pathogenesis of multiple sclerosis. Regulation of CXCL12 expression in astrocytes by soluble myelin basic protein. Journal of neuroimmunology, 177(1-2):27–39.

Casteleijn E, Kuiper J, van Rooij HC, Kamps JA, Koster JF, van Berkel TJ. 1988. Endotoxin stimulates glycogenolysis in the liver by means of intercellular communication. The Journal of biological chemistry, 263(15):6953–6955.

Chandrasoma P, Taylor CR. 1997. Concise pathology. Dritte Aufl. New York: McGraw-Hill Publishing Co.

Chen H-T, Tsou H-K, Hsu C-J, Tsai C-H, Kao C-H, Fong Y-C, Tang C-H. 2011. Stromal cell-derived factor-1/CXCR4 promotes IL-6 production in human synovial fibroblasts. Journal of cellular biochemistry, 112(4):1219–1227.

Chosay JG, Essani NA, Dunn CJ, Jaeschke H. 1997. Neutrophil margination and extravasation in sinusoids and venules of liver during endotoxin-induced injury. The American journal of physiology, 272(5 Pt 1): G1195-200.

Chung SW, Liu X, Macias AA, Baron RM, Perrella MA. 2008. Heme oxygenase-1-derived carbon monoxide enhances the host defense response to microbial sepsis in mice. The Journal of clinical investigation, 118(1):239–247.

Collins T, Read MA, Neish AS, Whitley MZ, Thanos D, Maniatis T. 1995. Transcriptional regulation of endothelial cell adhesion molecules. NF-kappa B and cytokine-inducible enhancers. FASEB journal: official publication of the Federation of American Societies for Experimental Biology, 9(10):899–909.

Copeland S, Warren HS, Lowry SF, Calvano SE, Remick D. 2005. Acute inflammatory response to endotoxin in mice and humans. Clinical and diagnostic laboratory immunology, 12(1):60–67.

Crump MP, Gong JH, Loetscher P, Rajarathnam K, Amara A, Arenzana-Seisdedos F, Virelizier JL, Baggiolini M, Sykes BD, Clark-Lewis I. 1997. Solution structure and basis for functional activity of stromal cell-derived factor-1; dissociation of CXCR4 activation from binding and inhibition of HIV-1. The EMBO journal, 16(23):6996–7007.

Dalton TP, Chen Y, Schneider SN, Nebert DW, Shertzer HG. 2004. Genetically altered mice to evaluate glutathione homeostasis in health and disease. Free radical biology & medicine, 37(10):1511–1526.

Deitch EA. 1998. Animal models of sepsis and shock. A review and lessons learned. Shock, 9(1):1–11.

Dejager L, Pinheiro I, Dejonckheere E, Libert C. 2011. Cecal ligation and puncture. The gold standard model for polymicrobial sepsis? Trends in microbiology, 19(4):198–208.

Delano MJ, Kelly-Scumpia KM, Thayer TC, Winfield RD, Scumpia PO, Cuenca AG, Harrington PB, O'Malley KA, Warner E, Gabrilovich S, Mathews CE, Laface D, Heyworth PG, Ramphal R, Strieter RM, Moldawer LL, Efron PA. 2011. Neutrophil mobilization from the bone marrow during polymicrobial sepsis is dependent on CXCL12 signaling. Journal of immunology, 187(2):911–918.

Devi S, Wang Y, Chew WK, Lima R, A-González N, Mattar CNZ, Chong SZ, Schlitzer A, Bakocevic N, Chew S, Keeble JL, Goh CC, Li JLY, Evrard M, Malleret B, Larbi A, Renia L, Haniffa M, Tan SM, Chan JKY, Balabanian K, Nagasawa T, Bachelerie F, Hidalgo A, Ginhoux F, Kubes P, Ng LG. 2013. Neutrophil mobilization via plerixafor-mediated CXCR4 inhibition arises from lung demargination and blockade of neutrophil homing to the bone marrow. The Journal of experimental medicine, 210(11):2321–2336.

Dinić S, Grdović N, Uskoković A, Đorđević M, Mihailović M, Jovanović JA, Poznanović G, Vidaković M. 2016. CXCL12 protects pancreatic β-cells from oxidative stress by a Nrf2-induced increase in catalase expression and activity. Proceedings of the Japan Academy. Series B, Physical and biological sciences, 92(9):436–454.

Ebong S, Call D, Nemzek J, Bolgos G, Newcomb D, Remick D. 1999. Immunopathologic alterations in murine models of sepsis of increasing severity. Infection and immunity, 67(12):6603–6610.

Edelstein CL. 2008. Biomarkers of acute kidney injury. Advances in chronic kidney disease, 15(3):222–234.

Fan H, Wong D, Ashton SH, Borg KT, Halushka PV, Cook JA. 2012. Beneficial effect of a CXCR4 agonist in murine models of systemic inflammation. Inflammation, 35(1):130–137.

Fink MP, Heard SO. 1990. Laboratory models of sepsis and septic shock. The Journal of surgical research, 49(2):186–196.

Fink MP. 2014. Animal models of sepsis. Virulence, 5(1):143–153.

Garnica MR, Souto JT, Silva JS, Andrade HF de. 2002. Stromal cell derived factor 1 synthesis by spleen cells in rodent malaria, and the effects of in vivo supplementation of SDF-1alpha and CXCR4 receptor blocker. Immunology letters, 83(1):47–53.

Goda S, Inoue H, Umehara H, Miyaji M, Nagano Y, Harakawa N, Imai H, Lee P, Macarthy JB, Ikeo T, Domae N, Shimizu Y, Iida J. 2006. Matrix metalloproteinase-1 produced by human CXCL12-stimulated natural killer cells. The American journal of pathology, 169(2):445–458.

Gonnert FA, Recknagel P, Seidel M, Jbeily N, Dahlke K, Bockmeyer CL, Winning J, Lösche W, Claus RA, Bauer M. 2011. Characteristics of clinical sepsis reflected in a reliable and reproducible rodent sepsis model. The Journal of surgical research, 170(1):e123-34.

Gonzalo JA, Lloyd CM, Peled A, Delaney T, Coyle AJ, Gutierrez-Ramos JC. 2000. Critical involvement of the chemotactic axis CXCR4/stromal cell-derived factor-1 alpha in the inflammatory component of allergic airway disease. Journal of immunology, 165(1):499–508.

Gruys E, Toussaint MJM, Niewold TA, Koopmans SJ. 2005. Acute phase reaction and acute phase proteins. Journal of Zhejiang University Science B, 6(11):1045–1056.

Guan S, Guo C, Zingarelli B, Wang L, Halushka PV, Cook JA, Fan H. 2015. Combined treatment with a CXCL12 analogue and antibiotics improves survival and neutrophil recruitment and function in murine sepsis. Immunology, 144(3):405–411.

Hansen IB, Ellingsen T, Hornung N, Poulsen JH, Lottenburger T, Stengaard-Pedersen K. 2006. Plasma level of CXC-chemokine CXCL12 is increased in rheumatoid arthritis and is independent of disease activity and methotrexate treatment. The Journal of rheumatology, 33(9):1754–1759.

Hendrix CW, Flexner C, MacFarland RT, Giandomenico C, Fuchs EJ, Redpath E, Bridger G, Henson GW. 2000. Pharmacokinetics and safety of AMD-3100, a novel antagonist of the CXCR-4 chemokine receptor, in human volunteers. Antimicrobial agents and chemotherapy, 44(6):1667–1673.

Hernandez PA, Gorlin RJ, Lukens JN, Taniuchi S, Bohinjec J, Francois F, Klotman ME, Diaz GA. 2003. Mutations in the chemokine receptor gene CXCR4 are associated with WHIM syndrome, a combined immunodeficiency disease. Nature genetics, 34(1):70–74.

Holmes CL, Russell JA, Walley KR. 2003. Genetic polymorphisms in sepsis and septic shock. Role in prognosis and potential for therapy. Chest, 124(3):1103–1115.

Hotchkiss RS, Karl IE. 2003. The pathophysiology and treatment of sepsis. The New England journal of medicine, 348(2):138–150.

Imaizumi T, Itaya H, Fujita K, Kudoh D, Kudoh S, Mori K, Fujimoto K, Matsumiya T, Yoshida H, Satoh K. 2000. Expression of Tumor Necrosis Factor- in Cultured Human Endothelial Cells Stimulated With Lipopolysaccharide or Interleukin-1. Arteriosclerosis, Thrombosis, and Vascular Biology, 20(2):410–415.

Ishii T, Nishihara M, Ma F, Ebihara Y, Tsuji K, Asano S, Nakahata T, Maekawa T. 1999. Expression of stromal cell-derived factor-1/pre-B cell growth-stimulating factor receptor, CXC chemokine receptor 4, on CD34+ human bone marrow cells is a phenotypic alteration for committed lymphoid progenitors. Journal of immunology, 163(7):3612–3620.

Jacob A, Zhou M, Wu R, Wang P. 2009. The role of hepatic cytochrome P-450 in sepsis. International journal of clinical and experimental medicine, 2(3):203–211.

Juarez J, Bendall L, Bradstock K. 2004. Chemokines and their receptors as therapeutic targets. The role of the SDF-1/CXCR4 axis. Current pharmaceutical design, 10(11):1245–1259.

Kalatskaya I, Berchiche YA, Gravel S, Limberg BJ, Rosenbaum JS, Heveker N. 2009. AMD3100 is a CXCR7 ligand with allosteric agonist properties. Molecular pharmacology, 75(5):1240–1247.

Kang K, Nan C, Fei D, Meng X, Liu W, Zhang W, Jiang L, Zhao M, Pan S, Zhao M. 2013. Heme oxygenase 1 modulates thrombomodulin and endothelial protein C receptor levels to attenuate septic kidney injury. Shock, 40(2):136–143.

Katz S, Jimenez MA, Lehmkuhler WE, Grosfeld JL. 1991. Liver bacterial clearance following hepatic artery ligation and portacaval shunt. The Journal of surgical research, 51(3):267–270.

Kim Y-S, Morgan MJ, Choksi S, Liu Z-G. 2007. TNF-induced activation of the Nox1 NADPH oxidase and its role in the induction of necrotic cell death. Molecular cell, 26(5):675–687.

Kishore SP, Bungum MK, Platt JL, Brunn GJ. 2005. Selective suppression of Toll-like receptor 4 activation by chemokine receptor 4. FEBS letters, 579(3):699–704.

Kolaczkowska E, Kubes P. 2013. Neutrophil recruitment and function in health and inflammation. Nature reviews. Immunology, 13(3):159–175.

Krams M, Frahm SO, Kellner U, Hrsg. 2010. Kurzlehrbuch Pathologie. Stuttgart: Thieme.

Lu D-Y, Tang C-H, Yeh W-L, Wong K-L, Lin C-P, Chen Y-H, Lai C-H, Chen Y-F, Leung Y-M, Fu W-M. 2009. SDF-1alpha up-regulates interleukin-6 through CXCR4, PI3K/Akt, ERK, and NF-kappaB-dependent pathway in microglia. European journal of pharmacology, 613(1-3):146–154.

Lu SC. 2009. Regulation of glutathione synthesis. Molecular aspects of medicine, 30(1-2):42–59.

Lukacs NW, Berlin A, Schols D, Skerlj RT, Bridger GJ. 2002. AMD3100, a CxCR4 antagonist, attenuates allergic lung inflammation and airway hyperreactivity. The American journal of pathology, 160(4):1353–1360.

Luo Y-p, Jiang L, Kang K, Fei D-s, Meng X-l, Nan C-c, Pan S-h, Zhao M-r, Zhao M-y. 2014. Hemin inhibits NLRP3 inflammasome activation in sepsis-induced acute lung injury, involving heme oxygenase-1. International immunopharmacology, 20(1):24–32.

Ma Q, Jones D, Borghesani PR, Segal RA, Nagasawa T, Kishimoto T, Bronson RT, Springer TA. 1998. Impaired B-lymphopoiesis, myelopoiesis, and derailed cerebellar neuron migration in CXCR4- and SDF-1-deficient mice. Proceedings of the National Academy of Sciences of the United States of America, 95(16):9448–9453.

Ma Q. 2013. Role of nrf2 in oxidative stress and toxicity. Annual review of pharmacology and toxicology, 53:401–426.

Maitra SR, Wojnar MM, Lang CH. 2000. Alterations in tissue glucose uptake during the hyperglycemic and hypoglycemic phases of sepsis. Shock, 13(5):379–385.

Majetschak M, Cohn SM, Nelson JA, Burton EH, Obertacke U, Proctor KG. 2004. Effects of exogenous ubiquitin in lethal endotoxemia. Surgery, 135(5):536–543.

Mao W, Yi X, Qin J, Tian M, Jin G. 2014. CXCL12 inhibits cortical neuron apoptosis by increasing the ratio of Bcl-2/Bax after traumatic brain injury. The International journal of neuroscience, 124(4):281–290.

Marquardt H, Schäfer S, Hrsg. 2004. Lehrbuch der Toxikologie. Zweite, völlig neu bearb. Aufl. Stuttgart: Wissenschaftliche Verlagsgesellschaft.

Martin G, Brunkhorst FM, Janes JM, Reinhart K, Sundin DP, Garnett K, Beale R. 2009. The international PROGRESS registry of patients with severe sepsis. Drotrecogin alfa (activated) use and patient outcomes. Critical care, 13(3):R103.

Maru Y, Hrsg. 2016. Inflammation and metastasis. Tokyo: Springer-Verlag.

Mebius RE, Kraal G. 2005. Structure and function of the spleen. Nature reviews. Immunology, 5(8):606–616.

Meiron M, Zohar Y, Anunu R, Wildbaum G, Karin N. 2008. CXCL12 (SDF-1alpha) suppresses ongoing experimental autoimmune encephalomyelitis by selecting antigen-specific regulatory T cells. The Journal of experimental medicine, 205(11):2643–2655.

Mezey E. 1982. Liver disease and protein needs. Annual review of nutrition, 2:21–50.

Micek ST, Lloyd AE, Ritchie DJ, Reichley RM, Fraser VJ, Kollef MH. 2005. Pseudomonas aeruginosa bloodstream infection. Importance of appropriate initial antimicrobial treatment. Antimicrobial agents and chemotherapy, 49(4):1306–1311.

Mikami S, Nakase H, Yamamoto S, Takeda Y, Yoshino T, Kasahara K, Ueno S, Uza N, Oishi S, Fujii N, Nagasawa T, Chiba T. 2008. Blockade of CXCL12/CXCR4 axis ameliorates murine experimental colitis. The Journal of pharmacology and experimental therapeutics, 327(2):383–392.

Monostory K, Dvorak Z. 2011. Steroid regulation of drug-metabolizing cytochromes P450. Current drug metabolism, 12(2):154–172.

Moore KW, Waal Malefyt R de, Coffman RL, O'Garra A. 2001. Interleukin-10 and the interleukin-10 receptor. Annual review of immunology, 19:683–765.

Morgan ET. 2001. Regulation of cytochrome p450 by inflammatory mediators. Why and how? Drug metabolism and disposition: the biological fate of chemicals, 29(3):207–212.

Morgan MJ, Liu Z-g. 2011. Crosstalk of reactive oxygen species and NF-κB signaling. Cell research, 21(1):103–115.

Müller-Werdan U, Schuster H-P, Werdan K, Hrsg. 2005. Sepsis und MODS. Vierte Aufl. Heidelberg: Springer-Verlag.

Mutschler E, Geisslinger G, Kroemer HK, Menzel S, Ruth P, Hrsg. 2013. Mutschler Arzneimittelwirkungen. Lehrbuch der Pharmakologie, der klinischen Pharmakologie und

Toxikologie; mit einführenden Kapiteln in die Anatomie, Physiologie und Pathophysiologie. Zehnte., vollständig überarbeitete und erweiterte Aufl. Stuttgart: Wissenschaftliche Verlagsgesellschaft.

Muyderman H, Wadey AL, Nilsson M, Sims NR. 2007. Mitochondrial glutathione protects against cell death induced by oxidative and nitrative stress in astrocytes. Journal of neurochemistry, 102(4):1369–1382.

Nagasawa T, Tachibana K, Kawabata K. 1999. A CXC chemokine SDF-1/PBSF. A ligand for a HIV coreceptor, CXCR4. Advances in immunology, 71:211–228.

Nagase H, Miyamasu M, Yamaguchi M, Imanishi M, Tsuno NH, Matsushima K, Yamamoto K, Morita Y, Hirai K. 2002. Cytokine-mediated regulation of CXCR4 expression in human neutrophils. Journal of leukocyte biology, 71(4):711–717.

Nakatani Y, Fukui H, Kitano H, Nagamoto I, Tsujimoto T, Kuriyama S, Kikuchi E, Hoppou K, Tsujii T. 2001. Endotoxin clearance and its relation to hepatic and renal disturbances in rats with liver cirrhosis. Liver, 21(1):64–70.

Nathan C. 2006. Neutrophils and immunity. Challenges and opportunities. Nature reviews. Immunology, 6(3):173–182.

Nemzek JA, Hugunin KMS, Opp MR. 2008. Modeling sepsis in the laboratory. Merging sound science with animal well-being. Comparative medicine, 58(2):120–128.

Novoa B, Bowman TV, Zon L, Figueras A. 2009. LPS response and tolerance in the zebrafish (Danio rerio). Fish & shellfish immunology, 26(2):326–331.

Page M, Hrsg. 2013. Patienten-Lexikon. Medizin leicht verständlich: München: Dorling Kindersley.

Park S, Kim D-G, Suh GY, Kang JG, Ju Y-S, Lee Y-J, Park JY, Lee SW, Jung K-S. 2012. Mild hypoglycemia is independently associated with increased risk of mortality in patients with sepsis. A 3-year retrospective observational study. Critical care, 16(5):R189.

Patel GP, Gurka DP, Balk RA. 2003. New treatment strategies for severe sepsis and septic shock. Current opinion in critical care, 9(5):390–396.

Pinsky MR, Vincent JL, Deviere J, Alegre M, Kahn RJ, Dupont E. 1993. Serum cytokine levels in human septic shock. Relation to multiple-system organ failure and mortality. Chest, 103(2):565–575.

Preyra I, Worster A. 2003. Hypoglycemia in bacterial septicemia. Canadian Journal of Emergency Medicine, 5(4):268–270.

Raetzsch CF, Brooks NL, Alderman JM, Moore KS, Hosick PA, Klebanov S, Akira S, Bear JE, Baldwin AS, Mackman N, Combs TP. 2009. Lipopolysaccharide inhibition of glucose production through the Toll-like receptor-4, myeloid differentiation factor 88, and nuclear factor kappa b pathway. Hepatology, 50(2):592–600.

Recknagel P, Gonnert FA, Halilbasic E, Gajda M, Jbeily N, Lupp A, Rubio I, Claus RA, Kortgen A, Trauner M, Singer M, Bauer M. 2013. Mechanisms and functional consequences of liver failure substantially differ between endotoxaemia and faecal peritonitis in rats. Liver international: official journal of the International Association for the Study of the Liver, 33(2):283–293.

Recknagel P, Gonnert FA, Westermann M, Lambeck S, Lupp A, Rudiger A, Dyson A, Carré JE, Kortgen A, Krafft C, Popp J, Sponholz C, Fuhrmann V, Hilger I, Claus RA, Riedemann NC, Wetzker R, Singer M, Trauner M, Bauer M. 2012. Liver dysfunction and phosphatidylinositol-3-kinase signalling in early sepsis. Experimental studies in rodent models of peritonitis. PLoS medicine, 9(11):e1001338.

Reinhart K, Brunkhorst FM, Bone H-G, Bardutzky J, Dempfle C-E, Forst H, Gastmeier P, Gerlach H, Gründling M, John S, Kern W, Kreymann G, Krüger W, Kujath P, Marggraf G, Martin J, Mayer K, Meier-Hellmann A, Oppert M, Putensen C, Quintel M, Ragaller M, Rossaint R, Seifert H, Spies C, Stüber F, Weiler N, Weimann A, Werdan K, Welte T. 2010. Prevention, diagnosis, therapy and follow-up care of sepsis. 1st revision of S-2k guidelines of the German Sepsis Society (Deutsche Sepsis-Gesellschaft e.V. (DSG)) and the German Interdisciplinary Association of Intensive Care and Emergency Medicine (Deutsche Interdisziplinäre Vereinigung für Intensiv- und Notfallmedizin (DIVI)). German medical science, 8:Doc14.

Remick DG, Newcomb DE, Bolgos GL, Call DR. 2000. Comparison of the mortality and inflammatory response of two models of sepsis. Lipopolysaccharide vs. cecal ligation and puncture. Shock, 13(2):110–116.

Remick DG, Ward PA. 2005. Evaluation of endotoxin models for the study of sepsis. Shock, 24 Suppl 1:7–11.

Riede U-N, Werner M, Freudenberg N, Hrsg. 2009. Basiswissen Allgemeine und Spezielle Pathologie. Heidelberg: Springer-Verlag.

Rittirsch D, Hoesel LM, Ward PA. 2007. The disconnect between animal models of sepsis and human sepsis. Journal of leukocyte biology, 81(1):137–143.

Rossi D, Zlotnik A. 2000. The biology of chemokines and their receptors. Annual review of immunology, 18:217–242.

Rubin LG, Schaffner W. 2014. Clinical practice. Care of the asplenic patient. The New England journal of medicine, 371(4):349–356.

Ruiz S, Vardon-Bounes F, Merlet-Dupuy V, Conil J-M, Buléon M, Fourcade O, Tack I, Minville V. 2016. Sepsis modeling in mice. Ligation length is a major severity factor in cecal ligation and puncture. Intensive care medicine experimental, 4(1):22.

Saiman Y, Jiao J, Fiel MI, Friedman SL, Aloman C, Bansal MB. 2015. Inhibition of the CXCL12/CXCR4 chemokine axis with AMD3100, a CXCR4 small molecule inhibitor, worsens murine hepatic injury. Hepatology research: the official journal of the Japan Society of Hepatology, 45(7):794–803.

Saini V, Marchese A, Majetschak M. 2010. CXC chemokine receptor 4 is a cell surface receptor for extracellular ubiquitin. The Journal of biological chemistry, 285(20):15566–15576.

Schattenberg JM, Galle PR, Schuchmann M. 2006. Akutes Leberversagen- Internistische Sicht. Praxis, 95(48):1873–1877.

Schütt C, Bröker B, Hrsg. 2011. Grundwissen Immunologie. Dritte Aufl. Heidelberg: Spektrum Akademischer Verlag.

Shoji Y, Uedono Y, Ishikura H, Takeyama N, Tanaka T. 1995. DNA damage induced by tumour necrosis factor-alpha in L929 cells is mediated by mitochondrial oxygen radical formation. Immunology, 84(4):543–548.

Singer M, Deutschman CS, Seymour CW, Shankar-Hari M, Annane D, Bauer M, Bellomo R, Bernard GR, Chiche J-D, Coopersmith CM, Hotchkiss RS, Levy MM, Marshall JC, Martin GS, Opal SM, Rubenfeld GD, van der Poll T, Vincent J-L, Angus DC. 2016. The Third International Consensus Definitions for Sepsis and Septic Shock (Sepsis-3). JAMA, 315(8):801–810.

Soderquist, Sundqvist, Vikerfors. 1999. Adhesion molecules (E-selectin, intercellular adhesion molecule-1 (ICAM-1) and vascular cell adhesion molecule-1 (VCAM-1)) in sera from patients with Staphylococcus aureus bacteraemia with or without endocarditis. Clinical and Experimental Immunology, 118(3):408–411.

Ssekitoleko R, Jacob ST, Banura P, Pinkerton R, Meya DB, Reynolds SJ, Kenya-Mugisha N, Mayanja-Kizza H, Muhindo R, Bhagani S, Scheld WM, Moore CC. 2011. Hypoglycemia at admission is associated with inhospital mortality in Ugandan patients with severe sepsis. Critical care medicine, 39(10):2271–2276.

Stamou KM, Toutouzas KG, Kekis PB, Nakos S, Gafou A, Manouras A, Krespis E, Katsaragakis S, Bramis J. 2006. Prospective study of the incidence and risk factors of postsplenectomy thrombosis of the portal, mesenteric, and splenic veins. Archives of surgery, 141(7):663–669.

Stortz JA, Raymond SL, Mira JC, Moldawer LL, Mohr AM, Efron PA. 2017. Murine Models of Sepsis and Trauma. Can We Bridge the Gap? ILAR journal, 58(1):90-105.

Tamamura H, Fujisawa M, Hiramatsu K, Mizumoto M, Nakashima H, Yamamoto N, Otaka A, Fujii N. 2004. Identification of a CXCR4 antagonist, a T140 analog, as an anti-rheumatoid arthritis agent. FEBS letters, 569(1-3):99–104.

Tamion F, Richard V, Renet S, Thuillez C. 2006. Protective effects of heme-oxygenase expression against endotoxic shock. Inhibition of tumor necrosis factor-alpha and augmentation of interleukin-10. The Journal of trauma, 61(5):1078–1084.

Teicher BA, Fricker SP. 2010. CXCL12 (SDF-1)/CXCR4 pathway in cancer. Clinical cancer research : an official journal of the American Association for Cancer Research, 16(11):2927–2931.

Thelen M, Thelen S. 2008. CXCR7, CXCR4 and CXCL12. An eccentric trio? Journal of neuroimmunology, 198(1-2):9–13.

Tötemeyer S, Sheppard M, Lloyd A, Roper D, Dowson C, Underhill D, Murray P, Maskell D, Bryant C. 2006. IFN-gamma enhances production of nitric oxide from macrophages via a mechanism that depends on nucleotide oligomerization domain-2. Journal of immunology, 176(8):4804–4810.

Triantafilou M, Lepper PM, Briault CD, Ahmed MAE, Dmochowski JM, Schumann C, Triantafilou K. 2008. Chemokine receptor 4 (CXCR4) is part of the lipopolysaccharide "sensing apparatus". European journal of immunology, 38(1):192–203.

Tsuchiya A, Imai M, Kamimura H, Takamura M, Yamagiwa S, Sugiyama T, Nomoto M, Heike T, Nagasawa T, Nakahata T, Aoyagi Y. 2012. Increased susceptibility to severe chronic liver damage in CXCR4 conditional knock-out mice. Digestive diseases and sciences, 57(11):2892–2900.

Tunc T, Cekmez F, Cetinkaya M, Kalayci T, Fidanci K, Saldir M, Babacan O, Sari E, Erdem G, Cayci T, Kul M, Kavuncuoglu S. 2015. Diagnostic value of elevated CXCR4 and CXCL12 in neonatal sepsis. The journal of maternal-fetal & neonatal medicine: the official journal of the European Association of Perinatal Medicine, the Federation of Asia and Oceania Perinatal Societies, the International Society of Perinatal Obstetricians, 28(3):356–361.

Underhill DM, Ozinsky A. 2002. Toll-like receptors. Key mediators of microbe detection. Current opinion in immunology, 14(1):103–110.

Valdés-Ferrer SI, Rosas-Ballina M, Olofsson PS, Lu B, Dancho ME, Ochani M, Li JH, Scheinerman JA, Katz DA, Levine YA, Hudson LK, Yang H, Pavlov VA, Roth J, Blanc L, Antoine DJ, Chavan SS, Andersson U, Diamond B, Tracey KJ. 2013. HMGB1 mediates splenomegaly and expansion of splenic CD11b+ Ly-6C(high) inflammatory monocytes in murine sepsis survivors. Journal of internal medicine, 274(4):381–390.

van den Berg F, Gifford L, Hrsg. 2005. Organsysteme verstehen und beeinflussen. Zweite überarbeitete und erw. Aufl. Stuttgart: Thieme.

Vary TC, Kimball SR. 1992. Regulation of hepatic protein synthesis in chronic inflammation and sepsis. The American journal of physiology, 262(2 Pt 1):C445-52.

Vianna RCS, Gomes RN, Bozza FA, Amâncio RT, Bozza PT, David CMN, Castro-Faria-Neto HC. 2004. Antibiotic treatment in a murine model of sepsis. Impact on cytokines and endotoxin release. Shock, 21(2):115–120.

Wang A, Fairhurst A-M, Tus K, Subramanian S, Liu Y, Lin F, Igarashi P, Zhou XJ, Batteux F, Wong D, Wakeland EK, Mohan C. 2009. CXCR4/CXCL12 hyperexpression plays a pivotal role in the pathogenesis of lupus. Journal of immunology, 182(7):4448–4458.

Ward PA, Lentsch AB. 1999. The acute inflammatory response and its regulation. Archives of surgery, 134(6):666–669.

Werner L, Guzner-Gur H, Dotan I. 2013. Involvement of CXCR4/CXCR7/CXCL12 Interactions in Inflammatory bowel disease. Theranostics, 3(1):40–46.

Wichterman KA, Baue AE, Chaudry IH. 1980. Sepsis and septic shock--a review of laboratory models and a proposal. The Journal of surgical research, 29(2):189–201.

Wung BS, Ni CW, Wang DL. 2005. ICAM-1 induction by TNFalpha and IL-6 is mediated by distinct pathways via Rac in endothelial cells. Journal of biomedical science, 12(1):91–101.

Yan J, Li S, Li S. 2014. The role of the liver in sepsis. International reviews of immunology, 33(6):498–510.

Yano T, Liu Z, Donovan J, Thomas MK, Habener JF. 2007. Stromal cell derived factor-1 (SDF-1)/CXCL12 attenuates diabetes in mice and promotes pancreatic beta-cell survival by activation of the prosurvival kinase Akt. Diabetes, 56(12):2946–2957.

Zou Q, Wen W, Zhang X-C. 2014. Presepsin as a novel sepsis biomarker. World journal of emergency medicine, 5(1):16–19.

8 Anhang

8.1 Supplemental Data Manuskript I

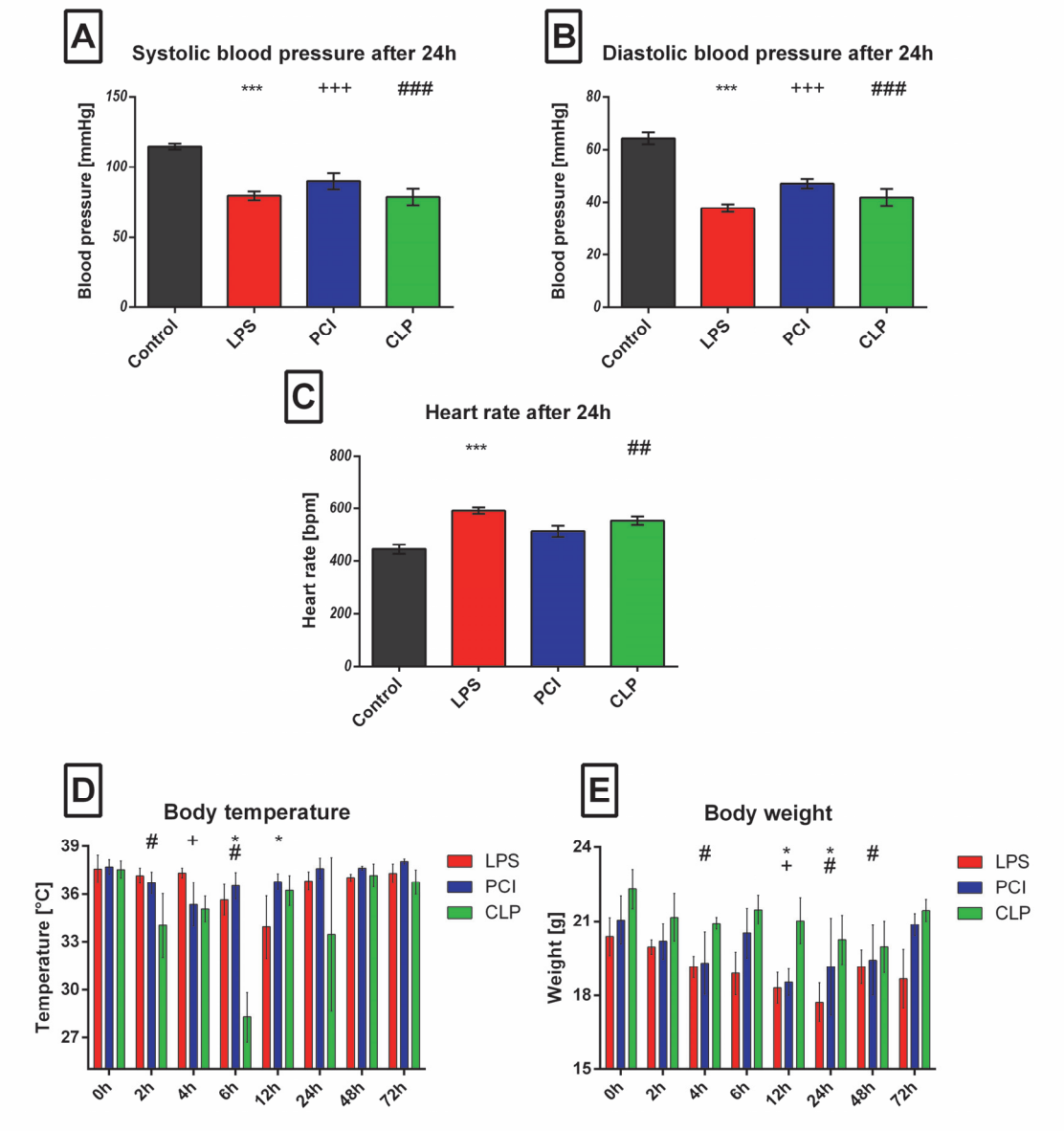

Additional File 1. Blood pressure, heart rate, body weight and body temperature.

At the time point indicated, mice were sacrificed and body weights as well as body temperatures were determined. Additionally, blood pressure values and heart rates were assessed after 24 h. Data are given as mean ± standard deviation (SD); n = 4-6 for each group and time point. Statistical significance was determined by using the non-parametric Kruskal-Wallis test, followed by pairwise Mann-Whitney U tests. Statistical comparisons were made versus the control of each group and are denoted as follows: LPS (asterisk, *), PCI (plus, +), CLP (diamond, #). A p value <0.05 (*,+,#) was considered statistically significant; a p value <0.01 (**,++,##) and a p value <0.001 (***,+++,###) are further specified.

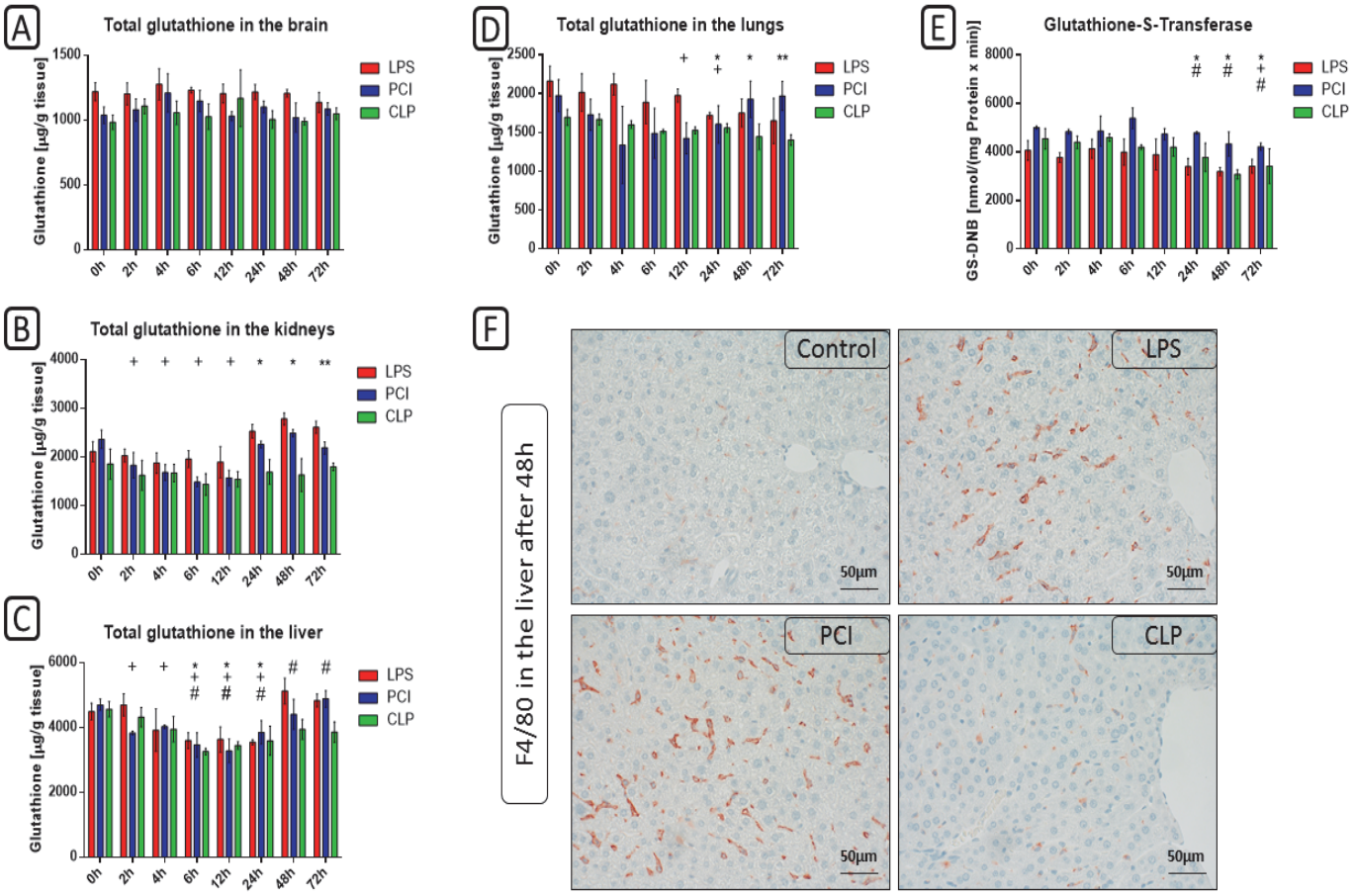

Additional File 2. Total glutathione concentration in different organs, glutathione-S-transferase activities and F4/80 expression in the livers.

At the time point indicated, mice were sacrificed and different organs were collected for the analysis of the total glutathione content (**a-d**). Furthermore, glutathione-S-transferase (GST) activities were determined in the 9000g liver supernatants (**e**). Data are given as mean ± standard deviation (SD); n = 4-6 for each group and time point. Statistical significance was determined by using the non-parametric Kruskal-Wallis test, followed by pairwise Mann-Whitney U tests. Statistical comparisons were made versus the control of each group and are denoted as follows: LPS (asterisk, *), PCI (plus, +), CLP (diamond, #). A p value <0.05 (*,+,#) was considered statistically significant; a p value <0.01 (**,++,##) and a p value <0.001 (***,+++,###) are further specified. The photomicrographs in (**f**) show representative livers after 48 h, displaying large amounts F4/80 positive cells after LPS and PCI treatment. In (**g**), HE stainings of PCI- and CLP-treated mice after 24 h are shown as a supplement to Fig 3D. PCI and CLP treatment caused almost no fat accumulation in the livers.

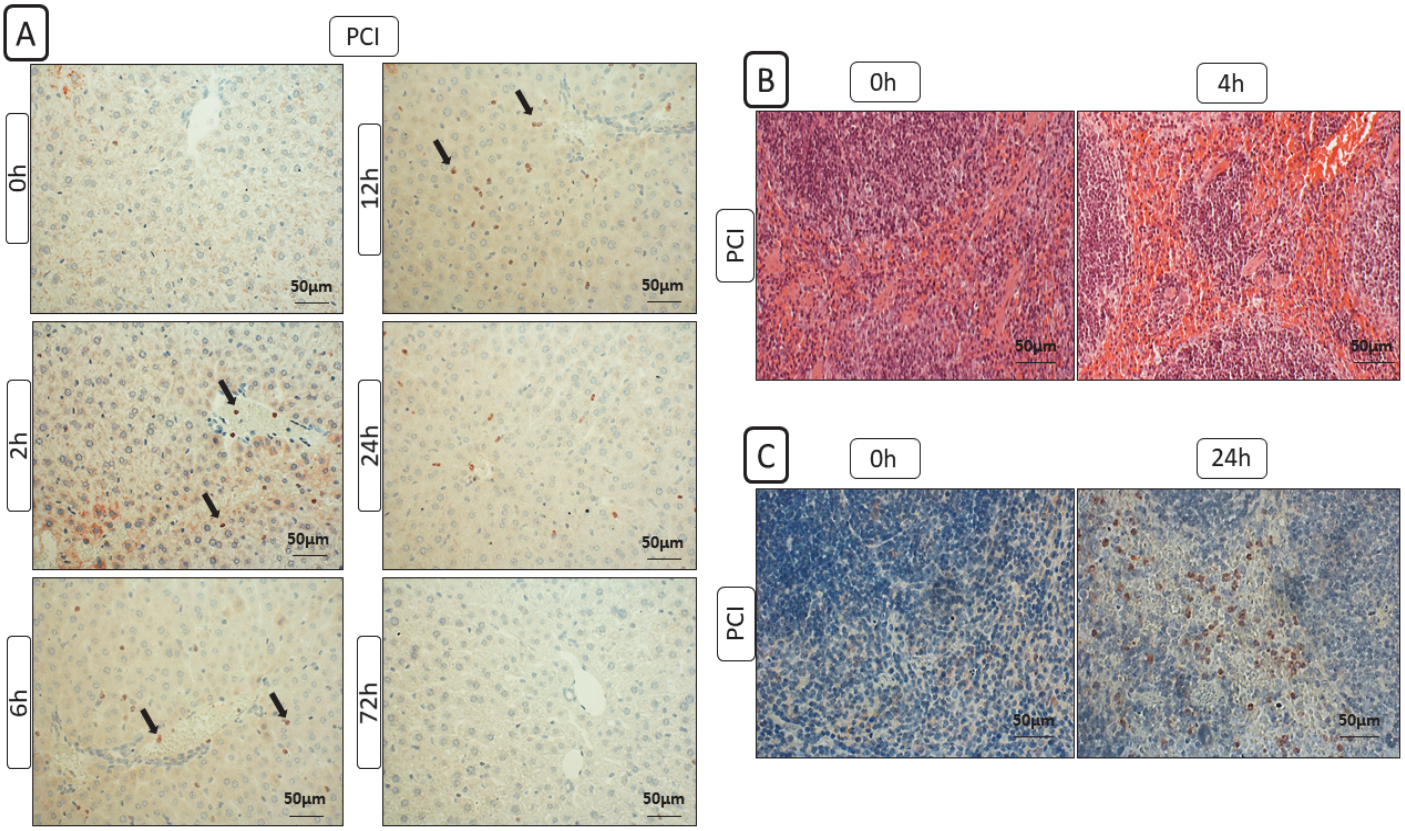

Additional File 3. iNOS expression in the livers and spleens as well as HE staining in the spleens of PCI-treated mice.

At the time point indicated, mice were sacrificed and livers and spleens were collected for immunohistochemical analysis. (**a**) Course of iNOS expression (red-brown color, counterstaining with hematoxylin; original magnification: 400×) in the livers of PCI-treated mice as supplements to Fig 4A and 4B. Arrows exemplarily show the infiltrated neutrophils. (**b**) HE-stained spleens 24 h after PCI treatment (original magnification: 400x). (**c**) iNOS expression patterns after PCI treatment at 24 h (original magnification: 400x) as a supplemental to Fig 6E.

8.2 Supplemental Data Manuskript II

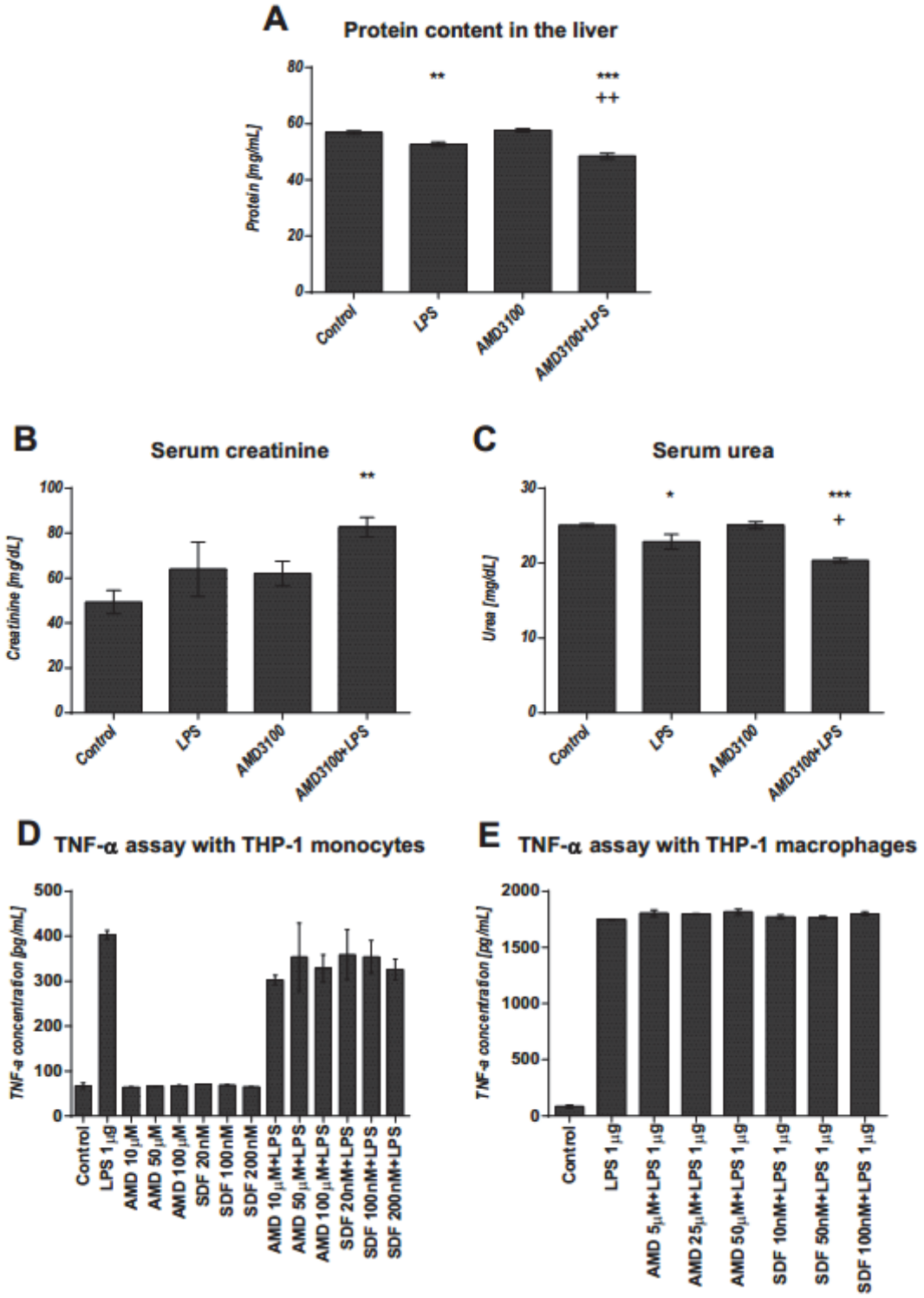

Additional File 1. Protein content in the liver, serum creatinine and urea levels and TNF alpha assay in THP-1 monocytes as well as macrophages.

C57BL/6N mice were treated either with LPS (5 mg/kg body weight), AMD3100 (5 mg/kg body weight), with both substances or with the solvent PBS (control). 24 h thereafter, the

mice were sacrificed and the livers were collected for the determination of the protein content in the 9000g supernatants by using the Biuret method (A). Also, the blood was obtained and serum creatinine as well as serum urea levels were measured (B, C). Data are given as mean ± standard error of the mean (SEM); n=7 for each group. Statistical significant differences between the different treatment groups were determined by using the one-way analysis of variance (ANOVA) and the Tukey post hoc test and are indicated as follows: *, $p \leq 0.05$; **, $p \leq 0.01$; ***, $p \leq 0.001$ vs. control animals; $^{+}$, $p \leq 0.05$; $^{++}$, $p \leq 0.01$; $^{+++}$, $p \leq 0.001$ vs. LPS treatment.

THP-1 cells were cultured in RPMI 1640 supplemented with 10% fetal bovine serum and 100 nM penicillin/streptomycin (all Capricorn Scientific, Ebsdorfergrund, Germany) and were cultured at a density of about 1.0×10^6/ml at 5% CO_2 at 37°C. To obtain THP-1 macrophages, cells were differentiated with PMA (phorbol 12-myristate 13-acetate; Sigma-Aldrich, St. Louis, MO) at a concentration of 40 ng/ml for three days. For the experiments, the cells were pretreated with AMD3100 or CXCL12, respectively, 30 minutes before LPS was added. After additional 12 hours, the media were collected and analyzed for TNF alpha concentration by using a TNF alpha ELISA Kit (Thermo Fisher Scientific, Massachusetts, USA) (D, E). Data are given as mean ± standard error of the mean (SEM); n=3 independent experiments.

8.3 Supplemental Data Manuskript III

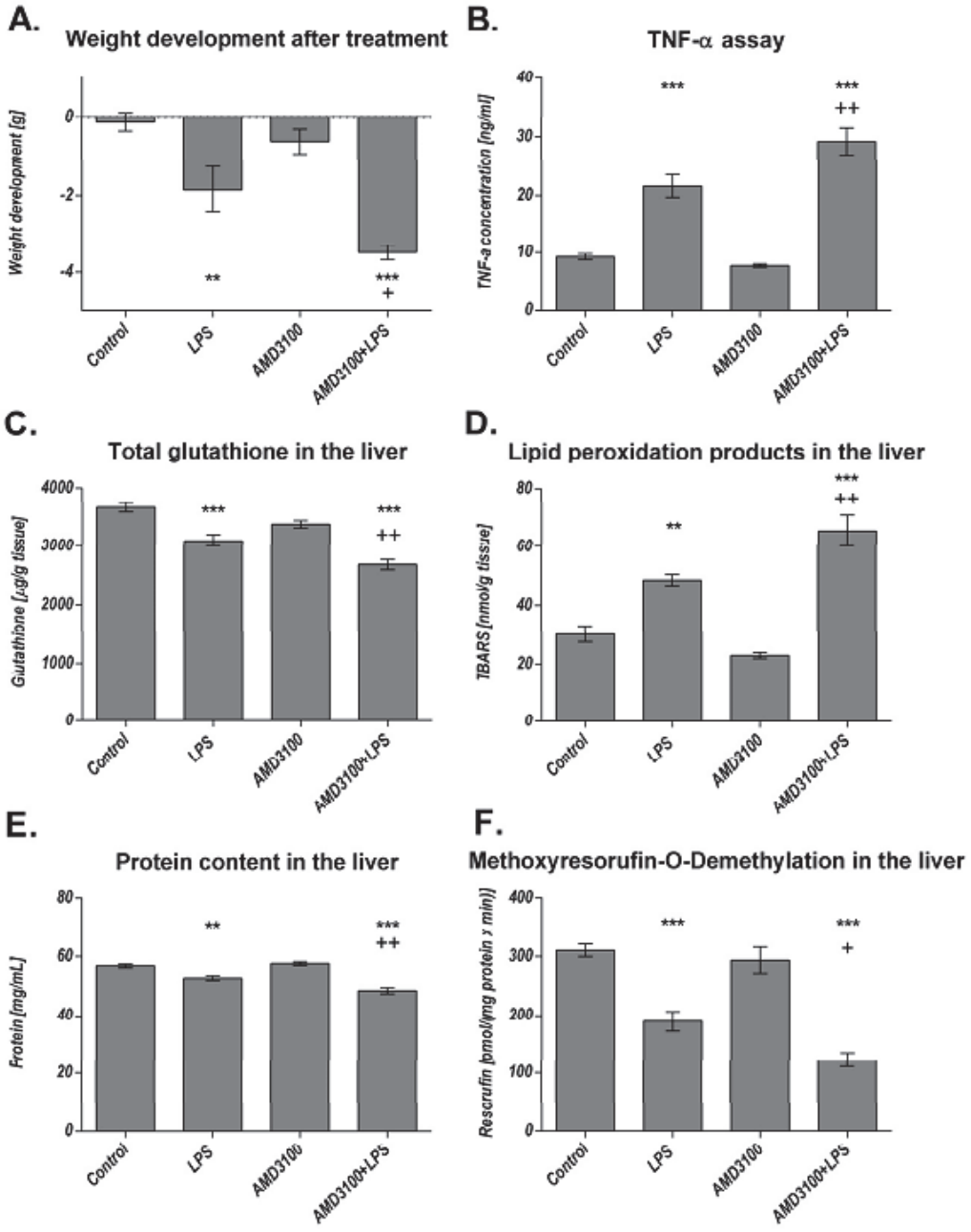

S1 Fig. Blockade of the CXCR4/CXCL12 axis with AMD3100 in endotoxemia.

Male adult C57BL/6N mice (12-weeks-old, body weight 25–30 g; Charles River Laboratories, Sulzfeld, Germany) were used. The animals were housed in plastic cages under standardized conditions (light-dark cycle 12/12 h, temperature 22 ± 2°C, humidity 50 ± 10%, pellet diet Altromin 1316, water ad libitum). A total of 28 mice was randomly divided into four groups

(n = 7 each): Control, LPS, AMD3100 and AMD3100 plus LPS. LPS (E. coli 0111:B4, Sigma Aldrich, Steinheim, Germany) was injected intraperitoneally (5mg/kg body weight), whereas AMD3100 (5 mg/kg body weight) was administered in PBS shortly after endotoxemia onset intraperitoneally. 24 hours after LPS treatment, mice were weighed and sacrificed in isoflurane anesthesia. Blood serum and livers were obtained and used for biochemical analysis. After combined treatment with AMD3100 plus LPS, significantly increased levels of serum TNF-α as well as lipid peroxidation products in the livers of mice when compared to the control or LPS group, respectively, were observed. In addition, a significant loss of body weight was observed which was accompanied by reduced protein, total glutathione and CYP activity levels in the livers of the co-treated mice. Statistical significance ($p \leq 0.05$) was determined by using the one-way analysis of variance (ANOVA) and the Tukey post hoc test. Data are given as mean ± standard error of the mean (SEM), n = 7; *, $p \leq 0.05$; **, $p \leq 0.01$; ***, $p \leq 0.001$ vs. control; $^{+}$, $p \leq 0.05$; $^{++}$, $p \leq 0.01$; $^{+++}$, $p \leq 0.001$ vs. LPS. These results clearly indicate that a blockade of the CXCR4/CXCL12 axis in endotoxemia is disadvantageous and worsens the disease. Undoubtedly, the chemokine receptor CXCR4 plays an important role in endotoxemia, and hence its activation becomes a promising treatment option not only for handling endotoxemia but also for other acute inflammatory diseases, especially when accompanied by an impaired liver function. The study was conducted under the licence of the Thuringian Animal Protection Committee. The principles of laboratory animal care and the German Law on the Protection of Animals as well as the Directive 2010/63/EU were followed.

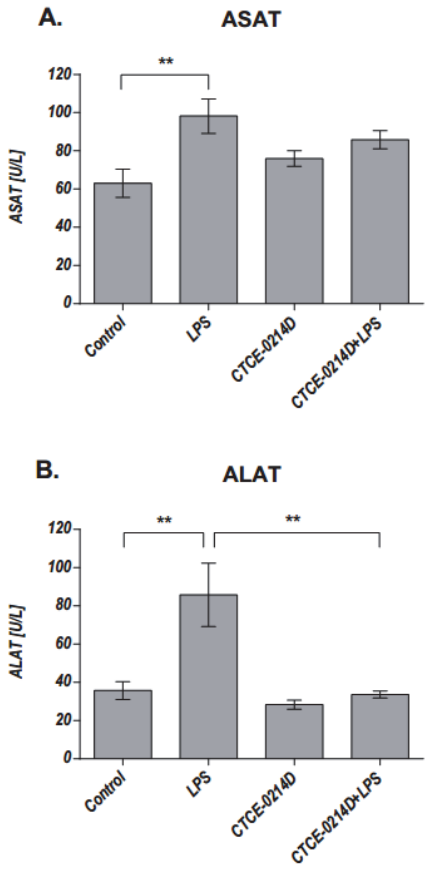

S2 Fig. Aspartate aminotransferase (ASAT) and alanine aminotransferase (ALAT) activities in the serum.

LPS caused a massive increase in the serum concentration of both enzymes when compared to the control group (ASAT: 63.0±7.4 U/L vs. 98.3±9.0 U/L, p = 0.005; ALAT: 35.7±4.6 U/L vs. 85.7±16.5 U/L; p = 0.002). However, CTCE-0214D was able to decrease the enzyme activities throughout. The ASAT activities (A) were reduced by about 15% when compared to the LPS group (p = 0.5), whereas the ALAT activities (B) showed a significant reduction by about 60% (p = 0.002). Remarkably, the ALAT activities of the control and of the CTCE-0214D plus LPS group are at the same level (35.7±4.6 U/L vs. 33.6±4.8 U/L, p = 0.98). As ALAT represents a more specific indicator of liver inflammation than ASAT, these findings underline the protective effects of CTCE-0214D on the livers impressively.

8.4 Ehrenwörtliche Erklärung

Hiermit erkläre ich, dass mir die Promotionsordnung der Medizinischen Fakultät der Friedrich-Schiller-Universität bekannt ist,

ich die Dissertation selbst angefertigt habe und alle von mir benutzten Hilfsmittel, persönlichen Mitteilungen und Quellen in meiner Arbeit angegeben sind,

mich folgende Personen bei der Auswahl und Auswertung des Materials sowie bei der Herstellung des Manuskripts unterstützt haben: apl. Prof. Dr. med. habil. Amelie Lupp,

die Hilfe eines Promotionsberaters nicht in Anspruch genommen wurde und dass Dritte weder unmittelbar noch mittelbar geldwerte Leistungen von mir für Arbeiten erhalten haben, die im Zusammenhang mit dem Inhalt der vorgelegten Dissertation stehen,

dass ich die Dissertation noch nicht als Prüfungsarbeit für eine staatliche oder andere wissenschaftliche Prüfung eingereicht habe und

dass ich die gleiche, eine in wesentlichen Teilen ähnliche oder eine andere Abhandlung nicht bei einer anderen Hochschule als Dissertation eingereicht habe.

Jena, 20.02.2017 Semjon Seemann

8.5 Danksagung

Besonders danken möchte ich Frau apl. Prof. Dr. med. Amelie Lupp für die umfängliche und beständig kompetente Unterstützung während der Erarbeitung meiner Dissertation. Ihre stetige Erreichbarkeit, ihre unaufhörliche Arbeitsmoral und die stets äußerst angenehme Atmosphäre in ihrer Arbeitsgruppe haben die gemeinsamen Veröffentlichungen und diese Arbeit erst ermöglicht. Zusätzlich möchte ich mich ausdrücklich für die zahlreichen konstruktiven Diskussionen, ihre finanzielle Unterstützung und den Rückhalt in besonders fordernden Situationen bedanken. Abseits der Dissertation hatte sie stets ein offenes Ohr für mich und mit ihrer natürlichen und positiven Art motivierte sie mich stets, mich allen Herausforderungen zu stellen.

Ferner möchte ich mich ausdrücklich bei meinen Eltern bedanken. Sie boten mir insbesondere eine seelisch-moralische Unterstützung und erklärten sich (ob freiwillig oder nicht) oft bereit, sich meine von Fachbegriffen geprägten Geschichten ein ums andere Mal anzuhören. Außerdem ermöglichten sie mir durch ihre Unterstützung in vielen alltäglichen Dingen, mich vollends auf die Verfassung der Manuskripte zu konzentrieren. Für ihren Rückhalt, ihre Liebe und ihre beständige Geduld bin ich ihnen unendlich dankbar.

Herrn Prof. Dr. rer. nat. Gerhard K.E. Scriba danke ich für die sehr freundliche Betreuung von pharmazeutischer Seite, die hilfreichen Korrekturen sowie die Übernahme des Zweitgutachtens dieser Arbeit.

Zu guter Letzt danke ich meinem engsten Freundeskreis für die anregenden Diskussionen, den stetigen Rückhalt und den nötigen Ausgleich.

8.6 Wissenschaftliche Beiträge

Publikationen

Seemann S, Lupp A. 2015. Administration of a CXCL12 analog in endotoxemia is associated with anti-inflammatory, anti-oxidative and cytoprotective effects in vivo. PLoS One, 10(9):e0138389.

Seemann S, Lupp A. 2016. Administration of AMD3100 in endotoxemia is associated with pro-inflammatory, pro-oxidative, and pro-apoptotic effects in vivo. J Biomed Sci, 23(1):68.

Seemann S, Zohles F, Lupp, A. 2017. Comprehensive comparison of three different animal models for systemic inflammation. J Biomed Sci, 2017, 24(1):60.

Poster und Kongressbeiträge

Löser K, Seemann S, Lenhardt I, Werz O, Lupp A. Influence of the frankincense resin extract Casperome® on the lipopolysaccharide (LPS) induced systemic inflammation and consecutive liver dysfunction in mice.
Poster auf dem "81st Annual Meeting of the German Society for Experimental and Clinical Pharmacology and Toxicology" in Kiel, März 2015

Seemann S, Lupp A. Activation of the chemokine receptor CXCR4 in endotoxemia is associated with protective effects in vivo.
Poster auf dem "Weimar Sepsis Update" in Weimar, September 2015.

Seemann S, Lupp A. Blockade of the chemokine receptor CXCR4 with AMD3100 in endotoxemia is associated with deleterious effects in vivo.
Poster auf dem "Weimar Sepsis Update" in Weimar, September 2015

Seemann S, Lupp A. The chemokine receptor CXCR4 agonist CTCE-0214D exerts protective effects in endotoxemia in vivo.
Vortrag auf dem "82st Annual Meeting of the German Society for Experimental and Clinical Pharmacology and Toxicology" in Berlin, März 2016

Seemann S, Lupp A. The chemokine receptor CXCR4 antagonist AMD3100 exerts deleterious effects in endotoxemia in vivo.
Poster auf dem “82st Annual Meeting of the German Society for Experimental and Clinical Pharmacology and Toxicology” in Berlin, März 2016

Seemann S, Maurer R, Stillhart C, Kleinebudde P, Page S. Wetting and dissolution behavior of milled hot-melt extrudates.
Poster auf dem “10th World Meeting on Pharmaceutics, Biopharmaceutics and Pharmaceutical Technology” in Glasgow, April 2016

Seemann S, Zohles F, Lupp A. Comparison of three different animal models for systemic inflammation.
Poster auf dem „Sepsis Weimar Update“ in Weimar, September 2017